ALFRED-WEGENER-INSTITUT
HELMHOLTZ-ZENTRUM FÜR POLAR- UND MEERESFORSCHUNG

775
2023

Berichte
zur Polar- und Meeresforschung

Reports on Polar and Marine Research

The Expedition PS133/2 of the Research Vessel POLARSTERN to the Scotia Sea in 2022

Edited by Sabine Kasten
with contributions of the participants

HELMHOLTZ

Die Berichte zur Polar- und Meeresforschung werden vom Alfred-Wegener-Institut, Helmholtz-Zentrum für Polar- und Meeresforschung (AWI) in Bremerhaven, Deutschland, in Fortsetzung der vormaligen Berichte zur Polarforschung herausgegeben. Sie erscheinen in unregelmäßiger Abfolge.

Die Berichte zur Polar- und Meeresforschung enthalten Darstellungen und Ergebnisse der vom AWI selbst oder mit seiner Unterstützung durchgeführten Forschungsarbeiten in den Polargebieten und in den Meeren.

Die Publikationen umfassen Expeditionsberichte der vom AWI betriebenen Schiffe, Flugzeuge und Stationen, Forschungsergebnisse (inkl. Dissertationen) des Instituts und des Archivs für deutsche Polarforschung, sowie Abstracts und Proceedings von nationalen und internationalen Tagungen und Workshops des AWI.

Die Beiträge geben nicht notwendigerweise die Auffassung des AWI wider.

Herausgeber
Dr. Horst Bornemann

Redaktionelle Bearbeitung und Layout
Susan Amir Sawadkuhi

Alfred-Wegener-Institut
Helmholtz-Zentrum für Polar- und Meeresforschung
Am Handelshafen 12
27570 Bremerhaven
Germany

www.awi.de
www.awi.de/reports

Der Erstautor bzw. herausgebende Autor eines Bandes der Berichte zur Polar- und Meeresforschung versichert, dass er über alle Rechte am Werk verfügt und überträgt sämtliche Rechte auch im Namen seiner Koautoren an das AWI. Ein einfaches Nutzungsrecht verbleibt, wenn nicht anders angegeben, beim Autor (bei den Autoren). Das AWI beansprucht die Publikation der eingereichten Manuskripte über sein Repositorium ePIC (electronic Publication Information Center, s. Innenseite am Rückdeckel) mit optionalem print-on-demand.

The Reports on Polar and Marine Research are issued by the Alfred Wegener Institute, Helmholtz Centre for Polar and Marine Research (AWI) in Bremerhaven, Germany, succeeding the former Reports on Polar Research. They are published at irregular intervals.

The Reports on Polar and Marine Research contain presentations and results of research activities in polar regions and in the seas either carried out by the AWI or with its support.

Publications comprise expedition reports of the ships, aircrafts, and stations operated by the AWI, research results (incl. dissertations) of the Institute and the Archiv für deutsche Polarforschung, as well as abstracts and proceedings of national and international conferences and workshops of the AWI.

The papers contained in the Reports do not necessarily reflect the opinion of the AWI.

Editor
Dr. Horst Bornemann

Editorial editing and layout
Susan Amir Sawadkuhi

Alfred-Wegener-Institut
Helmholtz-Zentrum für Polar- und Meeresforschung
Am Handelshafen 12
27570 Bremerhaven
Germany

www.awi.de
www.awi.de/en/reports

The first or editing author of an issue of Reports on Polar and Marine Research ensures that he possesses all rights of the opus, and transfers all rights to the AWI, including those associated with the co-authors. The non-exclusive right of use (einfaches Nutzungsrecht) remains with the author unless stated otherwise. The AWI reserves the right to publish the submitted articles in its repository ePIC (electronic Publication Information Center, see inside page of verso) with the option to "print-on-demand".

Titel: Polarstern vor dem Nordenskjöld Gletscher in der Cumberland Bay East, Südgeorgien.
(Foto: Dennis Koehler, AWI)

Cover: Polarstern in front of Nordenskjöld Glacier in Cumberland Bay East, South Georgia.
(Photo: Dennis Koehler, AWI)

The Expedition PS133/2 of the Research Vessel POLARSTERN to the Scotia Sea in 2022

Edited by

Sabine Kasten

with contributions of the participants

Please cite or link this publication using the identifiers
https://hdl.handle.net/10013/epic.b76dbf89-acd8-4ece-8798-ed9ba9cade45
https://doi.org/10.57738/BzPM_0775_2023
ISSN 1866-3192

Expedition PS133/2 / Island Impact Leg 2

20 November 2022 – 19 December 2022

Punta Arenas – Cape Town

Chief scientist
Sabine Kasten

Coordinator
Ingo Schewe

Contents

1. ÜBERBLICK UND EXPEDITIONSVERLAUF

Sabine Kasten DE.AWI

Das Hauptziel der Expedition PS133/2 “Island Impact” an Bord der *Polarstern* war es, die Quellen und Transportwege von Eisen (Fe), anderen Nährstoffen (sowohl Makronährstoffe als auch Spurenelemente/-metalle) und Kohlenstoffverbindungen in die Schelfgewässer der Insel Südgeorgien und weiter stromabwärts im südlichen antarktischen Zirkumpolarstrom (ACC) zu verstehen. Wir untersuchten die wichtigsten von der Insel stammenden (Schelf-)Quellen von Fe, Nährstoffen und anderen Spurenelementen, einschließlich der Auswirkungen des Eintrags dieser Verbindungen durch Schmelzwasser, Grundwasseraustritte und aktive Methan-Austritte. Die Arbeiten umfassten zudem die Untersuchung der Frage, wie das Austreten von Methan die benthischen Faunengemeinschaften sowie den Umsatz von Kohlenstoff und anderen Verbindungen sowie die Elementflüsse steuert. Darüber hinaus haben wir untersucht, wie dieses von den Inseln stammende Fe und andere potenzielle Fe-Quellen die Biogeochemie und Ökosystemstruktur im atlantischen Sektor des Südozeans beeinflussen. Die Expedition wird durch das Helmholtz-Forschungsprogramm “ Changing Earth – Sustaining our Future” Topic 2, Subtopics 1 und 4, Topic 4, Subtopic 1 und Topic 6, Subtopics 2 und 3 unterstützt.

Polarstern beendete den vorherigen Fahrtabschnitt PS133/1 und erreichte am 16. November den Hafen von Punta Arenas. Am Morgen des 17. November verholte *Polarstern* zur Pier Muelle Mardones. Während des kurzen Aufenthaltes an der Pier wurden die notwendigen Containerverladungen und das Bunkern dank der guten Organisation und Unterstützung der Schiffsleitung, des Vertreters der Reederei, der Kollegen und Kolleginnen des AWI sowie des Engagements der Besatzung erfolgreich abgeschlossen. Darüber hinaus fanden Treffen mit der Fahrtleiterin Christine Klaas und Kapitän Stefan Schwarze zur Übergabe zwischen den beiden Fahrtabschnitten statt. Am Abend gegen 21:00 Uhr verließ *Polarstern* die Pier und ging auf Reede.

Die Hauptgruppe der Fahrtteilnehmenden kam am 18. November in Punta Arenas an. Sie wurden am späten Nachmittag des 19. November von Bussen an ihren Hotels abgeholt und zum Hafen gebracht. Der Transport zum Hafen war ursprünglich für 11:30/12:00 Uhr geplant, verzögerte sich jedoch wegen der Schließung des Hafens aufgrund starker Winde. Am frühen Abend ließ der Wind nach, der Hafen wurde wieder geöffnet und die Teilnehmenden der Expedition PS133/2 konnten mit Hilfe von Schleppern auf *Polarstern* einschiffen. Am frühen Nachmittag des Sonntags, 20. November, verließ *Polarstern* Punta Arenas und begann den zweiten Fahrtabschnitt PS133/2 der Forschungsexpedition “Island Impact”. An Bord befand sich ein internationales Team von Forschenden des Alfred-Wegener-Instituts Helmholtz-Zentrum für Polar- und Meeresforschung, des British Antarctic Survey, der Fachbereiche Geowissenschaften und Biologie/Chemie der Universität Bremen, des GEOMAR Helmholtz-Zentrums für Ozeanforschung Kiel, das MARUM - Zentrum für Marine Umweltwissenschaften, des Max-Planck-Instituts für Marine Mikrobiologie Bremen, des Instituto Antártico Argentino, der Polnischen Akademie der Wissenschaften, der Universitäten zu Köln, Heidelberg, South Florida und Southampton sowie eine argentinische Beobachterin des Servicio de Hidrografia Naval, Ministerio de Defensa (Abb. 1.1).

Während des Transits durch die Magellanstraße und den Südatlantik zu unserem Forschungsgebiet Südgeorgien wurden die Container und Transportkisten mit der sehr geschätzten Hilfe der Schiffsbesatzung entladen. Die Großgeräte wurden an Deck aufgebaut und die Labore und Arbeitsräume vorbereitet und eingerichtet. Nach 4 Tagen Fahrt erreichten wir am 24. November unsere erste Station westlich von Südgeorgien mit dem Ziel, die Wassersäule zu charakterisieren und Wasser in einem Gebiet mit niedrigen Chlorophyllkonzentrationen im Oberflächenwasser zu gewinnen. An dieser Station setzten wir zum ersten Mal das neue, spurenmetallfreie Rosetten/CTD-System des AWI ein und sammelten eine große Menge an Oberflächenwasser, um an Bord Inkubationsexperimente durchzuführen. Nach einem kurzen Transit erreichten wir am 25. November unsere nächste Station im Bereich von Shag Rock. Diese Station wurde ausgewählt, da es Hinweise auf aktive Methanaustritte gab, die auf typische chemosynthetische Muscheln zurückzuführen waren, die im Mageninhalt des in diesem Gebiet gefangenen Schwarzen Seehechts gefunden wurden. Um aktive Methanaustritte zu lokalisieren, führten wir einen hydroakustischen Survey entlang der ehemaligen Langleinenprofils durch. Unsere nächste Station erreichten wir am 26. November, um an einer Lokation nordwestlich von Südgeorgien/Islas Georgias del Sur, die sich durch hohe Chlorophyllkonzentrationen im Oberflächenwasser auszeichnete, große Mengen an Wasser für Experimente an Bord zu sammeln.

Abb. 1.1: Fahrtteilnehmende der Expedition PS133/2 vor dem Nordenskjöld Gletscher in der Cumberland Bay East.

Fig. 1.1: Cruise participants of expedition PS133/2 in front of Nordenskjöld glacier in Cumberland Bay East.

Nach Abschluss der Arbeiten an dieser Station fuhren wir zu einem Bereich im Church Trough, in dem auf der Basis früherer Expeditionen aktive Methanaustritte und in den Sedimenten befindliche Gashydrate bekannt waren. Die Vermessungs- und Beprobungsaktivitäten in diesem Gebiet umfassten eine Flare Drift mit dem EK80, ein Profil mit dem HYDROSWEEP DS3, Wasserproben mit der CTD/Rosette sowie Sedimentproben mit Multicorer und Schwerelot, das mit einem Plastikschlauch ausgestattet war. Leider fanden wir keine Hinweise auf aktive Methanaustritte, und die geborgenen Sedimente enthielten keine Gashydrate.

Am 26. und 27. November setzten wir die Arbeiten in der Wassersäule und den Sedimenten im Gebiet auf dem Schelf vor der Possession Bay und der Antarctic Bay fort und führten außerdem einen HYDROSWEEP DS3-Survey durch. Anschließend fuhren wir in die innere Possession Bay, wo wir die Wassersäule und den Meeresboden beprobten, der - wie das PARASOUND-Sedimentecholot zeigte - durch mächtige und größtenteils ungestörte Sedimente gekennzeichnet ist. Aufgrund der vorherrschenden Wetterbedingungen beschlossen wir am 28. November, in die King Haakon Bay and Trough im Südwesten des Archipels zu fahren, die eines unserer Hauptuntersuchungsgebiete darstellte. Die Arbeiten in diesem Gebiet umfassten umfangreiche Wasser- und Sedimentbeprobungen an zwei Prozessstationen, nämlich der Prozessstation 1 “KHB1” in der äußeren King Haakon Bay (südlich des Eingangs zur King Haakon Bay) in der Nähe des Zusammenflusses mit den Jacobsen und Annenkov Troughs und der Prozessstation 2 “KHB2” in der inneren King Haakon Bay. An mehreren weiteren Stationen in diesem Arbeitsgebiet wurden Wasser- und Sedimentproben entnommen. Darüber hinaus kam im Schelfbereich des Annenkov Trough in der Nähe einer Lokation, die während der *Meteor*-Expedition M134 mit einem ROV untersucht wurde, eine Rauschert Dredge zum Einsatz, um Makro- und Megabenthosspezies zu gewinnen. Im inneren Bereich der King Haakon Bay wurden Zodiacs eingesetzt, um die Wassersäule in Küstennähe zu beproben und zu charakterisieren und Probenahmeteams an Land im Bereich des Peggotty Bluff im innersten Fjordgebiet zu bringen. Die Probenahmeteams an Land sammelten Boden-, Flusssediment- und Vegetationsproben sowie Wasserproben aus Schmelzwasserströmen und -tümpeln sowie Grundwasseraustritten.

In der Nacht vom 30. November auf den 1. Dezember beendeten wir die Arbeiten im Untersuchungsgebiet King Haakon Bay und Trough und fuhren über den Church Trough zurück zum nördlichen Schelf von Südgeorgien/Islas Georgias del Sur. Im Bereich des Church Trough wurden zwei Einsätze des mit einem Kunststoffschlauch ausgestatteten Schwerelotes durchgeführt, und dieses Mal konnten wir mit beiden Sedimentkernen erfolgreich Gashydrate bergen. *Polarstern* fuhr dann in Richtung Osten zum Schelf vor der Cumberland Bay, wo die Wassersäule an einer Station charakterisiert und beprobt wurde, bevor wir in die Cumberland Bay einfuhren. Bei der Einfahrt in die Cumberland-Bucht herrschte eine Föhn-Wettersituation mit starken Winden und einem starken Temperaturanstieg auf bis zu 16°C. Wir erreichten die Prozessstation 2 “CB2 - Grytviken Flare” in der Nacht und begannen ein umfangreiches Programm zur Beprobung der Wassersäule, das u.a. den Einsatz von treibenden Sedimentfallen, eines Wassersäulen-Kamerasystems, eines Unterwasser-Massenspektrometers zur Analyse der Konzentration von gelöstem Methan in der Wassersäule und von In-situ-Pumpen umfasste. Wir beendeten die Arbeiten an der Station “CB2 - Grytviken Flare” mit der Entnahme von Sedimentproben mit Hilfe von Multicorer und Schwerelot. In der Nacht zum 3. Dezember führten wir einen HYDROSWEEP/PARASOUND-Survey auf dem Schelf vor der Cumberland Bay durch und fuhren am Morgen zurück in die Cumberland Bay East, um mit den Arbeiten an der Prozessstation 1 “CB1 - Off Nordenskjöld Glacier” zu beginnen. Die Arbeiten an dieser Station begannen mit dem Ausbringen der Sedimentfalle. Neben einem umfangreichen Programm zur Beprobung der Wassersäule und dem Einsatz von drei Multicorern an Bord der *Polarstern* ließen wir auch die beiden Zodiacs zu Wasser, um die Wassersäule und die Sedimente mit Hilfe einer Hand-CTD, Niskin-Flaschen und einem kleinen Schwerelot in der Nähe der Front des marin-terminierenden Nordenskjöld-Gletschers zu beproben. In der darauffolgenden

Nacht vom 3. auf den 4. Dezember wurde das ozeanographische CTD/Rosetten-System am Eingang des Moraine Fjords eingesetzt und ein Transekt von drei kombinierten CTD/Rosetten- und Wassersäulenkamera-Stationen (Rosina) durch die Cumberland Bay East gefahren. Nach einem sehr erfolgreichen Wasserbeprobungsprogramm an diesen drei Stationen fuhr *Polarstern* zurück zur Prozessstation “CB1 - Off Nordenskjöld Glacier”, um die Sedimentfalle zu bergen.

Am Morgen des 4. Dezember kehrten wir zum Eingang des Moraine-Fjords zurück und setzten die beiden Zodiacs aus, um die Probenahmeteams an Land zu bringen, wo sie Wasser-, Boden-, Sediment- und Vegetationsproben nahmen. Während die Teams in der Nähe an Land an den Stränden und Uferstellen tätig waren, wurden an Bord der *Polarstern* ein Multicorer- und zwei Schwerelot-Einsätze gefahren. Leider war die Beprobung der Sedimente nicht erfolgreich. Wir beendeten die Arbeiten am Eingang des Moraine Fjords mit zwei Planktonnetzeinsätzen. Nach der Rückkehr des letzten Zodiacs zur *Polarstern* kehrten wir zur Prozessstation “CB1 - Off Nordenskjöld Glacier” zurück und führten erfolgreich zwei Schwerelot-Einsätze durch.

In der Nacht vom 4. auf den 5. Dezember erreichten wir unsere dritte Prozessstation im Untersuchungsgebiet der Cumberland Bay, die sich am Zusammenfluss von Cumberland Bay West und East in der äußeren Cumberland Bay befindet - genannt “CB3 - Confluence Zone”. Hier begannen mit der Beprobung der Wassersäule. Am frühen Morgen des 5. Dezember verließen wir die Station “CB3 - Confluence Zone” und fuhren zurück in die Cumberland Bay East in Richtung Grytviken und der Forschungsstation King Edward Point (KEP), die vom British Antarctic Survey betrieben wird. Im Vorfeld der Reise war beim Government of South Georgia and the South Sandwich Islands (GSGSSI) ein Antrag eingereicht worden, der bewilligt wurde. Auf dieser Grundlage wurden wir von den Regierungsbeamten zu einem ganztägigen Besuch auf Grytviken und KEP eingeladen. Wir nutzten die Gelegenheit, um umfangreiche Wasser-, Boden-, Sediment- und Vegetationsproben in und um Grytviken zu nehmen. Außerdem besuchte eine Delegation von Wissenschaftlerinnen und Mitgliedern der Schiffsführung - darunter die Fahrtleiterin und der Kapitän der *Polarstern* - die Forschungsstation KEP. Wir wurden in den Labors und anderen Einrichtungen von KEP herumgeführt und hielten eine Präsentation über die im Rahmen der Expedition PS133/2 von *Polarstern* durchgeführten Forschungsarbeiten. Der Besuch wurde sehr positiv aufgenommen und hat wichtige Verbindungen geknüpft, die sicherlich die künftige wissenschaftliche Zusammenarbeit in diesem Gebiet fördern werden.

Am späten Nachmittag des 5. Dezember verließen wir Grytviken und fuhren zum Schelf vor der Cumberland Bay, wo wir in den folgenden zwei Tagen Wassersäulen- und Sedimentprobenahmen sowie HYDROSWEEP-Untersuchungen an mehreren Stationen durchführten. Diese erstreckten sich vom inneren bis zum äußeren Schelfbereich und schlossen ein Transekts entlang des Cumberland Bay Trough ein. Am 7. Dezember beendeten wir die Wasser- und Sedimentprobennahmen an der Prozessstation “CB3 - Confluence Zone”. Am Abend des 7. Dezembers erreichten wir die Prozessstation 4 “CB4 - Shelf”, die sich im Schelfbereich vor der Cumberland Bay befindet und die letzte Station im Untersuchungsgebiet der Cumberland Bay darstellte. Hier führten wir ein umfangreiches Wassersäulenprogramm und die Beprobung des Oberflächensediments mit Hilfe des Multicorers durch. *Polarstern* verließ die Prozessstation “CB4 - Shelf” gegen Mitternacht und erreichte am Morgen des 8. Dezembers unser letztes Untersuchungsgebiet den äußeren Drygalskii-Trog an der südöstlichen Spitze Südgeorgiens/Islas Georgias del Sur. Hier führten wir eine PARASOUND-Vermessung durch und beabsichtigten zudem, einen Schwerlotkern zu gewinnen. Der Einsatz des Schwerelotes musste jedoch aufgrund der schlechten Wetter- und Seegangsbedingungen abgebrochen werden. Am frühen Nachmittag des 8. Dezember verließen wir unser Untersuchungsgebiet Südgeorgien/Islas Georgias del Sur und fuhren zu einer Position nordöstlich von Südgeorgien/ Islas Geogias de Sur, wo während des vorangegangenen Fahrtabschnitts PS133/1 ein Lander ausgesetzt worden war, der nicht geborgen werden konnte.

Während des Transits zur Lander-Station feierten wir am 9. Dezember den 40. Geburtstag von *Polarstern*. Neben diversen Pressemitteilungen, Videogrußbotschaften und Interviews von Bord wurde dieses Jubiläum der *Polarstern* am Abend im “Blauen Salon” des Schiffes gebührend gefeiert. Die Crew hatte den Salon im Vorfeld liebevoll dekoriert, Kapitän Moritz Langhinrichs hielt eine sehr schöne Rede auf das Schiff und wir bekamen das Geburtstagsvideo zu sehen, das die *Polarstern* über die Jahrzehnte ihrer beeindruckenden Arbeit zeigte. Es war eine gelungene Feier in einem sehr schönen und festlichen Rahmen.

Wir erreichten die Lander-Position gegen Mittag des 10. Dezember und unternahmen mehrere Versuche, den Lander sowohl mit dem POSIDONIA-System an Bord als auch mit einem ins Wasser abgesenkten Hydrophons zu orten. Wir erhielten jedoch kein eindeutiges Signal, dass der Lander ausgelöst wurde. Auch fast 3 Stunden nach dem Auslösen des Landers konnte er weder durch POSIDONIA noch durch ein Funksignal geortet oder an der Meeresoberfläche gesichtet werden. Wir beschlossen daher, die Lander-Station am späten Nachmittag des 10. Dezember zu verlassen und begannen unseren Transit in Richtung Kapstadt.

Während des 9-tägigen Transits nach Kapstadt wurde die Expeditionsausrüstung gepackt, die Labore gereinigt und Beiträge für den wissenschaftlichen Fahrtbericht geschrieben. In den ersten Tagen der Überfahrt setzten mehrere Gruppen die Bearbeitung von Proben fort und führten in den Labors Inkubationsexperimente durch und beendeten sie. Außerdem fanden regelmäßig wissenschaftliche Sitzungen statt, auf denen die vorläufigen Ergebnisse unserer Arbeiten an Bord vorgestellt und diskutiert wurden, sowie wissenschaftliche Abendvorträge, zu denen auch die Besatzungsmitglieder herzlich eingeladen waren.

Am Mittag des 19. Dezember lief *Polarstern* in den Hafen von Kapstadt ein. Der Fahrtverlauf der Expedition sowie ein Überblick der bearbeiteten Stationen finden sich in den Abbildungen 1.2 und 1.3. Die Expedition PS133/2 “Island Impact” war wissenschaftlich äußerst erfolgreich und ein wunderbares Erlebnis. Alle Fahrtteilnehmenden haben die herzliche, freundliche und vertrauensvolle Atmosphäre an Bord des Schiffes sehr genossen. Insbesondere von den jüngeren Fahrtteilnehmenden, die zum Teil zum ersten Mal an einer Schiffsexpedition teilgenommen haben, erhielten wir zahlreiche Rückmeldungen, dass es für sie eine unvergessliche und augenöffnende Erfahrung war, an dieser Expedition an Bord der *Polarstern* teilzunehmen und das Leben und Arbeiten an Bord zu erleben. Im Namen des gesamten Wissenschaftsteams der Expedition PS133/2 möchte ich mich daher bei Kapitän Moritz Langhinrichs und der gesamten Besatzung der *Polarstern* für die hervorragende Unterstützung und Hilfsbereitschaft bei der Koordination, Vorbereitung und Durchführung unserer wissenschaftlichen Arbeiten an Bord ganz herzlich bedanken.

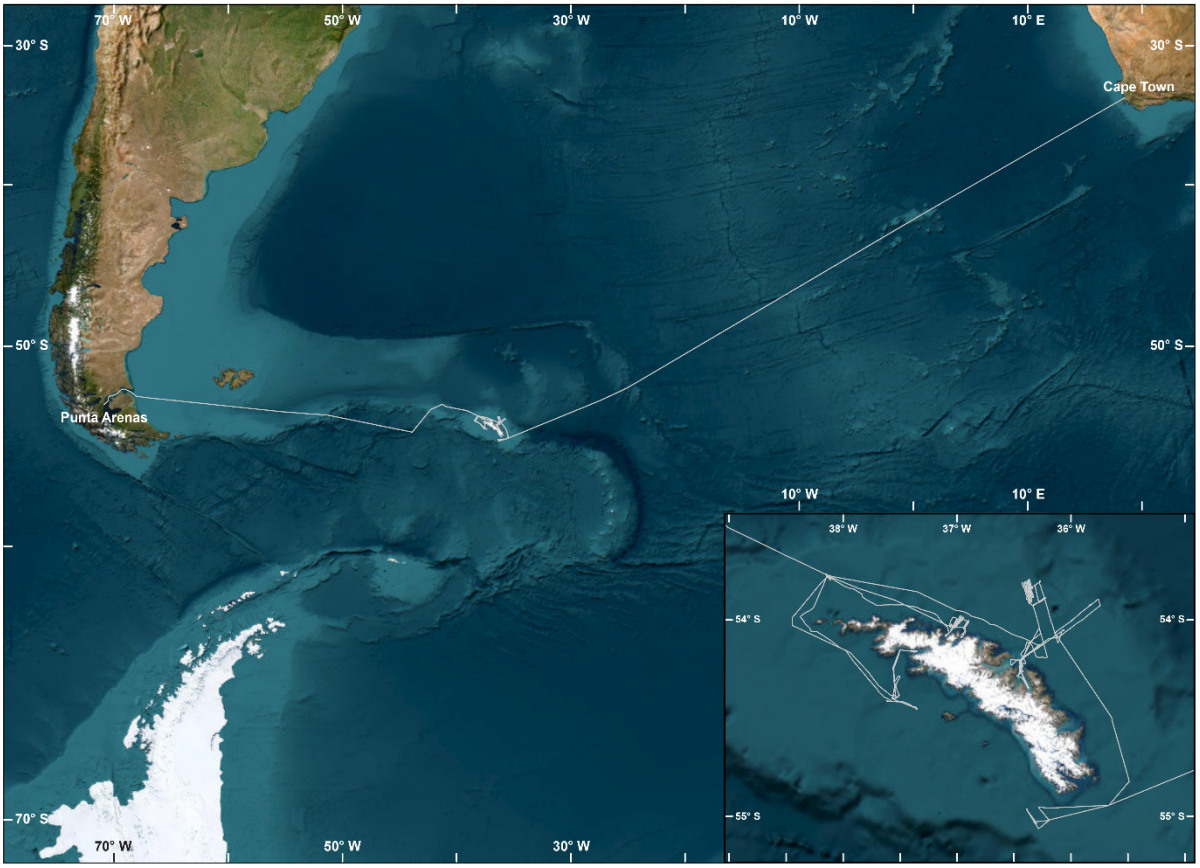

Abb. 1.2: Fahrtroute der Expedition PS133/2 (Basemap courtesy of Esri ArcGIS®). Siehe https://doi.pangaea.de/10.1594/PANGAEA.957577 für eine Darstellung des Master tracks in Verbindung mit der Stationsliste für PS133/2

Fig. 1.2: Cruise track of expedition PS133/2 (Basemap courtesy of Esri ArcGIS®). See https://doi.pangaea.de/10.1594/ PANGAEA.957577 to display the master track in conjunction with the station list for PS133/2

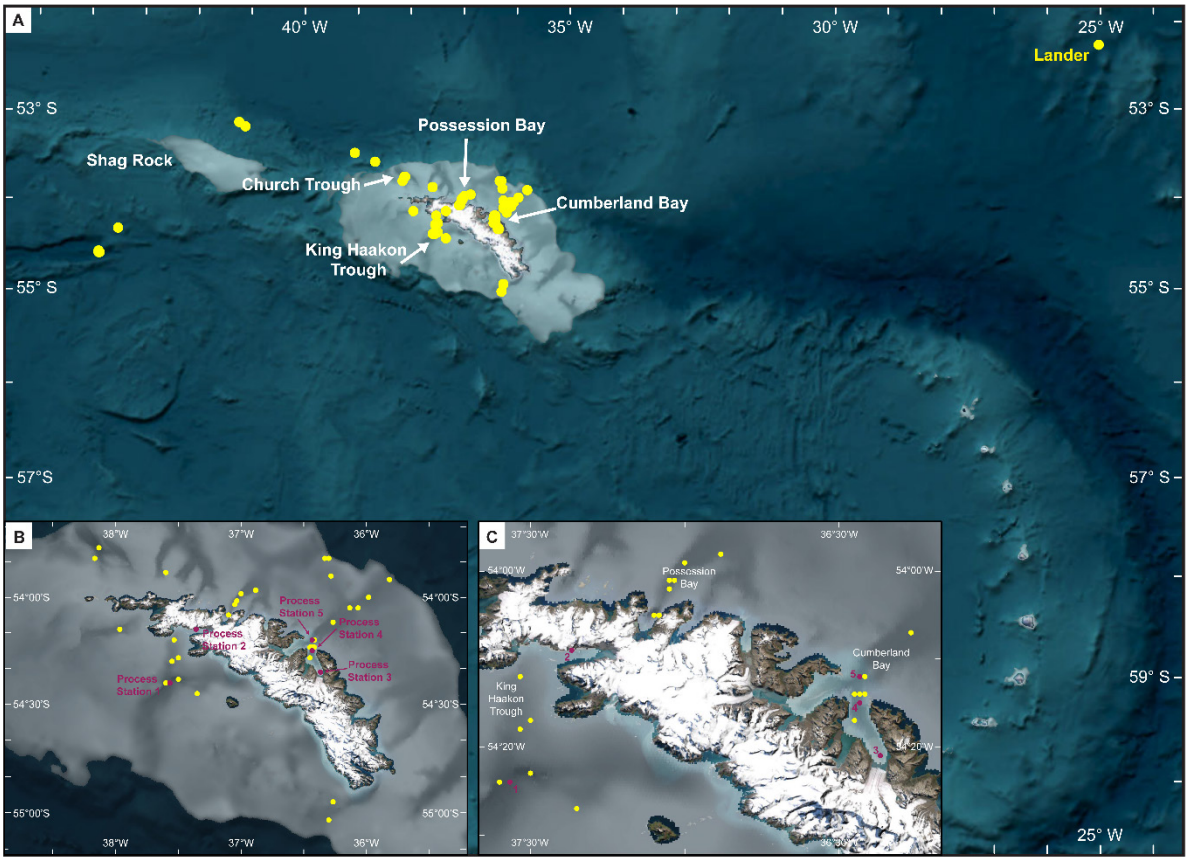

Abb. 1.3: A) Übersichtskarte von Südgeorgien und den Südlichen Sandwichinseln mit den wichtigsten Orten und allen Stationen der Expedition PS133/2. B) Zoom-In des Schelfs von Südgeorgien. Die gelben Punkte markieren die regulären Stationen, während die violetten Punkte die fünf Prozessstationen zeigen. Die Grytviken Flare befindet sich an der Position der Prozessstation 4. C) Zoom-In der drei Fjorde Possession Bay, King Haakon Bay und Cumberland Bay, in denen der Großteil der Forschungsarbeiten durchgeführt wurde (Basemap courtesy of Esri ArcGIS®).

Fig. 1.3: A) Overview map of South Georgia and the South Sandwich Islands showing the most important locations and all stations from cruise PS133/2. B) Zoom-In of the South Georgia shelf. Yellow dots demarcate regular stations while the purple dots show the five process stations. The Grytviken Flare is at the location of Process Station 4. C) Zoom-In on the three fjords Possession Bay, King Haakon Bay and Cumberland Bay, where most research was carried out (Basemap courtesy of Esri ArcGIS®).

SUMMARY AND ITINERARY

The main goal of expedition PS133/2 “Island Impact” on board *Polarstern* was to understand the sources and transport pathways of iron (Fe), other nutrients (both macronutrients and trace elements/metals) and carbon compounds into the shelf waters of South Georgia and further downstream in the Southern Antarctic Circumpolar Current (ACC). We investigated the main island-derived (shelf) sources of Fe, nutrients and other trace elements including the impact of injection of these compounds by glacial melt water, groundwater seepage and methane bubble ebullition. Work also included the study of how methane seepage controls benthic faunal communities as well as material turnover and element fluxes. We further investigated how the local island-derived Fe and other potential Fe sources contribute to the downstream biogeochemistry and ecosystem structure in the Atlantic sector of the Southern Ocean. The expedition is supported by the Helmholtz Research Programme “Changing Earth – Sustaining our Future” Topic 2, Subtopics 1 and 4, Topic 4, Subtopic 1 and Topic 6, Subtopics 2 and 3.

Polarstern finished the previous expedition leg PS133/1 and reached the harbour of Punta Arenas on 16 November. In the morning of 17 November *Polarstern* went to pier at Muelle Mardones. During the short layover at the pier, the necessary container loading and bunkering operations were successfully completed thanks to the good organization of the ship’s command, the representative of the shipping company, colleagues from AWI and the dedication of the crew. Furthermore, meetings with outgoing Chief Scientist Christine Klaas and Master Stefan Schwarze for handover between the two cruise legs took place. In the evening at around 21:00 h *Polarstern* had to leave the pier and went to roadstead.

The main group of cruise participants arrived in Punta Arenas on 18 November. They were picked up at their hotels by busses in the late afternoon of 19 November and brought to the harbour. Transport to the harbour was initially planned for 11:30/12:00 h but was delayed due to closure of the harbour as a consequence of strong winds. In the early evening winds decreased, the harbour opened, and cruise participants of expedition PS133/2 could embark *Polarstern* by means of tugboats. In the early afternoon of Sunday 20 November *Polarstern* left Punta Arenas, beginning the second leg PS133/2 of research expedition “Island Impact”. On board was an international team of researchers from the Alfred Wegener Institute Helmholtz Centre for Polar and Marine Research, the British Antarctic Survey, the Faculties of Geosciences and Biology/Chemistry at the University of Bremen, the GEOMAR Helmholtz Centre for Ocean Research Kiel, the MARUM – Center for Marine Environmental Sciences, the Max Planck Institute for Marine Microbiology Bremen, the Instituto Antártico Argentino, the Polish Academy of Sciences, the Universities of Cologne, Heidelberg, South Florida, Southampton as well as an Argentinian observer from the Servicio de Hidrografia Naval, Ministerio de Defensa (Fig. 1.1).

During transit through the Strait of Magellan and the South Atlantic Ocean to our research area at South Georgia/Islas Georgias del Sur, container and transport boxes were unloaded with highly appreciated help from the ship’s crew. Large equipment was assembled on deck, and labs and workspaces were prepared and installed. After 4 days of transit, we reached our first station west of South Georgia/Islas Georgias del Sur on 24 November with the aim of characterizing the water column and collecting water in an area of low surface-water chlorophyll concentrations. At this station we performed this leg’s first deployment of AWI’s new trace-metal clean Rosette/CTD system and collected a large volume of surface water to

perform on-board incubation experiments. After transit, we reached our next station at Shag Rock on 25 November. This station was targeted as there had been a suggestion for active deep-water methane seepage based on a specimen of a typical chemosynthetic clam genus found in the stomach content of a Patagonian Toothfish caught in the area. In order to locate active methane seeps we performed a hydroacoustic survey across the former longline track. On 26 November we reached our next station to collect large volumes of water for on-board experiments at a site northwest of South Georgia/Islas Georgias del Sur that was characterized by high surface-water chlorophyll concentrations.

After completion of work at this station we proceeded to a site in Church Trough where active methane seepage and sediment-hosted gas hydrates were known to occur based on previous expeditions. Survey and sampling activities in the area included a flare drift with the EK80, a profile with HYDROSWEEP DS3, water sampling with the CTD/rosette as well as sediment sampling by means of a multiple corer and a gravity corer with a soft plastic liner. Unfortunately, we did not find evidence of active methane seepage and the retrieved sediments did not contain gas hydrates.

We progressed to water column and sediment work in the area off Possession Bay and Antarctic Bay on 26 and 27 November and performed a HYDROSWEEP DS3 survey. Afterwards we transited into the inner Possession Bay where we sampled the water column and the seafloor, the latter characterized by thick and mostly undisturbed sediments which were confirmed by echo-prints from the PARASOUND sediment echosounder. Based on prevailing weather conditions, on 28 November, we decided to transit to King Haakon Bay and King Haakon Trough in the Southwest of the archipelago representing one of our main study areas. Work in this area included extensive water and sediment sampling at two process stations – namely Process Station 1 ”KHB1” located in the outer King Haakon Bay (South of the entrance to King Haakon Bay) near the confluence with Jacobsen and Annenkov throughs and Process Station 2 ”KHB2” situated in the inner King Haakon Bay. Water and sediment sampling was performed at several other stations in the working area. In addition, a Rauschert Dredge was used on the shelf of the Annenkov Trough near a location surveyed by ROV during *Meteor*-Expedition M134 to recover macro- and megabenthos species. Zodiacs were used in the innermost King Haakon Bay area to sample and characterize the water column close to shore and bring sampling teams on shore in the area of Peggotty Bluff. The on-shore sampling teams collected soil, stream sediment and vegetation samples as well as water samples from meltwater streams, ponds and groundwater seeps.

We finished work in the King Haakon Bay and Trough study area in the night of 30 November and went back to the northern shelf of South Georgia via Church Trough. In Church Trough two deployments of the gravity corer equipped with soft plastic liners were performed, and this time we successfully recovered gas hydrates from both sediment core deployments. *Polarstern* then headed east towards the shelf off Cumberland Bay where the water column was characterized and sampled at one station, before we transited into Cumberland Bay. While transiting into Cumberland Bay, we were facing a Föhn weather situation with strong winds and a sharp increase in temperature to up to 16°C. We arrived at Process Station 2 “CB2 - Grytviken Flare” at night and started an extensive water column sampling program that among others included deployment of drifting traps, a water column camera system (ROSINA), an in situ underwater mass spectrometer for the analysis of dissolved methane concentrations in the water column, and in situ pumps. We terminated work at station “CB2 –Grytviken Flare” with sediment sampling using the multiple and gravity corers. During the night of 3rd Dec, we performed a HYDROSWEEP/PARASOUND survey on the shelf off/outside Cumberland Bay and in the morning went back into Cumberland Bay East to start work at Process Station 1 “CB1 – Off Nordenskjöld Glacier”. Work at this site started with the deployment of the sediment trap. Besides an extensive water column sampling program and deployment of three multiple

corers from the *Polarstern*, we also launched two zodiacs to sample the water column and sediments by means of hand-held CTD, niskin bottles and a small gravity corer close to the front of the marine-terminating Nordenskjöld Glacier. The following night, 3 to 4 of December, was dedicated to the deployment of the oceanography CTD/rosette system at the entrance of Moraine Fjord and a transect of three combined CTD/rosette and water column camera (ROSINA) stations across Cumberland Bay East. After a very successful water column sampling program at these three stations, *Polarstern* went back to Process Station “CB1 – Off Nordenskjöld Glacier” to recover the sediment trap.

In the morning of 4 December, we returned to the entrance of Moraine Fjord and launched two zodiacs to transfer sampling teams to shore to collect water, soil, sediment, and vegetation samples. While the onshore teams were active at the beaches and shore sites nearby, two gravity corer and one multiple corer deployments were carried out on board *Polarstern*. Unfortunately, sampling of sediments was not successful. We finished work at the entrance of Moraine Fjord with two plankton net deployments. After return of the last zodiac to *Polarstern* we went back to Process Station “CB1 – Off Nordenskjöld Glacier” and successfully deployed and retrieved two gravity cores.

In the night of 4 to 5 December, we arrived at our third Process Station in the Cumberland Bay study area located at the confluence of Cumberland Bay West and East in outer Cumberland Bay– named „CB3 – Confluence Zone“, and started our water column sampling program. In the early morning of 5 December we left station „CB3 – Confluence Zone“ and headed back into Cumberland Bay East towards Grytviken and the research station King Edward Point (KEP) operated by the British Antarctic Survey. Prior to the cruise, a visit proposal had been submitted to the Government of South Georgia and the South Sandwich Islands (GSGSSI) that was granted. Based on this, we were invited by the Government Officers for a full-day visit to Grytviken and KEP. We used the opportunity to perform comprehensive water, soil, sediment and vegetation sampling at and around Grytviken. Furthermore, a delegation of scientists and members of the ship’s command, including the Chief Scientist and the Master of *Polarstern*, visited the research station KEP. We were shown around in the laboratories and other facilities of KEP and gave a presentation on the research performed in the framework of *Polarstern* expedition PS133/2 to the KEP staff. The visit was very well received and has established important links that will certainly foster future scientific cooperation in the area.

In the late afternoon of 5 December, we left Grytviken and headed to the outer shelf off Cumberland Bay where for the next 2 days we performed water column and sediment sampling as well as HYDROSWEEP surveys at several sites, reaching from the inner to the outer shelf area , including a transect along Cumberland Bay Trough. On 7 December we finished water sampling and sediment sampling work at process station „CB3 – Confluence Zone“. We reached Process Station 4 „CB4 – Shelf“ located at the shelf area off Cumberland Bay in the evening of 7 December, which represented the last station in the Cumberland Bay study area. Here, we performed an extensive water column program and sampling of the surface sediment by means of multiple corer. *Polarstern* left Process Station „CB4 – Shelf“ at around midnight and reached our last study area, the outer Drygalskii Trough,- located at the southeastern tip of South Georgia/Islas Georgias del Sur in the morning of 8 December. Here we performed a PARASOUND survey and also intended to take a gravity core. However, due to heavy weather and sea state conditions deployment of the gravity corer had to be abandoned. We left our study area South Georgia in the early afternoon and headed towards a site northeast of South Georgia. There a benthic lander had been deployed during the previous leg PS133/1 but recovery attempts had failed.

During transit to the lander station, we celebrated the 40. Anniversary of *Polarstern* on 9 December. Besides several press releases, video greetings and interviews from on-board,

we celebrated *Polarstern*'s 40. anniversary in the evening in a dignified manner in the 'Blue Salon' of the ship. The crew had lovingly decorated the salon beforehand, Master Moritz Langhinrichs gave a very nice speech celebrating the achievements of the vessel and we watched AWI's birthday video showing *Polarstern*'s impressive research over the decades. It was a successful celebration in a very nice and festive setting.

We reached the lander position around noon on 10 December and tried to locate and communicate with the lander's release systems, both with the POSIDONIA system on board and with a hydrophone lowered into the water. However, we did not receive any clear signal that the lander was released. Even after almost 3 hours after potential release of the lander, it could neither be located by POSIDONIA or radio signal, nor spotted by eye at the sea surface. Therefore, we decided to leave the lander station in the late afternoon and started our transit towards Cape Town.

During the 9-day transit to Cape Town, expedition equipment was packed, labs were cleaned and contributions to the cruise report were written. On the first days of the transit several groups continued processing samples and were running and finishing incubation experiments in the labs. We had regular scientific meetings to present and discuss preliminary results of our work performed onboard as well as more general science talks in the evenings, to which also the crew members were cordially invited.

Around noon of 19 December *Polarstern* arrived in the harbour of Cape Town. The cruise track of the expedition and an overview of stations sampled are shown in Figures 1.2 and 1.3. Overall, the expedition PS133/2 "Island Impact" has been scientifically extremely successful and a wonderful experience. All scientific cruise participants have enjoyed the warm, friendly, and trusting atmosphere on board the ship. Especially from the more junior cruise participants, some of whom participated in a ship expedition for the first time, we received numerous feedback that it was an unforgettable and eye-opening experience for them to participate in this expedition on board the *Polarstern* and to experience life and work on board. On behalf of the entire science team of expedition PS133/2, I would like to express my sincere thanks to Master Moritz Langhinrichs and the entire crew of the *Polarstern* for their excellent support and helpfulness during the coordination, preparation and execution of our scientific work on board.

WEATHER CONDITIONS DURING PS133/2

Michael Knobelsdorf, Frank Otte DE.DWD

On Sunday, 20 November 2022, *Polarstern* left the port of Punta Arenas for South Georgia with a one-day delay. The destination was the shelf waters of South Georgia. Here and also further downstream in the Antarctic Circumpolar Current, the main sources of iron, nutrients, trace elements and various carbon compounds originating from the island were to be investigated.

The weather at departure was dominated by a high north of the Falkland Islands. Thus, the sun was shining frequently until Monday, 21.11. There were northerly winds around 6 Bft, which briefly increased to 7 to 8 Bft with the passage of a cold front on Tuesday, 22. November. Significant seas rose to 4m and intermittent rain occurred under overcast skies. Air temperatures initially remained around 10 degrees.

On Wednesday (23.11.) and Thursday (24.11), the influence of a high north of the Falkland Islands extended to South Georgia. Thus, it was initially cloudy in many cases due to fog or low clouds. Significant seas were from 2 to 3 m within a northwesterly swell.

On Friday, 25.11. the sun was shining frequently within a southerly wind of 6 Bft at 4 degrees. During the weekend (26.11 and 27.11) *Polarstern* was crossed by a cold front of a low over the Weddell Sea. At the edge of the strong high northeast of the Falkland Islands a strong southwesterly flow over South Georgia prevailed. On the downwind side, partly katabatic winds with gusts up to 11 Bft occurred. Within a sun cloud mix, the air dried strongly at times. This was associated with large temperature fluctuations in a short period of time. The significant seas were partly 2 to 3m in the sheltered bays with a mostly westerly swell.

On Monday, 28.11. and Tuesday, 29.11., an Atlantic high pressure ridge extended to South Georgia while gradually weakening. The west to northwest wind with foehn gusts up to 8 Bft continued in King Haakon Bay in the northwest of South Georgia. Subsequently some Föhn weather like conditions were experienced, the relative humidity dropped by half pushing quite dry air in the area. Significant seas showed 2 m in the shelter of the bay with a mostly northwesterly swell. During the night of Wednesday, 30.11., a band of rain passed in conjunction with a cold front. In the wake of the front pressure increased, isolated showers occurred, later mostly sunny with southwesterly winds around 7 Bft dominated. The significant sea showed wave heights up to 3m within a mostly westerly swell.

In the following days until Monday 4.12. *Polarstern* was in Cumberland Bay on the northeast side of South Georgia. Mostly weak high pressure influence prevailed, the partly quite strong northwesterly current persisted. In many cases, the sun was shining during typical Föhn weather events. Thus, in the night of Friday, 2.12. there was the typical Föhn wall over the peaks of the mountains, at the same time the classic lenticularis clouds formed. Foehn gusts up to 11 Bft from the northwest occurred. This situation was even surpassed in the night to Sunday, 03.12. Thus, there were temperatures of partly over 17 degrees in a phase lasting several hours. This was not caused by Föhn winds alone. In the height there was a quite warm air mass, in combination with the Föhnwind it contributed to the strong temperature increase. Temperatures of 17 degrees and more were measured in the evening with a humidity of 30 percent. Initially, a significant sea of up to 2 m was measured, which was hardly noticeable from Monday, 5.12 on.

On Tuesday, 6.12. a weak cold front crossed Cumberland Bay in South Georgia. Subsequently, atmospheric pressure increased, widespread sunshine, isolated snow showers at only 0 degrees on Wednesday, 07.12. with a wind chill about minus 3 degrees. Within the bay, significant seas of 4m in places decreased noticeably. On Thursday, 08.12., the high influence over the island diminished as a storm low development appeared north of the Falkland Islands. Most of the day was overcast with rain at 2 degrees in a northwesterly wind of 8 Bft with gusts of 10 to 11 Bft. Significant seas were up to 4 m. As *Polarstern* had reduced speed to 9 knots, it was able to stay in the centre of the low on Friday, 09.12., while transiting towards Cape Town. For a short time there were only light winds, however after the passage of the storm low the airstream shifted southwest and the wind increased to 7 to 8 Bft. This resulted in poor visibility, with precipitation of rain and snow at 0 degrees.

On Saturday, 10.12, there were strong southwesterly winds of 7 to 8 Bft with gusts up to 9 Bft. Quite cold air flowed in, accompanied by frequent snow showers at 0 degrees within occasional sunshine. On Sunday, 11.12. a small depression moved in the direction of *Polarstern*. The associated cold front crossed the region, in the afternoon it was mostly sunny with a slight increase in pressure. The northwest wind temporarily increased to 7 to 8 Bft. The significant wave was about 4m, the temperature rose to 6 to 8 degrees.

Further down to Cape Town, high pressure ridges and lows crossed the cruising area. On Tuesday, 13.12., after the passage of a cold front, the weather calmed down briefly due to rising air pressure, before another low approached in the afternoon. It brought again northwesterly winds of 7 to 8 Bft, with the significant wave increasing from 2 m at the beginning to 5 meters at times. The weather was cloudy with fog, at times rainy with air and water temperatures around 8 degrees.

On Wednesday, 14.12, a weak ridge brought a relief in the weather, the winds eased substantially with the significant wave showing only a swell of about 2 m. Towards the evening another low close to Gough Island approached, the northwest wind increased to 7 to 8 Bft. On the next following day, 15.12. *Polarstern* was still under the influence of the above mentioned low while moving south and loosing its influence on *Polarstern*. In the wake of the low a SW'ly airstream set in with winds up to 7 to 8 Bft and a temporarily significant wave height of 5 m.

On the further itinerary through the subtropical high close to South Africa light S'ly winds with 5 Bft dominated. Quite often the sun was shining with temperatures hovering around 15 degrees.

On Friday, 16.12. *Polarstern* reached the subtropical high close to South Africa. The initially 6 to 7 Bft SW'ly winds dropped further to 5 Bft within a significant wave height of about 3 m within a SW'ly swell. It was mostly cloudy with temperatures around 12 degree. On the weekend with variable cloudiness moderate S'ly winds of 5 Bft were experienced, at times less. The temperatures showed 15 to 19 degrees.

On Monday, 19.12.2022, around 13:00 ships time *Polarstern* reached Cape Town The weather showed a mix of sun and clouds with S to SE winds of 5 to 6 Bft. Temperatures were hovering around 20 degrees.

2. HYDROACOUSTICS

Katharina Streuff[1,2], Neele Köhler[1,2], [1]DE.UNI-Bremen
Nina-Marie Lešić[1,2], Catalina Rubiano[3] [2]DE.MARUM
not on board: Miriam Römer[1,2], Alastair Graham[3], [3]GOV.FLORIDA

Grant-No. AWI_PS133/2_01

Objectives

Although previous studies have compiled and/or used bathymetric maps around South Georgia to elucidate some of the continental shelf morphology (Graham et al., 2008; 2017; Hodgson et al., 2014, Lešić et al., 2022), large parts of which are related to glacial activity (see trough systems in Fig. 2.1), the bathymetric coverage around the sub-Antarctic island is still very patchy. Research cruises to the area therefore offer the potential to map areas where the seafloor is poorly resolved. Together with surveys of the PARASOUND sediment echosounder, multibeam echosounder data offer valuable opportunities to resolve glacial landforms and (post-)glacial sediment sequences in order to reconstruct the evolution of the South Georgia ice cap during past glacial intervals. Furthermore, newly acquired multibeam data can be incorporated into ocean mapping efforts such as GEBCO and thus actively contribute to resolving more and more areas of the undiscovered deep.

Echosounding systems can also be used to visualise anomalies in the water column, which are often associated with sites of methane seepage at the seafloor. Actively emitting gas bubble seepage in South Georgia was first detected and described during *Polarstern* expedition ANT-XXIX/4 in 2013 (Bohrmann et al., 2013). While other such sources have been detected in numerous regions in our oceans, these were the first active seeps found south of the Antarctic Polar Front. Although only a few surveys were possible near South Georgia during this cruise, a total of 133 gas seeps were detected using the hydroacoustic systems. Correlation of the seep locations with the bathymetry of the shelf was enabled by the compilation of the extensive ship-based echosounder data published by Graham et al. (2017). Initial interpretations of the distribution of these detected gas bubble seeps indicated that emissions were found exclusively in areas of glacial troughs along the shelf and within fjords (Römer et al., 2014). Analyses revealed that the gas bubbles contained almost only methane, which was produced by microbial decomposition of organic material (Geprägs et al., 2016).

More intensive investigations of this newly discovered gas system were undertaken in 2017 during the *Meteor* expedition M134 (Bohrmann et al., 2017), which involved the systematic investigation of gas seeps in eight shelf troughs around South Georgia (Fig. 2.1). A total of 2,647 nautical miles around South Georgia were mapped with sediment echosounder and multibeam echosounder. Several thousands of gas seeps were detected as acoustic anomalies in the water column (Fig. 2.1). Almost all of the seeps were found to correlate with gas accumulations in the sediments, and again, to be concentrated mainly in the inner fjord systems and glacial troughs, where there is increased deposition of organic matter and increased microbial methane production.

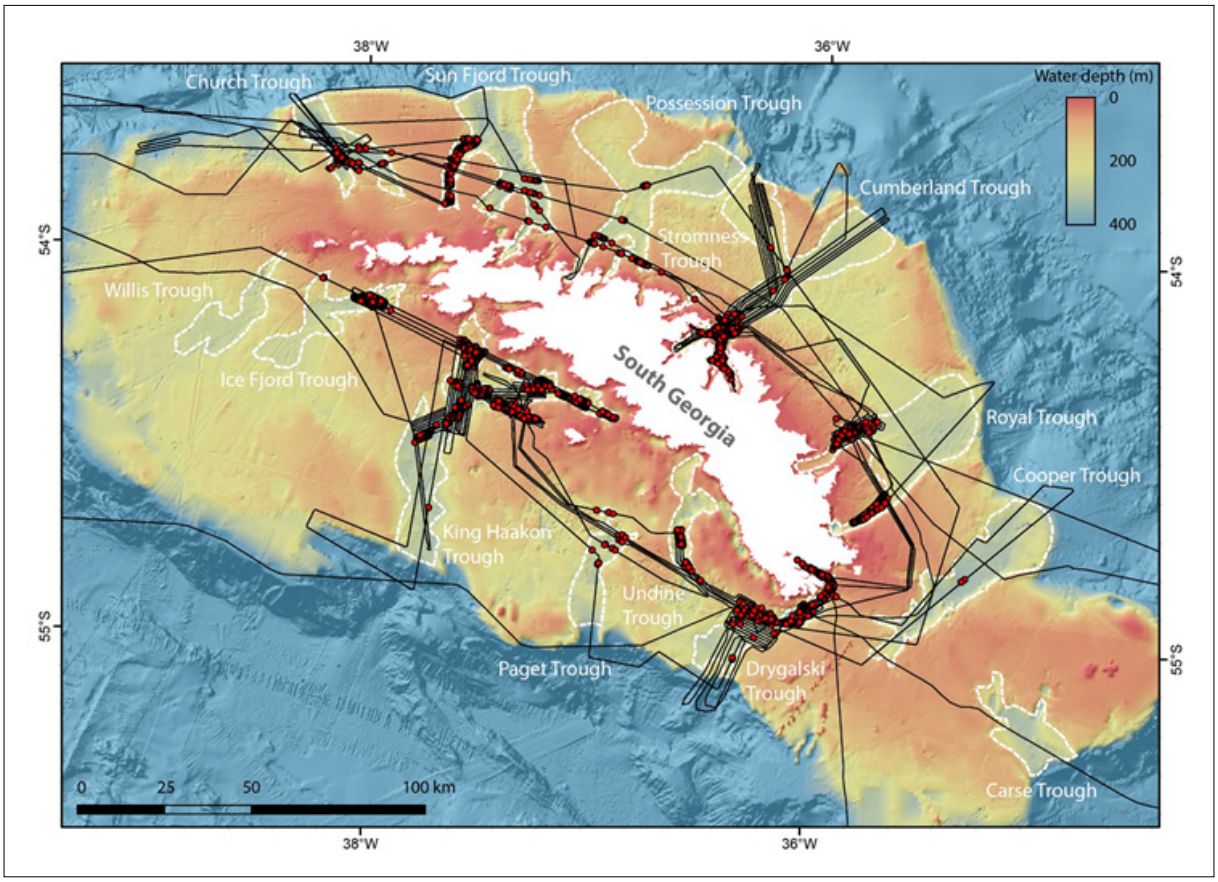

Fig. 2.1: Bathymetric representation of the shelf area around South Georgia. Glacial troughs cut into the shallow shelf (white dashed areas). Thousands of gas bubble seeps (red dots) were detected during the two previous expeditions ANT-XXIX/4 and M134 (black lines).

In addition to anomalies in the water column indicating (new) sites of active methane emmission, the data produced by the splitbeam echosounder can be used to quantify flow rates. The sediment echosounder provides additional data about gas sources but also gas concentrations and their pathways in the shallow subsurface. Bathymetry and backscatter maps generated by the multibeam also help to identify and characterize morphological structures associated with gas seeps. With one main objective being the continued mapping of the continental shelf around South Georgia and the acquisition of more data to better understand past glacial dynamics in the area, the second objective of the hydroacoustic team was to use the echosounders to answer the following research questions:

- How much gas (almost exclusively methane) escapes around South Georgia?
- How variable are these seeps, i.e. what kind of fluctuations do we have to expect that need to be included in a quantification approach?
- How are the gas emissions distributed and what distribution patterns can be observed? In order to achieve an overall estimate of gas emissions from individual measurements we have to extrapolate. This in turn will only be realistically possible if the distribution patterns are known.

Work at sea

Three hydroacoustic systems were used during expedition PS133/2, the Hydrosweep DS3 multibeam echosounder, the Simrad EK80 fish splitbeam echosounder and the Atlas PARASOUND sediment echosounder. All systems were watched over continuously through an established shift system during our time on the continental shelf of South Georgia, in order to minimize system failures and resulting data losses or to react quickly should they occur. Bathymetry, backscatter, and water column data were recorded using the Hydrosweep DS3 MBES – a specialized sonar comprised of an embedded transducer system that is flush-mounted within the hull and protected by an ice-shield. Hydrosweep operation – turning it on and off, starting/stopping pinging, etc. – was conducted using the Hydromap Control software. Position information was gathered by the mast-mounted Trimble GNSS and fed into the Hydrins Inertial Navigation System (INS) to provide the MBES position and motion (pitch, roll and heave) corrections while underway. The Hydrosweep DS3 utilizes the 14 to 17 kHz frequency range for use in water depths of up to 8250 m. While underway, both in transit and at the study areas, swath width was manually adjusted in the Teledyne PDS software program. Additionally, three separate grid sizes (50-,100-, and 200-m) were calculated for shallow (~0-100 m), intermediate (~1,000-2,500 m), and deep water (>2,500 m) mapping use.

The Hydrosweep ran continuously throughout the cruise with the exception of transit through EEZs and when the ship's crew attempted to recover an acoustically pinging lander from the previous cruise leg, PS133/1. When idling at a scientific station, the Hydrosweep remained pinging, however data storage was paused and then resumed upon transit to the next station.

Bathymetric data was collected in three different formats: the original Hydrosweep ASD format, the internal PDS format, and the Teledyne S7K format. As they were collected, the S7Ks were exported to Caris HIPS and subsequently georeferenced so they could then be cleaned throughout the cruise. Data were regularly backed up to an external hard drive system as well as individual hard drives. Due to the immense size of water column data produced by the Hydrosweep, following backup, the oldest raw data were occasionally deleted from the main PDS computer in order to create space for the new incoming data being acquired.

The Simrad EK80 wide band echosounder, or "fish echosounder", was intended to image potential anomalies in the water column at a higher resolution than that obtained by the Hydrosweep. Particularly in the shallow shelf areas around South Georgia, the EK80 was the most suitable instrument because it allows for the detection af algae, fish, plankton and gas bubbles. To detect methane flares during these drifts as well on the South Georgia shelf, the EK80 echosounder was operated in "Normal Operation" mode with a fixed frequency of 18 kHz and a ping interval of 5000 ms. Pulse duration was adjusted on the go but normally needed to be set to the maximum of 8.192 ms, in order to achieve an acceptable signal to noise ratio. Once *Polarstern* arrived on the shelf of South Georgia, the EK80 was continuously pinging, except during station work. While data were being acquired throughout the entire time in the research area, in order to keep data volume to a manageable amount, storage was turned on only periodically during flare drifts, in other areas where gas bubbles had been detected previously, or where we observed anomalies in the water column.

The third hydroacoustic system used during expedition PS133/2 was the PARASOUND P70 echosounder, which is useful for single beam echosounder investigations in the water column to detect anomalies, but is commonly used as a sediment echosounder. Like the Hydrosweep the echosounder was controlled through the software tandem Hydromap Control and Parastore. The system is capable to penetrate up to 200 m of sediments with a maximum transmission power of 70kW. It utilizes the parametric effect based on nonlinear relation of pressure and density during sonar propagation (Spiess and Breitzke, 1990). For our purposes the primary high frequency (PHF) at 18-20 kHz and the secondary low frequency (SLF) at ~4 kHz were of most

interest, as the PHF is used to detect anomalies, such as gas bubbles, plankton, fish and other particles in the water column, whereas the SLF offers a higher lateral resolution more suited to resolving sediment reflectors and imaging small-scale structures on the seafloor. During hydroacoustic surveys and during transit time the pulse characteristics of the PARASOUND were usually set to quasi-equidistant transmission, because signal distribution across the seafloor is superior, which thus yields better results to visualize sedimentary sequences. The system was set to single pulse and full water column when traversing over areas of interest for gas bubble detection. During flare drift surveys, however, the PARASOUND (and the Hydrosweep) were usually switched off due to interferences with the EK80. Raw data were stored as *.asd files, while the software PARASTORE saved .ps3 and .sgy files that can be used for interpretation at a later stage.

All hydroacoustic systems were calibrated regularly by applying updated sound velocity profiles (SVPs) of the changing water column. During transit to and from South Georgia, sound velocity profiles were calculated based on the World Ocean Atlas Database. While on the continental shelf sound velocity profiles were calculated using data collected by regular Seabird CTD deployments, which provided real-time values of sound velocity in the water column. This was done by first converting the binary CTD data to ASCII format using the SBE Data Processing software. Next, the data was imported into the Sound Speed Manager software where it was processed and exported (continually throughout the cruise) to the data acquisition computer for real-time sound velocity corrections.

Preliminary results

Over the course of the cruise roughly 4500 nautical miles of data were recorded (Fig. 2.2). In order to maximize use of time during transits across areas with data gaps, we followed along the edges of existing data where gaps existed, to try and fill in as many blanks as possible. In addition to the three aforementioned flare drifts (see Fig. 2.3) at vessel speeds below 2 kn, but on average 0.5 kn, hydroacoustic data were gathered during transits at a vessel speed of 10 to 10.5 kn, and during several surveys usually conducted at 5 kn. A total of two bathymetric surveys were carried out on the shelf of northern South Georgia, one close to and in Possession Bay, and one on the outer shelf off Cumberland Bay (Fig. 2.2, Tab. 2.1). In addition, five PARASOUND profiles across two troughs were recorded: three cross profiles in Cumberland Bay, another two in Drygalski Trough (Tab. 2.1).

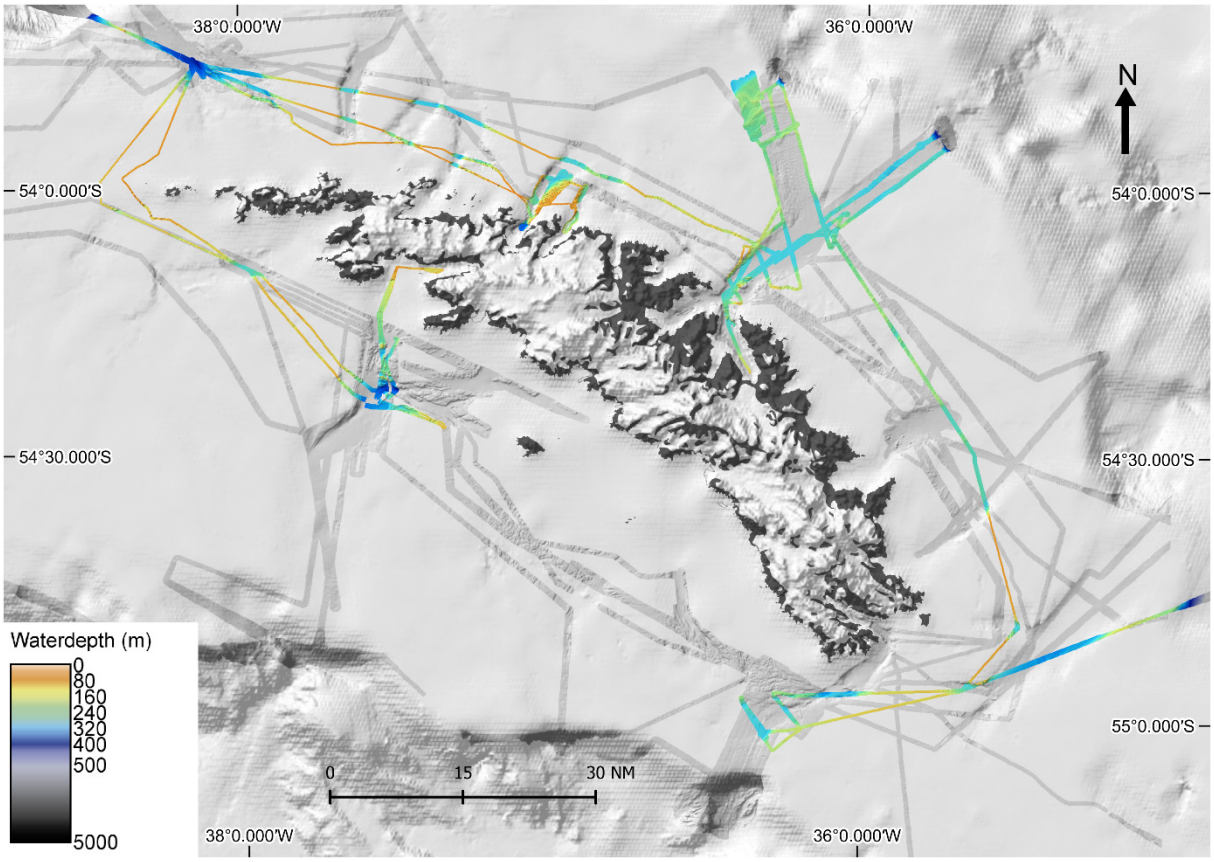

Fig. 2.2: Overview of Hydrosweep bathymetric data recorded during cruise PS133/2. Greyscale data represent data collected during previous cruises. Target areas for new high-resolution data included Church Trough, Possession Bay, King Haakon Bay, and Cumberland Bay. Data shown are projected in WGS 84 at a 100 m grid size.

Three “flare drift” profiles were run specifically to detect and investigate previously sighted flares, one in Church Trough, one on the way to King Haakon Bay in the south of the island, and one in Cumberland Bay across Grytviken Flare (Fig. 2.3, Tab. 2.1). During these profiles the ship was going as slowly as possible (normally around 0.5 kn on average) trying to drift over the sites of interest. Since *Polarstern* is a large and heavy vessel, however, the nautical officers were struggling to keep the ship in position, especially in rough seas, and it was not always possible to directly cross the flare site. The one west of King Haakon Bay was also not a “proper” drift profile, as the vessel merely slowed to speeds between 1 and 5 kn for about an hour during transit time. Rough weather prevented stable positioning of the ship, however, and the profile was aborted after approximately 45 minutes. Flare profiles with the splitbeam echosounder did not show any flares in the water column; however, this is likely an artefact owing to faulty settings, too much noise in the water column or an inappropriate frequency used (the optimum frequency for imaging gas bubbles is 38 kHz, but the available transducer was a fixed-frequency transducer set to 18 kHz). This assumption is based on the fact that flares were observed in the recorded PHF data of the PARASOUND sediment echosounder (see below).

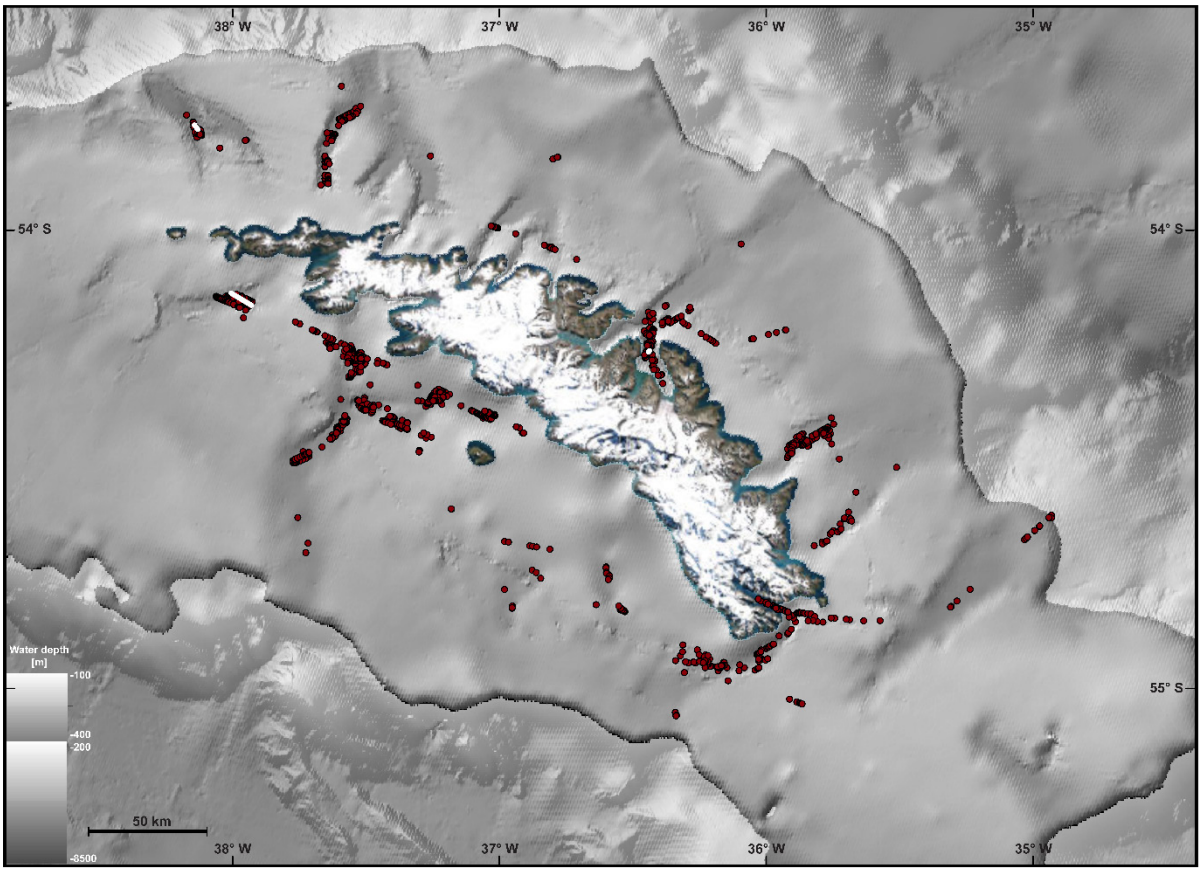

Fig. 2.3: Overview of the three Flare Drifts (white, thick lines) conducted during expedition PS133/2 shown in relation to the gas bubble flares mapped during previous Meteor cruise M134 (dark red symbols).

Tab. 2.1: Details on the hydroacoustic surveys completed during expedition PS133/2. Type denotes the kind of survey carried out, with FD = Flare Drift, FP = Flare Profile, HS = Hydrosweep, i.e. bathymetric survey, and PS = PARASOUND profiling. The PARASOUND profiles were logged as one station each, one in Cumberland Bay and one in Drygalski Trough.

Date, Station No. & Type	Start Time (UTC)	Start Location	End Time (UTC)	End Location	Study Area
26/11/2022 PS133/2_7-1 FD	06:05:31	53° 46,025' S 38° 08,547' W 385.4 m	09:05:20	53° 46,576' S 38° 07,831' W 372.8 m	Church Trough
27/11/2022 PS133/2_13-1 HS	02:51:04	54° 01,467' S 37° 03,869' W 263.5 m	13:34:58	54° 05,008' S 37° 05,912' W 358.3 m	Shelf outside Possession Bay
27/11/2022 FP	07:26:35	54° 09,293' S 37° 59,587' W 229.1 m	08:08:02	54° 09,984' S 37° 56,553' W 233.9 m	Shelf south of western South Georgia

02/12/2022 PS133/2_32-10 FD	06:10:54	54° 16,072' S 36° 26,519' W 260.1 m	07:58:06	54° 15,937' S 36° 26,249' W 257.6 m	Cumberland Bay, Grytviken Flare
03/12/2022 PS133/2_33-1 PS	02:40:06	54° 02,670' S 36° 16,574' W 191.0 m	07:47:21	54° 13,388' S 36° 24,482' 132.1 m	Cross profiles outside Cumberland Bay
06/12/2022 PS133/2_44-1 HS	01:29:14	54° 06,743' S 36° 07,012' W 236.6 m	23:27:13	54° 08,128' S 36° 22,772' W 198.9 m	Outer shelf outside Cumberland Bay
06/12/2022 PS133/2_51-1 PS	09:01:29	54° 57,376' S 36° 16,888' W 222.2 m	11:49:00	54° 58,283' S 36° 23,054' W 250.0 m	Outer Drygalski Trough

The first bathymetric survey on the shelf outside of Possession Bay demonstrated the challenge in getting good data coverage on the South Georgia shelf owing to the rugged and dynamic nature of the seafloor. Due to rapidly changing depths, the swath angle had to be constantly monitored and adjusted so as not to lose coverage when the seafloor rapidly became shallower. Despite all efforts a few holes in the data could, unfortunately, not be avoided, because depth variations in the range of 60 m in a matter of a few pings and a slightly sluggish response time of the Hydrosweep made it extremely tricky to keep track. Furthermore, in these variable water depths, the beam angle was not always stable with one or more beam signals being lost in the water column. Nevertheless, the data provided a good overview of the southeastern margin of Possession Fjord and the adjacent very hummocky shelf, possibly related to ancient bedrock terrain being modified by glacial, fluvial, or even subaerial erosion during previous ice ages. The second survey was mostly successful. It covered parts of the outer shelf adding on to some previous data coverage revealing parts of ice-marginal moraines, which, again, resulted in quite variable water depths. However, the seafloor was more wavy than hummocky in this region, and it was therefore much easier to attain a stable swath angle.

The PARASOUND data obtained throughout the cruise were of highly variable quality. There were initial problems to get the echosounder started and it took about a day to get it up and running. The problem was never quite resolved but seemed to be fixed by changing two plugs in the hardware. However, data quality throughout the cruise was extremely variable (see Fig. 2.4) and partially very noisy, a circumstance which could not be improved by modifying the settings in PARASTORE. Although poor data quality seemed to often coincide with steep terrain and/or windier weather, the data quality also suffered in the fjords or in coastal areas, i.e. at places where and at times when the seafloor was smooth and even and the ship was sheltered from the rough weather of the South Atlantic. Nevertheless, PARASOUND surveys were successful throughout and resolved cross-trough profiles showing both flanks and thick sediment packages in the center of the troughs. Acoustic stratification and the nearly horizontal orientation of reflections are characteristic for (postglacial) hemipelagic sedimentation in a mostly low to moderate-energy depositional environment (e.g. Ó Cofaigh et al., 2016). Furthermore, the PARASOUND system detected multiple gas flares on the shelf of South Georgia (Fig. 2.4A), even in locations where the EK80 splitbeam echosounder showed no anomalies. Due to variable data quality and a lot of noise in the water column, however, these were not usually very pronounced (Fig. 2.4B). Postprocessing of the PHF data showed that the cruise track crossed a total of approximately 200 sites of active gas seepage, some of them coinciding with the location of the drift profiles and previous locations of active gas seepage. Evaluation of the water column data recorded by the Hydrosweep may yield further flares but will only happen after the cruise.

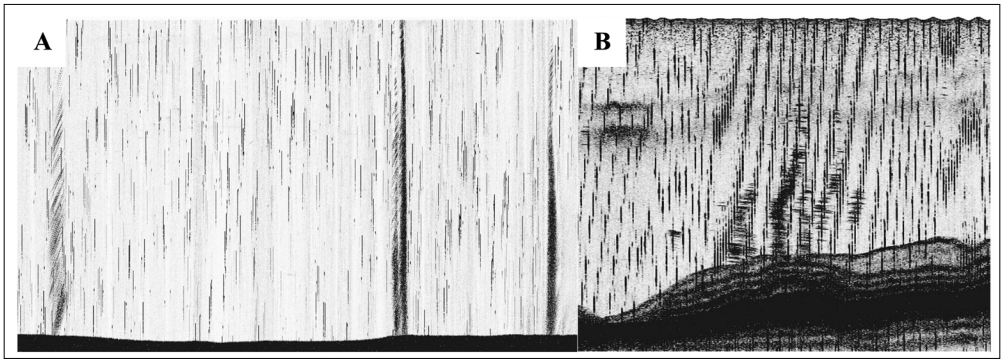

Fig. 2.4: Examples of the two best visible gas flares detected in the primary high frequency of the PARASOUND sediment echosounder from A) Grytviken, Cumberland Bay, and B) Ice Fjord, SW South Georgia. A) and B) show the variability in PARASOUND data quality throughout the cruise and the difficulty of recognizing flares in some areas.

Data management

Multiple backups of the data obtained during this cruise were stored to external hard disks which were brought ashore. After the cruise, they were saved on the servers available for this purpose at MARUM and will be archived, published and disseminated according to international standards by the World Data Center PANGAEA Data Publisher for Earth & Environmental Science (https://www.pangaea.de) within three years after the end of the cruise (Tab. 2.2).

Tab. 2.2: Type and volume of data acquired during cruise PS133/2

Data	Volume	Archiving
PARASOUND (ATLAS)		
.asd files for 3.5 kHz frequency (sediment profiles) and 19 kHz frequency (water column)	140 GB	Max. 3 months after cruise MARUM und PANGAEA
.ps3 and .sgy files for both frequencies	400 GB	Open access after 3 years
Multibeam (HYDROSWEEP)		
Bathymetry and water column raw data	5.7 TB	Max. 3 months after cruise
Processed .s7k files	114 GB	Max. 6 months after cruise MARUM und PANGAEA Open access after 3 years
Splitbeam (SIMRAD)		
18 kHz frequency raw data	45 GB	Max. 3 months after cruise MARUM und PANGAEA Open access after 3 years

This expedition is supported by the Helmholtz Research Programme “Changing Earth – Sustaining our Future” Topic 2, Subtopics 1 and 4, Topic 4, Subtopic 1 and Topic 6, Subtopics 2 and 3 and additional funding by MARUM – Center for Marine Environmental Sciences, University of Bremen to Project “Hydroacoustic Island Impact”.

In all publications based on this expedition, the **Grant No. AWI_PS133/2_1** will be quoted and the following publication will be cited:

Alfred-Wegener-Institut Helmholtz-Zentrum für Polar- und Meeresforschung (2017) Polar Research and Supply Vessel POLARSTERN Operated by the Alfred-Wegener-Institute. Journal of large-scale research facilities, 3, A119. http://dx.doi.org/10.17815/jlsrf-3-163.

References

Bohrmann G et al. (2017) R/V METEOR Cruise Report M134, Emissions of Free Gas from Cross-Shelf Troughs of South Georgia: Distribution, Quantification, and Sources for Methane Ebullition Sites in Sub-Antarctic Waters, Port Stanley (Falkland Islands) - Punta Arenas (Chile), 16 January - 18 February 2017. Ber. MARUM – Zent. für Mar. Umweltwiss., Fachbereich Geowiss., Univ. Bremen, 317. 1–220. https://doi.org/urn:nbn:de:gbv:46-00106081-12

Bohrmann G (2013) The expedition of the research vessel “Polarstern” to the Antarctic in 2013 (ANT-XXIX/4). Berichte zur Polar- und Meeresforschung „Expedition reports“, 668. Alfred Wegener Inst. for Polar and Marine Res., Bremerhaven. https://doi.org/10.2312/BzPM_0668_2013

Graham AGC, Kuhn G, Meisel O, Hillenbrand CD, Hodgson DA, Ehrmann W, Wacker L, Wintersteller P, dos Santos Ferreira C, Römer M, White D, Bohrmann G (2017) Major advance of South Georgia glaciers during the Antarctic Cold Reversal following extensive sub-Antarctic glaciation. Nature Comm. 8:14798. https://doi.org/10.1038/ncomms14798

Geprägs P, Torres ME, Mau S, Kasten S, Römer M, Bohrmann G (2016) Carbon cycling fed by methane seepage at the shallow Cumberland Bay, South Georgia, sub-Antarctic, Geochem. Geophys. Geosyst. 17. https://doi.org/10.1002/2016GC006276

Ó Cofaigh C, Hogan KA, Dowdeswell JA, Streuff KT (2016) Stratified glacimarine basin-fills in West Greenland fjords. In: Dowdeswell JA, Canals M, Jakobsson M, Todd BJ, Dowdeswell EK, Hogan KA (eds) Atlas of Submarine Glacial Landforms: Modern, Quaternary and Ancient. Geol. Soc. Lond. Mem. 46:99–100. https://doi.org/10.1144/M46.83

Römer M, Torres ME, Kasten S, Kuhn G, Graham AGC, Mau S, Little CTS, Linse K, Pape T, Geprägs P, Fischer D, Wintersteller P, Marcon Y, Rethemeyer J, Bohrmann G (2014) First evidence of widespread active methane seepage in the Southern Ocean, off the sub-Antarctic island of South Georgia. Earth and Planet. Sci. Lett. 403:166-177.

Spiess V, Breitzke M (1990) Das Parasound-Sedimentecholotsystem – Funktionsweise, Anwendungsbeispiele und digitale Datenerfassung, Jahrestag. der Dtsch. Geolog. Ges., Bremen. http://hdl.handle.net/10013/epic.21196

Veloso M, Greinert J, Mienert J, De Batist M (2015) A new methodology for quantifying bubble flow rates in deep water using splitbeam echosounders: Examples from the Arctic offshore NW-Svalbard. Limnol. Oceanogr. Methods 13:267–287. https://doi.org/10.1002/lom3.10024

3. MARINE GEOLOGY

Katharina Streuff[1,2], Simon Porrmann[1,2], Lucia Cattana[3], Neele Köhler[1,2], Male Köster[4], Norbert Lensch[4], Nina-Marie Lešić[1,2], Catalina Rubiano[5], Josefine-Friederike Weiss[4]
not on board: Alastair Graham[5], Miriam Römer[1,2]

[1]DE.UNI-Bremen
[2]DE.MARUM
[3]AR.Armada
[4]DE.AWI
[5]GOV.FLORIDA

Grant-No. AWI_PS133/2_02

Objectives

Because of its unique location in the Southern Ocean, the island of South Georgia is superbly situated to study the climatic and oceanic forcing of sub-polar environments over various timescales (Rosqvist et al., 1999). Described as a 'sentinel for change' in the Southern Hemisphere (Graham et al., 2017), the island's ice cap is extremely sensitive to environmental perturbations and therefore detailed records of how it has changed over time and space can provide important insights into past climatic changes (Gordon et al., 2008). In addition, because South Georgia serves as a scaled-down analogue for a marine-terminating ice sheet, the dynamics and behaviour of the ice cap can provide valuable clues as to how the larger Antarctic Peninsula ice sheet may respond to future environmental changes as the ocean and atmosphere of the polar regions warm. Unlike many other regions of the polar Antarctic, South Georgia's fjords are shallow, typically ice-free in summer, and accessible by ship, meaning they are easily mapped at high-resolution with sonars, and sediments there are readily obtainable (Hodgson et al., 2014). The sediments within the fjords are locally thick owing to a high sediment flux from the island's glacial systems and glacial turnover is fast, meaning the time between changes in the glacier catchments and time of deposition at the sea bed is often negligible. As such, these sub-polar marine environments provide ideal natural laboratories for studying glacial sedimentation processes, the processes of landform generation, as well as detailed studies of glacial outputs including assessing temporal changes in ice and sediment flux, as well as meltwater dynamics.

The evolution of the terrestrial and near-shore portion of South Georgia's ice cap is much better constrained than its marine counterpart (Barlow et al., 2016; Bentley et al., 2007, 1989a, 1978; Clapperton et al., 1989b; Graham and Hodgson, 2016; Oppedal et al., 2018; Rosqvist et al., 1999; Rosqvist and Schuber, 2003; White et al., 2017), due to a lack of offshore data and investigations. Only recently have studies used the shelf geomorphology and the sediment records from very selected offshore locations to constrain the evolution of the South Georgia ice cap throughout past glacial intervals (Graham et al., 2008, 2017; Hodgson et al., 2014; Lešić et al., 2022). They showed that South Georgia's modern-day fjords radiate from the island and thus mark the former pathways of large outlet glaciers and ice streams. Landforms lining the troughs give first insights into glacial dynamics within the troughs, suggesting that arteries of fast-flowing ice occupied these topographic depressions in the past and operated over both bedrock and sedimentary substrates. On the outer shelf and within the troughs, large ridges and banks are also common, interpreted as terminal, lateral, and recessional moraines marking former positions of ice sheets on the shelf and their subsequent reorganization during deglaciation. As a result of this relatively "fresh" seafloor geomorphology and evidence from

other maritime-Antarctic islands (Heard Island and Kerguelen Island), it has been postulated that the ice cap was significantly larger during at least one past glacial than it is today. The subsequent retreat of the ice cap is recorded in well-preserved morainal banks, subglacial bedforms, and stepped moraine sequences that show a net overall recession of ice margins to the modern coastline along cross-shelf troughs and across shallower banks (Graham et al., 2017). Using these combined terrestrial and marine records, studies have now reconstructed the Last Glacial Maximum (LGM) ice cap to have terminated at or very near the shelf break (Barlow et al., 2016; Barnes et al., 2016; Graham et al., 2008, 2017; Lešić et al., 2022). Several re-advances of the ice cap since then are inferred from prominent sea-floor moraines that are mapped regionally in the same physiographic position from one fjord to the next (Hodgson et al., 2014). One of these moraine positions, at the mouth of topographically-constrained fjords, is believed to correlate to an ice-cap wide re-advance during the Antarctic Cold Reversal (c. 14.7–13 ka B.P; Pedro et al., 2016), demonstrating a sensitive glacial response on the island to abrupt hemispheric-scale climatic shifts during the last deglaciation. The Holocene environmental record of glacier change is relatively well-constrained for the land-based South Georgia ice cap; however, the same records are poorly resolved for the offshore environment despite high potential for such events to be archived in the fjord sediments. Similarly, evidence from the offshore marine environment and South Georgia is still very limited. As a result, the understanding of glacial change on South Georgia is still rudimentary, especially when compared to our knowledge of glacial variability from other geographic locations in the Antarctic (Bentley et al., 2014). Consequently, a lot of questions regarding the glacial evolution over time remain unanswered, for instance 1) are the morainal sequences at the heads of inner and outer shelf basins around the island co-temporaneous, and related to regional climatic episodes, or local topographically-controlled stillstands?; 2) How did presence and persistence of shelf-ice cover affect the productivity history of the South Georgia margin?; 3) which role did meltwater play in past ice flow, bed shaping, and in forcing glacier retreat?; 4) how does the acoustic stratigraphy of the shelf relate to Quaternary cycles of ice-cap waxing and waning?; 5) were sections of the submerged sea-floor within some of the island's glacial fjords subaerial during past sea-level low-stands, allowing for the formation of buried peats that now seem to serve as a source of methane venting at the sea bed (cf. Geprägs et al., 2016; Römer et al., 2014)?; and 6) when and in response to which external forcing was rapid glacier retreat observed from visual and satellite observations (Cook et al., 2010)?

One of the main objectives of the marine geology investigations during cruise PS133/2 was to answer some or all of the above questions by obtaining high-resolution coastal records from diatom-bearing marine muds near several glacier margins. Because the cruise focused on two areas, King Haakon Bay and Cumberland Bay, situated on either side of the island, there is significant opportunity from the acquired sediment cores to assess sedimentary processes and environments within two climatically variable fjords of South Georgia. Furthermore, some of the obtained records should help constrain the spatial patterns of ice-cap change and evaluate whether glacier retreat has been driven primarily by atmospheric or oceanic drivers. Sediment cores from the continental shelf have the potential to not only deduce the glacial history of the region, but also to provide insights into regional palaeoceanography.

In line with the above questions and the main objective of the *IslandImpact* proposal, 'to reconstruct depositional history related to glacial/interglacial variations in sedimentation regimes', the marine geoscientific work on the expedition concentrated on the targets outlined below.

1. Hydrosweep swath bathymetry and PARASOUND sub-bottom profiler data added new high-resolution bathymetric information on glacial morphology and shelf sequence stratigraphy (see also Chapter 2 – Hydroacoustics). These serve as a foundation to seafloor geomorphological interpretations.

2. Sediment sequences collected with a gravity corer (GC) support the hydroacoustic information and, together with surface sediments obtained via multiple corer (MUC), can be used to reconstruct the glacial history of the island since the Last Glacial Maximum.

3. Sediment coring along transects from glacier front to the inner or mid-shelf provide temporal and local environmental information (see also Chapter 4 – Sediment Geochemistry) and help resolve modern glacial processes and past environmental variability. The latter, in turn, contribute to the wider understanding of Fe delivery to the continental shelf.

Work at sea

Onboard *Polarstern* it was necessary to seamlessly integrate coring efforts with the hydroacoustic systems. Sediment profiling data as well as bathymetric data from the Hydrosweep provided the basis for selecting suitable coring sites (see Chapter 2 – Hydroacoustics). At the majority of stations gravity cores were complemented with the according surface samples obtained via the MUC. Most cores were processed onboard. Because the MUCs provide the basis for most sediment geochemical and biological work, information on how they were processed can be found int the according chapters below. Gravity cores were sampled using a gravity corer of 3, 5, 10, or 15 m length, depending on the nature of the sediments and their thickness at the coring site. All gravity cores were cut into 1m sections, which were kept in the cold storage at +4° C until further analyses. An overview over the acquired gravity cores is provided in Tab. 3.1.

After cutting the cores into sections, nondestructive measurements were conducted on the whole-round gravity core sections using a GEOTEK Multisensor Core Logger (MSCL). The Instrument measures the magnetic susceptibility and the sound velocity of the pressure wave through the sediments. Additionally, core diameter and ambient temperature were logged and used for data processing (see Tab. 3.2 for a comprehensive list of parameters and sensors). To prevent the sensors from temperature-driven drifts, the cores were stored at room temperature for at least 12 hours before logging. Once the cores adapted to the surrounding temperature, MSCL measurements were performed on all recovered sections at a resolution of 1 cm, using an automatic pusher installed as part of the device. Data provided by the MSCL were used to get first insights into the sediment properties of South Georgia fjord sediments. Magnetic susceptibility was of special interest to better understand the terrestrial influence and to compare it to the pore water iron profile. Furthermore, magnetic susceptibility data is intended to be used to compare nearby cores and correlate peaks in the logs. On stations where two gravity cores were taken, MSCL logs were also used to check the core-to-core consistency for the station. The p-wave velocity gives another parameter that can be used to determine sediment properties and to correct sound velocities for hydroacoustic data. All data obtained on the cruise were processed onboard. This includes quality control of the data, as well as correction of the data obtained at core section boundaries. The cores that were logged onboard are indicated in the right-hand column of Tab. 3.1.

With the exception of three long cores and two short cores resulting from unsuccessful deployment, after logging, all cores were split into work half and archive half for further analysis. Usually two gravity cores were taken at each site, one for geochemical and biological sampling (see Chapters 4 and 10), and one for geological analysis. The latter included lithological logging of the sediment surface (see A.5 in the appendix) by describing the sediment according to preliminary grain size, colour – using the Munsell colour chart, visible internal structure such as layering or stratification and the presence or absence of particulars such as shells, minerals or dropstones. In cores from the continental shelf, shear strength measurements were performed every 10 to 20 cm using a shear torvane to get a first idea about potential glacial influence

after deposition. The cores were then sampled for further analyses at the home laboratory including TC/TOC analyses and (more detailed) measurements of grain size, water content, as well as wet and dry bulk density. Every 10 to 20 cm two samples were taken, one with cut-off 10ml syringes stored in glass vials for the measurements of carbon content, water content and density, and one containing the remaining ~1 cm-thick sediment slab at the same depth. The latter were transferred to whirlpak sampling bags and will be used for grain size analysis and fraction separation for radiocarbon dating and potential palaeoceanographic investigations. The working and archive halves of all cores were transferred into D-tubes after processing and stored in a cooling container at +4° C, where they will remain until arrival in Bremerhaven.

Tab. 3.1: List of gravity cores taken for geochemical and geological analyses. For more information see also the station list in A.4 in the appendix.

Station Number	**Station Start**			**Study Area**	**Core barrel**	**Recovery**	**MSCL**
	Latitude	**Longitude**	**Depth [m]**				
PS133/2_12-3	54° 01,616’ S	037° 02,975’ W	257	Outer Posession Bay	10 m	758 cm	Yes
PS133/2_15-6	54° 05,059’ S	037° 05,981’ W	357.8	Inner Posession Bay	10 m	715 cm	Yes
PS133/2_15-7	54° 05,067’ S	037° 06,044’ W	357.5	Inner Posession Bay	10 m	602 cm	Yes
PS133/2_17-13	54° 24,033’ S	037° 34,053’ W	348.2	King Haakon Trough	10 m	895 cm	Yes
PS133/2_17-14	54° 24,109’ S	037° 33,996’ W	342.9	King Haakon Trough	10 m	904 cm	Yes
PS133/2_23-11	54° 09,569’ S	037° 23,206’ W	154.1	Innermost King Haakon Bay	15 m	1088 cm	Yes
PS133/2_23-13	54° 09,527’ S	037° 23,094’ W	154	Innermost King Haakon Bay	15 m	~1000 cm	Yes
PS133/2_26-1	54° 24,810’ S	037° 36,970’ W	357.8	King Haakon Trough	10 m	985 cm	Yes
PS133/2_32-16	54° 15,872’ S	036° 26,261’ W	263.8	Cumberland Bay, Grytviken Flare	10 m	930 cm	Yes
PS133/2_35-9	54° 20,749’ S	036° 22,748’ W	159	Innermost Cumberland Bay	10 m	Six sections	Yes
PS133/2_35-10	54° 20,746’ S	036° 22,737’ W	158.9	Innermost Cumberland Bay	10 m	431 cm	Yes
PS133/2_37-4	54° 17,581’ S	036° 27,616’ W	140.4	Moraine Fjord, Grytviken	10 m	Banana, ~140 cm	No
PS133/2_37-6	54° 17,541’ S	036° 27,593’ W	144.6	Moraine Fjord, Grytviken	5 m	Banana, ~50 cm	No
PS133/2_42-10	54° 12,515’ S	036° 26,522’ W	264	Confluence Zone, outer Cumberland Bay	10 m	778 cm	Yes
PS133/2_42-11	54° 12,507’ S	036° 26,545’ W	264.8	Confluence Zone, outer Cumberland Bay	10 m	Eight sections	Yes

Station Number	Station Start			Study Area	Core barrel	Recovery	MSCL
	Latitude	Longitude	Depth [m]				
PS133/2_43-1	54° 03,236' S	036° 04,193' W	257	Inner shelf off Cumberland Bay	5 m	369 cm	Yes
PS133/2_46-1	53° 54,423' S	036° 17,010' W	229.1	Outer continental shelf off Cumberland Bay	5 m	232 cm	Yes
PS133/2_47-1	53° 49,191' S	036° 18,971' W	221.8	Outer continental shelf off Cumberland Bay	3 m	Only core catcher	No

Tab. 3.2: List of measured parameters by the MSCL.

Parameter	Device	Frequency	Pulse	Comments
Magnetic susceptibility	Coil sensor: BARTINGTON MS-3	Alternating field frequency: 565 kHz	Count time: 5 s	Precision: $0.1*10^{-5}$ Magnetic field strength: c. 80 A/m
P-Wave velocity and core diameter	Plate-transducers, diameter 4 cm	Transmitter pulse frequency: 500 kHz	Pulse repetition rate: 1 kHz	Recorded pulse resolution: 50 ns
Core thickness	Penny + giles, type HLP190 calibrated with distance piece			
Temperature	Bimetal sensor, calibrated with Hg-thermometer			

Preliminary results

Fig. 3.1 shows three of the magnetic susceptibility logs measured onboard. For station PS133/2_42, which is located in the Cumberland Bay fjord, two deployments of the GC resulted in the recovery of parallel cores 42-10 and 42-11. When comparing the magnetic susceptibility logs, they show a close correlation in general, but are offset by up to 50 cm. This is most likely due to position drifts between deployments that lead to small differences in the core location (see also Table 3.1) and was observed in most double coring stations. The third log in figure 3.1 shows the magnetic susceptibility of core 43-1 that was recovered on the mid-shelf outside of Cumberland Bay. The core shows a generally lower magnetic signature than the two from the inner fjord, although core-to-core correlation could be successfully done between major peaks in the upper 500 cm of 42-10/11 and the upper 250 cm of 43-1 (Fig. 3.1). The similarity in peaks confirms that magnetic sediment signals from the fjord also prevail on the shelf, likely due to similar sediment provenance. Therefore, the correlated peaks might be used as a proxy for terrestrial input through the Cumberland Bay fjord. In contrast, the discrepancy between sediment thickness shows that the sedimentation rate is much lower on the shelf than in the fjord, as would be expected due to the former's more distal location.

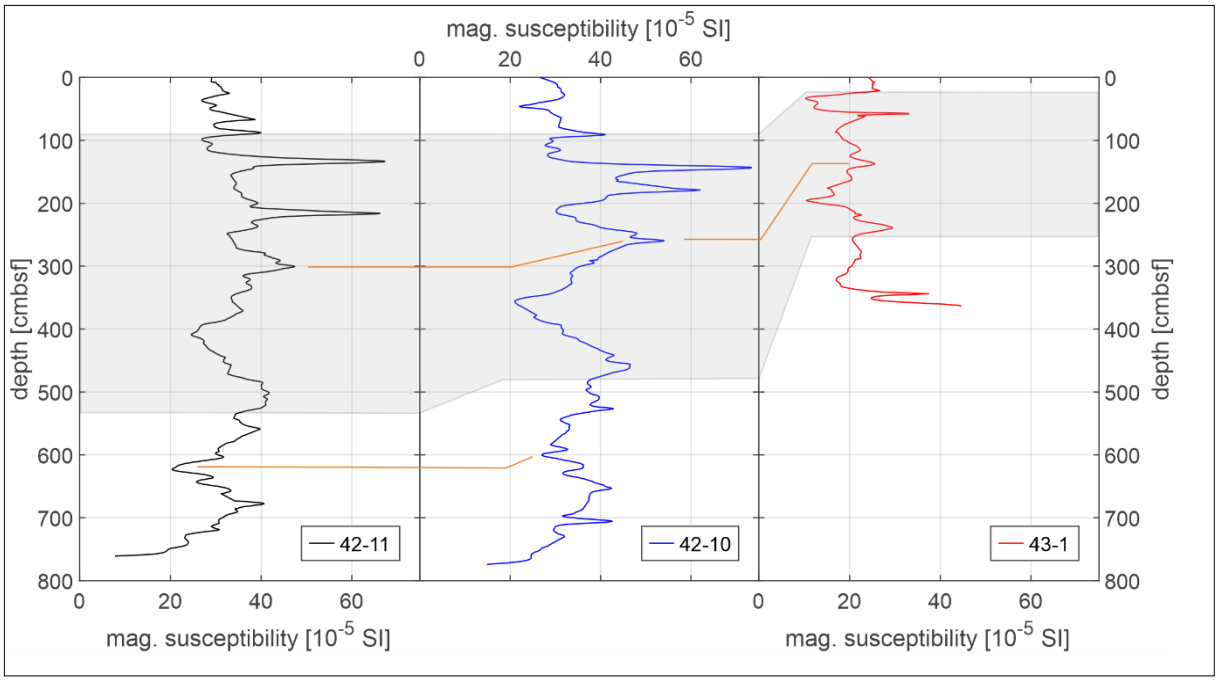

Fig. 3.1: The graphs show magnetic susceptibility logs of sediment cores 42-11, 42-10 and 43-1. Station 42 is located in the Cumberland Bay fjord while station 43 is located on the shelf off Cumberland Bay.

As already shown by the PARASOUND profiling (Chapter 2), sediment cover was thickest closest to the glaciers in the innermost fjords and thinned with increasing distance from the source. Furthermore, basin fills were usually stratified and horizontally layered, as expected from glacimarine settings. Gravity cores taken from the inner fjord basins on the northern side of the island usually recovered the full length of the core barrel and mostly contained soft, very organic-rich mud, whereas a core (47-1) from the outer shelf off Cumberland Bay recovered only the core catcher containing stiff diamicton (see also A.5 in the appendix). First tentative interpretations suggest that fjord sedimentation in northern South Georgia is mostly governed by glacial runoff and leads to the accumulation of fine-grained, water-rich muds deposited at exceedingly high sedimentation rates. Occasional sand patches and rare dropstones suggest that input from iceberg melt and meltwater streams is present but almost completely outrun by the extremely high input from suspension settling. Conversely, on the northern shelf of South Georgia hemipelagic sedimentation prevails. Organic matter appears to be less concentrated and the sediment cover is much thinner suggesting a drastic decrease in sedimentation rate from the fjord to the outer shelf. This effect is very nicely pronounced in cores 43-1 and 46-1, taken from the mid- and the outer shelf off Cumberland Bay, respectively. The more proximal core, 43-1, is longer than the more distal one, suggesting that less material reaches the core location on the outer shelf. Both cores recovered a stiff diamicton at their base, which the corer could not penetrate further. The stiffness as well as the observed very high concentration of large, angular dropstones, some gravel and sand all contained in a muddy matrix suggests that this diamicton could be a remnant from one of the past glacials, likely the Last Glacial Maximum. As both cores were taken from areas close to bathymetric ridges, we assume that the diamicton likely represents the material from glacial moraines marking past positions of ice extent on the continental shelf off South Georgia (Graham et al., 2008, 2017). In King Haakon Bay, the gravity core taken from the inner fjord was not split because the core halves will be shared between microbiology and geology and need to be shipped to Bremen before analyses can take place. Sediments taken from the outer King Haakon Trough also attest to the very thick

sediment cover concentrated in the trough basin and showed fine-grained, partially laminated mud with a high content of organic material in the form of gastropods and bivalve fragments. A mottled appearance and a strong smell of H_2S further supported an interpretation as organic-rich sediment and indicates anoxic conditions in the sediments. Some core sections revealed small ikaite crystals most likely attesting to the (former) presence of gas hydrates.

The results from the sediment cores will be integrated with the hydroacoustic data after the cruise in order to provide more holistic interpretations of depositional environments on and around the South Georgia block.

Data management

Marine geological data will be archived, published and disseminated according to international standards by the World Data Center PANGAEA Data Publisher for Earth & Environmental Science (https://www.pangaea.de) within two years of the end of the cruise. By default, the CC-BY license will be applied.

Any other data will be submitted to an appropriate long-term archive that provides unique and stable identifiers for the datasets and allows open online access to the data.

This expedition is supported by the Helmholtz Research Programme “Changing Earth – Sustaining our Future” Topic 2, Subtopics 1 and 4, Topic 4, Subtopic 1 and Topic 6, Subtopics 2 and 3.

In all publications based on this expedition, the **Grant No. AWI_PS133/2_02** will be quoted and the following publication will be cited:

Alfred-Wegener-Institut Helmholtz-Zentrum für Polar- und Meeresforschung (2017) Polar Research and Supply Vessel POLARSTERN Operated by the Alfred-Wegener-Institute. Journal of large-scale research facilities, 3, A119. http://dx.doi.org/10.17815/jlsrf-3-163.

References

Barlow NLM, Bentley MJ, Spada G, Evans DJA, Hansom JD, Brader MD, White DA, Zander A, Berg S (2016) Testing models of ice cap extent, South Georgia, sub-Antarctic. Quat Sci Rev 154:157–168. https://doi.org/10.1016/j.quascirev.2016.11.007

Barnes DKA, Sands CJ, Hogg OT, Robinson BJO, Downey RV, Smith JA (2016) Biodiversity signature of the Last Glacial Maximum at South Georgia, Southern Ocean. J Biogeog 43(12):2391–2399. https://doi.org/10.1111/jbi.12855

Bentley MJ, Evans DJA, Fogwill C, Hansom J, Sugden D, Kubik P (2007) Glacial geomorphology and chronology of deglaciation, South Georgia, sub-Antarctic. Quat Sci Rev 26(5-6):644–677. https://doi.org/10.1016/j.quascirev.2006.11.019

Bentley MJ, Ó Cofaigh C, Anderson JB, Conway H, Davies B, Graham AGC, Hillenbrand C-D, Hodgson DA, Jamieson SSR, Larter RD, Mackintosh A, Smith JA, Verleyen E, Ackert RP, Bart PJ, Berg S, Brunstein D, Canals M, Colhoun EA, Crosta X, Dickens WA, Domack EW, Dowdeswell JA, Dunbar R, Ehrmann W, Evans J, Favier V, Fink D, Fogwill CJ, Glasser NF, Gohl K, Golledge NR, Goodwin I, Gore DB, Greenwood SL, Hall BL, Hall K, Hedding DW, Hein AS, Hocking EP, Jakobsson M, Johnson JS, Jomelli V, Jones RS, Klages JP, Kristoffersen Y, Kuhn G, Leventer A, Licht KJ, Lilly K, Lindow J, Livingstone SJ, Massé G, McGlone MS, McKay RM, Melles M, Miura H, Mulvaney R, Nel W, Nitsche FO, O’Brien PE, Post AL, Roberts SJ, Saunders KM, Selkirk PM, Simms AR, Spiegel C, Stolldorf TD, Sugden DE, van der Putten N, van Ommen T, Verfaillie D, Vyverman W, Wagner B, White DA, Witus AE, Zwartz D (2014) A community-based geological reconstruction of Antarctic Ice Sheet deglaciation since the Last Glacial Maximum. Quat Sci Rev 100:1–9. https://doi.org/10.1016/j.quascirev.2014.06.025

Clapperton CM, Sugden DE, Birnie J, Wilson MJ (1989a) Late-glacial and Holocene glacier fluctuations and environmental change on South Georgia, Southern Ocean. Quat Res 31(2):210–228. https://doi.org/10.1016/0033-5894(89)90006-9

Clapperton CM, Sugden DE, Birnie RV, Hanson JD, Thom G (1978) Glacier fluctuations in South Georgia and comparison with other island groups in the Scotia Sea. In: Bakker EMVZ (ed) Antarctic glacial history and world palaeoenvironments. Balkema, Rotterdam, p 98-104

Clapperton CM, Sugden DE, Pelto M (1989b) Relationship of Land Terminating and Fjord Glaciers to Holocene Climatic Change, South Georgia, Antarctica. In: Oerlemans J (ed) Glacier Fluctuations and Climatic Change. Glaciology and Quaternary Geology, vol 6. Springer Netherlands, Dordrecht, p 57-75

Cook AJ, Poncet S, Cooper APR, Herbert DJ, Christie D (2010) Glacier retreat on South Georgia and implications for the spread of rats. Antarct Sci 22(3):255–263. https://doi.org/10.1017/S0954102010000064

Geprägs P, Torres ME, Mau S, Kasten S, Römer M, Bohrmann G (2016) Carbon cycling fed by methane seepage at the shallow Cumberland Bay, South Georgia, sub-Antarctic. Geochem, Geophys, Geosys 17(4):1401-1418. https://doi.org/ 10.1002/2016gc006276

Gordon JE, Haynes VM, Hubbard A (2008) Recent glacier changes and climate trends on South Georgia. Glo Pla Cha 60(1-2):72–84. https://doi.org/10.1016/j.gloplacha. 2006.07.037

Graham AGC, Fretwell PT, Larter RD, Hodgson DA, Wilson CK, Tate AJ, Morris P (2008) A new bathymetric compilation highlighting extensive paleo-ice sheet drainage on the continental shelf, South Georgia, sub-Antarctica. Geochem, Geophys, Geosys 9(7). https://doi.org/10.1029/2008gc001993

Graham AGC, Hodgson DA (2016) Terminal moraines in the fjord basins of sub-Antarctic South Georgia. Geol Soc, Lon, Mem 46(1):67-68. https://doi.org/ 10.1144/M46.165

Graham AGC, Kuhn G, Meisel O, Hillenbrand C-D, Hodgson DA, Ehrmann W, Wacker L, Wintersteller P, Dos Santos Ferreira C, Römer M, White DA, Bohrmann G (2017) Major advance of South Georgia glaciers during the Antarctic Cold Reversal following extensive sub-Antarctic glaciation. Nat comm 8:14798. https://doi.org/ 10.1038/ncomms14798

Hodgson DA, Graham AGC, Griffiths HJ, Roberts SJ, Ó Cofaigh C, Bentley MJ, Evans DJA (2014) Glacial history of sub-Antarctic South Georgia based on the submarine geomorphology of its fjords. Quat Sci Rev 89:129–147. https://doi.org/10.1016/ j.quascirev.2013.12.005

Lešić N-M, Streuff KT, Bohrmann G, Kuhn G (2022) Glacimarine sediments from outer Drygalski Trough, sub-Antarctic South Georgia – evidence for extensive glaciation during the Last Glacial Maximum. Quat Sci Rev 292. https://doi.org/10.1016/ j.quascirev.2022.107657

Oppedal LT, Bakke J, Paasche Ø, Werner JP, van der Bilt WGM (2018) Cirque Glacier on South Georgia Shows Centennial Variability over the Last 7000 Years. Frontiers Earth Sci 6(2). https://doi.org/10.3389/feart.2018.00002

Pedro JB, Bostock HC, Bitz CM, He F, Vandergoes MJ, Steig EJ, Chase BM, Krause CE, Rasmussen SO, Markle BR, Cortese G (2016) The spatial extent and dynamics of the Antarctic Cold Reversal. Nat Geosci 9(1):51–55. https://doi.org/10.1038/ ngeo2580

Römer M, Torres M, Kasten S, Kuhn G, Graham AGC, Mau S, Little CTS, Linse K, Pape T, Geprägs P, Fischer D, Wintersteller P, Marcon Y, Rethemeyer J, Bohrmann G (2014) First evidence of widespread active methane seepage in the Southern Ocean, off the sub-Antarctic island of South Georgia. Earth Pla Sci Letters 403:166–177. https://doi.org/10.1016/j.epsl.2014.06.036

Rosqvist GC, Rietti-Shati M, Shemesh A (1999) Late glacial to middle Holocene climatic record of lacustrine biogenic silica oxygen isotopes from a Southern Ocean island. Geology 27(11):967. https://doi.org/10.1130/0091-7613(1999)027<0967: LGTMHC>2.3.CO;2

Rosqvist GC, Schuber P (2003) Millennial-scale climate changes on South Georgia, Southern Ocean. Quat Res 59(3):470–475. https://doi.org/10.1016/S0033-5894(03)00036-X

White D, Bennike O, Melles M, Berg S, Binnie S (2017) Was South Georgia covered by an ice cap during the Last Glacial Maximum? Geol Soc, Lon, Spec Pub. SP461.4. https://doi.org/10.1144/sp461.4

4. SEDIMENT GEOCHEMISTRY

Male Köster[1], Ingrid Dohrmann[1], Tanja Glawatty[1], Sabine Kasten[1,2,3], Maja Victoria Leusch[3], Daniel Müller[1], Christina Nadolsky[1]

[1]DE.AWI
[2]DE.MARUM
[3]DE.UNI-Bremen

Grant-No. AWI_PS133/2_03

Objectives

Our main objective is to determine and quantify the different sources and transport pathways of iron (Fe), other nutrients (PO_4^{3-}, NO_3^-, H_4SiO_4) and trace metals into the fjords and coastal area off South Georgia. Possible sources and transport pathways of dissolved Fe, nutrients and trace metals include a) weathering and erosion of Fe-rich rocks, b) glacial melt, c) submarine groundwater discharge, d) post-depositional reduction and diffusion of Fe across the sediment/water interface, e) dust input and f) mixing of Fe-rich pore water into the water column by means of methane bubble ebullition and bioturbation/bioirrigation.

Sediment investigations performed in Cumberland Bay Fjord and other fjords of South Georgia have revealed high levels of dissolved Fe and PO_4^{3-} concentrations in surficial and sub-surface pore-waters of sediments high in methane and affected by active bubble ebullition. Hydrocarbon seepage – both in the form of fluid migration and ebullition of free gas – can exert a strong control on the transport mode and fluxes of elements across the sediment/water interface (e.g., Wallmann et al., 1997; Torres et al., 2003). The ebullition of free gas can produce a mixing of solutes and sediments – similar to bioturbation (e.g., Haeckel et al., 2007), which might represent an important pathway for transferring interstitial constituents into the overlying bottom water. The effect of hydrocarbon seepage on enhancing solute mixing and element fluxes from the seabed into the water column was shown for Ba, Ca, CO_2, DIC and silica (e.g., Wallmann et al., 1997; Torres et al., 2003). However, nothing is known about how and to which extent fluid seepage or mixing induced by the escape of gas bubbles affect the transport, speciation and fate of macro and micro nutrients and other interstitial constituents (Fe, NO_3^-, PO_4^{3-}, trace metals) from the pore water into the overlying water. We postulate that abundant bubble ebullition as found in the fjords and troughs of South Georgia and other fjords and troughs of the archipelago might represent an important - yet unconsidered – transport mechanism for Fe and other interstitial constituents across the sediment/water interface, which might be more important than molecular diffusion.

Furthermore, indications of sub-aerial seepage of Fe^{2+}-rich groundwater and subsequent oxidation of Fe^{2+} in contact with atmospheric oxygen in beach areas of the inner Cumberland Bay Fjord were found during expeditions ANT-XXIX/4 and M134 (Bohrmann, 2013; Bohrmann et al., 2017). Submarine groundwater discharge is typically found along many coastal zones worldwide (e.g., Schlüter et al., 2004). It is likely that weathering of the Fe-rich rocks found on South Georgia (Curtis, 2011) and both the sub-aerial and submarine discharge of Fe^{2+}-rich groundwater may represent an important – yet so far mostly unexplored – source and transport pathway of reactive Fe (colloidal, freshly precipitated Fe oxyhydroxide of low crystallinity, or possibly complexed with humic acids) into the coastal zone of South Georgia and most likely

other (sub-)Antarctic settings. Therefore, gas bubble-induced solute mixing and transport of interstitial compounds into the water column, and sub-aerial and submarine discharge of Fe^{2+}-rich groundwater represent additional potential sources and transport mechanisms, which have remained relatively unexplored as yet.

There is still uncertainty about the biogeochemical pathways leading to the high levels of dissolved Fe (and PO_4^{3-}) observed in the pore-waters of the fjord sediments (e.g., Wunder et al., 2021). Thus, another objective is to identify the processes that mediate Fe reduction both in surface sediments and below the sulfate/methane transition (SMT). Possible processes include organoclastic Fe reduction or the methane-mediated Fe reduction, which has been shown in lab experiments (e.g., Beal et al., 2009) and postulated for high-accumulation marine environments (Riedinger et al., 2014; Oni et al., 2015). Identifying the microbial Fe-reducing communities within the sediment (e.g., Oni et al., 2015) will help to answer this question. Stable Fe isotopes ($\delta^{56}Fe$) have also proven to be valuable tracers to assess the potential sources as well as transport and reaction pathways of Fe – including microbial Fe reduction (e.g. Henkel et al., 2016, 2018).

Work at sea

During the cruise, pore-water and solid-phase samples were collected by means of multiple corer (MUC) and gravity corer (GC) deployments in the Cumberland Bay Fjord, the King Haakon Bay as well as in the Possession Bay. In addition, pore-water and solid-phase samples were collected in shallow waters of the Cumberland Bay Fjord using a hand-held gravity corer on-board a Zodiac.

After arrival of the cores on deck of *RV Polarstern*, the MUC cores were cut into 1 to 2 cm thick slices, which were placed into 50 ml centrifuge tubes. In the cases where headspace was observed in the centrifuge tube, the sample was flushed with N_2 to avoid oxidation. At each station in the King Haakon Bay and Cumberland Bay Fjord, two additional MUC cores were used for *ex-situ* oxygen measurements and $\delta^{56}Fe$ analyses.

The gravity cores were cut into 1 m segments and split into work and archive halves after multi-sensor core logging (see Chapter 3). Pore water was extracted using rhizons with an average pore size of 0.15 µm (Seeberg-Elverfeldt et al., 2005) either from sealed centrifuge tubes in the case of MUC samples or directly from GC working halves. For gravity cores, pore-water samples were taken in intervals of 20 cm. In order to avoid any dilution or oxidation during the pore-water sampling by rhizons, the first ml of the freshly extracted pore water was discarded. Solid-phase samples were collected with 10 ml cut-off syringes at the pore-water sampling intervals. Furthermore, 3 ml cut-off syringe samples were taken from segment cuts directly on deck (1 m vertical resolution, “immediate sampling”) as well as in the middle of each segment once the cores were split into work and archive halves (1 m vertical resolution; “later sampling”) for the analysis of dissolved methane (CH_4) concentrations. The “later sampling” was generally 1 to 2 days after core retrieval since the GCs needed to equilibrate to room temperature prior to multi-sensor core logging as whole-round cores. The 3 ml of bulk sediment were transferred to 20 ml glass vials prefilled with 5 ml NaOH, thereby creating a headspace volume of 12 ml (see Chapter 7 for description of measurement).

In addition to the MUC and GC deployments, pore-water and solid-phase samples from three cores – retrieved with the hand-held gravity corer on-board a Zodiac in the Cumberland Bay East (SB1-3) – were collected. The core SB1 was retrieved close to the Nordenskjöld Glacier while SB2 and SB3 were taken close to Grytviken (Tab. 4.1).

Tab. 4.1: Sediment cores collected during Zodiac sampling close to the Nordenskjöld Glacier and off Grytviken.

Area	PS133/2-	Date	Sample ID	Water depth [m]	Coordinates	
Close to Nordenskjöld Glacier	36-1	03.12.2022	SB1	12	S 54° 22.026’	W 36° 23.686’
Off Grytviken	37-5	04.12.2022	SB2	13	54°16’55’’S	36°30’18’’W
Off Grytviken	37-5	04.12.2022	SB3	21	54°16’59’’S	36°30’4’’W

On-board pore-water analyses include the determination of alkalinity, dissolved Fe (Fe^{2+}), nitrate (NO_3^-), nitrite (NO_2^-), ammonium (NH_4^+), phosphate (PO_4^{3-}) and silica (SiO_2) as well as oxygen concentrations. ***Alkalinity*** was determined on a 1 ml aliquot of sample by titration with 100 or 50 mM HCl. The pH measurements were performed using a Mettler Toledo micro-electrode. The samples were titrated with a digital burette to a pH of approximately 3.9 (pH 3.4 – 4.1) and both titration volume and final pH were recorded. The alkalinity was calculated using a modified equation from Grasshoff et al. (1999). For each measurement, the certified seawater standard IAPSO (certified alkalinity of 2.325 mmol/l) was titrated three times. The deviation of the mean value from the certified value was included in the calculation of the alkalinity.

Dissolved Fe (Fe^{2+}) was detected photometrically (DR Lange HACH 3900 photometer) at a wavelength of 565 nm. An aliquot of 1 ml of the extracted pore water was pre-treated with 50 µl of ascorbic acid and then added to 50 µl Ferrospectral solution to complex dissolved Fe for colorimetric measurement. In the case of high dissolved Fe concentrations (>1 mg/l), the samples were diluted with oxygen-free artificial seawater.

A QuAAtro continuous segmented flow analyser (Seal Analytical, The Netherlands) was used for the simultaneous determination of the pore-water concentrations of nitrate (NO_3^-), nitrite (NO_2^-), ammonium (NH_4^+), phosphate (PO_4^{3-}) and silica (SiO_2). For the determination of ***nitrate and nitrite***, nitrate is reduced to nitrite at pH 8 in a copperized cadmium reduction coil. The nitrite reduced from nitrate plus any nitrite react under acidic conditions with sulphanilamide to form a diazo compound that then couples with N-1-naphthylethylenediamine dihydrochloride (NEDD) to form a reddish-purple azo dye measured photometrically at 520 nm. Nitrate and nitrite concentrations were only determined in pore-water samples from the MUC cores. ***Ammonium*** was analysed fluriometrically using the ortho-phtalaldehyde (OPA) method. ***Phosphate*** was determined using the molybdenum blue method (Grasshoff et al., 1999). Ammonium molybdate solution was added to the pore-water aliquot and spiked with ascorbic acid solution. The phosphomolybdate complex was reduced to molybdenum blue and measured photometrically at 880 nm. ***Silica*** was also measured photometrically as a silica molybdate complex at 820 nm. The Certified Reference Materials (CRM) KANSO Lot.CO-0730 and KANSO Lot.CL-1229 were measured with each set of samples to check analytical reproducibility of the analyses.

The ***oxygen concentrations in the supernatant bottom seawater*** of the MUC cores were determined using the iodometric titration after Winkler (1888). The titration was performed using a multi-step oxidation of dissolved oxygen to iodine using the iodide ion in presence of an alkaline solution of manganese(II) ions, while the amount of generated iodine was then determined by titration with a standard thiosulfate solution (Grasshoff et al., 1999).

Ex-situ oxygen measurements were performed in a cool room (+4°C) on MUC cores with supernatant bottom seawater using the fiberoptical retractable needle-type oxygen microsensor (OXR50-HS; HS:High Speed; diameter: 50 µm; Pyroscience, Germany). The temperature of the supernatant bottom seawater was measured simultaneously using a teflon-coated temperature sensor (TSUB21; diameter 2.1 mm; Pyroscience, Germany). Both sensors were connected to the 4-cannel compact USB-powered fiber-optic meter FireSting-PRO (Pyroscience, Germany). The oxygen sensor was attached to a micromanipulator with a motorized z-axis (MU1; Pyroscience Germany) and the oxygen concentrations were measured every 100 µm over a total profile length of 2.5 cm. A 2-point calibration was performed with air-saturated seawater and Ar-flushed seawater prior to each measurement.

Pore-water aliquots for the determination of ***sulfate*** (SO_4^{2-}) and ***chloride*** (Cl^-) concentrations were collected for shore-based analyses. Samples containing ***hydrogen sulfide*** were fixed with 5% ZnAc. In addition, subsamples of approximately 1 ml of pore water were acidified with double sub-boiling distilled HCl for ***major and minor cation*** (e.g., Al, Ba, Ca, Mg, Mn, Fe, Si, P and S) analyses. For the measurement of ***dissolved inorganic carbon*** (DIC) concentrations, subsamples of approximately 2.2 ml were treated with 10 µl $HgCl_2$. Furthermore, pore-water aliquots of up to 10 ml were acidified with 250 µl double sub-boiling distilled HCl for shore-based δ^{56}***Fe analyses***. All pore-water aliquots were stored at +4°C. Samples for ^{210}***Pb analyses*** were collected from MUC cores at 1 cm intervals and stored at +4°C for the determination of sedimentation rates. The ***solid-phase samples*** were transferred into gas-tight aluminium bags, flushed with N_2 and subsequently vacuum-sealed. The vacuum-sealed bags were stored frozen (–20° C) under anoxic conditions for shore-based inorganic geochemical, mineralogical and sedimentological analyses.

Preliminary results

During this cruise, pore-water and solid-phase samples were collected from 10 MUC and 12 GC deployments as well as from 3 hand-held gravity cores as detailed in Table 4.2. Results of geochemical pore-water analyses are described below for sediments from three selected cores retrieved on a transect from the inner towards the outer Cumberland Bay. Site PS133/2-35 is located in the inner Cumberland Bay East in the vicinity of the Nordenskjöld Glacier (Fig. 4.1).

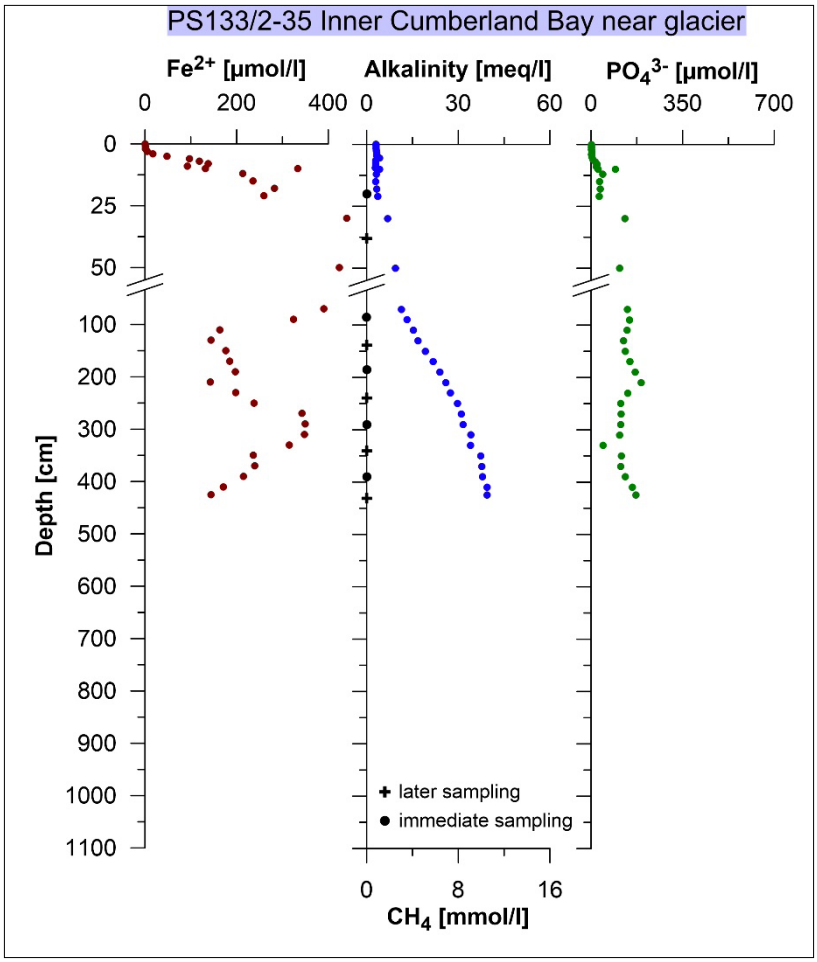

Fig. 4.1: Dissolved iron (Fe^{2+}) concentrations (red filled circles), alkalinity (blue filled circles), dissolved methane concentrations (black filled circles: immediate sampling; black filled crosses: later sampling) and phosphate (PO_4^{3-}) concentrations in MUC and GC samples from site PS133/2-35 in the inner Cumberland Bay in the vicinity of the Nordenskjöld Glacier.

Dissolved Fe could be measured over the entire core length at site PS133/2-35 and reaches maximum concentrations of 440 µmol/l at 30 cm. Alkalinity increases with depth up to 40 meq/l in the deepest sample. An increase in alkalinity is generally associated with continued degradation of organic matter in the sediments. Dissolved methane (CH_4) was not detected. Phosphate (PO_4^{3-}) concentrations slightly increase from approximately 2 µmol/l close to the sediment/water interface up to 40 µmol/l in the upper 10 cm. Below 50 cm, the phosphate concentrations fluctuate around 130 µmol/l.

Site PS133/2-32 is located at the so-called Grytviken Flare in the northern part of the Cumberland Bay East, where active gas emission had been observed during *Meteor* cruise M134 in 2017 (Bohrmann et al., 2017) and *RV Polarstern* cruise ANT/XXIX-4 in 2013 (Bohrmann, 2013; Fig. 4.2).

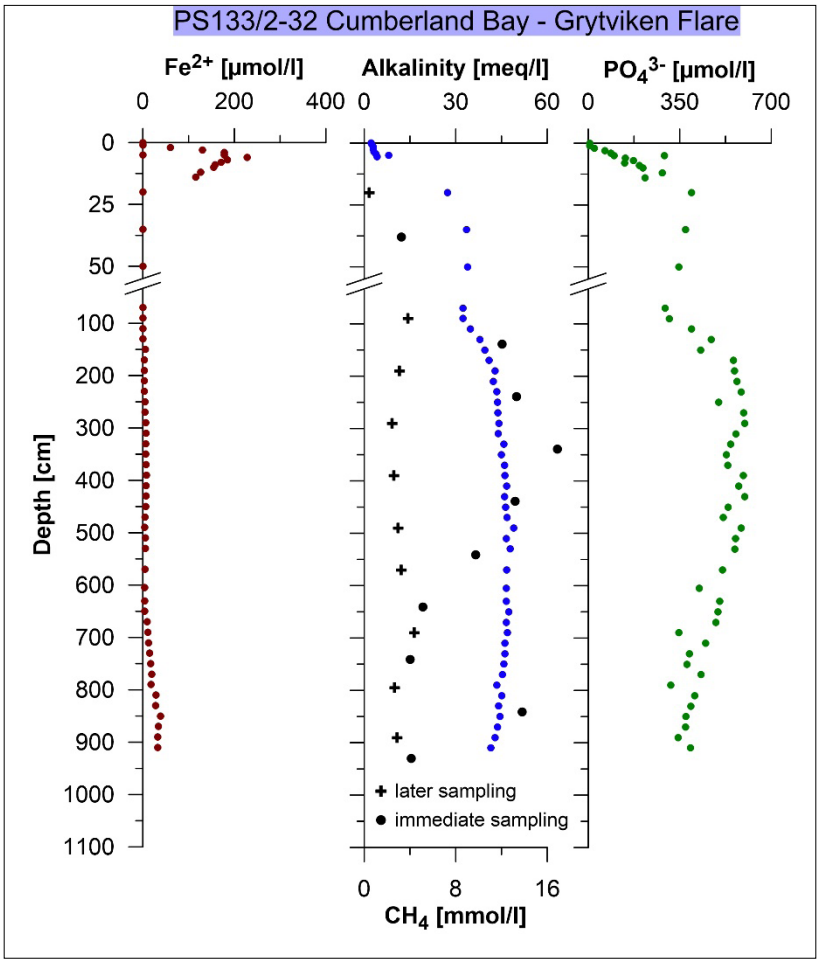

Fig. 4.2: Dissolved iron (Fe^{2+}) concentrations (red filled circles), alkalinity (blue filled circles), dissolved methane concentrations (black filled circles: immediate sampling; black filled crosses: later sampling) and phosphate (PO_4^{3-}) concentrations in MUC and GC samples from site PS133/2-32 located at Grytviken Flare in the northern part of the Cumberland Bay East.

At this site, the pore-water profile of dissolved Fe shows a maximum of 230 µmol/l at approximately 6 cm, suggesting microbially mediated Fe oxide reduction in this zone. Dissolved Fe concentrations are relatively low (<10 µmol/l) between 25 and 650 cm and slighty increase up to 38 µmol/l further below. The sediment interval between 25 and 650 cm is additionally characterized by hydrogen sulfide odor. Alkalinity generally increases with depth up to approximately 50 meq/l at 530 cm, followed by a slight decrease towards the core end. Methane is elevated below 30 cm and reaches maximum concentrations of almost 17 mmol/l at around 340 cm. Samples, that were taken when the GC was split into work and archive halves (later sampling) have considerably lower methane concentrations compared to the samples that were already taken on deck (immediate sampling). This offset in methane concentrations is likely caused by methane outgasing due to pressure changes after core retrieval. Phosphate reaches maximum concentrations of ~400 µmol/l at 20 cm in the surface sediments. In the deeper sediments, the phosphate concentrations increase up to 600 µmol/l at approximately 300 cm and decreases down to ~350 µmol/l further below. Furthermore, an ikaite ($CaCO_3$ * $6H_2O$) mineral was found at 612 cm.

Site PS133/2-42 is located in the so-called Confluence Zone between Cumberland Bay East and West (Fig. 4.3).

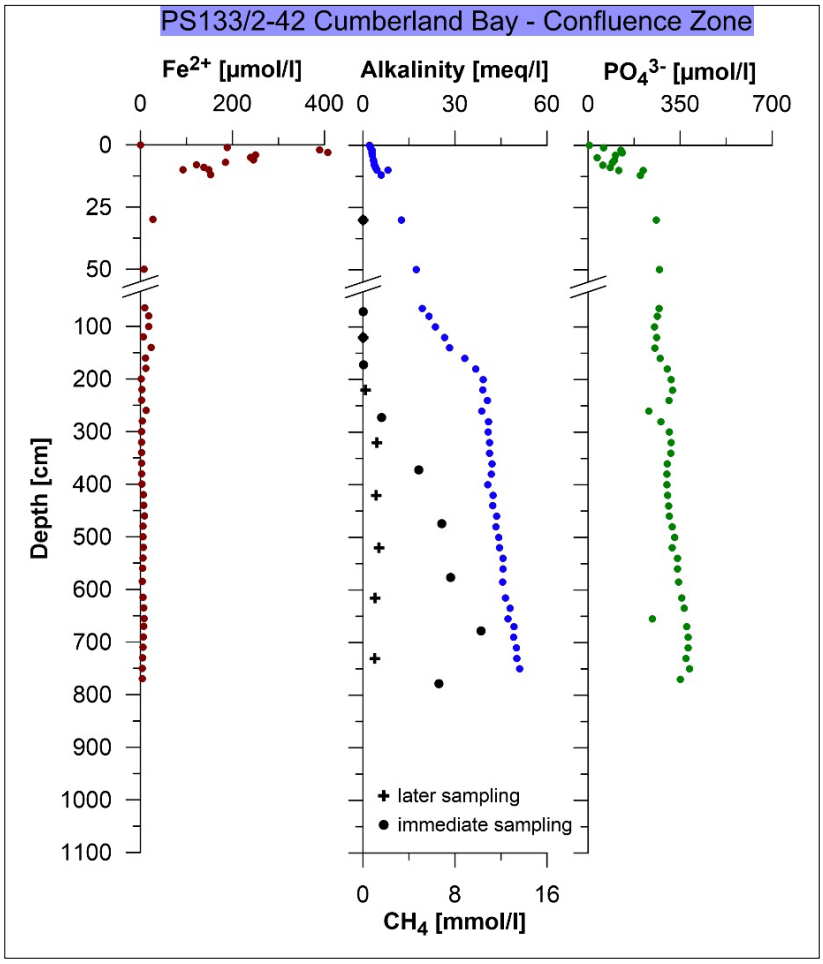

Fig. 4.3: Dissolved iron (Fe^{2+}) concentrations (red filled circles), alkalinity (blue filled circles), dissolved methane concentrations (black filled circles: immediate sampling; black filled crosses: later sampling) and phosphate (PO_4^{3-}) concentrations in MUC and GC samples from site PS133/2-42 located at the Confluence Zone between Cumberland Bay East and West.

Dissolved Fe at the Confluence Site has maximum concentrations of up to 410 µmol/l at 3 cm and is, thus, within the range of dissolved Fe concentrations at site PS133/2-35 in the inner Cumberland Bay. While sulfide odor was detected below 65 cm, dissolved Fe concentrations are relatively low (<20 µmol/l) compared to the concentrations in the surface sediments. Alkalinity generally increases with depth up to 50 meq/l. The profile gradient, however, becomes more linear at approximately 200 cm. At the same time, methane concentrations increase below 200 cm up to 10 mmol/l at 680 cm. The alkalinity kink, concurrent with the increase in methane concentrations, suggests the location of the sulfate-methane transition (SMT) at approximately 180 to 220 cm. At this depth, a consortium of anaerobic methane-oxidizing archaea and sulfate-reducing bacteria concurrently reduce downward diffusing sulfate and oxidize methane produced deeper in the sediment (e.g., Hinrichs et al., 1999; Boetius et al., 2000). Phosphate increases with depth and reaches maximum concentrations of ~380 µmol/l. In general, the phosphate concentrations at the Confluence Site are higher compared to the Glacier Site, but lower compared to the Grytviken Flare Site. An ikaite was found in the core catcher of the gravity corer.

To conclude, while site PS133/2-35 in the inner Cumberland Bay close to the Nordenskjöld Glacier displays high dissolved Fe concentrations over the entire core length, the sites at Grytviken Flare and in the Confluence Zone display a build-up of dissolved Fe only in the surface sediments. The deeper sediments at these sites, in contrast, are characterized by sulfidic conditions. These observations suggest that Fe oxide reduction dominates over sulfate reduction in the inner Cumberland Bay close to the glacier, while sulfate reduction (either organoclastic or AOM-driven sulfate reduction) is more dominant in the outer Cumberland Bay East.

Tab. 4.2: Investigated sites where geochemical samples were taken during this cruise with parameters analysed on board and aliquots of samples stored and conserved.

PS133/2-	**Fe^{2+}**	**$\delta^{56}Fe$**	**HS^-** (600 µl Zn acet.)	**ICP-OES** (25 µl HCl dd)	**SO_4^{2-}, Cl^-**	**NO_3^-/NO_2^-**	**NH_4^+**	**SiO_2**	**PO_4^{3-}**	**Alkalinity**	**DIC**	**O_2**	**CH_4**	**Sediment** (anoxic)	**^{210}Pb**
9-2 MUC	X	-	X	X	X	X	X	X	X	X	X	-	X	X	-
9-3 GC	-	-	X	X	X	-	X	X	X	X	X	-	X	X	-
12-1 MUC	X	-	-	X	X	X	X	X	X	X	X	-	X	X	-
12-3 GC	X	X	X	X	X	-	X	X	X	X	X	-	X	X	-
15-3 MUC	X	-	-	X	X	X	X	X	X	X	X	X	X	X	X
15-6 GC	X	X	X	X	X	-	X	X	X	X	X	-	X	X	-
15-7 GC	-	-	-	-	-	-	-	-	-	-	-	-	X	-	-
17-11 MUC	X	X	X	X	X	X	X	X	X	X	X	X	X	X	X
17-14 GC	-	-	X	X	X	-	X	X	X	X	X	-	X	X	-
23-9 MUC	X	X	X	X	X	X	X	X	X	X	X	X	X	X	X
23-11 GC	X	X	-	X	X	-	X	X	X	X	X	-	X	X	-
23-13 GC	-	-	-	-	-	-	-	-	-	-	-	-	X	-	-
29-1 GC	-	-	-	-	-	-	-	-	-	-	-	-	X	-	-
29-2 GC	-	-	X	X	X	-	X	X	X	X	X	-	X	-	-
32-16 GC	X	X	X	X	X	-	X	X	X	X	X	-	X	X	-
32-18 MUC	X	X	-	X	X	X	X	X	X	X	X	X	X	X	X
35-6 MUC	X	X	-	X	X	X	X	X	X	X	X	X	X	X	X
35-10 GC	X	X	-	X	X	-	X	X	X	X	X	-	X	X	X

PS133/2-	**Fe^{2+}**	**$\delta^{56}Fe$**	**HS^-** (600 µl Zn acet.)	**ICP-OES** (25 µl HCl dd)	**SO_4^{2-}, Cl^-**	**NO_3^-/NO_2^-**	**NH_4^+**	**SiO_2**	**PO_4^{3-}**	**Alkalinity**	**DIC**	**O_2**	**CH_4**	**Sediment** (anoxic)	**^{210}Pb**
SB1	-	X	-	X	X	X	X	X	X	X	X	-	-	X	-
SB2	-	X	-	X	X	X	X	X	X	-	X	-	-	X	-
SB3	-	X	-	X	X	X	X	X	X	-	-	-	-	X	-
42-8 MUC	X	X	-	X	X	X	X	X	X	X	X	X	X	X	X
42-10 GC	X	X	X	X	X	-	X	X	X	X	X	-	X	X	-
50-6 MUC	X	X	X	X	X	X	X	X	X	X	X	X	-	X	X
50-7 MUC	X	-	X	X	X	-	-	-	-	-	-	-	X	X	-

Data management

Environmental data will be archived, published and disseminated according to international standards by the World Data Center PANGAEA Data Publisher for Earth & Environmental Science (https://www.pangaea.de) within two years after the end of the cruise at the latest. By default, the CC-BY license will be applied.

Any other data will be submitted to an appropriate long-term archive that provides unique and stable identifiers for the datasets and allows open online access to the data.

This expedition was supported by the Helmholtz Research Programme “Changing Earth – Sustaining our Future” Topic 2, Subtopics 1 and 4, Topic 4, Subtopic 1 and Topic 6, Subtopics 2 and 3.

In all publications based on this expedition, the **Grant No. AWI_PS133/2_03** will be quoted and the following publication will be cited:

Alfred-Wegener-Institut Helmholtz-Zentrum für Polar- und Meeresforschung (2017) Polar Research and Supply Vessel POLARSTERN Operated by the Alfred-Wegener-Institute. Journal of large-scale research facilities, 3, A119. http://dx.doi.org/10.17815/jlsrf-3-163.

References

Beal EJ, House CH, Orphan VJ (2009) Manganese- and iron-dependent marine methane oxidation. Science 325:184–187. https://doi.org/10.1126/science.1169984.

Boetius A, Ravenschlag K, Schubert CJ, Rickert D, Widdel F, Gieseke A, et al. (2000) A marine microbial consortium apparently mediating anaerobic oxidation of methane. Nature 407: 623-626. https://doi.org/10.1038/35036572.

Bohrmann G (2013) The expedition of the research vessel “Polarstern” to the Antarctic in 2013 (ANT-XXIX/4). Reports on Polar and Marine Research, Bremerhaven, Alfred Wegener Institute for Polar and Marine Research, 668:169 p. https://doi.org/10.2312/BzPM_0668_2013.

Bohrmann G, et al. (2017) R/V METEOR Cruise Report M134, Emissions of Free Gas from Cross-Shelf Troughs to South Georgia: Distribution, Quantification, and Sources for Methane Ebullition Sites in Sub-Antarctic Waters. Berichte, MARUM – Zentrum für Marine Umweltwissenschaften, Fachbereich Geowissenschaften, Universität Bremen, 317:220 p.

Curtis M (2011) Geological Map of South Georgia. BAS GEOMAP 2 Series, Cambridge, British Antarctic Survey.

Grasshoff K, Kremling K, Ehrhardt, M (ds) (1999) Methods of seawater analysis, 3rd edition. Wiley-VCH, Weinheim, New York.

Haeckel M, Boudreau BP, Wallmann K (2007) Bubble-induced porewater mixing: A 3-D model for deep porewater irrigation. Geochimica et Cosmochimica Acta 71:5135–5154. https://doi.org/10.1016/j.gca.2007.08.011.

Henkel S, Kasten S, Poulton SW, Staubwasser M (2016) Determination of the stable iron isotopic composition of sequentially leached iron phase in marine sediments. Chemical Geology 421:93–102. https://doi.org/10.1016/j.chemgeo.2015.12.003.

Henkel S, Kasten S, Hartmann JF, Silva Busso A, Staubwasser M (2018) Iron cycling and stable Fe isotope fractionation in Antarctic shelf sediments, King George Island. Geochimica et Cosmochimica Acta 237:320–338. https://doi.org/10.1016/j.gca.2018.06.042.

Hinrichs K-U, Hayes J-M, Sylva SP, Brewer PG, DeLong EF (1999) Methane-consuming archaebacteria in marine sediments. Nature 398: 802-805. https://doi.org/10.1038/19751.

Oni O, Miyatake T, Kasten S, Richter-Heitmann T, Fischer D, Wagenknecht L, Kulkarni A, Blumers M, Shylin SI, Ksenofontov V, Costa BFO, Klingelhöfer G, Friedrich MW (2015) Distinct microbial populations are tightly linked to the profile of dissolved iron in the methanic sediments of the Helgoland mud area, North Sea. Frontiers in Microbiology 6:365. https://doi.org/10.3389/fmicb.2015.00365.

Riedinger N, Formolo MJ, Lyons TW, Henkel S, Voßmeyer A, Kasten S (2014) An inorganic geochemical argument for coupled anaerobic oxidation of methane and iron reduction in marine sediments. Geobiology 12:172–181. https://doi.org/10.1111/gbi.12077.

Seeberg-Elverfeldt J, Schlüter M, Feseker T, Kölling M (2005) Rhizon sampling of porewaters near the sediment-water interface of aquatic systems. Limnology and Oceanography, Methods 3:361–371. https://doi.org/10.4319/lom.2005.3.361.

Schlüter M, Sauter EJ, Andersen CE, Dahlgaard H, Dando PR (2004) Spatial distribution and budget for submarine groundwater discharge in Eckernförde Bay (Western Baltic Sea). Limnology and Oceanography 49:157–167. https://doi.org/10.4319/lo.2004.49.1.0157.

Torres ME, Bohrmann G, Dubé TE, Poole, FG (2003) Formation of modern and Paleozoic stratiform barite at cold methane seeps on continental margin. Geology 31:897–900. https://doi.org/10.1130/G19652.1.

Wallmann K, Linke P, Suess E, Bohrmann G, Sahling H, Schlüter M, Dählmann A, Lammers S, Greinert J, von Mirbach N (1997) Quantifying fluid flow, solute mixing, and biogeochemical turnover at cold vents of the eastern Aleutian subduction zone. Geochimica et Cosmochimica Acta 61:5209–5219. https://doi.org/10.1016/S0016-7037(97)00306-2.

Winkler LW (1888) Die Bestimmung des in Wasser gelösten Sauerstoffes. Berichte der Deutschen Chemischen Gesellschaft 21: 2843–2855.

Wunder LC, Aromokeye DA, Yin X, Richter-Heitmann T, Willis-Poratti G, Schnakenberg A, Otersen C, Dohrmann I, Römer M, Bohrmann G, Kasten S, Friedrich MW (2021) Iron and sulfate structure microbial communities in (sub-)Antarctic sediments. The ISME Journal 15:3587–3604. https://doi.org/10.1038/s41396-021-01014-9.

5. THE IMPACTS OF VARIOUS IRON SOURCES ON BIOAVAILABILITY OF IRON AND PLANKTON COMMUNITY COMPOSITION

Florian Koch[1], Joshua Hübner[1], Jasmin Stimpfle[1], [1]DE.AWI
Bernd Krock[1]
not on board: Scarlett Trimborn[1], Christian Völkner[1]

Grant-No. AWI_PS133/2_04

Objectives

In 30-50 % of the world's oceans plankton biomass is low even though nutrients and light are plentiful (de Baar et al., 2005). Rather than macronutrients such as nitrate or phosphate, in these high nutrient low chlorophyll (HNLC) regions it is the scarcity of certain trace metals (TM) such as iron (Fe) and/or vitamins, which govern primary production and/or plankton species composition (Martin and Fitzwater, 1988; de Baar et al., 2005; Bertrand et al., 2007; Koch et al., 2011). The Southern Ocean (SO) is the world's largest HNLC region, and responsible for roughly 40 % of all oceanic uptake of anthropogenic carbon and an area where iron limitation to phytoplankton has been reported (de Baar et al., 2005; Boyd and Ellwood, 2010; Trimborn et al., 2015). In addition, the SO is an important region contributing disproportionally to upwelling of deep water and formation of intermediate and bottom waters linking the Pacific, Indian and Atlantic Oceans and thus being of global importance in climate regulation, biodiversity and biogeochemical cycles (Buesseler, 1998; Lumpkin and Speer, 2007).

Extensive open water phytoplankton blooms occur along the flow of the southern Antarctic Circumpolar Current downstream of the island South Georgia. The sources and magnitude of iron (Fe) inputs fueling productivity in these land-remote areas are poorly known. These substantial algal blooms require significant Fe inputs, but the actual Fe supply mechanisms and their relative importance for primary production and biogeochemical processes along the flow of the southern Antarctic Circumpolar Current (S-ACC) remain largely unconstrained. Current hypotheses for the main Fe sources fuelling the large blooms along the S-ACC downstream of South Georgia are: i) Entrainment into the mixed layer of Fe-enriched deep waters originating around South Georgia through winter mixing and deep sources east of the large S-ACC bloom. ii) External sources such as atmospheric dust and icebergs and iii) lateral advection and recycling of particle associated Fe (living matter and detritus), potentially mediated by zooplankton feeding activity. Currently, we lack observational data on the relative importance of each of these different Fe supply mechanisms. The aim of our group on expedition PS133/2 was to identify and quantify Fe and other TM pools from South Georgia (38°W). We focused on three Fjords: King Haakon Bay, Possession Bay and Cumberland Bay. The second goal was to investigate the bioavailability of different Fe sources for natural SO phytoplankton communities. In addition, the presence/prevalence of harmful algal species and phytotoxins around South Georgia was investigated for the first time.

As part of the overall goal of cruise PS133/2 we aimed to:

- characterize the vertical and horizontal distribution patterns, stocks and origin of Fe and other TMs as well as Vitamin B_{12}, comparing King Haakon Bay, Cumberland Bay and Possession Bay.
- measure primary and bacterial production rates in the euphotic zone
- determine pico- and nanoplankton biomass at 20 m water depth
- assess Fe and vitamin B_{12} uptake rates, trace metal ratios, photophysiological status at 20 m water depth
- assess the distribution of several key phycotoxin producing phytoplankton species and determine their abundances around South Georgia
- determine the Fe bioavailability of different Fe sources collected from King Haakon Bay and Cumberland Bay to a natural phytoplankton community
- to compare the potential Fe/Mn/vitamin limitation of a coastal and off shelf phytoplankton community

Work at sea

In order to characterize the vertical profiles of trace metal chemistry (dissolved and particulate Fe, dissolved and particulate Fe isotopes, Fe chemical speciation, concentrations of ligands and humic-acid like substances) seawater was sampled at 9 stations on the shelf, and in King Haakon Bay and Cumberland Bay, South Georgia Island. In addition to the vertical profiles, at each station, primary- and bacterial production rates, Fe and vitamin B_{12} uptake and cycling rates, trace metal ratios, photophysiological status from 20 m water depth were measured. At 2 stations, seawater was sampled with a TM clean Teflon pump and used to conduct experiments investigating the impact of different Fe sources on phytoplankton community composition. In addition, dilution series experiments were conducted in order elucidate the role of microzooplankton grazing on carbon cycling. Finally, open-ocean and coastal water was 0.2 μm filtered, amended with 6 different Fe-sources and bioavailability experiments were conducted, using a natural coastal phytoplankton community.

More specifically:

1. At 9 stations (Table 5.1), seawater was collected with AWI's new, state of the art, trace metal clean sampling infrastructure including a Teflon CTD equipped with OTE bottles (12 L/bottle capacity) and winch. All samples were brought to, and processed in a custom build, clean room container. At these stations, ultra-clean CTD casts were used to sample for concentrations of dissolved trace metals (Fe, Mn, Zn, Co and Cu), particulate Fe, ligands, humic acid-like substances and Fe chemical speciation from 0 m – bottom at 5-8 depths. From up to 8 depths, samples for dissolved and particulate stable Fe isotopes were collected in collaboration with Michael Staubwasser (Chapter 6). Samples for colloidal Fe and B-vitamins were also taken from 20 m water depth.

Tab. 5.1: Stations sampled on expedition PS133/2. HA-like, PP and BP refer to humic acid like compounds, primary production and bacterial production, respectively, while AdEX and DilX denote trace metal manipulation experiments and dilution series grazing experiments, respectively. With the exception for PS133/2-27, all stations were sampled with the trace metal clean CTD equipped with Teflon coated GoFlo bottles.

Station	Depths sampled	Fe chemistry	HA-Like	TMQuota	PP and BP	Fe and B_{12} uptake rates	AdEX	DilX
PS133/2-1*	6	x	x	x	x	x	x	x
PS133/2-5	8	x	x	x	x	x		
PS133/2-11	5	x	x	x	x	x		
PS133/2-17	6	x	x	x	x	x		
PS133/2-23	4	x	x	x	x	x		
PS133/2-27*	1	x					x	x
PS133/2-32	5	x	x	x	x	x		
PS133/2-42	5	x	x	x	x	x		
PS133/2-45	5	x	x	x	x	x		
PS133/2-50	5	x	x	x	x	x		

**denotes stations at which the Teflon pump was used to fill bottles or tanks for the experiments. For all other stations, parameters were obtained from a depth of 20 m.*

2. At all 9 sampling stations, seawater from 20 m water depth was used to determine size fractionated (0.2-2 and > 2 µm) primary- and bacterial production rates using ^{14}C-bicarbonate and ^{3}H-leucine, respectively. Using a Fast repetition rate fluorometer, the photophysiological status of the sampled phytoplankton community at 20 m water depth was also assessed.

3. Uptake rates of Fe and B_{12} were measured at each station using ^{55}Fe and ^{57}Co-B_{12}. In addition, samples for the intracellular content of the trace metals (Fe, Mn, Zn, Co and Cu) of phytoplankton were taken. Cycling of Fe and Vitamin B_{12} were estimated by incubation whole natural seawater for 48 hours and measuring changes in Fe and Vitamin B_{12} concentrations.

4. At eleven stations, two net vertical tows from 30 m water depth to surface were conducted using a 20 µm meshsize Apstein plankton net in order to collect phytoplankton for subsequent phycotoxin analysis and molecular species identification back in the lab (Table 5.2). Additionally, for the duration of the cruise, Solid Phase Absorption Toxin Tracking (SPATT) bags were used as a sensitive *in situ* monitoring method to examine dissolved marine biotoxins due passive adsorption onto porous synthetic resin from the ship's clean underway sampling system. Furthermore, during the transect from South Georgia to Cape Town plankton was continuously sampled from the ship's underway sampling system. For smaller than 20 µm size plankton, 20 L of Niskin bottle water from the euphotic zone were sampled and filtered over 5 µm polycarbonate filters at gentle vacuum (< 200 mbar).

Tab. 5.2: Stations sampled for phycotoxins. CTD = Niskin bottle water; APN = 20 µm mesh size phytoplankton net.

Station number	Date	Time [UTC]	LAT [°S]	LAT ['S]	LON [°W]	LON ['W]	Device
1	24.11.2022	16:30	54	36.270	43	53.303	CTD/APN
5	26.11.2022	00:30	53	12.498	41	8.083	CTD/APN
7	26.11.2022	06:30	53	46.576	38	7.831	CTD
11	26.11.2022	18:00	54	2.136	37	3.420	CTD/APN
15	27.11.2022	16:00	54	5.047	37	5.977	CTD/APN
17	28.11.2022	15:00	54	24.057	37	3.410	CTD/APN
23	29.11.2022	17:00	54	5.019	37	6.098	CTD/APN
24	30.11.2022	11:00	54	12.770	37	32.322	CTD/APN
31	01.12.2022	19:30	54	7.717	36	16.522	CTD
32	02.12.2022	02:00	54	15.857	26	0.234	CTD/APN
35	03.12.2022	10:00	54	21.160	36	22.045	CTD/APN
37	03.12.2022	23:56	54	17.631	36	27.579	CTD/APN
42	05.12.2022	01:46	54	12.610	36	25.989	CTD
42	07.12.2022	00:15	54	12.529	36	26.449	CTD/APN
50	07.12.2022	19:40	54	3.912	36	8.424	CTD/APN

5. At 2 stations (*PS133/2-1* and *PS133/2-27*), seawater was pumped directly on board with the help of a Teflon membrane pump. For this, a LDPE Hose was lowered to 20 m water depth and ~1,500 L seawater was pumped directly into a trace metal clean container where 2,5 L polycarbonate bottles and tanks were filled for three different kinds of experiments:

    1. At sites *PS133/2-1* and *PS133/2-27* triplicate bottles were amended with 0,5nM FeCl, 1nM MnCl, 100pM B_{12} and a combination thereof. The aim of these experiments was to assess whether the offshore and coastal phytoplankton communities of South Georgia were limited or co-limited by either of the trace nutrients. The duration of the experiments ranged between 4 and 10 days at the low (*PS133/2-1)* and high (*PS133/2-27*) biomass station respectively. All incubations were grown in a temperature-controlled growth chamber (2 °C) at 30 µmol photons m^{-2} s^{-1} daylight irradiance under a light-dark cycle of 14,5:9,5 h. Macronutrient concentrations (nitrate, phosphate, silicate and ammonium) and total chlorophyll *a* concentrations were measured at least every second day over the course of the experiments. Similarly, the physiological state of the cells was determined via fast repetition rate fluorometry (FRRf, Chelsea) onboard. At the beginning and end of the experiments, samples for taxonomic species composition, cell density and chemical parameters were taken that will be more described in the following. To determine taxonomic composition aliquots of 100 ml unfiltered seawater were preserved with Lugols solution at a final concentration of 1 %. Preserved samples were stored at 4°C in the dark until further analysis by light and epifluorescence microscopy back at the AWI. For bacterial and picoplankton composition via flow cytometry, seawater was transferred into cryovials and stored at -80 °C until they will be analysed at home. Seawater pH was measured onboard using a calibrated pH/ion meter (Methrom, three-point calibration). Information on the efficiency of photochemistry in PSII after dark acclimation for 1h and during varying light exposure was obtained using FRRf

by exposure to increasing irradiance (from 11 up to 600 µmol photons m^{-2} s^{-1}). Samples for particulate organic carbon (POC) were filtered onto precombusted (500° C; 12 h) GFF filters and stored in precombusted petri dishes (500° C; 12 h) at -20° C. To test aggregation capacity and carbon export potential of all resulting communities, 900 ml aliquots were taken from each triplicate bottle at the end of the incubation experiment and combined in a roller tank to induce aggregation via differential settling. The tanks were rotated at 1 rotation per minute (rpm) over 48h at a constant temperature of 2°C in the dark. After 48 h, all tanks were filmed with a Canon EOS 650 to record aggregate formation, size/volume, and sinking velocity. At the end of the roller tank incubation, aggregated material was collected for POC content determination.

2. At stations *PS133/2-1* and *PS133/2-27* a dilution series experiment was set up by mixing whole seawater with 0.2 µm filtered seawater at 100 %, 75 %, 50 % and 30 %. The aim of these experiments was to estimate microzooplankton grazing rates. All bottles were incubated in a climate-controlled laboratory at ambient light and temperature conditions and for 24-72 h depending on the experiment. At the end of the experiments, samples for POC/PON, flow cytometry, chlorophyll a and dissolved macronutrient were taken. 700 ml from each triplicate of each dilution were then combined to be analyzed back at the lab for dissolved B-vitamins.

3. Finally, the bioavailability of different Fe sources from King Haakon Bay and Cumberland Bay were tested. Berenice Ebner (Chapter 6) collected 5 different iron sources from both systems (Table 5.3). A subsample from each source was used to condition 0.2 µm filtered seawater collected from stations *PS133/2-1* and *PS133/2-27.* Briefly: 2.5 L of filtered seawater was spiked with the unfiltered Fe-source, for an approximate target addition of 1 nM Fe. The bottles were then allowed to condition under ambient light and temperature conditions before being filtered. Samples were taken for Fe-chemistry, ligands, HA-like and dissolved nutrients. In addition, triplicate 125mL polycarbonate bottles were spiked with 55Fe and allowed to equilibrate with each Fe-source conditioned water for 24 hours. During this conditioning, 20 L of a coastal phytoplankton community was gently concentrated down to 400 ml using Amicons with a 3 µm pore size polycarbonate filter. This plankton concentrate was then added to the conditioned, labeled water and incubated under ambient light and temperature conditions for 24 hours. At the same time, a subset of bottles was spiked with plankton and 14C-bicarbonate in order to measure primary production.

Tab. 5.3: Iron source samples collected by B. Ebner on South Georgia and used for the bioavailability experiments.

Sample	ID	Collection date	Location	Lat [°S]	Long [°W]
Schmelzwasser1	SW1	29.11.22	King Haakon Bay	54° 08’ 42”	37° 16’ 34”
Schmelzwasser2	SW2	29.11.22	King Haakon Bay	54°08’ 43’’	37°16’33’’
Fe-Quelle	FeQ	29.11.22	King Haakon Bay	54° 08’ 41”	37° 16’ 43”
Küstenwasser	KW	04.12.22	Moraine Fjord	54°22’9’’	36°29’38’’

Sample	ID	Collection date	Location	Lat [°S]	Long [°W]
Schmelzwasser	SmW	04.12.22	Moraine Fjord	54°22'9''	36°29'38''

Preliminary results

1. The expected data set will characterize the trace metal distribution and biogeochemistry in the open waters downstream of South Georgia. Our study will provide vertical profiles of TMs in this biologically active area and elucidate their vertical distribution and possible sources. The analysis of TMs will take place on various mass spectrometers back at the Alfred Wegener Institute.

2. Primary production and bacterial production rates were measured on board and revealed a biologically productive system. Primary production rates ranged from 28-158 µgC l^{-1} d^{-1}, with the lowest and highest rates being observed at sites *PS133/2-1* and *PS133/2-50*, respectively (Table 5.4). At all stations except station *PS133/2-50*, the larger (>2 µm) phytoplankton dominated primary production. Bacterial production generally followed this trend, with the lowest and highest rates measured at sites *PS133/2-1* and *PS133/2-17* (0.19 and 1.59 µgC m^{-3} d^{-1}, respectively; Table 5.4)

Tab. 5.4: Primary (PP) and bacterial (BP) production rates measured in water collected from 20 m with the UCTD Rosette. Primary production was size fractionated using different pore size polycabonate filters.

	PP (ugC l^{-1} d^{-1})			BP (ugC l^{-1} d^{-1})
	Total	**0.2-2µm**	**>2µm**	
133/2-1	28.0	6.5	21.5	0.19
133/2-5	90.2	13.6	76.7	1.09
133/2-11	58.7	9.1	49.6	0.27
133/2-17	125.0	-1.0	125.9	1.59
133/2-23	54.7	-4.2	58.9	0.81
133/2-32	63.0	13.7	49.3	0.30
133/2-45	33.3	15.0	18.3	0.30
133/2-42	17.7	6.2	11.6	0.21
133/2-50	158.3	109.4	48.9	0.32

3. The calculation of Fe and B_{12} uptake rates rely on dissolved Fe and B_{12} concentrations. These will be measured back at the AWI and rates will subsequently be calculated.

4. Both amendment experiments yielded interesting preliminary results. The offshore community (site *PS133/2-1*) responded to the addition of B_{12} and the combination of FeB_{12} and FeMn, by an increase in the total primary production rates of the resulting phytoplankton communities relative to the control (Fig. 5.1) For the B_{12} addition this increase was due to a large increase in primary production of the

autotrophic picoautotrophs (phytoplankton < 2 µm). In contrast the increase of total primary production in the FeB_{12} and FeMn treatments could be attributed to the > 2 µm phytoplankton group (Fig. 5.1). Most interestingly was that the addition of Fe did not result in a significant increase of total primary production. Since Mn alone did also not increase primary production, the observed increase in the FeMn was due to colimitation. Back at the AWI other parameters, (POC/PON, light microscopy, flow cytometry) will further investigate on how these manipulations changed the plankton community composition. In contrast the coastal experiment conducted at site PS133/2-27 did not result in obvious differences in the primary production of the resulting communities. In contrast to the other station, however, primary production was dominated (100%) by the >2µm size fraction.

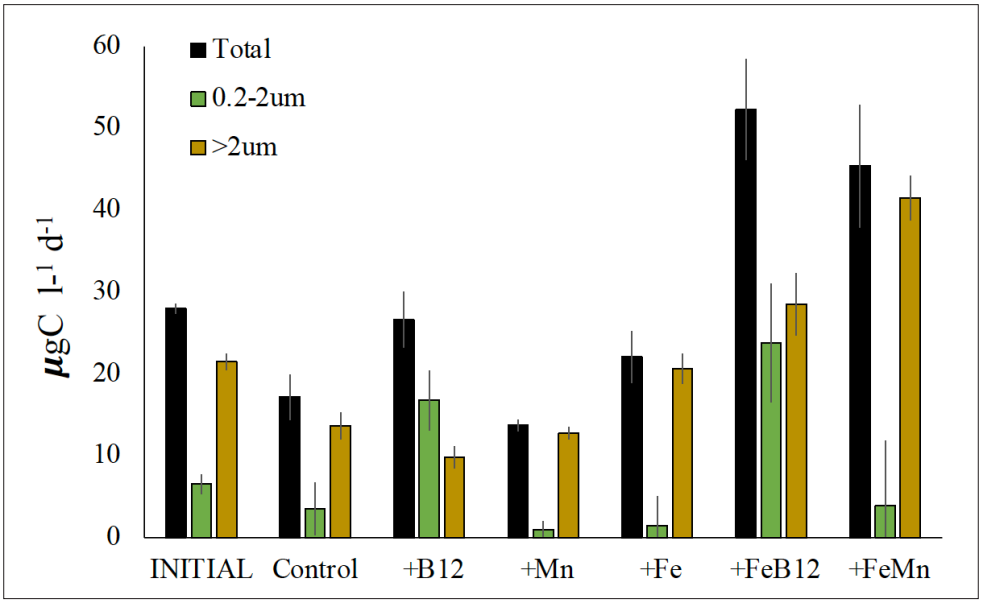

Fig. 5.1: Nutrient amendment experiments conducted with water from expedition PS133/2-1. Primary production of each resulting plankton community was measured at the end of the experiment. The treatments were 100pM B_{12}, 1nM Mn, 0.5 Fe and a combination thereof. Values denote mean ± standard deviation.

Only the chlorophyll a for the dilution experiment at PS133/2-1 was analyzed on bord. Results highlighted that net growth rate of the total primary producers was 0.28 d^{-1} (Fig. 5.2). The intrinsic growth rate (theoretical growth rate in the absence of grazers) however, was almost double (0.53 d^{-1}) while the grazing rate of 0.26 d^{-1} signified that half of the biomass was grazed down each day.

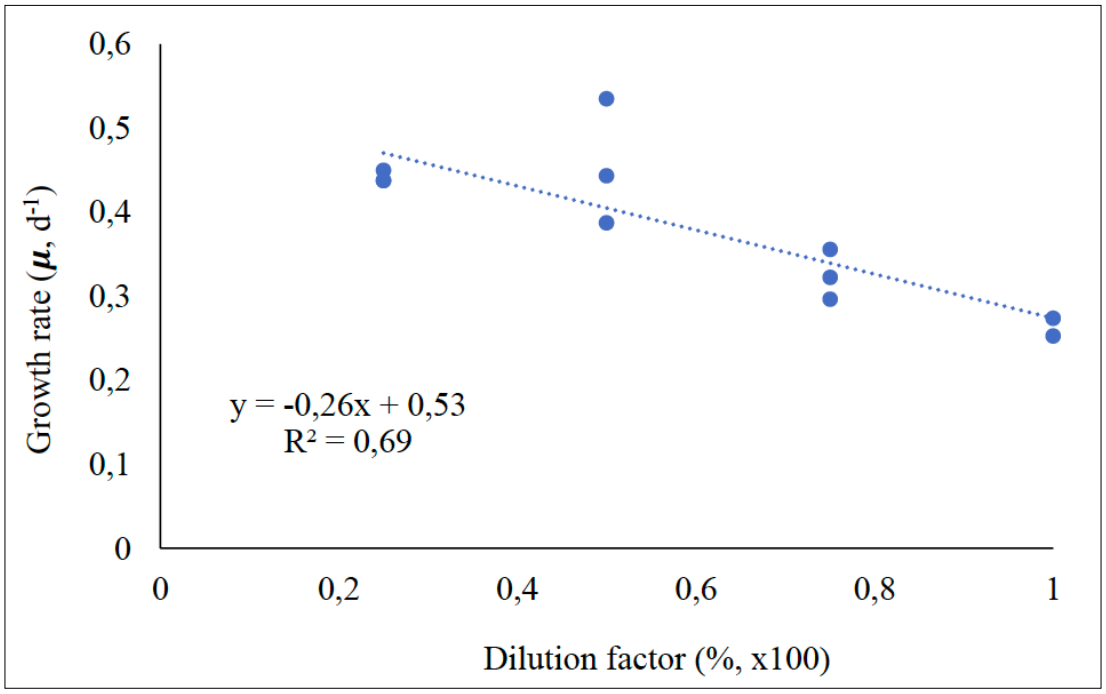

Fig. 5.2: Dilution experiments conducted with water from station PS133/2-1. Chlorophyll a based growth rates were calculated for every dilution. The slope of the linear regression denotes the microzooplankton grazing rate and the y-intercept represents the theoretical chlorophyll a-based growth in the absence of grazing.

Finally, the last set of experiments tried to highlight the potential bioavailability of several potential Fe sources to a model phytoplankton community. These experiments were partially successful. The set conducted with water from PS133/2-1, produced interesting results. Although an attempt was made to add a similar amount of Fe from each source, the exact amount added will only be known once the samples have been analyzed back at the AWI. Until this the results are speculative at best. Interesting, however is that the different Fr-sources resulted in different uptake rates, suggesting differences in their bioavailability.

Rate measurements of primary and secondary production, coupled to uptake and recycling rates of TMs and vitamins will shed light on the cycling and dynamics between these essential trace nutrients and the pelagic plankton community. In addition, the three types of targeted experiments should shed light on the role of the various TM/vitamins, Fe-sources and the importance of microzooplankton grazing different groups. Lastly, samples of phytotoxins collected will, for the first time, explore the extent to which potentially harmful or ecosystem disruptive algae are present and if Fe plays a role in their ecology.

Data management

Environmental data will be archived, published and disseminated according to international standards by the World Data Center PANGAEA Data Publisher for Earth & Environmental Science (www.pangaea.de) within two years after the end of the cruise at the latest. By default the CC-BY license will be applied.

Molecular data (DNA and RNA data) will be archived, published and disseminated within one of the repositories of the International Nucleotide Sequence Data Collaboration (INSDC, www.insdc.org) comprising of EMBL-EBI/ENA, GenBank and DDBJ).

Any other data will be submitted to an appropriate long-term archive that provides unique and stable identifiers for the datasets and allows open online access to the data.

This expedition was supported by the Helmholtz Research Programme “Changing Earth – Sustaining our Future” Topic 2, Subtopics 1 and 4, Topic 4, Subtopic 1 and Topic 6, Subtopics 2 and 3.

In all publications based on this expedition, the **Grant No. AWI_PS133/2_04** will be quoted and the following publication will be cited:

Alfred-Wegener-Institut Helmholtz-Zentrum für Polar- und Meeresforschung (2017) Polar Research and Supply Vessel POLARSTERN Operated by the Alfred-Wegener-Institute. Journal of large-scale research facilities, 3, A119. http://dx.doi.org/10.17815/jlsrf-3-163

References

Bertrand EM et al. (2007) Vitamin B-12 and iron colimitation of phytoplankton growth in the Ross Sea. Limnologie and Oceanogr. 52:1079–1093. https://doi.org/10.4319/lo.2007.52.3.1079

Boyd PW, Ellwood MJ (2010) The biogeochemical cycle of iron in the ocean. Nature Geoscience 3:675–682. https://doi.org/10.1038/ngeo964

Buesseler KO (1998) The decoupling of production and particulate export in the surface ocean. Global Biogeochemical Cycles 12:297–310. https://doi.org/10.1029/97GB03366

de Baar HJW et al. (2005) Synthesis of iron fertilization experiments: From the iron age in the age of enlightenment. Journal of Geophysical Research-Oceans 110:1–24. https://doi.org/10.1029/2004JC002601

Koch F, Marcoval MA, Panzeca C, Bruland K-W, Sanudo-Wilhelmy SA, Gobler CJ (2011) The effect of vitamin B-12 on phytoplankton growth and community structure in the Gulf of Alaska. Limnology and Oceanography 56:1023–1034. https://doi.org/10.4319/lo.2011.56.3.1023

Lumpkin R, Speer K (2007) Global ocean meridional overturning. Journal of Physical Oceanography 37:2550–2562. https://doi.org/10.1175/JPO3130.1

Martin JH, Fitzwater SE (1988) Iron deficiency limits phytoplankton growth in the Northeast Pacific Subarctic. Nature 331:341–343. https://doi.org/10.1038/331341a0

Trimborn S, Hoppe CJM, Taylor BB, Bracher A, Hassler C (2015) Physiological characteristics of open ocean and coastal phytoplankton communities of Western Antarctic Peninsula and Drake Passage waters. Deep-Sea Research Part I-Oceanographic Research Papers 98:115–124. https://doi.org/10.1016/j.dsr.2014.12.010

6. DISSOLVED AND SUSPENDED PARTICULATE IRON ISOTOPES AT THE COAST AND ON THE SHELF OF SOUTH GEORGIA

Michael Staubwasser[1], Jun Hao Chang[1], [1]DE. UNI-Köln
Berenice Ebner[2], Ingrid Stimac[2], [2]DE.AWI
not on board: Susann Henkel[2]

Grant-No. AWI_PS133/2_05

Grant-No. DFG STA 936/9-1

Objectives

A high phytoplankton concentration in the generally Fe-limited Southern Ocean downstream of South Georgia and other Southern Ocean islands suggests active Fe-fertilization from a land source (Robinson et al., 2016). On-board experimentation conducted on this cruise by Koch et al. (Chapter 5) already confirmed Fe-limitation of phytoplankton growth in these waters. The flux of Fe from glaciated islands can be high and is initially in the form of particulate reactive Fe-oxihydroxides derived from sub-glacial terrestrial Fe(II) weathering (e.g. Bhatia et al., 2013). Such Fe is believed to be a significant contributor to biological Fe-demand in the open ocean (van der Merwe et al., 2019). The conversion mechanism of reactive particulate Fe (pFe) into bio-available dissolved Fe (dFe) may take place directly in the water column and involve different forms of dFe-pFe exchange, e.g. ligand-promoted dissolution and desorption-adsorption processes, as well as maintaining high dFe levels by subsequent biologic Fe-recycling (Boyd et al., 2017). Alternatively, reductive dissolution of island-derived pFe during early diagenesis in near-surface sediment pore waters on the shelf may release dFe into the water column and be mixed back into the photic zone. Specific Fe-isotope signatures may resolve these two principal sources (Henkel et al., 2018).

The first objective of this cruise was a systematic sampling of dFe and pFe in the waters surrounding South Georgia for subsequent Fe-isotopes analysis. Ideally, sampling should cover the entire transport pathway from source end-members – i.e. glacial outflow along the shore and pore fluids from shelf sediments – through the mixing zone of the shelf water column, and into the open ocean centers of phytoplankton productivity.

The second objective is to determine Fe-isotope fractionation factors for marine dFe-pFe interaction in an on-board experiment – for analysis on return. These fractionation factors are essentially unknown for alkaline seawater conditions. Instead, the community applies fractionation factors – or rather the sign of these factors – taken from lab experiments conducted under acidic conditions (Beard and Johnson, 2004). Because Fe-isotope source end-member compositions are used to calculate dissolved Fe-source contributions to the global ocean Fe-budget (Conway and John, 2014), dFe-pFe exchange particularly at the input boundaries – e.g. the nepheloid seafloor bottom layer for early diagenetic seafloor Fe reflux – will likely modify end-member input Fe-isotope compositions. For the question of glaciated ocean island Fe-input to the Southern Ocean, dFe-pFe exchange in the water column may

affect the isotopic composition of both glacial outwash nano-particulate Fe and shelf-bottom diagenetic Fe-reflux. To derive an estimate of the “bulk system” fractionation factor for dFe-pFe exchange in seawater, a time series experiment was designed where pFe from source and open ocean isotopic end-members are enriched by ultra-filtration and subsequently inserted into ultra-filtered waters of presumed low and high ligand concentration. If marine dFe-pFe isotope fractionation factors can be determined, not only would it be possible to calculate a refined Fe source contribution budget, but also to estimate directly the utilization efficiency of Fe from ocean island sources by phytoplankton.

Work at sea

At a total of 9 stations, 59 seawater samples were collected with the AWI’s trace metal clean sampling infrastructure including a Teflon CTD equipped with Ocean Test Equipment (OTE) bottles (12L/bottle capacity) and winch. For stations’ coordinates and map display see Oetjens et al. (Chapter 11). A standardized depth profiling scheme was observed with up to 8 samples until 1,000 m or – on the shelf – until 10/20 m above the sea floor (Tab. 6.1). In addition, 19 samples of surface and near-bottom water were sampled inside King Haakon Bay, Cumberland Bay, and Grytviken with manually operated GoFlo bottles during three separate Zodiac runs. Here, King Haakon Bay receives glacial streams and particle-loaded ice from a small calving glacier, Cumberland Bay receives almost exclusively ice from the calving Nordenskjöld glacier, and Grytviken receives only streams from the hinterland. All bays show a particle-rich low-salinity surface layer of 2-20 m thickness (Fig. 6.1). All water samples (12 l from clean CTD casts, 5 or 8 l from manual GoFlo bottles) were filtered in the AWI clean-container with individual 0.4 µm Whatman cartridge filters for every sample. Besides the filtered and acidified (pH ≈ 2.1) water samples, cartridge filters were also kept and stored frozen for subsequent pFe-isotopes analysis. A filter performance comparison profile was sampled at station 5 for the Acropak 0.2 µm filters recommended by GEOTRACES but which could not be delivered in time for the cruise. Finally, during three landfalls the sub-glacial weathering end-member – in particular fluvial waters and sediments enriched with reactive ferric oxihydroxide nano-particles from glacier outwash – was also sampled on the shore in King Haakon Bay and in Grytviken (Fig. 6.2). Both water and sediment were also sampled from the beach. Complementary pore-water samples from MUC and gravitiy sediment cores on the shelf and inside the bays were taken on-board for Fe-isotopes analysis by Köster et al. (Chapter 4).

In order to identify dFe-pFe isotope exchange and determine the unknown marine Fe-isotope fractionation factors of this exchange, we ultra-filtered 50 l volumes of low chlorophyll water from station 1 (20 m), and high chlorophyll water from station 5 (20 m), respectively with 10 kDa Sartorius VivaFlow 200 cartridges. The ultra-filtered water was split into six experiment series of six 1 l aliquots each, and spiked with ^{54}Fe enriched Fe stabilized in oxalic acid to a final sample concentration of 2 nM added ^{54}Fe / l in 0.1 mmol / l oxalic acid. This constitutes an approximate doubling of the natural dFe concentration expected in this environment (van der Merwe et al., 2019). Into these six series, marine particles in two particle size distributions – 10 kDa to 0.2 µm and > 0.2 µm – enriched by ultrafiltration from stations 5 (plankton-rich surface water), 11 (shelf bottom water), and 23 (glacial outflow layer from Haakon Bay surface) – were reinserted. The final sample particle concentration was approximately three times the natural concentration. Over the course of 15 days, samples were then filtered again at specific time points. The > 0.2 µm fraction was stored on filter discs, the concentrated 10 kDa to 0.2 µm retentate (typically 50 – 100 ml, i.e. 10 – 20 fold concentration) and the < 10 kDa filtrate were kept for later analysis. The last samples of each series was stored for filtration in the lab at the University of Cologne on return.

Tab. 6.1: Table of stations and water depths with clean-CTD sampling for Fe-isotopes.

Sta 1	Sta 5	Sta 11	Sta 17	Sta 23	Sta 32	Sta 42	Sta 45	Sta 50
20 m	20 m	20 m	20 m	20 m	20 m	20 m	20 m	20 m
40 m	40 m	40 m	40 m	40 m	40 m	40 m	40 m	40 m
60 m	80 m	80 m	80 m	80 m	80 m	80 m	80 m	80 m
100 m	150 m	150 m	150 m	10 m above bottom	120 m	150 m	150 m	150 m
150 m	200 m	200 m	200 m		10 m above bottom	10 m above bottom	10 m above bottom	10 m above bottom
300 m	300 m	20 m above bottom	20 m above bottom					
500 m	500 m							
Failed	1,000 m							

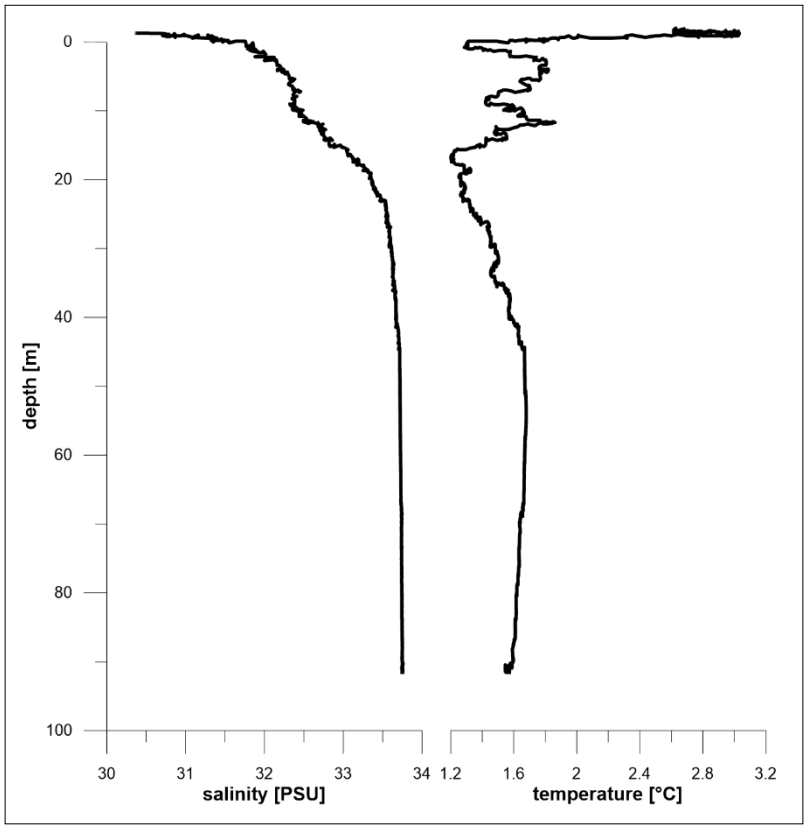

Fig. 6.1: CTS Profile inside Cumberland Bay (54°22'38"S, 36°22'38"W) showing a ~ 20 thick surface layer of low salinity caused by meltwater from the Nordenskjöld glacier. The meltwater layer is has a visibly high particle load and can be traced by the ship's beam transmission sensor in westerly directions in the open ocean off the bay's mouth. (Data and figure provided by Dennis Köhler.)

Preliminary results

Because analyses have yet to be performed by MC-ICP-MS at the mass spectrometry facility of the University of Cologne, there are no preliminary Fe-isotope results to report on at this point.

Data management

We anticipate to archive all analytical data at the World Data Center PANGAEA Data Publisher for Earth & Environmental Science (www.pangaea.de) within three years after the end of the cruise. Scientific results will be published according to international standards.

This expedition was supported by the Helmholtz Research Programme “Changing Earth – Sustaining our Future” Topic 2, Subtopics 1 and 4, Topic 4, Subtopic 1 and Topic 6, Subtopics 2 and 3. Further funding was provided by the German Research Foundation DFG in the framework of Grant DFG STA 936/9-1.

In all publications based on this expedition, the **Grant No. AWI_PS133/2_03** will be quoted and the following publication will be cited:

Alfred-Wegener-Institut Helmholtz-Zentrum für Polar- und Meeresforschung (2017) Polar Research and Supply Vessel POLARSTERN Operated by the Alfred-Wegener-Institute. Journal of large-scale research facilities, 3, A119. http://dx.doi.org/10.17815/jlsrf-3-163.

Fig. 6.2: Two glacial outflow streams on the northeastern shore of King Haakon Bay with nano-particulate Fe-oxihydroxide enrichment. Fotos by Berenice Ebner.

References

Beard BL, Johnson CM (2004) Fe Isotope Variations in the Modern and Ancient Earth and Other Planetary Bodies. Reviews in Mineralogy & Geochemistry 55:319–357.

Bhatia MP, Kujawinski EB, Das SB, Breier CF, Henderson PB, Charette MA (2013) Greenland meltwater as a significant and potentially bioavailable source of iron to the ocean. Nature Geoscience 6:274–278. https://doi.org/10.1038/ngeo1746

Boyd PW, Ellwood MJ, Tagliabue A, Twining BS (2017). Biotic and abiotic retention, recycling and remineralization of metals in the ocean. Nature Geoscience 10:167–173. https://doi.org/10.1038/ngeo2876

Conway TM, John SG (2014) Quantification of iron sources to the North Atlantic Ocean. Nature 511 215–215. http://dx.doi.org/10.1038/nature13482

Henkel S, Kasten S, Hartmann JF, Silva-Busso A, Staubwasser M (2018) Iron cycling and stable Fe isotope fractionation in Antarctic shelf sediments, King George Island. Geochimica et Cosmochimica Acta 237: 320-338. https://doi.org/10.1016/j.gca.2018.06.042

Robinson J, Popova EE, Srokosz MA, Yool A (2016). A tale of three islands: Downstream natural iron fertilization in the Southern Ocean. Journal of Geophysical Research Oceans 121: 3350–3371. https://doi.org/10.1002/2015JC011319

van der Merwe P, Wuttig K, Holmes T, Trull TW, Chase Z, Townsend AT, Goemann K, Bowie AR (2019) High Lability Fe Particles Sourced From Glacial Erosion Can Meet Previously Unaccounted Biological Demand: Heard Island, Southern Ocean. Frontiers in Marine Sciences 6:332. https://doi.org/10.3389/fmars.2019.00332

7. METHANE MEASUREMENTS – SEDIMENT, WATER COLUMN AND ATMOSPHERE

Torben Gentz[1], Ingeborg Bussmann[1], [1]DE.AWI
Malte Höhn[1], Katrin Linse[2] [2]UK.BAS
not on board: Evelyn Workman[2]

Grant-No. AWI_PS133/2_06

Objectives

Methane is a potent greenhouse gas, which has a 28-36 times higher global warming potential than carbon dioxide on a 100-year timescale (Myhre et al., 2013). The concentration of methane in the atmosphere has been increasing since the industrial revolution and presently concentrations are approximately 2.6 times higher than the pre-industrial level (Saunois et al., 2020). Consequently, reducing methane emissions and subsequently atmospheric methane concentrations are an important step to keep the “Paris Agreement” of 1.5° C of global heating (Cain et al., 2022). Therefore, global sources and sinks of methane need to be explored.

The oceanic contribution to the global atmospheric methane budget is not yet fully investigated (Saunois et al., 2020). Oceanic methane sources include production by phytoplankton and methane seeps from the seabed. Due to only a few datasets available for the global ocean, emissions remain highly uncertain, especially in polar regions. A recent investigation estimated methane emissions in the Southern Ocean based on underway measurements from cold temperate to Antarctic areas (Bui et al., 2018). Several studies (Römer et al., 2014; Del Valle et al., 2017; Spain et al., 2020; Thurber et al., 2020) reported the first observations of methane seepage from shallow nearshore waters in Antarctica and sub-Antarctic islands. In 2017, methane seeps were shown to be abundant within the fjords and continental margin of South Georgia based on results obtained during expedition M134 of *METEOR*.

The extent of increased methane concentrations within the water column and its potential consumption was assessed by discrete water sampling and by high spatial resolution measurements with an Underwater mass spectrometer (UWMS). The air sampling during cruise PS133/2 was complementary to the sediment and water column sampling aiming to detect methane concentrations from locations with confirmed methane seepage.

With this combined data set, we are able to quantify the contribution of the Southern Ocean and its methane seeps to the local carbon budgets in response to regional climate change and interaction with the adjacent ocean. The transport, reaction pathways and fluxes between sediment, coastal sea and atmosphere will be quantified.

Work at sea

Dissolved methane concentrations:

We analysed 210 duplicate water samples from the CTD-rosette’s Niskin bottles. The water samples were taken from the surface, near surface (at ~10 to 20 m depth), at several intermediate

depths as well as close to the seafloor (Table 7.1). For analysis the water samples were filled into air-tight glass bottles. A headspace was created with nitrogen (Alphagaz 1, AirLiquide) and after equilibration for temperature and gas exchange, the samples were analysed for methane with an Agilent gas chromatograph (GC) with FID. The settings of the GC were an oven temperature of 60°C, an injector temperature of 200°C and a detector temperature of 220°C. The carrier gas was nitrogen (see above) with hydrogen and synthetic air as burning gases. The calculation of the methane concentration was performed according to Magen et al. (2014).

For further information see Table 7.1 at the end of the chapter.

The *in-situ* concentration of methane was mapped in the vicinity of Grytviken Flare in Cumberland Bay (Table 7.2) by a new designed UWMS in high temporal and spatial resolution (Gentz et al., 2014). The UWMS is able to analyse the dissolved gas composition in aquatic systems in about one second, which results in a high-resolution mapping of dissolved methane concentrations in the water column of the different fjord habitats.

Tab. 7.2: Sample list for the use of the UWMS.

Station	Longitude	Latitude	Water Depth (m)	Sampling water depth (m)		
PS133/2_32-11	54°15.867'S	036°26.293'W	263	240	215	180

Methane oxidation rates:

To determine the biological sink of dissolved methane i.e., the methane oxidation rate (MOX), water samples were spiked with radiolabelled methane. After 2 days of incubation at near in situ conditions (2°C) the amount of produced radiolabelled water was determined with a liquid scintillation counter and the MOX calculated (Bussmann et al., 2015). In addition, six experiments on the influence of methane concentration and of nutrient limitation on MOX were performed on board.

LosGatos greenhouse gas analyser work:

Ambient methane concentrations were measured continuously by a LosGatos® greenhouse gas analyser (GGA). The GGA was calibrated regularly on board with gas sampling bags of standard gas and pure nitrogen. The inlet of the air was situated at the "crow's nest" with an additional water trap. With this dataset and additional information on wind speed and dissolved methane concentrations the methane flux can be calculated at high spatial resolution.

Air sampling by hand-held pump:

On board, air samples were collected in tedlar bags using a small battery powered pump at regular intervals, before dawn (~2 am) and mid-day (~2 pm) in international waters and around South Georgia (Table 7.3). The tedlar bags were stored in the +4°C cold room after sampling until leaving the vessel in Cape Town. The filled tedlar bags were transported back to the UK on arrival for isotopic analysis of the methane at the greenhouse gas laboratory at Royal Holloway University of London (France et al., 2022). At sampling event 15, the hand pump stopped working and sampling was ended.

Tab. 7.3: Sample list for hand pump collected air samples.

Sample ID	Date 2022	Time [UTC]	Station PS133-2	Location	Ship [kt]	Wind [m/s)]	Wind [°)]	Air [°C]	Air [hP]
1	24.11.	14:55	1_1	starboard front					995
2	25.11.	04:05	2_1	starboard front	10	6.3	230	2.2	1005
3	25.11.	16:00	4_1	starboard front	4.3	7.3	275	3.5	1010
4	26.11.	03:58	6_1	port aft	11	12.8	311	3.4	1005
5	26.11.	16:01	10_1	starboard front	10.5	17	270	3.7	991.5
6	27.11.	03:45	14_1	starboard front	5.5	15.4	271	3.3	1002
7	27.11.	15:45	15_4	starboard front	0.2	16.1	235	3.3	1006
8	28.11.	04:04	16_1	starboard front	7.5	11.4	250	2.3	1011
9	28.11.	16:08	17_6	starboard front	0.6	9.7	263	3.4	1009
10	29.11.	02:52	19_2	starboard front	0.5	6.6	312	2.2	1009
11	29.11	16:40	23_3	starboard front	0.3	4.9	353	8.3	996
12	30.11	03:30	23_12	starboard front	0	5.5	88	6.7	984
13	01.12.	16:00	30_1	starboard front	9.3	17.9	280	4.3	1069
14	02.12.	16:03	32_12	starboard front	0.3	16.6	339	6.9	1000
15	03.12.	04:00	34_1	starboard front					

Sediment sampling:

Sediment samples (3 ml) from MUC and gravity corer from various depths were fixed with 5 ml NaOH in 20 ml glass vials. This headspace was also analysed on board. These samples are listed in Chapter 4.

Three gravity cores equipped with a plastic hose were taken in the “Church Trough”, a known location for gas hydrates (Bohrmann et al. 2017). We allowed the collected gas hydrates to thaw, stored them as gas in gas-tight glass vials and analysed them on board for gas composition (Table 7.4). The radiocarbon age of the gas hydrates will be analysed at the MICADAS-facility at AWI-Bremerhaven. A new method for this application was recently established.

Tab. 7.4: Sample list for the collection of gas hydrates.

Station	Longitude	Latitude	Depth	Core length	Samples taken
PS133/2_9-3	53°46,204'S	038°08.420'W	378m	240 cm	/
PS133/2_29-1	53°46,205'S	038°08.416'W	378m	245 cm	7
PS133/2_29-2	53°46,203'S	038°08.408'W	378m	345 cm	9

Preliminary results

Dissolved methane concentrations:

Concentrations of dissolved methane in the water column revealed a broad range, from below saturation (1 nmol/L) to high concentrations near the bottom of Possession Bay and King Haakon Bay (196 nmol/L). In Figure 7.1 a transect from inside King Haakon Bay towards the shelf is shown with the respective dissolved methane concentrations determined on board.

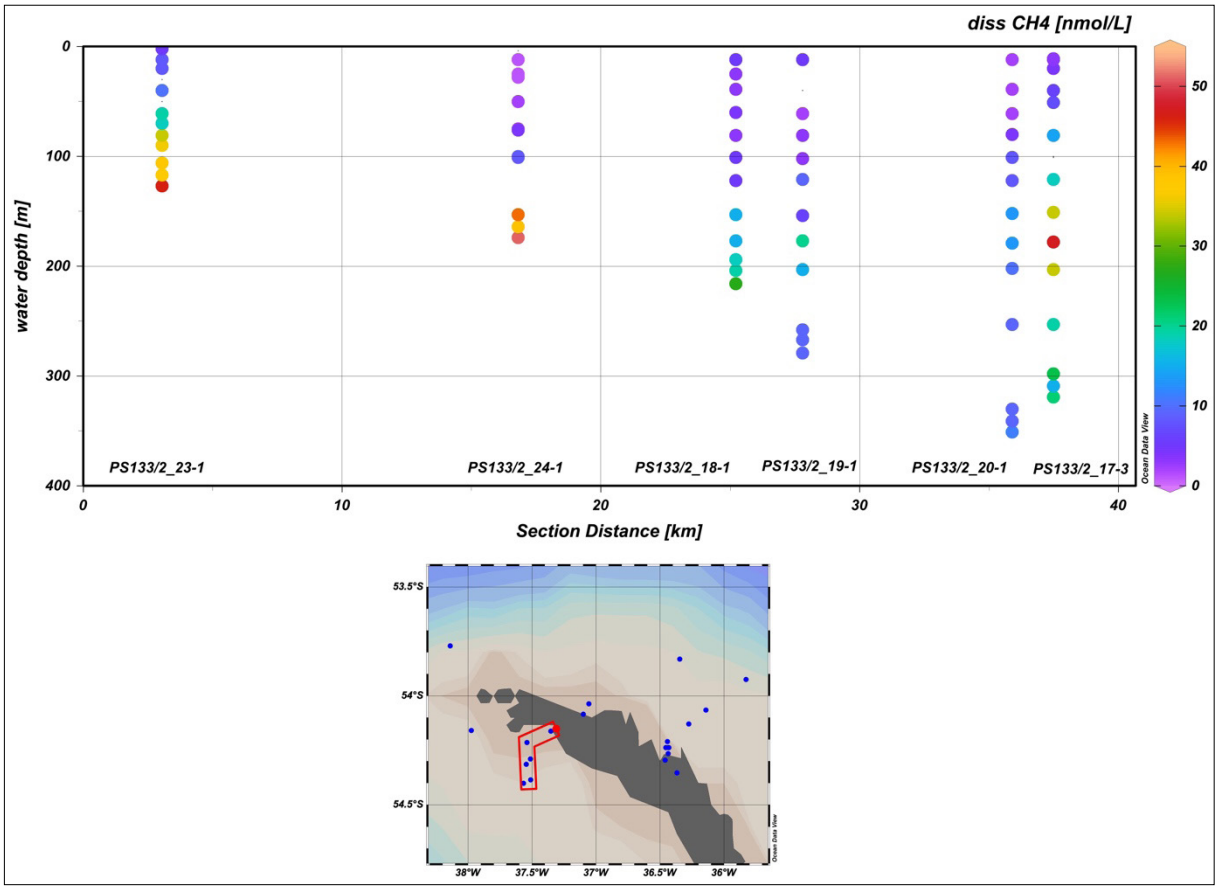

Fig. 7.1: Dissolved methane concentrations along a transect from inside King Haakon Bay towards the shelf.

Methane oxidation rates:

The methane oxidation rates were overall rather low, with most surface samples being below the detection limit (Fig. 7.2). Highest activities were encountered in the bottom water of Possession Bay with 3.4 nmol/l/d, while at the surface only 0.07 nmol/L/d were determined. Several experiments were performed to test if the methane oxidation rate was limited by nutrients (PO4 and NO3), trace elements or methane. However, the addition of these compounds did not result in increased MOX. Also, the addition of glacier water did not reveal any differences.

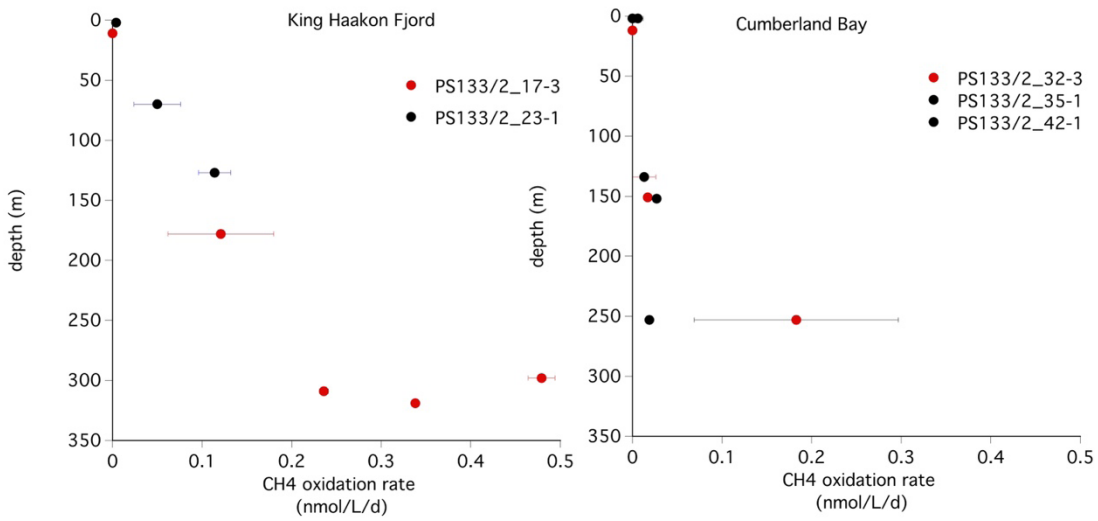

Fig. 7.2: Methane oxidation rates in King Haakon Bay and Cumberland Bay, the red colour indicates stations with elevated MOX, either at the inner Fjord or before the sill.

Gas hydrates:

Three gravity cores with foil as liner were taken at nearly the same position (Table 7.4). Two cores were relatively short (240 cm) and no or only a small amount of hydrates were found (GC 9-3 and 29-1). Gravity core 29-2 showed 2 different structures of the gas hydrates. In 240 cm depth the hydrates were thicker and rounded while in greater depth gas hydrates showed flat and plate-like shapes (Fig. 7.3). In total 16 samples of gas hydrates were taken. Gas analysis on board showed a gas composition of up to 67 % methane. The radiocarbon age of the gas hydrate-derived methane will be analysed at the MICADAS-facility at the AWI in Bremerhaven

Fig. 7.3: Gas hydrates found in the gravity core taken in Church Trough. Gas hydrates from core 29-2 had the form of tubes at shallow depth (245 cm) and as plates in greater depth (340 cm) as shown on the left and right photo.

High resolution mapping of methane concentrations in the water column using the UWMS:

In cooperation with the bathymetric group on board *Polarstern* (use of Simrad EK80 as well as PARASOUND) no gas-flares were detected, even at seep-locations known from previous cruises (Bohrmann et al., 2017). A deployment of the UWMS was performed at the former Grytviken Flare discovered during expedition M134 of *Meteor* in 2017. Measurements were taken at three different water depths (Fig. 7.4). Main goal for this deployment was to observe changes in methane concentration over time in the bottom water layer to understand if time dependent outgassing of methane from sediment takes place.

The continuous measurement of the UWMS for up to 1h at the same water depth (240 m, 215 m and 180 m) showed a well-mixed water layer that does not show indication of extreme outgassing of methane by gas seeps while measuring.

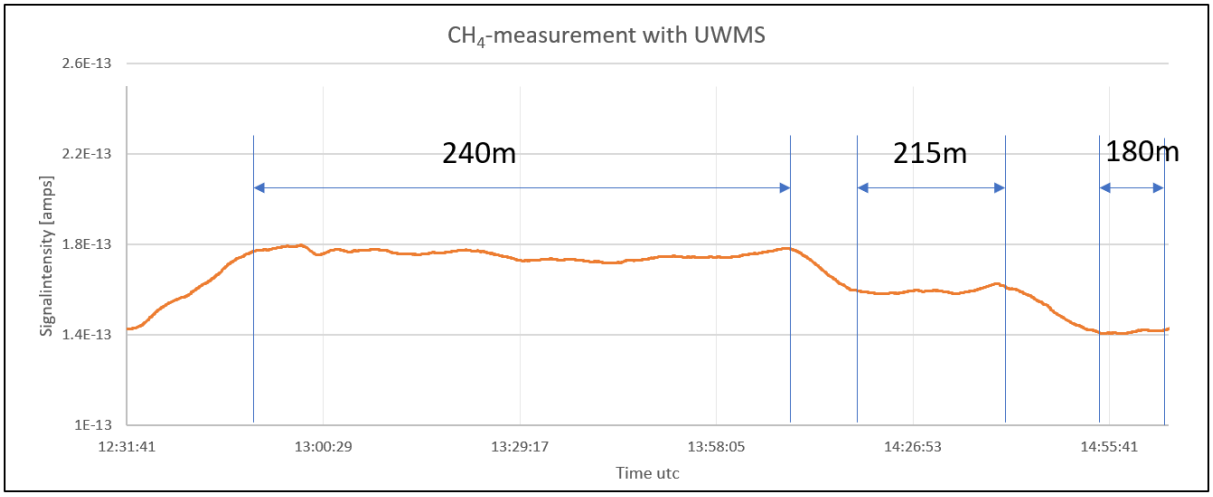

Fig. 7.4: Dissolved methane concentrations analysed during the UWMS deployment at three different water depths at Grytviken Flare (station 32-11).

Data management

Environmental data will be archived, published and disseminated according to international standards by the World Data Center PANGAEA Data Publisher for Earth & Environmental Science (https://www.pangaea.de) within two years after the end of the cruise at the latest. By default, the CC-BY license will be applied.

Atmospheric methane isotopic data will be submitted to, archived, published and disseminated by the UK Polar Data Centre (PDC) hosted at the British Antarctic Survey.

This expedition was supported by the Helmholtz Research Programme “Changing Earth – Sustaining our Future” Topic 2, Subtopics 1 and 4, Topic 4, Subtopic 1 and Topic 6, Subtopics 2 and 3.

In all publications based on this expedition, the **Grant No. AWI_PS133/2_06** will be quoted and the following publication will be cited:

Alfred-Wegener-Institut Helmholtz-Zentrum für Polar- und Meeresforschung (2017) Polar Research and Supply Vessel POLARSTERN Operated by the Alfred-Wegener-Institute. Journal of large-scale research facilities, 3, A119. http://dx.doi.org/10.17815/jlsrf-3-163.

References

Bui OTN, Kameyama S, Yoshikawa-Inoue H, Ishii M, Sasano D, Uchida H, Tsunoga U (2018) Estimates of methane emissions from the Southern Ocean from quasi-continuous underway measurements of the partial pressure of methane in surface seawater during the 2012/13 austral summer. Tellus B: Chemical and Physical Meteorology 70:1–15. https://doi.org/10.1080/16000889.2018.1478594

Bussmann I, Matousu A, Osudar R, Mau S (2015) Assessment of the radio 3H-CH4 tracer technique to measure aerobic methane oxidation in the water column. Limnology and Oceanography: Methods 13:312–327. http://doi/10.1002/lom3.10027

Bohrmann G et al. (2017) R/V METEOR Cruise Report M134, Emissions of Free Gas from Cross-Shelf Troughs to South Georgia: Distribution, Quantification, and Sources for Methane Ebullition Sites in Sub-Antarctic Waters. Berichte, MARUM – Zentrum für Marine Umweltwissenschaften, Fachbereich Geowissenschaften, Universität Bremen, 317:220 p.

Cain M, Jenkins S, Allen MR, Lynch J, Frame DJ, Macey AH, Peters GP (2022) Methane and the Paris Agreement temperature goals. Philosophical Transactions of the Royal Society A: Mathematical, Physical and Engineering Sciences 380:2215. https://doi.org/10.1098/rsta.2020.0456

Del Valle RA, Yermolin E, Chiarandini J, Sanchez Granel A, Lusky JC (2017) Methane at the NW of Weddell Sea, Antarctica. Journal of Geological Research Article ID 5952916. https://doi.org/10.1155/2017/5952916

France J, Fisher R, Lowry D, Allen G, Andrade M, Bauguitte S, Bower K, Broderick TJ, Daly M, Forster G, Gondwe M, Helfter C, Hoyt AM, Jones A, Lanoiselle M, Moreno I, Nisbet-Jones P, Oram DE, Pasternak D, Pitt J (2022) $\delta^{13}C$ methane source signatures from tropical wetlands and rice field emissions. Philosophical Transactions of the Royal Society of London A: Mathematical, Physical and Engineering Sciences 380:2215. https://doi.org/10.1098/rsta.2020.0449

Gentz T, Damm E, Schneider von Deimling J, Mau S, McGinnis DF, Schlüter, M (2014) A water column study of methane around gas flares located at the West Spitsbergen continental margin. Continental Shelf Research 72:107–118. https://doi.org/10.1016/j.csr.2013.07.013

Magen C, Lapham LL, Pohlman JW, Marshall K, Bosman S, Casso M (2014). A simple headspace equilibration method for measuring dissolved methane. Limnology and Oceanography: Methods 12:637–650. http://doi:10.4319/lom.2014.12.637

Myhre G, Shindel D, Bréon F-M, Collins W, Fuglestvedt J, Huang J, Koch D, LamarqueJ-F, Lee D, Mendoza B, Nakajima T, Robock A, Stephens G, Takemura T, Zhang H (2013) Anthropogenic and Natural Radiative Forcing: Climate Change 2013: The Physical Science Basis. Contribution of Working Group I to the Fifth Assessment Report of the Intergovernmental Panel on Climate Change Cambridge University Press, Cambridge, United Kingdom and New York, NY, USA.

Römer M, Torres M, Kasten S, Kuhn G, Graham AGC, Mau S, Little C, Linse K, Pape T, Gepräg, P, Fischer D, Wintersteller P, Marcon Y, Rethemeyer J, Bohrmann G and shipboard scientific party ANT-XXIX/4 (2014) First evidence of widespread methane emissions around a Sub- Antarctic Island (South Georgia). Earth and Planetary Science Letters 403:166–177. https://doi.org/10.1016/j.epsl.2014.06.036

Saunois M, Stavert AR, Poulter B, Bousquet P, Canadell JG, Jackson RB (2020) The Global Methane Budget 2000–2017. Earth System Science Data 12:1561–1623. https://doi.org/10.5194/essd-12-1561-2020

Spain EA, Johnson SC, Hutton B, Whittaker JM, Lucieer V, Watson, SJ (2020) Shallow seafloor gas emissions near Heard and McDonald Islands on the Kerguelen Plateau, Southern Indian Ocean. Earth and Space Science 7. https://doi.org/10.1029/2019EA000695

Thurber AR, Seabrook S, Welsh RM (2020) Riddles in the cold: Antarctic endemism and microbial succession impact methane cycling in the Southern Ocean. Proceedings of the Royal Society B.2872020113420201134. http://doi.org/10.1098/rspb.2020.1134

Tab. 7.1: Sample list of water samples taken from the CTD-rosette at the respective water depths in meters, samples for measurement of methane oxidation rate are indicated in bold.

Station	Date time (UTC)	Longitude	Latitude	Water Depth [m]													
CTD 9-1	26.11.22 10:16	53° 46,219' S	038° 08,310' W	21	300	304	326	335									
CTD 11-1	26.11.22 18:48	54° 02,115' S	037° 03,326' W	11	20	49	101	202									
CTD 15-1	27.11.22 13:39	54° 05,019' S	037° 05,952' W	25	50	76	101	127	152	176	217	227	253	277	303	323	333
CTD 17-3	28.11.22 13:10	54° 24,079' S	037° 34,030' W	11	20	40	51	81	101	121	151	178	203	253	298	309	319
CTD 18-1	29.11.22 00:36	54° 17,346' S	037° 30,830' W	12	25	39	60	81	101	122	153	176	194	204	216		
CTD 19-1	29.11.22 02:38	54° 18,629' S	037° 32,566' W	12	40	61	81	102	121	154	177	203	258	267	279		
CTD 20-1	29.11.22 05:04	54° 23,097' S	037° 30,638' W	13	39	61	80	101	122	152	179	202	253	330	341		
CTD 23-1	29.11.22 13:55	54° 09,675' S	037° 21,201' W	2	12	20	40	61	70	81	90	106	117	127			
CTD 24-1	30.11.22 10:40	54° 12,770' S	037° 32,322' W	4	12	25	28	50	75	100	153	164	174				
CTD 28-1	01.12.22 01:41	54° 09,446' S	037° 58,510' W	3	25	50	75	101	152	177	224	234	246				
CTD 31-1	01.12.22 18:50	54° 07,724' S	036° 16,513' W	13	26	51	102	153	178	246	256	265					
CTD 32-3	02.12.22 01:34	54° 15,899' S	036° 26,234' W	12	25	41	80	101	151	176	203	243					
CTD 35-1	03.12.22 10:07	54° 21,168' S	036° 22,072' W	2	25	35	50	76	100	112	122	134					
CTD 37-1	03.12.22 23:56	54° 17,631' S	036° 27,579' W	3	25	50	76	101	114	126							
CTD 38-1	04.12.22 01:00	54° 14,226' S	036° 27,161' W	2	51	75	102	151	184								
CTD 39-1	04.12.22 02:39	54° 14,110' S	036° 26,242' W	4	51	76	102	151	197								
CTD 40-2	04.12.22 05:01	54° 14,257' S	036° 25,701' W	4	50	75	101	126	163								
CTD 42-1	05.12.22 01:46	54° 12,610' S	036° 25,989' W	2	20	40	61	81	101	152	177	202	232	242	253		
CTD 45-5	07.12.22 00:15	54° 12,529' S	036° 26,449' W	5	21	41	61	81	100	125	151	183	193	203			
CTD 48-1	07.12.22 14:08	53° 55,506' S	035° 49,618' W	4	41	62	101	152	176	202	246	256	267				
CTD 50-1	07.12.22 19:40	54° 03,912' S	036° 08,424' W	6	41	61	101	151	177	202	237	247	257				

8. NATURAL RADIONUCLIDES AND PARTICLE CHARACTERIZATION

Walter Geibert[1], Dennis Köhler[1], [1]DE.AWI
Rhiannon Jones[2]; Ilona Sekudewicz[3] [2]UK.SOTON
[3]PL.PAS

Grant-No. AWI_PS133/2_07

Outline

The timescales of the fluxes of dissolved substances from land to ocean can be studied with soluble natural radionuclides like radium and radon. Radium and radon are released to the ocean by sediments, and following their release, they decay with a specific half-life. This process creates a mathematical relation between the inventory of radium or radon present and its supply by sediments. This can be used to estimate fluxes from ground and pore waters into the ocean, and to follow their distribution. Here, we combine the information from short-lived radium isotopes ^{224}Ra and ^{223}Ra (the latter possibly expected to be very low) with the long-lived radium isotopes ^{226}Ra and ^{228}Ra. In addition, we study ^{222}Rn/^{226}Ra disequilibria near the seafloor for a tentative assessment of gas fluxes. We link the information from radium to information from particle composition in order to assign sources, identify transport mechanisms and reveal chemical properties that control trace element budgets of the Southern Ocean.

Objectives

Our objectives were

1. to measure radium together with trace element ratios on potential groundwater sources to the ocean
2. to determine the inventory of several radium isotopes and ^{222}Rn (at least ^{224}Ra and ^{226}Ra) in one or more fjords
3. to measure ^{226}Ra and (where possible) the ^{228}Th/^{228}Ra ratio in nepheloid layers, if observed
4. to sample particles transported offshore and measure their elemental composition, in combination with the radium signature of the surrounding water and hydrographic information

Work at sea

All samples taken from onboard and on the beach are listed in Table 8.1; samples and measurements taken from the zodiac are listed separately in tables below. Our work at sea was split in three aspects:

1. sampling of large-volume samples (typically 60-120L) from the standard CTD rosette for **short-lived radium** (Jones/Sekudewicz), absorbed onto manganese coated fiber.

In addition, 2 L samples for ^{226}Ra and 1 L samples for ^{222}Rn (Köhler/Geibert) were taken from the CTD rosette. These samples were complemented by supernatant water from multicores, where available.

2. Collection of suspended particles for elemental analyses on **filters** together with **Mn-coated absorbers** for radium isotopes by means of *in-situ* pumps as part of the comprehensive process stations (Köhler/Geibert); see Table 8.2 for an overview.

3. Sampling of beach waters and groundwater seepages for ^{224}Ra and ^{226}Ra (entire team).

Fig. 8.1: Radium sampling of a large volume sample (40 L in total) on Grytviken beach. The sample was pre-concentrated on South Georgia before being analysed on board Polarstern.

In addition to sampling as it was originally planned above, CTD Transects with a handheld Seabird “Seacat” CTD profiler and a hand-held gravity corer (“UWItec”) were conducted from a zodiac in nearshore sites (King Haakon Bay), close to the glacier in Cumberland Bay East, in Moraine Fjord and near Grytviken (see Tables 8.3, 8.4, 8.5 and 8.6). The first deployment only included the actual CTD sensors; the later deployments also included turbidity, chlorophyll, pH and oxygen sensors.

Tab. 8.1: Overview of the number of different sample types taken during cruise PS133/2.

Station	**1**	**9**	**11**	**15**	**17**	**18**	**23**	**24**	**31**	**32**	**35**	**37**	**38**	**39**	**40**	**42**	**B**
# large volume samples from CTD / beach	4	3	3		5	2	4	-	-	4	1	1	3	3	3	4	1
MUC supernatant	-	2 L	-		5.4 L	-	4.7 L	-	-	22.8 L	7.8 L	-	-	-	-	9.6 L	-
#^{226}Ra 2L samples	5	2	1		4	-	4	-	-	4	2	-	2	2	2	-	1
#^{222}Rn samples	1	4	-	4	4	-	-	4	4	4	-	-	-	-	-	4	-
ISP filters					7					6						4	
ISP Mn cartridges					5x2					4x2						4x2	

Tab. 8.2: Detailed overview of the in situ pump deployments during cruise PS133/2.

Station	**Pump ID**	**Manufact.**	**Type**	**Type**	**#**	**Filters**	**Depth [m]**	**Vol [L]**
17-2	AWI_ISPCh01	Challenger		ISP	1	PES+Mn	20	226
17-2	AWI_ISPCh02	Challenger		ISP	2	PES+Mn	80	129
17-2	AWI_ISPCh03	Challenger		ISP	3	PES+Mn	150	100
17-2	AWI_ISPCh04	Challenger		ISP	4	PES+Mn	175	149
17-2	AWI_ISPCh05	Challenger		ISP	5	PES+Mn	250	0
17-2	AWI_ISP03	McLane	WTS-LV	Dual Filter	6	PES	300	183
						QMA	300	159
17-2	AWI_ISP01	SeaFeather CTD	Demo		7	PES	315	0
32-12	AWI_ISPCh01	Challenger		ISP	1	PES+Mn	20	210
32-12	AWI_ISPCh02	Challenger		ISP	2	PES+Mn	80	119
32-12	AWI_ISPCh03	Challenger		ISP	3	PES+Mn	125	200
32-12	AWI_ISPCh04	Challenger		ISP	4	PES+Mn	150	149
32-12	AWI_ISP03	McLane	WTS-LV	Dual Filter	5	PES	200	193
						QMA	200	170
32-12	AWI_ISP01	SeaFeather CTD	Demo		6	PES	250	0
42-7	AWI_ISPCh01	Challenger		ISP	1	PES+Mn	20	129
42-7	AWI_ISPCh02	Challenger		ISP	2	PES+Mn	80	90
42-7	AWI_ISPCh03	Challenger		ISP	3	PES+Mn	125	305

Station	Pump ID	Manufact.	Type	Type	#	Filters	Depth [m]	Vol [L]
42-7	AWI_ISPCh04	Challenger		ISP	4	PES+Mn	150	120
42-7	AWI_ISP01	SeaFeather CTD	Demo		5	PES	250	12

Tab. 8.3: Detailed overview of zodiac CTD deployments and discrete samples in King Haakon Bay (Team: Stimac, Köster, Köhler, Bäcker).

Lat	Lon	Water depth [m]	Water sample	CTD cast #	Uwitec core #	Comments
54° 08' S	37° 16' W	11	k4 - 5 m	49		
54° 08' S	37° 16' W	15		50		
54° 08' S	37° 16' W	12		51		Kattein 10 L 1/2
54° 08.847' S	37° 16.878' W	13	surface	52		Kattein 10 L 2/2
54° 08.854' S	37° 16.881' W	14	k3 - 5 m			
54° 08.871' S	37° 16.867' W	15			1 (failed)	
54° 09.771' S	37° 17.241' W	38				ice sample
54° 09.804' S	37° 17.398' W	31	k1 - 30 m	53		high particle load, water colored like milk
54° 09.837' S	37° 17.577' W	5	k2 - 5 m (failed)	54		high particle load, water colored like milk
54° 09.899' S	37° 17.672' W	5	k2 - 5 m	55		high particle load, water colored like milk
54° 09.929' S	37° 17.974' W	32			2 (failed)	high particle load, water colored like milk
54° 09.909' S	37° 19.039' W	55	k5	56		
54° 09.914' S	37° 19.324' W		G1 - 5 m	57		
54° 09.619' S	37° 20.071' W	13	G2 - 10 m (failed)	58		
54° 09.619' S	37° 20.071' W	12	G2 - 10 m	59		

Tab. 8.4: Detailed overview of zodiac CTD deployments and discrete samples near Nordenskjöld glacier (Team: Köhler, Höhn, Anselin, Buchholz).

Lat	Lon	CTD cast #	Water sample
54°22'28''S	36°23'42''W	67	
54°22'30''S	36°23'50''W	68	
54°22'25''S	36°23'44''W	69	
54°22'42''S	36°23'4''W	70	
54°22'39''S	36°23'2''W	71	
54°22'30''S	36°22'23''W	72	
54°23'7''S	36°21'20''W	73	

Lat	Lon	CTD cast #	Water sample
54°23’9’’S	36°20’59’’W	74	
54°23’12’’S	36°22’3’’W	75	
54°23’10’’S	36°21’35’’W	76	
54°23’7’’S	36°21’43’’W	77	
54°22’40’’S	36°22’36’’W	78	5 - surface
54°22’8’’S	36°22’31’’W	79	
54°21’32’’S	36°22’2’’W		24 - surface

Tab. 8.5: Detailed overview of zodiac CTD deployments and discrete samples taken in Moraine Fjord (Team: Stimac, Köhler, Höhn, Bäcker).

Lat	Lon	Water depth [m]	Water sample	CTD cast #
54°20’5’’S	36°29’00’’W	195	G4 - surface	80
54°20’6’’S	36°29’1’’W	195	K5 - 50 m	
54°18’46’’S	36°28’26’’W	24	K24 - surface	81

Tab. 8.6: Detailed overview of zodiac CTD deployments and discrete samples in Grytviken (Team: Stimac, Köhler, Höhn, Bäcker).

Lat	Lon	Water depth	Water sample	CTD cast #	UWItec core #
54°16’55’’S	36°30’19’’W	12		82	1
54°16’55’’S	36°30’18’’W	13			2
54°16’54’’S	36°30’19’’W	12			3
54°16’54’’S	36°30’19’’W	12			4
54°16’59’’S	36°30’7’’W	20		83	5
54°16’58’’S	36°30’8’’W	20			6
54°16’59’’S	36°30’4’’W	21			7
54°17’6’’S	36°29’51’’W	16	3 - surface	84	
54°17’8’’S	36°29’48’’W	16			8
54°17’6’’S	36°29’46’’W	17			9

The sampling devices used were:

1. Submersible pumps (in-situ pumps), one of which (“Seafeather10k”) delivers CTD and other sensor data. Models: 1x “Seafeather 10k smart”, 1 x “McLane”, 6x “Challenger”
2. Standard-CTD (operated by Physical Oceanography)

On board detection/measurement systems were:

1. Radium delayed coincidence counter (RaDeCC) for ^{224}Ra, ^{223}Ra and indirectly ^{228}Th and ^{228}Ra/^{226}Ra ratios
2. Rad-7 (manufactured by Durridge Inc.), a specific ^{222}Rn gas counter, modified to measure discrete one liter water samples

3. Triathler (manufactured by Hidex), liquid scintillation counting system for ^{222}Rn and indirectly ^{226}Ra in discrete samples (not used during cruise)
4. Seabird “Seacat” CTD profiler, equipped with a variable number of additional sensors.

On board processing/measurement techniques were:

1. Gravitative filtration of large-volume water samples (80-120 L) over manganese coated fiber, followed by a measurement of ^{224}Ra (half-life 3.6 days)
2. Freezing of filters from *in-situ* pumps
3. ^{222}Rn on Rad-7 via de-bubbling of 1 L samples
4. Filtration of particle samples from South Georgia (river water/surface water) and collection/freezing of particles from glacier ice.

Deviations from the plan

While many samples and data could be obtained as planned, or in addition to what had originally been planned (see above), other aspects of our work were less successful.

In terms of sampling, we found the underway sampling system to give unreasonably high counts for ^{224}Ra that were unlikely to reflect actual environmental levels. This had been observed before (Rutgers van der Loeff, pers. comm.) and is most likely due to adsorption of the ^{224}Ra progenitor ^{228}Th to the walls of the ship’s seawater supply system. Therefore, no large-volume surface samples from a constant water depth could be evaluated.

A part of the sampling on the beach (the moraine wall in front of Penguin River in Cumberland Bay East) was unsuccessful. Due to a difficult landing on the beach, combined with abundant seals, no sampling equipment could be taken there and consequently no samples were taken there. Instead, sampling was conducted later on the beach in Grytviken.

The laser cutter for filters was eventually not used due to insufficient lab space. Filters were immediately frozen instead.

Many electronical parts of the equipment had suffered substantial damage during transit to expedition PS133/2. This concerned at least two Radecc-counters, several in situ pumps, 2 CTD sensor systems, and one Rad7 counter. This required adaptation and a moderate reduction of the sampling programme throughout the cruise. On-board processing of time sensitive radioisotopes was also moderated, as sample run time was limited due to a reduced set of instruments.

Preliminary results

Onboard counting of short-lived radium:

In general, the observed activities were very low compared to many other studies from coastal systems, but comparable to what has been reported from Kerguelen Islands (Sanial et al.2015). In spite of relatively large sample volumes, ^{224}Ra is found to be near its detection limit, and ^{223}Ra often below it. The notable exceptions are water samples from very close to the seafloor, or taken nearshore at the very surface. The beach sample seemed comparable to other surface samples. Underway samples had high ^{224}Ra activities, too, but indirect contamination vie ^{228}Th adsorbed onto the ship’s intake system is a distinct possibility here, precluding its interpretation. MUC supernatants also were elevated, as expected, and can be used to constrain the ^{223}Ra/^{224}Ra ratio of the sediment source. The low activities point overall to low supply from terrestrial sediments and/or rapid exchange rates with the open ocean. Given

the fact that the fjords are deep compared to other coast types, and that the slopes are mostly covered by rock, not sediments, this is not unexpected. These factors would also apply to other trace metals, so their source must be seen at the surface or the sediment-covered seafloor.

Onboard counting of ^{222}Rn via Rad-7:

In general, ^{222}Rn was near the detection limit of this method. However, elevated activities were seen near the seafloor. ^{226}Ra analyses in the home laboratory are needed to quantify $^{222}Rn_{excess}$.

Onboard inspection of in-situ pump filters:

The filters of the in-situ pumps revealed that particles had been collected in spite of overall relatively low sample volumes in the low 100 s of liters, in particular near the surface. CTD profiles and sensor data from the offline-CTD of “Seafeather10k” still need to be evaluated.

CTD profiles (hand-held)

First profiles have been downloaded and indicate rapid subglacial and surface freshwater discharge, especially near Nordenskjöld Glacier. A full evaluation of the comprehensive dataset still stands out.

Planned post-cruise analyses:

1. Re-counts of the Mn-fiber samples to determine supported ^{223}Ra and ^{224}Ra for finalizing $^{224}Ra_{ex}$
2. Precise ^{226}Ra on small volume (<2L) sea water samples with ICP-MS; this information will then be brought together with onboard ^{222}Rn measurements to see if a disequiibrium between ^{222}Rn and ^{226}Ra was present.
3. $^{228}Ra/^{226}Ra$ ratios in leached Mn-fiber and Mn-cartridges by gamma spectrometry
4. Electron microscopy, including energy dispersive X-Ray spectroscopy (EDX) to characterize elemental distribution on filter aliquots
5. Quantitative bulk element analyses on filter samples

Data management

Environmental data will be archived, published and disseminated according to international standards by the World Data Center PANGAEA Data Publisher for Earth & Environmental Science (https://www.pangaea.de) within two years after the end of the cruise at the latest. By default, the CC-BY license will be applied.

Any other data will be submitted to an appropriate long-term archive that provides unique and stable identifiers for the datasets and allows open online access to the data.

This expedition was supported by the Helmholtz Research Programme “Changing Earth – Sustaining our Future” Topic 2, Subtopics 1 and 4, Topic 4, Subtopic 1 and Topic 6, Subtopics 2 and 3.

In all publications based on this expedition, the **Grant No. AWI_PS133/2_07** will be quoted and the following publication will be cited:

Alfred-Wegener-Institut Helmholtz-Zentrum für Polar- und Meeresforschung (2017) Polar Research and Supply Vessel POLARSTERN Operated by the Alfred-Wegener-Institute. Journal of large-scale research facilities, 3, A119. http://dx.doi.org/10.17815/jlsrf-3-163.

References

Sanial V et al. (2015) Use of Ra isotopes to deduce rapid transfer of sediment-derived inputs off Kerguelen. Biogeosciences 12:1415–1430. https://doi.org/10.5194/bg-12-1415-2015

9. MACRO- AND MEGABENTHIC METHANE SEEP FAUNA

Katrin Linse[1], Madeline P.B.C. Anderson[1], [1]UK.BAS
Sabine Kasten[2]; [2]DE.AWI
not on board: Philip R Hollyman[1], [3]UK.NCL
William D.K. Reid[3], Jason Newton[4] [4]UK.GLA

Grant-No. AWI_PS133/2_08

Objectives

Methane is confirmed as one of the potent climate change gases with a global warming potential higher than carbon dioxide (Wadham et al., 2012). Marine methane in the Southern Ocean (SO) is estimated to comprise about a quarter of the Earth's marine methane (Michaud et al., 2017). In recent years, first records of methane seepages from the seafloor and raised methane concentrations in the overlying water column have been reported from sub-Antarctic islands and the Antarctic shelf (Römer et al., 2014; Geprägs et al., 2016; de Valle et al., 2017; Spain et al., 2019). Research to date has focussed on the Arctic, with investigations on the origins, amounts and effects on the ecosystem of methane emissions (Åström et al., 2018, 2020), but there has been minimal research in the SO. More specifically, significant gaps exist in relation to the responses of the SO benthic faunal communities to methane and their role in whether seepage areas are sources or sinks.

To date research on methane as a climate change gas with global warming potential has focussed on terrestrial methane (Wadham et al., 2012; Michaud et al., 2017). Marine methane in the SO could play an important role in a) climate change and b) may also impact SO biodiversity and ecosystem function as a result of the increased marine methane seepage caused by warming of the Antarctic continental shelf.

Evidence of methane seepage has come from a number of sources including the detection of raised methane in sediments at the eastern Antarctic Peninsula, gas flares on the Kerguelen Plateau, gas hydrate in the South Georgia shelf and methane seepage including bacterial mats in nearshore, shallow waters of the Ross Sea (Bohrmann et al., 2017; del Valle et al., 2017; Spain et al., 2019; Thurber et al., 2020). However, to date no living chemosynthetic mega- or macrofauna, generally associated with deep-sea methane seepage have been reported from the SO seepage sites.

The benthic fauna of South Georgia is highly diverse (1,445 species; Hogg et al., 2011), and marked by a cumulative dominance of endemic and range-edge species, as well as by a high number of recorded rare species. Before the discovery of methane seepage by Römer et al. (2014) no confirmed cold seep activities were known from the continental shelf of South Georgia and to date no chemosynthetic benthic fauna has been reported. Bell et al. (2016) studied the composition and trophic structure of macrofauna from southwestern troughs, characterized by elevated methane levels in the sediments, and reported on very limited contribution of methane–derived carbon to the food web. Linse and Hogg during cruise M134 (Bohrmann et al., 2017) noted higher macrofaunal abundances in samples from the methane-elevated sediments in the southwestern troughs of South Georgia than in samples from seepage sites

in the northern ones, but neither community composition nor trophic interactions have been fully investigated across the full range of methane seepage conditions. In the eastern Antarctic Peninsula, benthic fauna from carbon-enriched sites suggests that these are from opportunistic taxonomic groups, which are often found in association with methane seepage but are not dependent on it (Bell et al., 2016, 2017). This pattern has been observed in other areas of the ocean where methane seepage occurs but lacks charismatic megafauna which are often observed in methane seep habitats (Åström et al., 2018, 2020). This suggests that the role of methane sustaining marine benthic food webs is being underestimated, and that identifying seepage locations may be too reliant on larger, visual cues.

This project will investigate the community composition, functional traits and trophodynamics of benthic fauna from methane seepage influenced habitats at South Georgia and compare it to benthic fauna from carbon enriched habitats in the SO, which are hypothesised or known to be influenced by methane seepage. The research will use a combination of the biogeochemical techniques (e.g. stable isotope and lipid analyses) to elucidate the food source of benthic fauna and establish the degree of dependence on methane sources; morphological analysis to identify species and establish potential functional traits; and statistical analysis to understand the response of the benthic communities to varying sediment geochemical conditions. There will be an emphasis on understanding the role of bivalves as potential indicator species of hydrocarbon- and carbon-enriched habitats in the SO, which will lead to a biogeographical analysis and the identification of potential future exploration sites.

The objectives of the benthic methane seep fauna project are:

- Study species richness, abundance, community composition, functional traits and small-scale distributions of macro- and megabenthic fauna in methane influenced habitats and link these to environmental parameters. Species distributions will be assessed vertically in the sediment and at different methane seepage sites – multicorer and Rauschert Dredge collections;
- Elucidate the trophic role of macrobenthic fauna in local South Georgia food web and their reliance on methane seep associated food sources – multicorer and Rauschert Dregde collections, stable isotope analyses of soft tissues and bivalve shells;
- Compare South Georgia methane seepage influenced habitat community composition with other SO and shallow water methane seep communities – literature records, multicorer collections.

Work at sea

We worked closely with the marine sedimentologists, microbiologists and geochemists on the methane-influenced habitats on the shelf of South Georgia, especially in the Cumberland Bay Fjord and the King Haakon Bay and their associated troughs 5 and 9 as model areas. We co-used tubes from the 8-tube (10 cm diameter) OKTOPUS Ltd multicorer (MUC) deployments for quantitative macrofauna assessments and performed a Rauschert Dredge (RD) deployment for qualitative megafauna collections (Fig. 9.1).

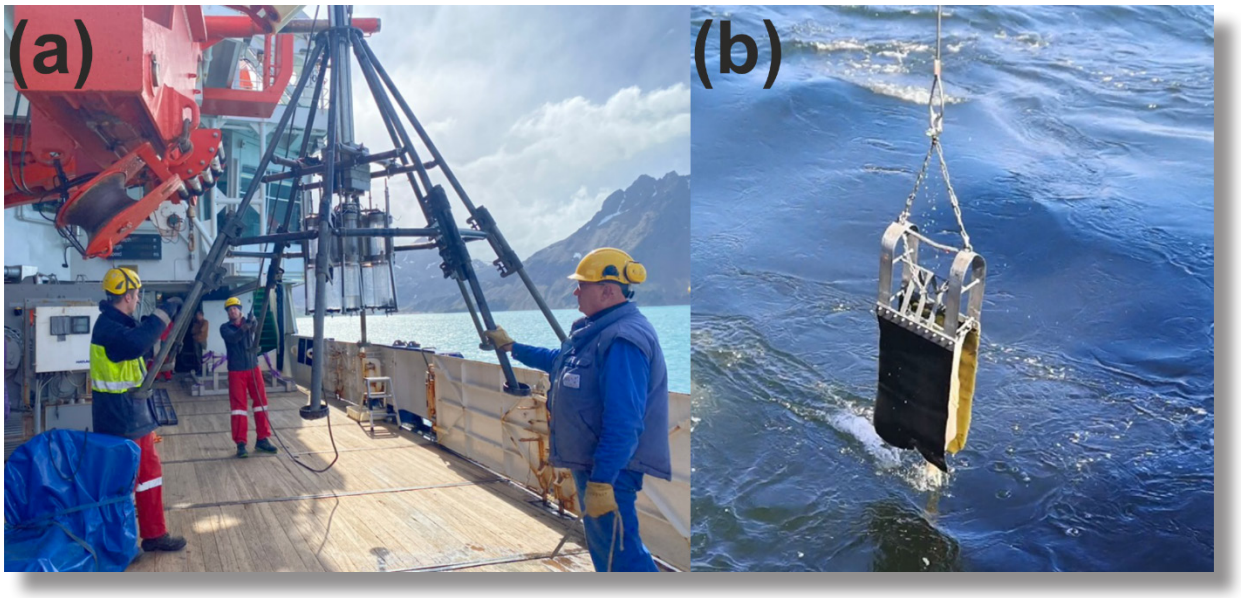

Fig. 9.1: a) Multicorer on deployment, b) Rauschert Dredge on deployment (photos: a) © Isabella Wilkie, b) © Madeline Anderson)

Multicorer work:

At those locations where MUC deployments were scheduled, two deployments were done to fulfil the requirements for MUC corer tubes. On arrival on deck, all tubes of the MUC were photographed to record sediment core length, layering and colour (see Appendix A.6). After tubes were assigned for geochemical and microbiological analyses of pore water, methane, solid phase, microbiology and isotopes, the remaining tubes were available for macrofauna analyses. For quantitative abundance analyses and comparison with previous macrofaunal studies, each tube was sliced at 0-2 cm and 2-5 cm layers using a core extruder, resulting in at least two individual samples per tube (Table 9.1). Mobile, larger macrofauna visible on the top of tubes or deeper than 5cm in the cores were sampled separately (Table 9.3). The sliced samples for macrofauna analysis were sieved in the wetlab through 300 µm sieves with ambient sea water (temperature of 2-5°C) and fixed in bulk in 96% ethanol or individually frozen. After at least 48 h ethanol fixation at -20°C, the bulk samples were ready to be sorted to different taxonomic levels, from order to morphospecies level, under a Meiji stereomicroscope, counted and transferred to appropriate curatorial vials. Sorting on board was aborted halfway through sample A001 (Table 9.2) as the vessel's movement and station schedules affected it.

Rauschert Dredge work:

The Rauschert Dredge was deployed once the shelf near the Annenkov Trough, while trawling in the vicinity of methane seepage to collect megafaunal specimens in Cumberland Bay near Grytviken Flare was had to be cut for time constrains. On arrival on deck, the catch was cleaned by sieving under ambient sea water, sorted to morphospecies, photographed, and fixed as full specimens or tissue samples in ethanol or frozen for later morphological and food web analyses.

All macrobenthic samples, which were all collected on the continental shelf of South Georgia, were transferred from *Polarstern* to the British Research Station King Edward Point for further analysis at the British Antarctic Survey, UK.

Preliminary (expected) results

At sea, benthic macrofauna samples from the MUC and RD depoyments were sorted, fixed according to their further analyses, and labelled with consequative numbers indicating their analyses (Tables 9.1 to 9.4). All samples were given general animal numbers “Axxx” and full specimens or tissue samples were fixed for barcoding and biodiversity analyses in 96 % ethanol and stored at -20°C. In total 179 “A-xxx” numbers were given out. 56 full specimens or tissue samples labelled “R-xxx” were fixed in RNAlater for genomic analysis and stored at -20°C. 108 full specimens or tissue samples labelled “ISO-xxx” were initially frozen at -80°C for stable isotope analyses and later transferred to -20°C. 54 tissue samples “CRYO-xxx” and 17 full specimens or tissue samples “BIO-xxx” were frozen at -80°C for lipid and genome analyses.

Multicorer work:

In total 43 core tubes from 8 locations were taken from 12 out of 15 MUC deployments.

Tab. 9.1: Quantitative unsorted MUC core samples. All fixed in 96 % ethanol. Slices of cores taken at 0 (sediment surface) - 2cm and 2-5 cm.

Station No.	Sampling Depth (m)	Location	MUC No.	Core	Depth (cm)	Vial ID
PS133-2_09_02	379	Church Trough	1	7	0-2	A-001
					2-5	A-002
				1	0-2	A-003
					2-5	A-004
				2	0-2	A-005
					2-5	A-006
PS133-2_12_01	257	Outside Posession Bay	2	5	0-2	A-011
					2-5	A-012
			3	1	0-2	A-013
					2-5	A-014
				2	0-2	A-015
					2-5	A-016
				3	0-2	A-017
					2-5	A-018
				4	0-2	A-019
					2-5	A-020
				5	0-2	A-021
					2-5	A-022
				6	0-2	A-023
					2-5	A-024
				7	0-2	A-025
					2-5	A-026
				8	0-2	A-027
					2-5	A-028

Station No.	Sampling Depth (m)	Location	MUC No.	Core	Depth (cm)	Vial ID
PS133-2_15_03	357	Posession Bay	4	6	0-2	A-029
					2-5	A-030
				2	0-2	A-032
					2-5	A-033
				3	0-2	A-034
					2-5	A-035
				4	0-2	A-036
					2-5	A-037
PS133-2_15_05			5	5	0-2	A-038
					2-5	A-039
				6	0-2	A-040
					2-5	A-041
				7	0-2	A-042
					2-5	A-043
				8	0-2	A-044
					2-5	A-045
PS133-2_17_12	343	outer King HT (near AT)	7	8	0-2	A-059
					2-5	A-060
				7	0-2	A-061
					2-5	A-062
				3	0-2	A-063
					2-5	A-064
				2	0-2	A-065
					2-5	A-066
				1	0-2	A-067
					2-5	A-068
PS133-2_23_10	154	inner King Haakon Bay	9	5	0-2	A-069
					2-5	A-070
				4	0-2	A-071
					2-5	A-072
				3	0-2	A-073
					2-5	A-074
				2	0-2	A-075
					2-5	A-076
				1	0-2	A-077
					2-5	A-078

Station No.	Sampling Depth (m)	Location	MUC No.	Core	Depth (cm)	Vial ID
PS133-2_32_17	256	Grytviken Bay	10	1	0-2	A-180
					2-5	A-181
				2	0-2	A-182
					2-5	A-183
				4	0-2	A-184
					2-5	A-185
				6	0-2	A-186
					2-5	A-187
				7	0-2	A-188
					2-5	A-189
PS133-2_32_18			11	5	0-2	A-190
					2-5	A-191
PS133-2_35_07	160	off Nordenskjöld Glacier	13	1	0-2	A-194
					2-5	A-195
				2	0-2	A-196
					2-5	A-197
				3	0-2	A-198
					2-5	A-199
				4	0-2	A-200
					2-5	A-201
PS133-2_35_08			14	1	0-2	A-202
					2-5	A-203
				8	0-2	A-204
					2-5	A-205
PS133-2_37_03	139	off KEP	15	1	4	A-207

Tab. 9.2: Incomplete sorting of MUC core sample vial A-001. Impressions of first taxa identified. Fixed in 96 % ethanol. 0-2 cm, core 7, MUC 1, depth 379 m, on 26/11/2022, station 09_02 from Church Trough.

Vial ID	Taxon	Phyla
A-047	Mysidacea	Arthropoda
A-048	Tanaidacea	Arthropoda
A-049	Polychaeta no tube	Annelida
A-050	Nematoda	Nematoda
A-051	Cumacea	Arthropoda
A-052	Copepoda harpacticoid	Arthropoda
A-053	Sipunculida	Sipunculida
A-054	Polychaeta tube	Annelida
A-055	Bivalvia	Mollusca
A-056	Gastropoda	Mollusca
A-057	Isopoda	Arthropoda
A-058	Ostracoda	Arthropoda

The first, subjective impression of sorting the 0-2 cm fraction of MUC core sample A-001 showed large numbers of harpacticoid copepods and few nematodes compared with macrofauna abundances of the MUC cores from the *Meteor* expedition M134.

Tab. 9.3: Qualitative MUC samples and/or subsampling taken. A-xxx samples in 96 % ETOH (apart from A-031 which was kept dry), ISO- and BIO- were frozen in -80°C then transferred to -20°C.

Station No.	Depth (m)	Kit No.	Core	Depth (cm)	Phyla	Vial ID
PS133-2_09_02	379	1	4	0-5	ALL	A-007
PS133-2_12_01	257	2	4	~0-5	ALL	A-008
			1	~0-5	ALL	A-009
			8	~0-5	ALL	A-010
			5	5+	Sipunculida	ISO-001
			5	5+	Sipunculida	ISO-002
		3	6	8	Annelida	ISO-003
PS133-2_12_02	256	2	5	?	Annelida	ISO-004
PS133-2_15_03	357	4	8	Top	Mollusca	A-031
PS133-2_15_05			6	Bottom	Sipunculida	A-046
						BIO-001
						CRYO-001
						ISO-005
						ISO-006
PS133-2_17_11	343	6	5	Surface	Arthropoda	BIO-002
			6	Bottom	Sipunculida	ISO-008
						ISO-009
						ISO-010
						ISO-011
						ISO-012
						ISO-013
						ISO-014
						ISO-015
PS133-2_17_12	343	7	3	Deep	Annelida	BIO-003
						ISO-007
PS133-2_32_18	256	11	2	Deep	Annelida	A-192
PS133-2_35_06	160	12	6	?	Mollusca	A-206
				Surface	Echinodermata	ISO-109
				?	Mollusca	ISO-110

Rauschert Dredge work:

One Rauschert Dredge was deployed on the shelf of Annenkov Trough near a site that has been investigated by ROV during M134 and showed dense abundances of filter feeding benthic macrofauna. A 10 min trawl of the 43 cm wide Rauschert Dregde resulted in a small, but well preserved collection of macro- and megabenthic specimens, which were sieved on deck and presorted, before selected specimens for further analyses were kept in ambient temperature sea water filled buckets until they were worked on (Table 9.4, Fig. 9.2). Excess marine invertebrate specimens were kept alive in ambient seawater filled bucket and returned to the ocean. No fish (vertebrates) were collected.

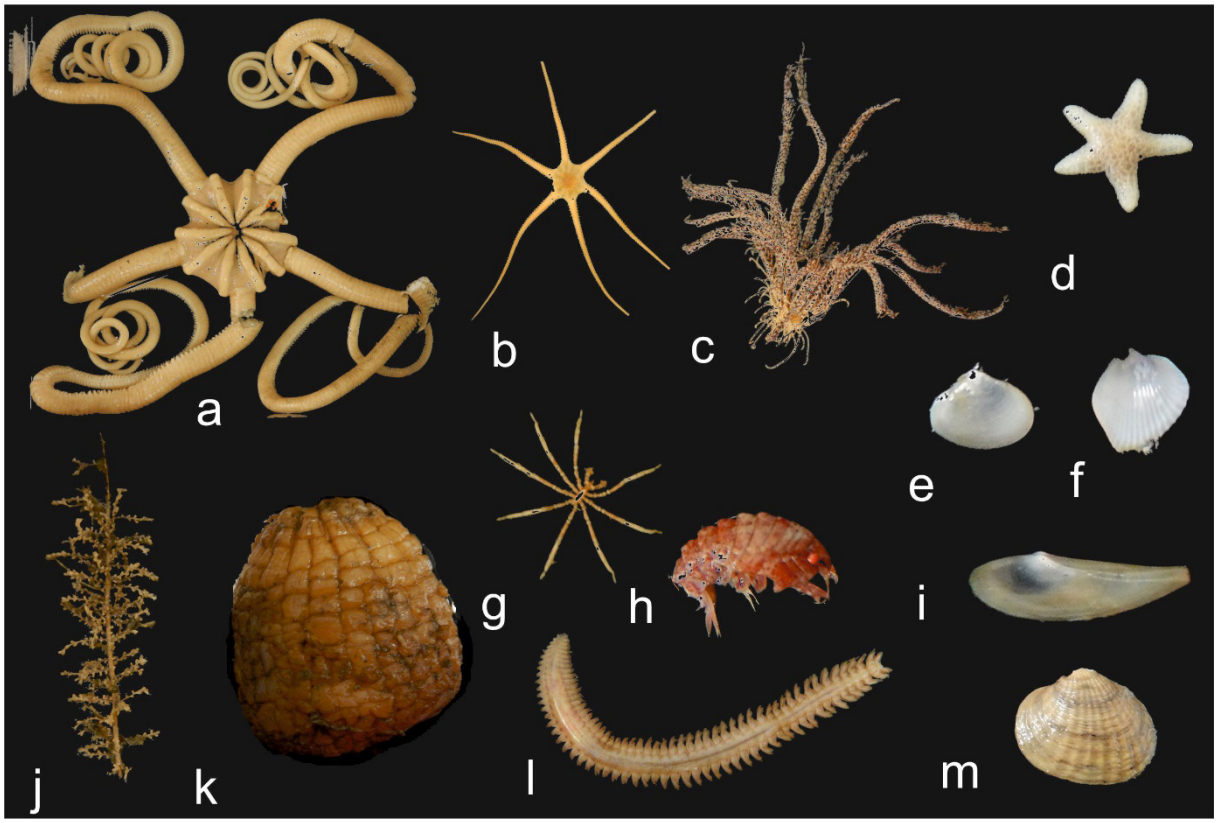

Fig. 9.2 Examples of benthic macro- and megafaunal invertebrates collected by the Rauschert Dredge: a) Austrotoma agassizi; b) ophiuroid; c) Promatocrinus sp.; d) asteroid; e) Ptychocardia vanhöffeni; f) Thracia meridionalis; g) pycnogonid; h) Epimeria cf. georgiana; i) Propeleda longicaudata; j) primnoid soft coral; k) Hormathia sp.; l) nephtyid polychaete; m) Cyclocardia astartoides. (photos: © Isabella Wilkie)

Tab. 9.4: A-numbers (96 % ethanol) and subsamples in R-xxx (RNAlater), CRYO-xxx & BIO-xxx (-80°C), and ISO- (-80°C → -20°C) from the Rauschert Dredge at 140 m water depth near the Annenkov Trough, qualitative, station number PS133-2_25_01, on 30 November 2022.

Vial ID	Subsample	N.	Taxon
A-080	R-001, BIO-004, CRYO-002, ISO-017	1	Cephalopoda
A-081	CRYO-003, ISO-028, BIO-005	1	Ophiuroidea
A-082	ISO-019	1	Pycnogonida
A-083	CRYO-004, BIO-006, ISO-020	1	Hydrozoa
A-084	CRYO-005, ISO-021, ISO-020, B-007	1	Hydrozoa
A-085	CRYO-006, ISO-022, ISO-023	1	Crinoidea
A-086	CRYO-007, ISO-024	1	Ophiuroidea
A-087	CRYO-008, ISO-025	1	Ophiuroidea
A-088	CRYO-009, ISO-026	1	Ophiuroidea
A-089	ISO-027, CRYO-010	1	Polychaeta
A-090	ISO-028, ISO-029	1	Crinoidea
A-091	CRYO-011, R-002, ISO-030	1	Pycnogonida
A-092	ISO-031a, CRYO-012, R-003	1	Polychaeta
A-093	ISO-031b, BIO-008	1	Ophiuroidea

Vial ID	Subsample	N.	Taxon
A-094	ISO-032a	1	Ophiuroidea
A-095	CRYO-013	1	Bryozoa
A-096	BIO-009, R-004	1	Gorgonaria
A-097	ISO-033, CRYO-014, R-005	1	Gorgonaria
A-098	ISO-034, CRYO-015, R-006	1	Gorgonaria
A-099	N	1	Gorgonaria
A-100	N	1	
A-101	ISO-035	1	Ophiuroidea
A-102	N	1	Polychaeta
A-103	ISO-036	1	Pycnogonida
A-104	CRYO-16, BIO-010, ISO-037	1	Porifera
A-106	ISO-032b	1	Ophiuroidea
A-109	CRYO-019, ISO-040	1	Hydrozoa
A-110	CRYO-020, ISO-041	1	Ascidiacea
A-111	ISO-042	1	Hirudinea
A-112	ISO-043, CRYO-021	1	Ophiuroidea
A-113	ISO-044, CRYO-022	1	Polychaeta
A-114	ISO-045, CRYO-023	1	Polychaeta
A-115	R-008	1	Hirudinea
A-116	R-009	1	Gorgonaria
A-117	N	1	Polychaeta
A-118	ISO-046, CRYO-024	1	Hydrozoa
A-119	ISO-047, CRYO-025, R-010	1	Porifera
A-120	ISO-048, CRYO-026, R-011	1	Bryozoa
A-121	ISO-051	1	Ophiuroidea
A-122	ISO-049	1	Ophiuroidea
A-123	ISO-050	1	Ophiuroidea
A-124	CRYO-027, ISO-052, R-012, BIO-011	1	Pycnogonida
A-124	R-016, BIO-012, BIO-013, CRYO-036, ISO-071, CRYO-37, ISO-072, CRYO-038, ISO-073, CRYO-039, ISO-074, CRYO-040, ISO-075	13	Amphipoda
A-125	ISO-053	1	Ophiuroidea
A-126	ISO-054	1	Ophiuroidea
A-127	ISO-055, CRYO-028	1	Ophiuroidea
A-128	R-013	1	Pycnogonida
A-129	ISO-086, CRYO-029	1	Ophiuroidea
A-130	ISO-058	1	Ascidiacea
A-131	ISO-059	1	Bryozoa
A-132	ISO-057	1	Pycnogonida
A-133	ISO-060, CRYO-030	1	Ophiuroidea
A-134	ISO-061, ISO-062, CRYO-031, ISO-063, R-014, ISO-064, ISO-065, CRYO-032, CRYO-033, R-015	1	Ophiuroidea
A-135	ISO-066	1	Ascidiacea
A-136	ISO-067, CRYO-034	1	Ascidiacea

Vial ID	Subsample	N.	Taxon
A-137	N	1	Gorgonaria
A-138	ISO-068	1	Polychaeta
A-139	C-035	1	Ophiuroidea
A-140	ISO-070	1	Ophiuroidea
A-141	ISO-069	1	Ophiuroidea
A-143	R-017, CRYO-041	7	Bivalvia
A-144	ISO-076, ISO-077, ISO-078, ISO-079, CRYO-042, CRYO-043, CRYO-044, BIO-014, R-018, R-019	14	Cumacea
A-145	R-020, ISO-080, CRYO-045	7	Bivalvia
A-146	CRYO-046, CRYO-047, ISO-083	6	Bivalvia
A-147	ISO-081, ISO-082, BIO-015, BIO-016	1	Bivalvia
A-148	CRYO-048, ISO-084, CRYO-049, ISO-085	2	Polychaeta
A-149	R-021, BIO-017	1	Isopoda
A-150	N	18	Amphipoda
A-151	ISO-087	1	Echinoidea
A-152	N	1	Polychaeta
A-153	N	2	Polychaeta
A-154	N	1	Polychaeta
A-155	ISO-088	1	Asteroidea
A-156	ISO-086, CRYO-050	1	Isopoda
A-157	R-022	1	Echinoidea
A-158	ISO-089	1	Polychaeta
A-159	CRYO-051, ISO-090	1	Holothuroidea
A-160	ISO-091	1	Decapoda
A-161	R-023, R-024, R-025, R-026	7	Bivalvia
A-162	N	7	Cumacea
A-163	N	4	Polychaeta
A-164	N	1	Pycnogonida
A-165	N	~3	Amphipoda
A-166	ISO-092, CRYO-052	2	Decapoda
A-167	ISO-093	1	Decapoda
A-168	R-030, R-031, ISO-094, ISO-095, ISO-096	10	Pycnogonida
A-169	ISO-097	2	Hexactinellida
A-170	R-032, R-033, R-034	9	Echinoidea
A-171	R-035, R-036, R-037, R-038, R-039	8	Isopoda
A-172	ISO-098, ISO-099, ISO-100, ISO-101	12	Polychaeta
A-173	N	2	Echinoidea
A-174	ISO-102	1	Asteroidea
A-175	ISO-103	1	Asteroidea
A-176	N	2	Amphipoda
A-177	ISO-104	1	Hydrozoa
A-178	R-040, R-041, R-042, R-043, R-044, R-045, R-046, R-047	26	Bivalvia

Vial ID	Subsample	N.	Taxon
A-179	R-048, R-049, R-050, R-051, R-052, R-053, ISO-105, ISO-106, R-054, CRYO-053, ISO-107, ISO-108, CRYO-054, R-055, R-056	33	Gastropoda
R-027	N	1	Isopoda
R-028	N	1	Isopoda
R-029	N	1	Bivalvia

The results of our planned stable isotope and food web analyses on benthic fauna will allow us to elucidate longer-term dietary signals (including those characteristic of feeding on pelagic copepods identified by fatty acid marker analysis) will allow to estimate what role methane seepage plays in the South Georgia food web and carbon draw down.

Data management

Environmental data will be archived, published and disseminated according to international standards by the World Data Center PANGAEA Data Publisher for Earth & Environmental Science (https://www.pangaea.de) within two years after the end of the cruise at the latest. By default, the CC-BY license will be applied.

Molecular data (DNA and RNA data) will be archived, published and disseminated within one of the repositories of the International Nucleotide Sequence Data Collaboration (INSDC, www.insdc.org) comprising of EMBL-EBI/ENA, GenBank and DDBJ).

Any other data will be submitted to an appropriate long-term archive that provides unique and stable identifiers for the datasets and allows open online access to the data.

After identification, macro- and megabenthic biodiversity data will be submitted to, archived, published and disseminated by the UK Polar Data Centre (PDC) hosted at the British Antarctic Survey. Physical collected specimens, when not destroyed for analyses, will be stored at the British Antarctic Survey until analyses publication and then archived in a natural history museum for international access.

This expedition is supported by the Helmholtz Research Programme “Changing Earth – Sustaining our Future” Topic 2, Subtopics 2.1 and 2.4, Topic 4, Subtopic 4.1 and Topic 6, Subtopics 6.2 and 6.3.

In all publications based on this expedition, the **Grant No. AWI_PS133/2_08** will be quoted and the following publication will be cited:

Alfred-Wegener-Institut Helmholtz-Zentrum für Polar- und Meeresforschung (2017) Polar Research and Supply Vessel POLARSTERN Operated by the Alfred-Wegener-Institute. Journal of large-scale research facilities, 3, A119. http://dx.doi.org/10.17815/jlsrf-3-163.

References

Åström EKL, Carroll ML, Ambrose JR, WG, Sen A, Silyakova A, Carroll J (2018) Methane cold seeps as biological oases in the high-Arctic deep sea. Limnology and Oceanography 63:S209–S231. https://doi.org/10.1002/lno.10732

Åström EKL, Sen A, Carroll ML, Carroll J (2020) Cold Seeps in a Warming Arctic: Insights for Benthic Ecology. Frontiers in Marine Science, https://doi.org/10.3389/fmars.2020.00244

Bell JB, Aquilina A, Woulds C, Glover AG, Little CTS, Reid WDK, Hepburn LE, Newton,J, Mills RA (2016) Geochemistry, faunal composition and trophic structure in reducing sediments on the southwest South Georgia margin. Royal Society Open Science 3:160284. http://dx.doi.org/10.1098/rsos.160284

Bell JB, Reid WDK, Pearce DA, Glover AG, Sweeting CJ, Newton J, Woulds C (2017) Hydrothermal activity lowers trophic diversity in Antarctic hydrothermal sediments. Biogeosciences 14:5705–5725.

Bohrmann G et al. 2017. R/V METEOR Cruise Report M134, Emissions of Free Gas from Cross-Shelf Troughs of South Georgia: Distribution, Quantification, and Sources for Methane Ebullition Sites in Sub-Antarctic Waters, Port Stanley (Falkland Islands) - Punta Arenas (Chile), 16 January - 18 February 2017. http://nbn-resolving.de/urn:nbn:de:gbv:46-00106081-12

Del Valle RA, Yermolin E, Chiarandini J, Sanchez Granel A, Lusky JC (2017) Methane at the NW of Weddell Sea, Antarctica. Journal of Geological Research Article ID 5952916. https://doi.org/10.1155/2017/5952916

Geprägs P, Torres ME, Mau S, Kasten S, Römer M, Bohrmann, G (2016) Carbon cycling fed by methane seepage at the shallow Cumberland Bay, South Georgia, sub-Antarctic. Geochemistry, Geophysics, Geosystems, 17(4):1401–1418. https://doi.org/10.1002/2016GC006276

Hogg OT, Barnes DKA, Griffiths HJ (2011) Highly diverse, poorly studied and uniquely threatened by climate change: an assessment of marine biodiversity on South Georgia's continental shelf. PLoS One 6:e19795. https://doi.org/10.1371/journal.pone.0019795

Michaud AB, Dore JE, AchbergerAM, Christner BC, Mitchell AC, Skidmore ML, Vick-Majors TJ, Priscu JC (2017) Microbial oxidation as a methane sink beneath the West Antarctic Ice Sheet. Nature Geoscience 10:582–586. https://doi.org/10.1038/ngeo2992

Römer M, Torres M, Kasten S, Kuhn G, Graham AGC, Mau S, Little C, Linse K, Pape T, Geprägs, P, Fischer D, Wintersteller P, Marcon Y, Rethemeyer J, Bohrmann G and shipboard scientific party ANT-XXIX/4 (2014) First evidence of widespread methane emissions around a Sub-Antarctic island (South Georgia). Earth and Planetary Science Letters 403:166–177. https://doi.org/10.1016/j.epsl.2014.06.036

Spain EA, Johnson SC, Hutton B, Whittaker JM, Lucieer V, Watson, SJ (2020) Shallow seafloor gas emissions near Heard andMcDonald Islands on the Kerguelen Plateau, Southern Indian Ocean. Earth and Space Science 7 https://doi.org/10.1029/2019EA000695

Thurber AR, Seabrook S, Welsh RM (2020) Riddles in the cold: Antarctic endemism and microbial succession impact methane cycling in the Southern Ocean. Proceedings of the Royal Socienty B.2872020113420201134. http://doi.org/10.1098/rspb.2020.1134

Wadham J, Arndt S, Tulaczyk S (2012) Potential methane reservoirs beneath Antarctica. Nature 488:633–637. https://doi.org/10.1038/nature11374

10. BIOGEOCHEMISTRY AND MICROBIOLOGY

Katja Laufer-Meiser[1], Josefine Friederike Weiß[2], Graciana Willis Poratti[3], Lea Wunder[4]
Not on board: Kathleen Stoof-Leichsenring[2], Michael Friedrich[4]

[1]DE.GEOMAR
[2]DE.AWI
[3]AR.IIA
[4]DE.UNI-Bremen

Grant-No. AWI_PS133/2_09

Objectives

The Biogeochemistry and Microbiology group has two main objectives: (1) To investigate microbial processes with a focus on iron and sulfur cycling in order to broaden our understanding on key anaerobic respiratory processes. In detail, we will investigate how they are controlled by the availability of electron acceptors, i.e. iron and sulfate; whichs availability is also impacted by glacial input in sediments around South Georgia (SG). (2) To investigate the identity of sedimentary ancient eurcaryotic DNA (sedaDNA) to draw conclusions on changes in biodiversity (of algae, animals and plants) over longer timescales under changing climate conditions.

For our first objective, we could show previously that the availability of electron acceptors (i.e. iron oxides and sulfate) has a strong impact on microbial communities in sediments from SG (Wunder et al., 2021). Intriguingly, known sulfate reducers appeared to be abundant in surface sediment, yet iron reduction was the dominant anaerobic respiratory process. To build up on these results, we plan to (a) study more sediment sites in transects from glacier to shelf, (b) determine rates of sulfate reduction (SRR) and anaerobic oxidation of methane (AOM, either coupled to sulfate reduction or the reduction of iron oxides), and (c) identify electron donors that might fuel sulfate reduction *in situ* using RNA stable isotope probing (SIP). Additionally, we plan to investigate the potential for the microbial degradation of the frequent algal sulfated sugar polymer fucoidan as well as lignin and lignin model compounds (vanillin). This includes the analysis of terrestrial samples as potential source of these compounds.

By applying kinetic iron extractions, we could show that in sediments of Svalbard fjords benthic cycling of iron is important for transforming iron from glacial sources (Laufer-Meiser et al., 2021). Also, within our first objective, we will investigate the reactivity of iron minerals towards microbial reduction in samples from glacial sources, the water column and sediment by kinetic iron extractions in order to see if we can find similar patterns as in Svalbrard fjords. Moreover, we will study microorganisms involved in iron cycling (by cultivation dependent and cultivation-independent methods) within the sediment samples.

For our second objective, analysis of sedaDNA will be done to identify the past taxonomic composition and turnover of various organisms throughout the sediment record. This can be discovered by either target-specific approaches like metabarcoding (Liu et al., 2021; Stoof-Leichsenring et al., 2022; Zimmermann et al., 2020, 2021) or total sedaDNA shotgun sequencing (Courtin et al., 2022; Schulte et al., 2021). This helps to understand biodiversity change under past natural climate and related environmental conditions as well as under intensified human impact during the recent past.

Work at sea

During expedition PS133/2 we collected sediment samples from MUC and gravity cores. Moreover, we collected samples of meltwater, glacial ice, sediment, soil and vegetation during sampling on land and from a Zodiac.

MUC work

Of each MUC deployment (listed in Table 10.1) the microbiology and biogeochemistry group obtained the following MUC cores:

- One core for SRR, Nucleic Acids (NA) extraction and CH_4
- One core for Fe-kinetics
- Two cores for sampling live sediments, except for stations 9, 12 and 15 where only one core was sampled
- One core, immediately frozen, for aDNA at selected stations

Tab. 10.1: List of MUC samples and types of subsamples that were taken.

Station and deployement name and area	Samples taken for
PS133/2_9-2, Church Trough	SRR, FeHCl, FeKin, dFe, NA, CH_4, live sediments
PS133/2_12-1, outer Posession Bay	SRR, FeHCl, FeKin, dFe, NA, CH_4, live sediments
PS133/2_15-3, inner Possession Bay	SRR, FeHCl, FeKin, dFe, NA, CH_4
PS133/2_15-5, inner Posession Bay	Live sediments, NA
PS133/2_17-11, King Haakon Trough	SRR, FeHCl, FeKin, dFe, MPN, NA, CH_4, live sediments
PS133/2_17-12, King Haakon Trough	Live sediments, NA
PS133/2_23-9, innermost King Haakon Bay	SRR, FeHCl, FeKin, dFe, MPN, NA, CH_4, live sediments
PS133/2_23-10, innermost King Haakon Bay	Live sediments, NA
PS133/2_32-18, Cumberland Bay, Grytviken Flare	SRR, FeHCl, FeKin, dFe, MPN, aDNA, NA, CH_4, live sediments
PS133/2_32-17, Cumberland Bay, Grytviken Flare	Live sediments, NA
PS133/2_35-6, innermost Cumberland Bay	SRR, FeHCl, FeKin, dFe, MPN, aDNA, NA, CH_4, live sediments
PS133/2_35-7, innermost Cumberland Bay	Live sediments, NA
PS133/2_42-8, Confluence Zone, outer Cumberland Bay	SRR, FeHCl, FeKin, dFe, MPN, aDNA, NA, CH_4, live sediments
PS133/2_42-9, Confluence Zone, outer Cumberland Bay	Live sediments, NA
PS133/2_50-7, mid-continental shelf off Cumberland Bay	SRR, FeHCl, FeKin, dFe, MPN, aDNA, NA, CH_4, live sediments
SRR = sulfate reduction rates; FeHCl = Fe extraction with HCl; FeKin = kinetic Fe extractions; dFe = dissolved Fe in porewater, MPN = most probable number incubations; NA= nucleic acids; aDNA= ancient DNA	

Processing of MUC cores:

For subsampling the core for SRR, nucleic acids and CH_4 a 2.5-cm coreliner was introduced (Fig. 10.1). The 2.5-cm coreliner had pre-drilled holes that were closed with a polyurethane-based elastic glue (Sikaflex 11FC). Afterwards, the MUC core was extruded and samples for nucleic and CH_4 were taken around the 2.5 cm coreliner. For nucleic acid samples 10 ml sediment samples were taken every 1 cm for the first 10 cm and every 2 cm for the rest of the core, using cut 5-mL syringes. The samples were then stored in 10 ml vials at -20°C. For CH_4 samples see the sediment geochemistry Chapter 4. Finally, for measuring SRR with the whole-core injection method (Jørgensen, 1978), the 2.5 cm subcore for SRR was closed with stoppers from top and bottom and incubated at 2°C for at least 24 h before 50 kBq of a ^{35}S-sulfate tracer/cm was injected and the subcores were incubated for 16-20 h at 2°C. The incubation was stopped by slicing the 2.5-cm subcore at 1 cm sections and adding the sediment to 50 ml vials containing 10 ml 20 % zinc acetate. SRR samples fixed in zinc acetate were stored at -20°C. For quantifying SRR the cold-chromium distillation method will be applied in the home laboratory at GEOMAR in Kiel (Kallmeyer et al., 2004; Røy et al., 2014).

The MUC core for Fe-kinetics was subsampled with a 6-cm diamenter coreliner, which was used to slice sediment under anoxic conditions at 2°C inside a glovebag as described in detail by Michaud et al. (2020). The core was sectioned at intervals of 1 cm from 0-4 cm sediment depth, 2 cm from 4-10 cm sediment depth, and at 3 cm intervals below. Of each slice, subsamples were taken for sequential HCl extractions (FeHCl), kinetic Fe-extractions (FeKin) and dissolved Fe (dFe). Samples for FeHCl and FeKin were placed into an anaerogen pack (containing an oxygen consuming pouch (AnaeroGen, ThermoFischer)) and stored frozen at 20°C. Samples for dFe were first centrifuged inside the glovebag for 15 minutes (Eppendorf Minispin, 13 400 rpm) and then the supernatant was transferred into spin-filters (0.45 μm nylon membrane, Norgen Biotek). The spin-filters were centrifuged for 3 minutes and finally 500 µl of the flow-through were added to 100 µl of 6 M HCl (1 M final concentration). dFe samples were stored at 4°C.

Fig. 10. 1*: Sampling MUC core with SRR subcore, taking sample for nucleic acids.*

From select sites, MPN (most probable number) incubations for microaerophilic Fe(II)-oxidizers, nitrate-reducing Fe(II)-oxidizers and Fe(III)-reducers were set up as described in Laufer et al., (2016). For Fe(II)-oxidizers, the section of the core containing the oxic-anoxic transition zone, as identified via microsensor measurements by the geochemistry group, was taken. For Fe(III)-reducers, the section of the core just below the oxic-anoxic transition zone was taken. At all sites, except PS133/2_50-7, oxygen was depleted at 0.5 cm sediment depth, such that a subsample of the 0-1 cm slice was used for Fe(II)-oxidizer MPNs and a subsample fo the 1-2 cm slice was used for Fe(III)-reducer MPNs. At site PS133/2_50-7 oxygen penetrated to 1.5 cm sediment depth, such that a subsample of the the 1-2 cm and 2-3 cm slice was used for preparation of Fe(II)-oxidizer and Fe(III)-reducer MPNs, respectively. After setup, MPNs were incubated at 4°C and will be further incubated for approximately 4-6 months until no further growth (by color change and microscopy) can be observed.

Cores for live sediments were sliced in 2 x 2 cm sections, filled into 250 ml glass bottles (= 4 cm sediment per bottle) and closed hermetically with butyl rubber stoppers and a plastic lid. The headspace of the bottles was flushed with N_2 (99.9999%) for approximately 15-20 minutes to eliminate O_2 and generate anaerobic conditions. The bottles were stored at 4°C (close to *in-situ* temperature) in the dark. In case that the cores for sampling living sediments came from different MUC deployments then the core used for more detailed nucleic acid sampling, a subsample for nucleic acid extraction was collected of the 4-cm section of the living sediment core. The “living” sediments will be used in the home laboratory in the University of Bremen to perform different types of incubation experiments, e.g., RNA Stable-Isotope-Probing (RNA-SIP).

The processing of cores for ancient DNA analysis will be done at the AWI in Potsdam to minimize risk of contamination. Therefore, the cores will be transported back as whole cores in tube foil at -20°C.

Gravity corer work

The following types of samples were taken of each gravity corer deployment on which sediment geochemistry was performed (Chapter 4) with some exceptions for aDNA samples (Tab. 10.2):

- Frozen for nucleic acid extraction
- Frozen for ancient DNA (aDNA)
- Living sediment
- Frozen pore water for lignin, fucoidan, methylated aromatic compound analysis

Samples for nucleic acid extractions were taken with 5 ml cut syringes by introducing the syringes into the cut-open gravity core before pore water extraction was started. After the pore water extraction was concluded, the syringes with the sediment were removed from the core and the sediment was stored in 10 ml tubes at -20°C. The samples were taken at the same depth as pore water and solid phase samples by the Sediment Geochemistry group (Chapter 4) in a depth interval of every 20 cm for the top 2 m followed by every 40 cm for the rest of the core.

Subsamples of the extracted pore water were frozen at -20°C for subsequent analyses of lignin, fucoidan and methylated aromatic compounds in the home laboratory in Bremen.

Living sediments were sampled after all other sampling was concluded by cutting out multiple 2 cm sections of the core along 1 m core pieces. The sediment was filled in 250 ml bottles (= pooled subsample of 1 m sediment per bottle), closed with butyl stoppers, flushed with N_2 and stored at 4°C in the dark, as described above.

Two gravity cores were taken at King Haakon Bay and innermost Cumberland Bay which were stored at 4°C and are transported back to Marum in Bremen, where they will be opened and one half will be stored completely for living sediment.

For subsampling the gravity core for ancient DNA only sterile devices were used. The subsamples were taken from cores from outer and inner Possession Bay, King Haakon Bay and King Haakon Trough and outer and inner Cumberland Bay area. Additionally, another core from the King Haakon Trough was subsampled. Two subsamples were taken with syringes every 50 cm over the total length of the core. All subsamples were frozen at -20°C and will be further processed in the clean paleogenetic laboratories of the AWI in Potsdam, Germany (https://www.awi.de/en/science/geosciences/polar-terrestrial-environmental-systems/labs-and-methods/paleogenetic-lab.html)

Tab. 10.2: List of gravity cores, total length and types of subsamples that were taken.

Station name and area	Length of the GC [cm]	Subsamples taken for
PS133/2_9-3, Church Trough	530	live sediments, NA
PS133/2_12-3, outer Possession Bay	745	aDNA, live sediment, NA
PS133/2_15-6, inner Possession Bay	685	aDNA, live sediment, NA
PS133/2_23-11, King Haakon Bay	1080	aDNA, NA
PS133/2_23-13, King Haakon Bay	*	live sediment+
PS133/2_17-14, King Haakon Trough	890	aDNA, live sediment, NA
PS133/2_26-1, King Haakon Trough		aDNA
PS133/2_32-16, outer Cumberland Bay	910	aDNA, live sediment, NA
PS133/2_35-10, mouth of Cumberland Bay	425	aDNA, NA
PS133/2_35-9, mouth of Cumberland Bay	*	live sediment+
PS133/2_42-10, shelf of Cumberland Bay	770	aDNA, live sediment, NA

**Length yet not available.*

These cores were kept at 4°C close and will be measured and split at MARUM, Bremen, at arrival for live sediments and geology. NA = nucleic acids; aDNA = ancient DNA

Sampling from the zodiac and on land

During sampling on land at the *innermost King Haakon Bay*, we sampled two visually different meltwater streams. At the first location (S 54° 08’ 42”, W 37° 16’ 34”) we sampled water from a meltwater stream with relatively turbid water (Fig. 10.2 A). At the second location (S 54°08’ 43’’ W37°16’33’’, Fig. 10.2 B) we collected meltwater from a meltwater stream with much less turbid water. Additionally, at both locations and at an additional third location (S 54° 08’ 41”, W 37° 16’ 36”) we collected fine sediment that accumulated at places within the meltwater river with low flow velocity. At a fourth location (S 54° 08’ 41”, W 37° 16’ 43”) we observed red precipitates indicating presence of Fe-rich water that apparently came from a groundwater seep (Fig. 10.2 C, D). At this location we also took water and sediment samples.

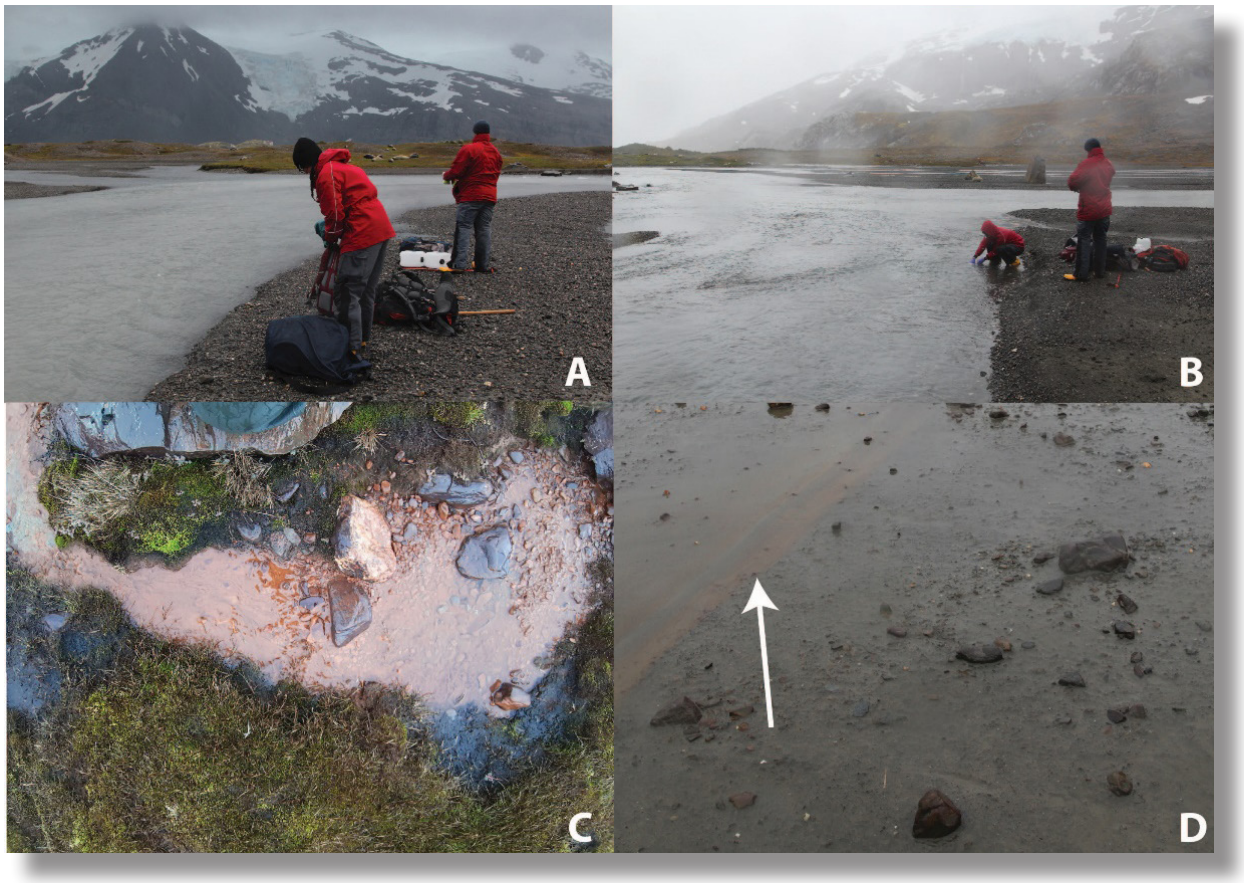

Fig. 10.2: Land-based sampling at the innermost King Haakon Bay. A: Turbid meltwater stream. B: Clear meltwater stream. C: Fe-rich groundwater seep. D: red flocks several meters (10-20 m) away from groundwater seep.

Vegetation and soil samples were taken from different locations in beach proximity. In general, the vegetation on land is very bare, but Tussock gras dominates areas close to the beach and areas where the glacier retreated longer ago (Fig. 10.3 A-C). These areas were also highly populated by fur seals and elephant seals, which likely influence the soil and terrestrial input by their remainings. In places where the ground is more baren, mainly moss and different *Acaena* species grow on rocky underground (Fig. 10.3 E). These plants stretch out widely with their roots/stalks and potentially contain lignin.

From each dominant Embryophyta one sample was taken for DNA marker analysis. Additionally, soil samples close to the vegetation were taken for DNA analysis. The vegetation samples were taken especially close to small rivers to investigate the terrestrial input into the marine ecosystem. Furthermore, root samples were taken for DNA analysis of roots that were introduced into small water ponds and small rivers.

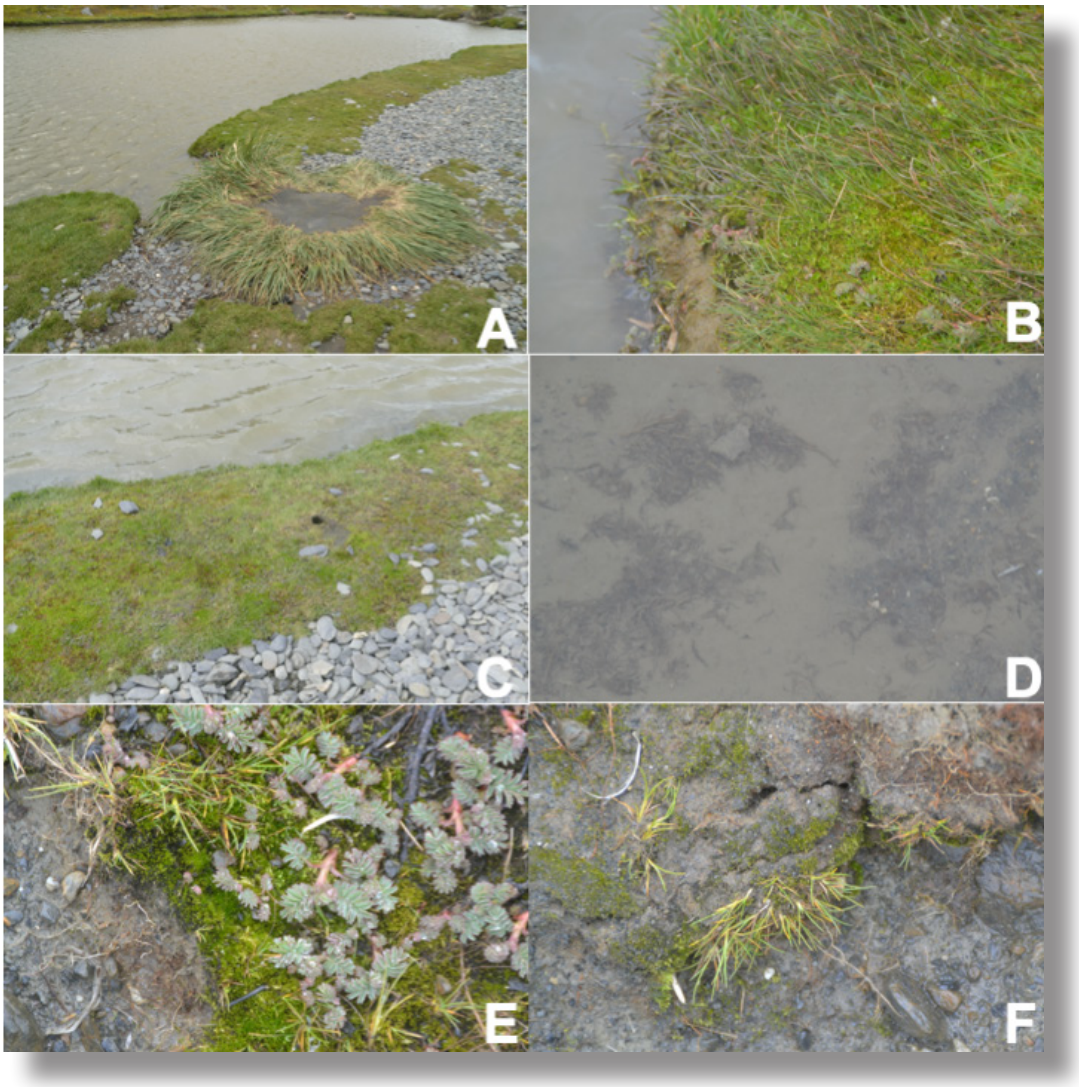

Fig. 10.3: Land-based sampling at the innermost King Haakon Bay. A: Small pond close to the beach with adjacent vegetation of bryophyta and Poaceae (Tussock grass). B: Close up of the vegetation. C: Example of soil sampling site at the same Station as A & B. D: Plants parts on sediment in a small river. E Vegetation on the river bank including Acaena spp. F: Vegetation on the river bank.

During sampling from a Zodiac within the *innermost Cumberland Bay*, just in front of the marine-terminating Nordenskjöld glacier (Fig. 10.4), we sampled glacial plume water, glacial ice, and sediment cores with a hand-held gravity corer. Glacial plume water was sampled at the stations S 54° 22.520' W 36° 23.707', S 54° 22.554' W 36° 23.871', S 54° 22.678' W 36° 23.058', and S 54° 23.092' W 36° 21.329'. For glacial ice samples we targeted small (ca. 30-50 cm diameter) ice-pieces that we collected all along the glacial front. The sediment core that the microbiology and geochemistry group was processing was sampled at S 54° 23.071' W 36° 21.031' at 57 m water depth.

Fig. 10.4: Sampling in front of the Nordenskjöld glacer. A: Glacal front on the right edge of the glacier. B: Turbid glacial meltwater plume in front of the right edge of the glacier. C: Piece of glacial ice. D: Close-up of glacial ice with frozen-in sediment and stones (dark spots).

During land-based sampling within *Moraine fjord*, we took our samples from a relatively turbid meltwater river, which apparently was one of the main rivers draining the glacier that was sitting further up in the mountains (Fig. 10.5 A). At the location S 54° 22.1399' W 036° 29.7256' we sampled meltwater and sediment from the river. At location S 54° 22'9'' W 36° 29'38'' we collected some pieces of glacial ice that originated from the smaller tidewater glaciers located at the head of Moraine fjord (Fig. 10.5 C).

Fig. 10.5: A: Approximate location of the sampling site in Moraine fjord. B: Meltwater river from where we took our samples. C: Small marine-terminating glaciers at the head of Moraine fjord. D: Glacial ice at the site where we landed with the zodiac.

During our visit in *Grytviken*, we attempted to sample meltwater from Penguin river, draining one of the larger land-terminating glaciers within Cumberland Bay (Fig. 10.6 A, C). However, due to the overwhelming abundance of fur seals along the beach preventing us from walking along the beach, and the steep slopes we would have had to climb down and up to reach the river via the kliff (Fig. 10.5 B), we were not successful. Instead, we took water samples from the drinking water reservoir just up the hill from Grytviken (Fig. 10.5 D). The water in the reservoir most likely comes mainly from snowmelt.

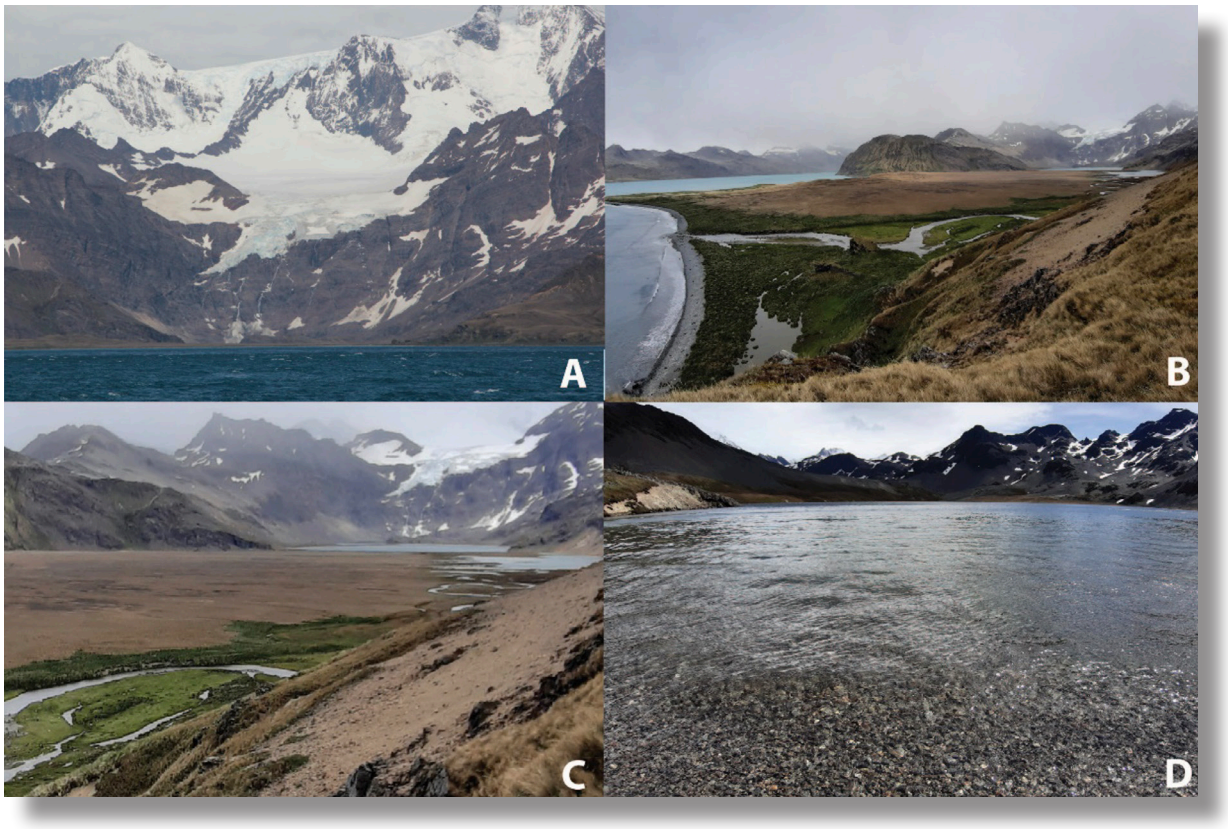

Fig. 10.6: A: Land-terminating glacier from which Penguin river originates. B: Mouth of Penguin river as seen from the top of the kliff. C: Close up of the glacier, it can be seen that the meltwater at first forms a lake and then flows into Penguin river. D: Sampling site at the reservoir at Grytviken.

The vegetation around Grytviken, Cumberland Bay, is much more established compared to the sampling site in King Haakon Bay, at the other side of the island. Here, thick meadows with different gras species and invasive species such as *Taraxacum officinalis* (Dandelion) dominate the vegetation. Sampling locations around Grytviken were located on top of the hills following creeks running above and below the gras and rocky areas downward to a thick vegetation stripe behind the beach, which was dominated by Tussock Grass and fur seals (Fig.10.7 A, B). Vegetation and soil samples were taken around the creeks and on the bottom of the creeks, similarly as in King Haakon Bay.

Tab. 10.3: List of zodiac and land-based samplings.

Station name and area	Types of samples taken
PS133/2_22_1&2, innermost King Haakon Bay	Meltwater, stream sediment, soil, vegetation
PS133/2_36_1&2, innermost Cumberland Bay	Plume water, glacial ice, sediment cores
PS133/2_37_5, Moraine Fjord, Grytviken	Meltwater, stream sediment, glacial ice, sediment cores
Grytviken	Water from reservoir, soil and vegetation from the hills and around the creeks

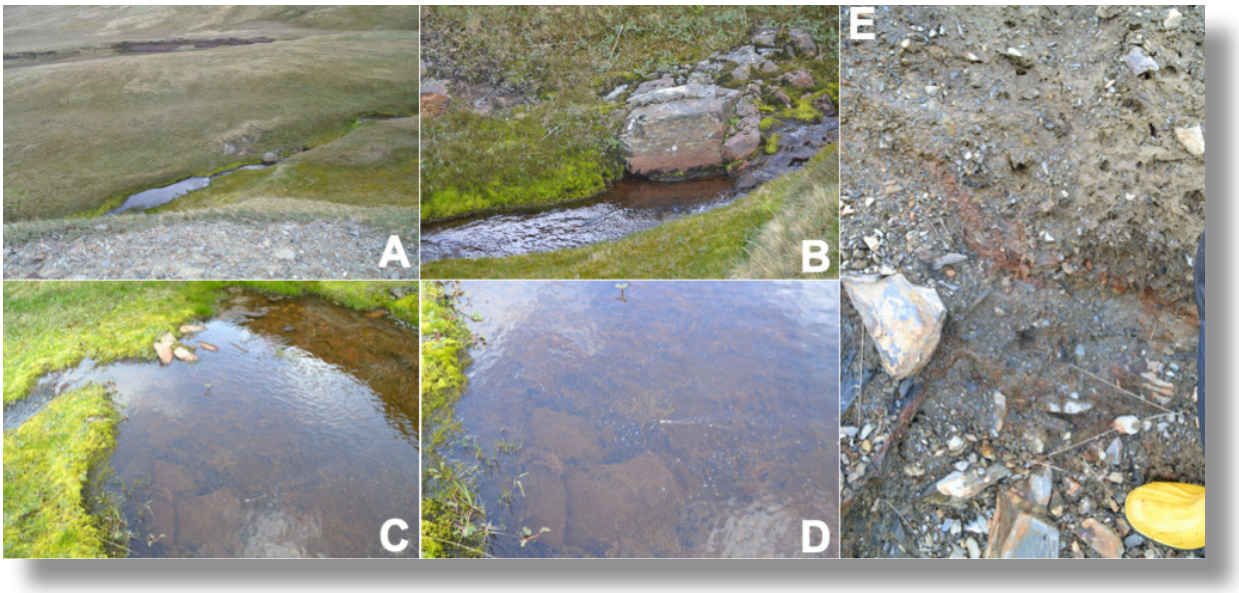

Fig. 10.7: A: Small river with vegetation growing around it on top of the hills. B: Close up of the vegetation on the river bank. C: Small pond with adjacent vegetation. D: Close up of roots that are introduced into the water and small water plants. E: Soil sampling site of a dried-up riverbed.

Processing of samples

All meltwater, stream sediment and glacial ice samples were frozen at -20°C and will be further processed in the home laboratory. The sediment cores were processed as described above for the 6 cm subcores taken from the MUC cores. The only difference was, that the cores were sliced in 1 cm sections throughout and that 1 cm^3 of sediment was additionally sampled and used for SRR incubations in glass-syringes that were closed with butyl stoppers. From the Grytviken site, additionally 0.5 cm^3 subsamples were fixed with 4% formaldehyde for 12 h, washed with PBS and stored in PBS/EtOH at -20°C for later analyisis via FISH (fluorescence *in-situ* hybridization).

All vegetation and soil samples were frozen at -20°C and will be further analyzed for DNA marker analysis at the AWI in Potsdam and for lignin content in Bremen, Germany.

Water sampling

During the station work and transit, seawater was filtered using the AutoFim. In total 35 filtrations were done for DNA sequencing at a depth of 11 meters at different sites around South Georgia (Fig. 10.8). All samples are stored at -20°C until further processing at the AWI in Bremerhaven.

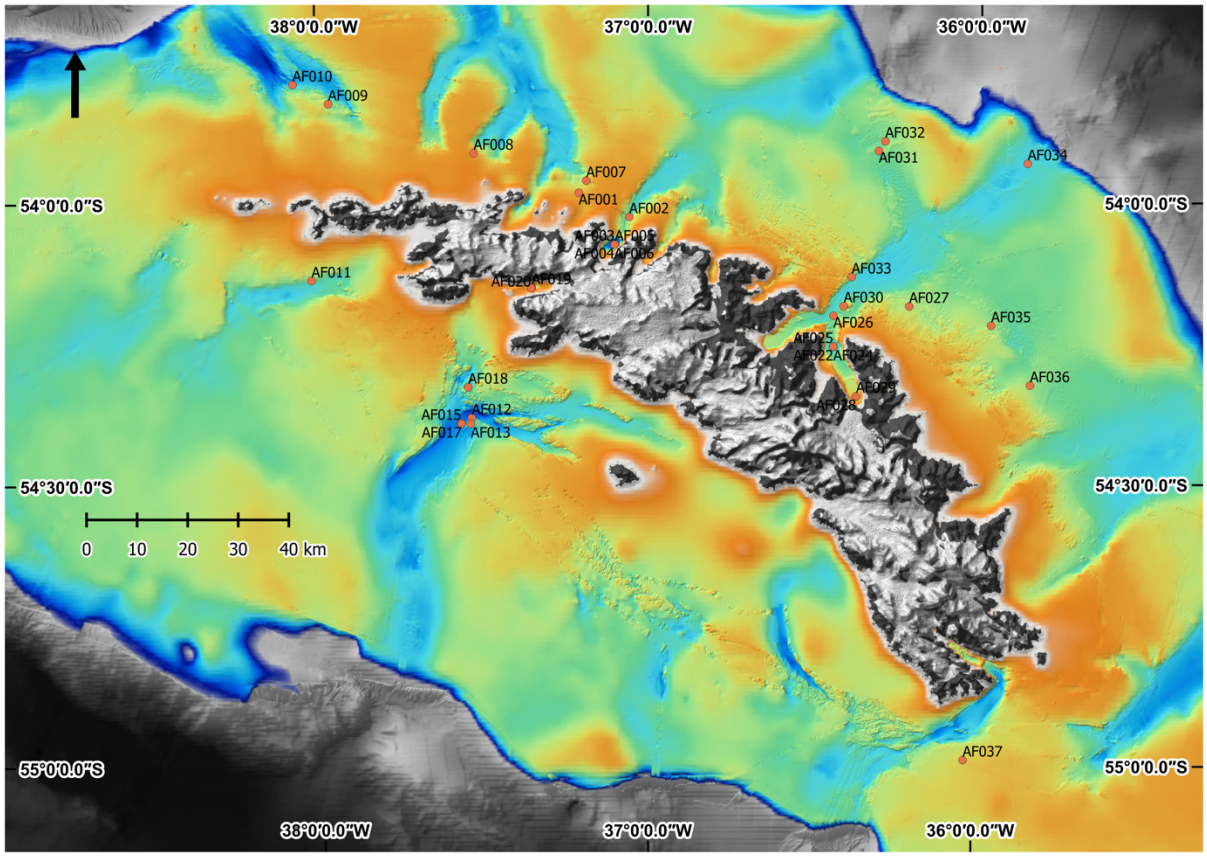

Fig. 10.8: Map of AutoFim filtration sites.

Preliminary and expected results

Expected results include SRR from surface sediments, the amount and reactivity of particulate iron in material from glacial sources, seawater and sediments, as well as numbers of Fe-oxidizers an -reducers present within the sediments (Tab. 10.1).

In the home laboratory at the University of Bremen, DNA and RNA will be extracted from the samples conserved for nucleic acid extraction and 16S rRNA (gene) sequencing will be performed in order to investigate the microbial community. The results will be compared to the geochemical data of the sediments and along the transects from glacier to shelf.

In order to further investigate potential activities, incubation experiments will be performed with living sediments, which is transported back anoxic at close to *in-situ* temperatures of 4°C. Especially the metabolic potentials of sulfate reducing microorganisms will by investigated by setting up stable isotope probing experiments (Yin et al., 2019) with ^{13}C labelled bicarbonate, sulfate and hydrogen as electron donor.

Applying the sedaDNA approach we expect to characterize changes of the local ecosystem and its environmental drivers in the past mainly covering centennial-millennial timescales depending on the resolution of sediment cores. As an example, previous sedaDNA analytics performed in our paleogenetic laboratories at AWI deciphered past diatom composition and its relation to sea-ice and climate dynamics in the North Pacific over the last 20ka (Zimmermann et al., 2021) and in the Fram Strait (30ka) (Zimmermann et al., 2020).

Data management

Environmental data will be archived, published and disseminated according to international standards by the World Data Center PANGAEA Data Publisher for Earth & Environmental Science (https://www.pangaea.de) within two years after the end of the expedition at the latest. By default, the CC-BY license will be applied.

Molecular data (DNA and RNA data) will be archived, published and disseminated within one of the repositories of the International Nucleotide Sequence Data Collaboration (INSDC, www.insdc.org) comprising of EMBL-EBI/ENA, GenBank and DDBJ). Additionally, DNA data and bioinformatic scripts for data analyses will be made publicly available on the data repository Dryad (https://datadryad.org) or GitHub.

Any other data will be submitted to an appropriate long-term archive that provides unique and stable identifiers for the datasets and allows open online access to the data.

This expedition was supported by the Helmholtz Research Programme “Changing Earth – Sustaining our Future” Topic 2, Subtopics 1 and 4, Topic 4, Subtopic 1 and Topic 6, Subtopics 2 and 3.

In all publications based on this expedition, the **Grant No. AWI_PS133/2_09** will be quoted and the following publication will be cited:

Alfred-Wegener-Institut Helmholtz-Zentrum für Polar- und Meeresforschung (2017) Polar Research and Supply Vessel POLARSTERN Operated by the Alfred-Wegener-Institute. Journal of large-scale research facilities, 3, A119. http://dx.doi.org/10.17815/jlsrf-3-163.

References

Courtin J, Perfumo A, Andreev AA, Opel T, Stoof-Leichsenring KR, Edwards ME, Murton JB, Herzschuh U (2022) Pleistocene Glacial and Interglacial Ecosystems Inferred from Ancient DNA Analyses of Permafrost Sediments from Batagay Megaslump, East Siberia. Environmental DNA 00:1-19. https://doi.org/10.1002/edn3.336

Jørgensen BB (1978) A Comparison of methods for the quantification of bacterial sulfate reduction in coastal marine-sediments.1. Measurement with radiotracer techniques. Geomicrobiology Journal 1:11–27. https://doi.org/10.1080/01490457809377721

Kallmeyer JTG, Ferdelman TG, Weber A, Fossing H, Jørgensen BB (2004) A cold chromium distillation procedure for radiolabeled sulfide applied to sulfate reduction measurements. Limnology and Oceanography Methods 2:171–18. https://doi.org/10.4319/lom.2004.2.171

Laufer-Meiser K, Michaud A B, Maisch M, Byrne J M, Kappler A, Patterson MO, Røy H, Jørgensen, B. B (2021) Potentially bioavailable iron produced through benthic cycling in glaciated Arctic fjords of Svalbard. Nature communications 12:1349. https://doi.org/10.1038/s41467-021-21558-w

Laufer K, Nordhoff M, Røy H, Schmidt C, Behrens S, Jørgensen BB, and Kappler A (2016) Coexistence of microaerophilic, nitrate-reducing, and phototrophic Fe(II) oxidizers and Fe(III) reducers in coastal marine sediment. Applied and Environmental Microbiology 82:1433–1447. https://doi.org/10.1128/AEM.03527-15

Liu S, Kruse S, Scherler D, Ree RH, Zimmermann HH, Stoof-Leichsenring KR, Epp LS, Mischke S, Herzschuh U (2021) Sedimentary Ancient DNA Reveals a Threat of Warming-Induced Alpine Habitat Loss to Tibetan Plateau Plant Diversity. Nature Communications 12:2995. https://doi.org/10.1038/s41467-021-22986-4

Michaud A, Laufer K, Findlay A, Pellerin A, Antler G, Turchyn AV, Røy H, Wehrmann LM, Jørgensen BB (2020) Glacial influence on the iron and sulfur cycles in Arctic fjord sediments (Svalbard). Geochim. Cosmochim. Acta 280:423–440. https://doi.org/10.1016/j.gca.2019.12.033

Røy H, Weber HS, Tarpgaard IH, Ferdelman TG, Jørgensen BB (2014) Determination of dissimilatory sulfate reduction rates in marine sediment via radioactive 35 S tracer. Limnology and Oceanography Methods 12:196–211. https://doi.org/10.4319/lom.2014.12.196

Schulte L, Bernhardt N, Stoof-Leichsenring K, Zimmermann HH, Pestryakova LA, Epp LS, Herzschuh U (2021) Hybridization Capture of Larch (Larix Mill.) Chloroplast Genomes from Sedimentary Ancient DNA Reveals Past Changes of Siberian Forest. Molecular Ecology Resources 21(3):801–15. https://doi.org/10.1111/1755-0998.13311

Stoof-Leichsenring KR., Huang S, Liu S, Jia W, Li K, Liu X, Pestryakova LA, Herzschuh U (2022) Sedimentary DNA Identifies Modern and Past Macrophyte Diversity and Its Environmental Drivers in High-Latitude and High-Elevation Lakes in Siberia and China. Limnology and Oceanography 67(5):1126–41. https://doi.org/10.1002/lno.12061

Yin X, Kulkarni AC, Friedrich MW (2019) DNA and RNA Stable Isotope Probing of methylotrophic methanogenic Archaea. In: Dumont, M. G., Hernández, García M (eds). Stable Isotope Probing: Methods and Protocols. Springer New York: New York, NY, pp 189-206.

Wunder LC, Aromokeye DA, Yin X, Richter-Heitmann T, Willis-Poratti G, Schnakenberg A, Otersen C, Dohrmann I, Römer M, Bohrmann G, Kasten S, Friedrich MW (2021) Iron and sulfate reduction structure microbial communities in (sub-) Antarctic sediments. The ISME journal 15(12):3587–3604. https://doi.org/10.1038/s41396-021-01014-9

Zimmermann HH, Stoof-Leichsenring KR, Kruse S, Nürnberg D, Tiedemann R, Herzschuh U (2021) Sedimentary Ancient DNA From the Subarctic North Pacific: How Sea Ice, Salinity, and Insolation Dynamics Have Shaped Diatom Composition and Richness Over the Past 20,000 Years. Paleoceanography and Paleoclimatology 36:e2020PA004091. https://doi.org/10.1029/2020PA004091

Zimmermann HH, Stoof-Leichsenring KR, Kruse S, Müller J, Stein R, Tiedemann R, Herzschuh U (2020) Changes in the Composition of Marine and Sea-Ice Diatoms Derived from Sedimentary Ancient DNA of the Eastern Fram Strait over the Past 30 000 Years. Ocean Science 16:1017–32. https://doi.org/10.5194/os-16-1017-2020

11. PHYSICAL OCEANOGRAPHY

Annika Oetjens[1], Joséphine Anselin[2;] [1]DE.AWI
not on board: Wilken-Jon von Appen[1], [2]UK.BAS
Ryan Mole[1], Emma Young[2]

Grant-No. AWI_PS133/2_10

Objectives

The Southern Ocean contains so-called high nutrient low chlorophyll areas in which macronutrients are abundant, but micronutrients (primarily iron) limit primary production (the growth of phytoplankton). The work on Island Impact leg 1 (PS133/1) preceding Expedition PS133/2 mapped out some of these areas and in particular the temperature/ salinity characteristics of the water masses that are or are not iron limited. Tracers such as iron are either passively advected with currents and mixed with water masses or they are modified by biological processes (primary production, remineralization). Coastal and shelf sea processes (e.g. around the archipelago of South Georgia) form new water masses with distinct temperature/salinity characteristics and they also introduce iron originating from land to the water column. Therefore, the identification of water masses on the shelf of South Georgia (and their origins) together with their iron concentrations allows for the computation of their contribution to iron concentrations across the Atlantic sector of the Southern Ocean.

Work at sea

All stations where hydrographic measurements were carried out during expedition PS133/2 in the vicinity of South Georgia are shown in Fig. 11.1. Hydrographic measurements performed during expedition PS133/2 were conducted using two CTD systems: CTD-OZE (Table 11.1) and CTD-clean (Table 11.2). Meta-data of all PS133/2 CTD stations are listed in Table 11.3.

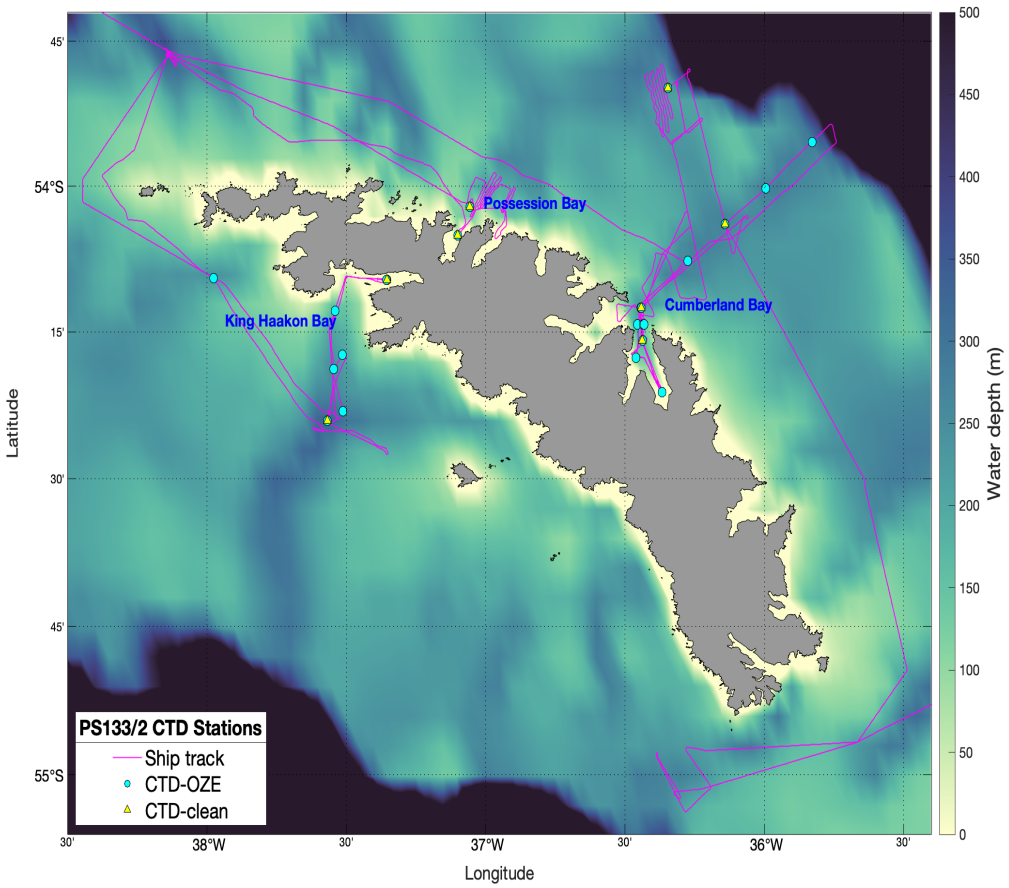

Fig. 11.1: Bathymetric map of South Georgia archipelago showing locations of CTD-OZE and CTD-clean stations from PS133/2. Note that the first four stations, located further offshore (001_02, 001_05, 005_01, 009_01) are not shown on the map. Bathymetry data was obtained from GEBCO Compilation Group (2022) GEBCO 2022 Grid (https://doi.org/10.5285/e0f0bb80-ab44-2739-e053-6c86abc0289c).

The sensors and rosette of CTD-OZE were provided by the Physical Oceanography group from DE.AWI ("CTD-OZE"). The sensors and rosette of CTD-clean were provided by the ecological chemistry group from DE.AWI ("CTD-clean"). Through the use of titanium and plastic instead of steel, it allows the sampling of trace metals, in particular iron. In the following, we describe the technical setup of the CTD rosette, followed by a description of the general procedure of performing CTD casts during the cruise. We then present further information on the actual deployments, including a description of initial test casts and an overview of technical issues throughout the cruise. Finally, a description of the technically set up of the vessel mounted ADCP is provided.

CTD-OZE

The standard sensor configuration of the CTD-OZE system throughout the cruise consisted of two temperature sensors, two conductivity cells, a pressure sensor, two oxygen sensors, two fluorescence sensors, a transmissiometer, and a phytosynthetically active radiation (PAR) sensor (see Tab. 11.1 for more details).

Furthermore, there was a Sea-Bird SUNA nitrate sensor (SN 1318) on the rosette. As this sensor has a depth rating of 2,000 m, it was not attached for the first cast. The device was programmed to start sampling – and record the data internally – as soon as power was supplied.

Power was supplied by the SBE911, so that data acquisition started when the CTD was turned on. The nitrate measurements had not yet been processed at the time of completion of this report, hence the absence of preliminary results.

In addition, an Underwater Vision Profiler (UVP) was attached to the rosette. More details on the UVP measurements can be found in the respective section. The UVP was set up to start automatically when lowered below 20 m and to stop recording when heaved for more than 30 m. Therefore, the usual procedure for a CTD deployment was as follows: lowering the rosette to 22 m, waiting for up to two minutes for the UVP and the CTD pump to turn on, heaving back to the surface. Then the downcast starts by lowering the rosette with 0.5 m/s. The lowering speed was further reduced when approaching the sea floor. The casts were stopped 10 m above ground.

Tab. 11.1: Sensor configurations for the CTD-OZE system used during cruise PS133/2.

	SN	**Calibration Date**	**Channel**	**Description**
CTD				SBE 911plus
Temperature (primary)	1373	2019-10-11	F0	SBE3plus
Conductivity (primary)	1198	2019-09-17	F1	SBE4c
Pressure	0321	2017-11-14	F2	SBE9, substituted by SN 0287 with calibration date 1992-11-20 for conf3 and with calibration date 2017-11-14 for conf4
Temperature	2929	2019-09-13	F3	SBE3plus
Conductivity	1199	2019-09-17	F4	SBE4c
Oxygen (primary)	2292	2022-02-09	V0	SBE43, substituted by SN 4303 with calibration date 2022-08-06 for conf2-conf4
Oxygen	3654	2022-02-09	V1	SBE43, substituted by SN 4305 with calibration date 2022-08-16 for conf2-conf4
Altimeter	51533	--	V2	Teledyne Benthos PSA916
Fluorescence	7239	2021-12-09	V3	WETLabs ECO CDOM Fluorometer
Fluorescence	1346	2016-01-15	V4	WETLabs ECO Chlorophyll Fluorometer
Beam Transmission	0814	2011-10-24	V5	WETLabs C-Star
Photosynthetically Active Radiation (PAR)	2197	2021-11-30	V6	SEA-BIRD PAR-LOG
Nitrate	1318	--	V7	Power only

CTD-clean

The standard sensor configuration of the CTD-clean system throughout the cruise consisted of two temperature sensors, two conductivity cells, a pressure sensor, one oxygen sensor, one fluorescence sensor, a transmissiometer, and a phytosynthetically active radiation (PAR) sensor (see Tab. 11.2 for more details). During cast 032_02 the pumps turned off and temperature, salinity and oxygen were no longer recorded correctly. This issue could not be resolved onboard. For the following casts, the clean CTD was therefore only deployed to close bottles and the profiles had to be taken from the CTD-OZE.

Tab. 11.2: Sensor configurations for the CTD-clean system used during cruise PS133/2.

	SN	Calibration Date	Channel	Description
CTD				SBE 911plus
Temperature (primary)	6519	2022-07-19	F0	SBE3plus
Conductivity (primary)	4964	2022-06-28	F1	SBE4c
Pressure	1431	2020-11-19	F2	SBE9
Temperature	6491	2022-07-19	F3	SBE3plus
Conductivity	4982	2022-06-28	F4	SBE4c
Oxygen (primary)	4047	2020-10-30	V0	SBE43
Empty	--	--	V1	--
Fluorescence	6450	2020-08-12	V2	WETLabs ECO Chlorophyll Fluorometer
Beam Transmission	2064	2020-11-20	V3	WETLabs C-Star
Altimeter	74480	2020-03-06	V4	Valeport VA500
Empty	--	--	V5	--
Photosynthetically Active Radiation (PAR)	2067	2020-11-11	V6	SEA-BIRD PAR-LOG
Empty	--	--	V7	--

For water sampling purposes the Niskin bottles were fired on the upcast after waiting for 45 s at each target depth for both sampling the ‘true’ ambient water mass and also allowing for lagging sensors to adjust. These water samples are partly used for calibrating the salinity, however due to the low depth range it was not possible to take samples while on the shelf. Results from on-board salinometry are presented in the subsequent section.

Tab. 11.3: Meta-data of all CTD stations from PS133/2. The station names refer to the file numbers and headers of the CTD data and correspond to the DSHIP entries.

Station	Time at depth [UTC]	Lat [°N]	Lon [°S]	Depth [m]	CTD	Comments
001-02	2022-11-24 15:37	-54.6065	-43.9018	4482	clean	
001-05	2022-11-25 00:06	-54.6002	-43.8999	4449	OZE	Test station, salinity samples
005-01	2022-11-26 01:02	-53.5003	-39.0802	2990	clean	Salinity samples taken
009-01	2022-11-26 10:53	-53.7699	-38.1404	379	OZE	
011-01	2022-11-26 19:13	-54.0356	-37.0568	249	OZE	
011-02	2022-11-26 20:35	-54.0358	-37.0570	248	clean	

Station	Time at depth [UTC]	Lat [°N]	Lon [°S]	Depth [m]	CTD	Comments
015-01	2022-11-27 14:04	-54.0842	-37.1000	359	OZE	
017-02	2022-11-28 12:29	-54.4013	-37.5674	344	clean	
017-03	2022-11-28 13:28	-54.4013	-37.5679	345	OZE	
017-08	2022-11-28 20:11	-54.4012	-37.5674	344	OZE	
018-01	2022-11-29 00:55	-54.2886	-37.5143	240	OZE	
019-01	2022-11-29 02:55	-54.3129	-37.5446	297	OZE	
020-01	2022-11-29 05:28	-54.3853	-37.5123	373	OZE	
023-01	2022-11-29 14:10	-54.1612	-37.3542	139	OZE	
023-05	2022-11-29 18:00	-54.1605	-37.3551	139	OZE	
023-07	2022-11-29 22:16	-54.1609	-37.3541	139	clean	Scan length error during upcast
024-01	2022-11-30 10:55	-54.2135	-37.5408	187	OZE	
028-01	2022-12-01 01:57	-54.1576	-37.9760	259	OZE	
031-01	2022-12-01 19:18	-54.1288	-36.2752	279	OZE	
032-02	2022-12-02 00:52	-54.2649	-36.4380	260	clean	Pumps turned off during upcast
032-03	2022-12-02 01:56	-54.2649	-36.4367	261	OZE	
032-06	2022-12-02 04:19	-54.2651	-36.4366	261	OZE	
035-01	2022-12-03 10:21	-54.3527	-36.3671	143	OZE	Salinity samples taken
035-04	2022-12-03 13:24	-54.3529	-36.3673	143	OZE	
037-01	2022-12-04 00:08	-54.2937	-36.4604	136	OZE	
038-01	2022-12-04 01:21	-54.2368	-36.4549	196	OZE	
039-01	2022-12-04 02:52	-54.2370	-36.4342	216	OZE	Drifted while at depth (bottom +10m)
040-02	2022-12-04 05:13	-54.2375	-36.4309	191	OZE	

Station	Time at depth [UTC]	Lat [°N]	Lon [°S]	Depth [m]	CTD	Comments
042-01	2022-12-05 02:10	-54.2086	-36.4432	264	OZE	
045-01	2022-12-06 06:44	-53.8310	-36.3460	209	OZE	
045-02	2022-12-06 07:41	-53.8312	-36.3456	212	clean	No T, C, Oxy data, only to close bottles
042-05	2022-12-07 00:34	-54.2088	-36.4423	264	OZE	
042-06	2022-12-07 01:24	-54.2086	-36.4427	264	clean	No T, C, Oxy data, only to close bottles
048-01	2022-12-07 14:23	-53.9240	-35.8278	276	OZE	
049-01	2022-12-07 17:35	-54.0038	-35.9957	281	OZE	Only profile, no bottles closed
050-01	2022-12-07 20:01	-54.0651	-36.1415	270	OZE	
050-02	2022-12-07 21:15	-54.0652	-36.1421	270	clean	No T, C, Oxy data, only to close bottles
055-01	2022-12-16 17:20	6.275	-39.483	1000	OZE	Last CTD

Salinometry

We obtained high precision salinity measurements with an Optimare Precision Salinometer (OPS, SN 006) for potential recalibration of the conductivity sensors. An overview of all taken samples as well as the results from the salinometry can be found in Tab. 11.4. The samples were taken from the Niskin bottles of both CTDs (CTD-OZE and CTD-clean). Before taking the actual sample, the bottles and rubber lid were rinsed 3 times. Then the bottles were closed, sealed (crimped) with an aluminum cap, and stored.

We measured the water samples in a single batch at the end of the sampling campaign. The day before the session, the salinity bottles were heated in a water bath to approximately 30°C, and then let cool down for about 10 h. The pressure within the bottles was released with an injection needle directly after the warm bath. Before using the OPS, the samples were shaken thoroughly for overcoming any stratification in the bottle. While sampled by the OPS, the opening of the bottles was sealed with parafilm to inhibit evaporation. The metal inlet tube of the OPS was cleaned with a Kim-wipe between samples.

A salinometry session starts with the standardization of the OPS using standard seawater. The respective bottle was sealed with the original cap and regularly sampled at the end of each session again. Each salinity measurement of a water sample from the Niskin bottles is calculated from the average of three individual OPS measurements that are allowed to differ by less than 0.0005 PSU. The salinity values measured by the two sensors of the CTD (Sal00 and Sal11) are calculated from the mean of 49 data scans recorded at the time of closing the Niskin bottle.

Tab. 11.4: All salinity values (PSU) calculated with the salinometer and the conductivity sensors of the two CTDs (CTD-OZE and CTD-clean).

	Expedition	Station	Depth	Salinity OPS	Salinity CTD Sal00	Difference Sal00-OPS	Salinity CTD-Sal11	Difference Sal11-OPS
	CTD-Oze							
1	PS133/2	001-05	3000	34.6934	34.6879	-0.0055	34.6862	-0.0072
2	PS133/2	035-01	75	33.8410	33.8373	-0.0037	33.8337	-0.0073
3	PS133/2	055-01	1000	34.2621				
4	PS133/2	001-05	1000	34.6845	34.6777	-0.0068	34.6763	-0.0082
5	PS133/2	001-05	1000	34.6854	34.6777	-0.0077	34.6763	-0.0091
6	PS133/2	001-05	3000	34.6939	34.6879	-0.0060	34.6862	-0.0077
7	PS133/2	035-01	75	33.8429	33.8373	-0.0056	34.8337	-0.0092
8	PS133/2	055-01	1000	34.2648				
	CTD-clean							
9	PS133/2	005-01	1000	34.7030	34.6964	-0.0066	34.6980	-0.0050
10	PS133/2	005-01	1000	34.7046	34.6964	-0.0082	34.6980	-0.0066

The first evaluation of the results shows that the salinities measured with the sensors were lower by up to 0.0092 PSU than the salinities measured with the OPS (Fig. 11.2). Both CTD sensors showed the same temporal trend apart from measurement 7. A more detailed error analysis will be conducted after the expedition.

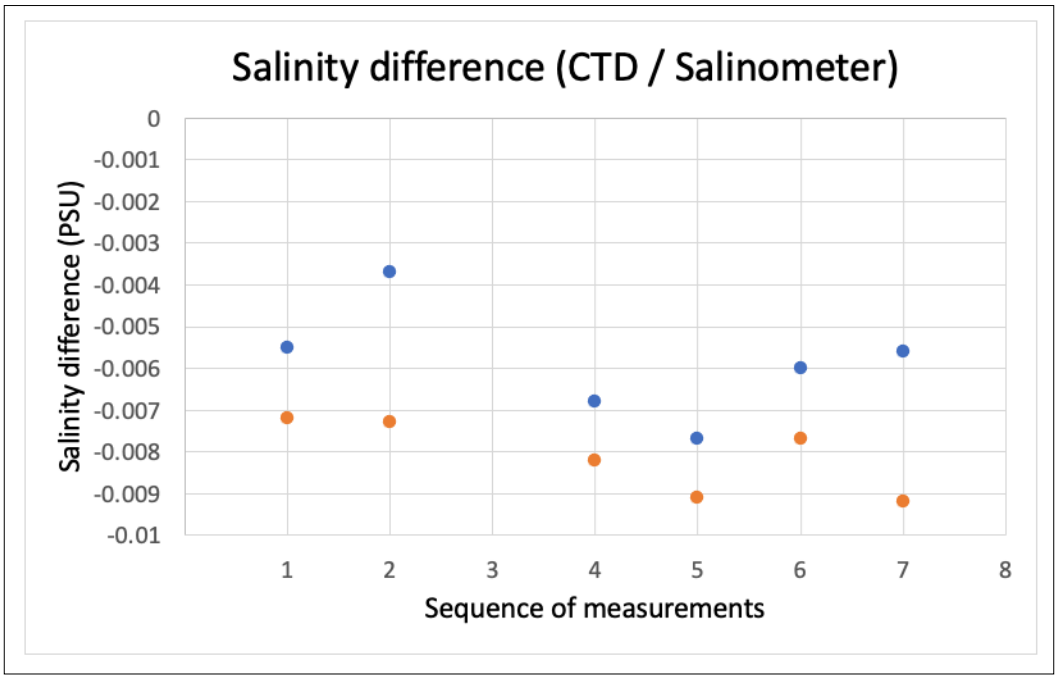

Fig. 11.2: Plot of the differences in salinity measured with the OPS salinometer and the CTD sensors of the CTD-OZE. The X-axis shows the time sequence of the measurements (as listed in Tab 11.5). The blue dots show the results from the CTD sensor Sal00. The orange dots show the results from the CTD sensor Sal11. Sample 3 and 8 do not yet have a corresponding CTD sensor measurements due to a technical issue during processing. This data gap will be addressed after the expedition.

Vessel mounted ADCP

The vessel mounted Acoustic Doppler Current Profiler (VMADCP) was in operation from 21 November 2022 11:17 until entering the 12 nm territorial waters of Cape Town at the end of the cruise. The RDI Ocean Surveyor instrument (150 kHz) was mounted at an angle of 45 degrees in the 'Kastenkiel' of *Polarstern* and provides a continuous time series of profiles of ocean current velocity in the upper 300 m of the water column while underway. The instrument was configured in narrowband mode and set up to use a 4 m bin size (configuration file cmd_OS150NB_trigger_off.txt as shown in Tab. 11.5), covering a range from 15 m to around 200 - 300 m depth depending on sea state, ship speed and the presence of back-scatterers in the water column.

Overall, the system functioned without any issues and all data was collected entirely in the data files (file format: PS133_2[three digit deployment number]_000[three digit file number].ENX, *.ENR, *.ENS, *.N1R, *.N2R, *.NMS, *.STA, *.LTA, *.VMO, *.LOG), as we did not apply any changes to the instrument configuration.

The setup of navigational input was used from the vessel's GPS system.

The software VmDas (Teledyne RD Instruments) was used to set the ADCP's operating parameters and to record the data. Finally, the data conversion was done using Matlab routines of the Ocean Surveyor Sputum Interpreter (OSSI) version 1.9 (osheader.m, osdatasip.m, osrefine.m, osbottom.m). The finishing processing will be done on land.

Tab. 11.5: VMADCP command file cmd_OS150NB_trigger_off.txt

```
;---------------------------------------------------------------------\
; ADCP Command File for use with VmDas software.
;
; ADCP type:     150 Khz Ocean Surveyor
; Setup name:    for Polarstern in 6/2014
; Setup type:    Low resolution, long range profile (Narrowband)
;
; NOTE:  Any line beginning with a semicolon in the first
;        column is treated as a comment and is ignored by
;        the VmDas software.
;
; NOTE:  This file is best viewed with a fixed-point font (e.g. courier).
; Modified Last: 12Jun2014
;---------------------------------------------------------------------/
```

; Restore factory default settings in the ADCP

cr1

; set the data collection baud rate to 9600 bps,

; no parity, one stop bit, 8 data bits

; NOTE: VmDas sends baud rate change command after all other commands in

; this file, so that it is not made permanent by a CK command.

cb411

; Set for narrowband single-ping profile mode (NP), 100 (NN) 4 meter bins (NS),

; 2 meter blanking distance (NF), 390 cm/s ambiguity vel (WV)

WP000

NP001

NN080

NS0400

NF0400

;WV390

; Disable single-ping bottom track (BP),

; Set maximum bottom search depth to 1200 meters (BX)

BP000

;BX12000

; output velocity, correlation, echo intensity, percent good

ND111100000

; Ping as fast as possible

TP000000

; Since VmDas uses manual pinging, TE is ignored by the ADCP

; and should not be set.

;TE0000000

; Set to calculate speed-of-sound, no depth sensor, external synchro heading

; sensor, pitch or roll being used, no salinity sensor, use internal transducer

; temperature sensor

EZ1011101

; Output beam data (rotations are done in software)

EX00000

; Set transducer misalignment (hundredths of degrees).

; Ignored here but set in VmDAS options.

;EA00000

; Set transducer depth (decimeters)

ED00110

; Set Salinity (ppt)

ES35

;set external triggering and output trigger; no trigger

CX0,0

;set external triggering and output trigger

;CX1,3

; save this setup to non-volatile memory in the ADCP

CK

Preliminary results

Profiles and T-S curves from Cumberland Bay East and from King Haakon Bay are shown in Fig. 11.3 and Fig. 11.4, respectively. It should be noted that the plots were created based on uncalibrated data. Data calibration will be performed following completion of the cruise.

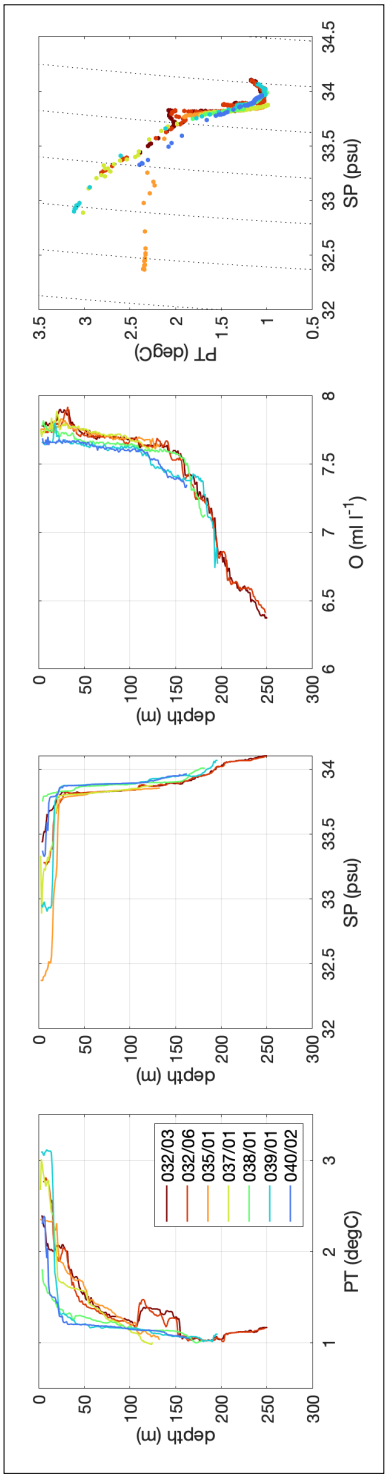

Fig. 11.3: Potential Temperature (PT), salinity (SP), oxygen (O) profiles, and Temperature-Salinity curves from a selection of stations in Cumberland Bay East. Plots created based on uncalibrated data.

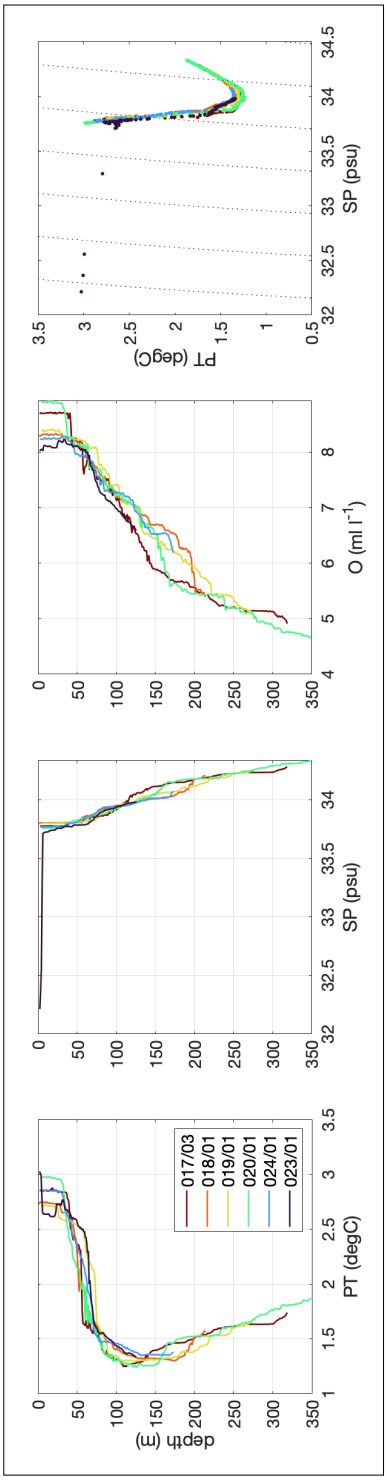

Fig. 11.4: Potential Temperature (PT), salinity (SP), oxygen (O) profiles, and Temperature-Salinity curves from a selection of stations in King Haakon Bay and shelf. Plots created based on uncalibrated data.

Data management

The raw CTD data from the two rosettes and the velocity data from the VMADCP will be made available through the World Data Center PANGAEA Data Publisher for Earth & Environmental Science (https://www.pangaea.de) within two years after the cruise. The finally processed CTD and velocity data will also be made available through PANGAEA when processing has been completed. By default, the CC-BY license will be applied.

This expedition is supported by the Helmholtz Research Programme “Changing Earth – Sustaining our Future” Topic 2, Subtopics 1 and 4, Topic 4, Subtopic 1 and Topic 6, Subtopics 2 and 3.

In all publications based on this expedition, the **Grant No. AWI_PS133/2_10** will be quoted and the following publication will be cited:

Alfred-Wegener-Institut Helmholtz-Zentrum für Polar- und Meeresforschung (2017) Polar Research and Supply Vessel POLARSTERN Operated by the Alfred-Wegener-Institute. Journal of large-scale research facilities, 3, A119. http://dx.doi.org/10.17815/jlsrf-3-163.

12. MARINE PARTICLES, SINKING FLUXES AND NUTRIENT CYCLING IN SURFACE SEDIMENTS

Morten Iversen[1,2], Hannah Marchant[2], [1]DE.AWI
Susanne Spahic[1], Isabella Wilkie[3] [2]DE.MARUM
not on board: Christian Konrad[1,2], Rudi Amann[3] [3]DE.MPIMM

Grant-No. AWI_PS133/2_11

12.1 Marine Particles and sinking Fluxes

Objectives

Our first set of objectives during expedition PS133-2 was based around understanding the dynamics and export of marine particles in the different environments surrounding South Georgia, on transects from the inner King Haakon and Cumberland Bay Fjords to the outer fjords and shelf regions. We used *in-situ* camera systems (ROSINA, JellyCam, UVP, and the *In-situ* Settling Cam) to determine the abundance and size-distribution of different particle types (ROSINA and UVP) and zooplankton species (JellyCam and UVP). We further directly measured *in-situ* settling velocities of individual particles by deploying the *In-situ* Settling Cam with the drifting trap. Export flux was directly measured with sediment traps equipped with gel traps (Fig. 12.1) and production of fecal pellets for further biogeochemical analyses were produced on board using *in-situ* collected zooplankton and phytoplankton. We further deployed Marine Snow Catchers to collect *in-situ* formed particles for determination of composition, settling velocities and microbial degradation.

Our main aims were to identify pathways for organic matter transport, transformation and turnover in the water column. To achieve this, we measured the following parameters in combination with hydrographic data:

- Measuring particle (plankton and aggregates) size-distribution, abundance and composition in the water column.
- Measuring export fluxes below the upper mixed layer depth and the permanent thermocline and determine the composition and characteristics of the sinking matter.
- Determine processes that influence particle dynamics and sinking fluxes.
- Determine the impact that particle formation, recycling and export has on nutrient stoichiometry.

Our second set of objectives was to examine bacterio- and phytoplankton interactions in the mixed surface layer of the water column and sediment, with a focus on the degradation of sugars via aerobic heterotrophy. In order to do so, we collected samples from both the water and sediment for cell counts (via microscopy and fluorescence in-situ hybridisation) and DNA sequencing for subsequent metagenomic analyses.

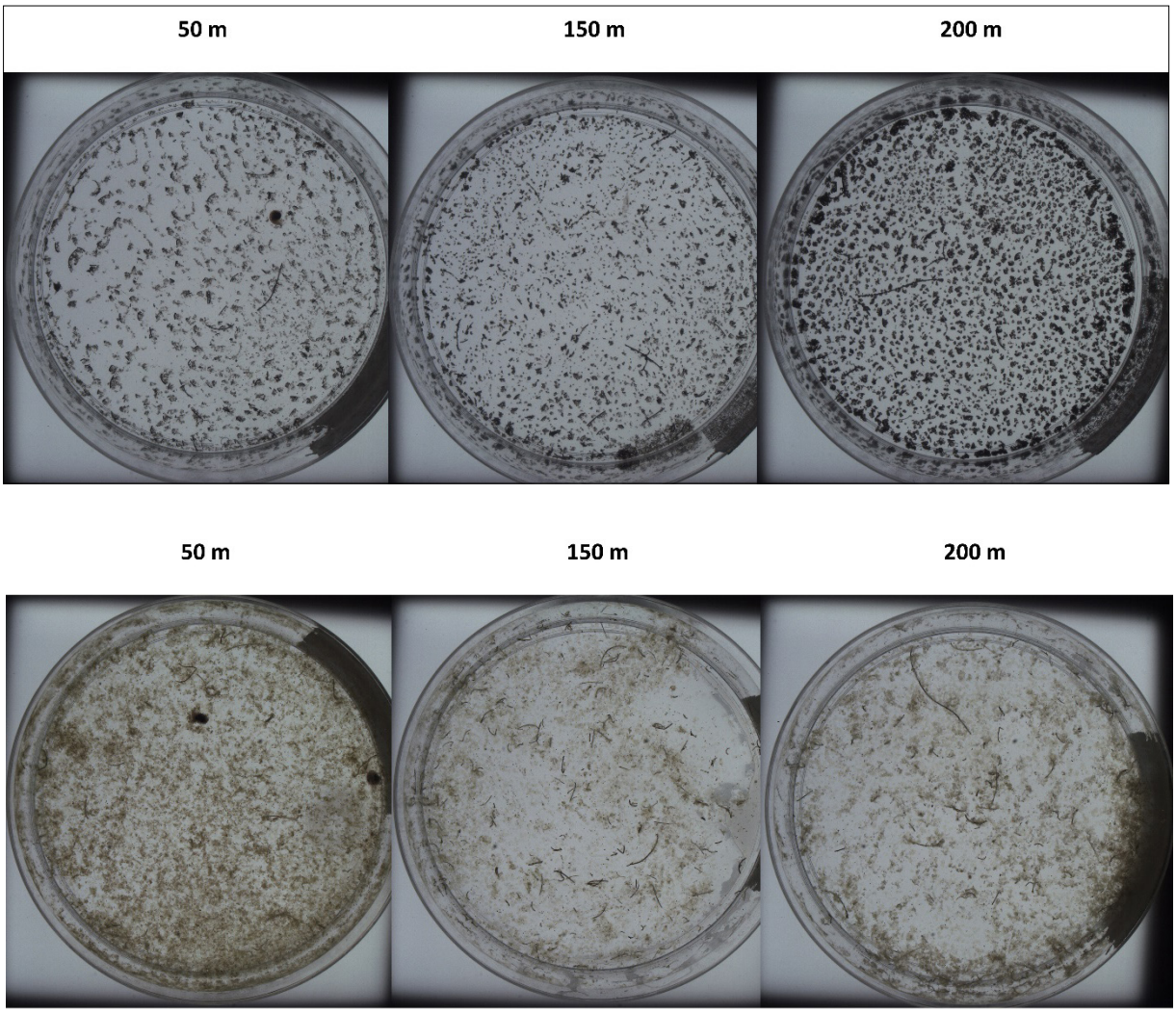

Fig. 12.1: Upper three gel traps were collected at Cumberland Bay Fjord while the lower three gel traps were collected at King Haakon Bay Fjord. The gel traps contain particles collected in-situ using the drifting trap array.

Work at sea

In-situ camera systems

Particle characteristics (size, shape, type and origin) will be determined from the transects of UVP5 underwater video profiling system attached to the CTD-rosette sampler and the ROSINA which was equipped with the JellyCam and a CTD. The coupled CTD and underwater camera systems allow quantification of the whole size-spectrum including the larger macrozooplankton and aggregates (ROSINA and JellyCam) and link their abundance and distributions to the different water masses. The UVP deployment list is provided in the section on the oceanographic CTD-Rosette deployments. Table 12.1 provides a list of the ROSINA deployments.

Table 12.1: Station number, study area, profile number, deployment date, deployment time, and deployment depth of the ROSINA deployments.

Station Number	Study area	Profile [#]	Date [YYYY-MM-DD]	Time [HH:MM]	Depth [m]
PS133/2_17-7	King Haakon Trough	ROSINA_01	2022-11-28	18:30	320
PS133/2_18-2	King Haakon Trough	ROSINA_02	2022-11-29	01:27	220
PS133/2_19-3	King Haakon Trough	ROSINA_03	2022-11-29	03:35	270
PS133/2_20-2	King Haakon Trough	ROSINA_04	2022-11-29	06:06	350
PS133/2_23-4	Innermost King Haakon Bay	ROSINA_05	2022-11-29	16:40	120
PS133/2_31-2	Shelf outside Cumberland Bay	ROSINA_06	2022-12-01	20:01	265
PS133/2_32-5	Cumberland Bay, Grytviken Flare	ROSINA_07	2022-12-02	03:14	240
PS133/2_35-3	Innermost Cumberland Bay	ROSINA_08	2022-12-03	12:12	130
PS133/2_38-2	CTD Transect outer Cumberland Bay	ROSINA_09	2022-12-04	01:49	180
PS133/2_39-2	CTD Transect outer Cumberland Bay	ROSINA_10	2022-12-04	03:21	210
PS133/2_40-1	CTD Transect outer Cumberland Bay	ROSINA_11	2022-12-04	04:17	150
PS133/2_42-2	Confluence Zone, outer Cumberland Bay	ROSINA_12	2022-12-05	02:39	245
PS133/2_48-2	CTD Transect along Cumberland Bay Trough	ROSINA_13	2022-12-7	15:00	260
PS133/2_49-2	CTD Transect along Cumberland Bay Trough	ROSINA_14	2022-12-7	17:53	270
PS133/2_50-3	Mid-continental shelf off Cumberland Bay	ROSINA_15	2022-12-7	21:55	255

Sediment trap deployments

Export fluxes were measured below the mixed layer at depths that were adjusted to the water column depth at the station. This was done using a free drifting array with up to three sediment trap stations (KC, Denmark) consisting of four cylindrical sinking matter collectors each (Fig.12.2, Table 12.2). The trap was adjusted so that it did not drift freely, but instead was moored to the seafloor by a 60 kg weight.

Table 12.2: Station number, study area, deployment and recovery times, trap depths, and In-situ Settling Cam (ISC) depths for the sediment trap moorings.

Station Number	Study area	Gear	Date [YYYY-MM-DD HH:MM]	ISC Depth [m]	Trap Depth(s) [m]
PS133/2_17-1	King Haakon Trough	DF-II-4 Deployment	2022-11-28 10:22	100	50, 150, 200
PS133/2_21-1	King Haakon Trough	DF-II-4 Recovery	2022-11-29 08:05	100	50, 150, 200

Station Number	Study area	Gear	Date [YYYY-MM-DD HH:MM]	ISC Depth [m]	Trap Depth(s) [m]
PS133/2_23-8	Innermost King Haakon Bay	DF-II-5 Deployment	2022-11-29 22:57	50	100
PS133/2_23-14	Innermost King Haakon Bay	DF-II-5 Recovery	2022-11-30	50	100
PS133/2_32-1	Cumberland Bay, Grytviken Flare	DF-II-6 Deployment	2022-12-01 22:59	100	50, 150, 200
PS133/2_32-14	Cumberland Bay, Grytviken Flare	DF-II-6 Recovery	2022-12-02 20:51	100	50, 150, 200
PS133/2_35-5	Innermost Cumberland Bay	DF-II-7 Deployment	2022-12-03 15:39	50	100
PS133/2_41-1	Innermost Cumberland Bay	DF-II-7 Recovery	2022-12-04 08:00	50	100

Material from three collectors at each depth level will be used for biogeochemical analyses of particulate organic matter composition, and molecular microscopic analysis of planktonic organisms. The fourth collector at each depth will be filled with a viscous gel to preserve size and shape of sinking particles (Fig 12.1). These were digitally analysed on board. We deployed two sediment traps in each fjord, King Haakon Bay Fjord and Cumberland Bay Fjord, one at near the glaciers at the head of the two fjords and one closer to the fjord mouth.

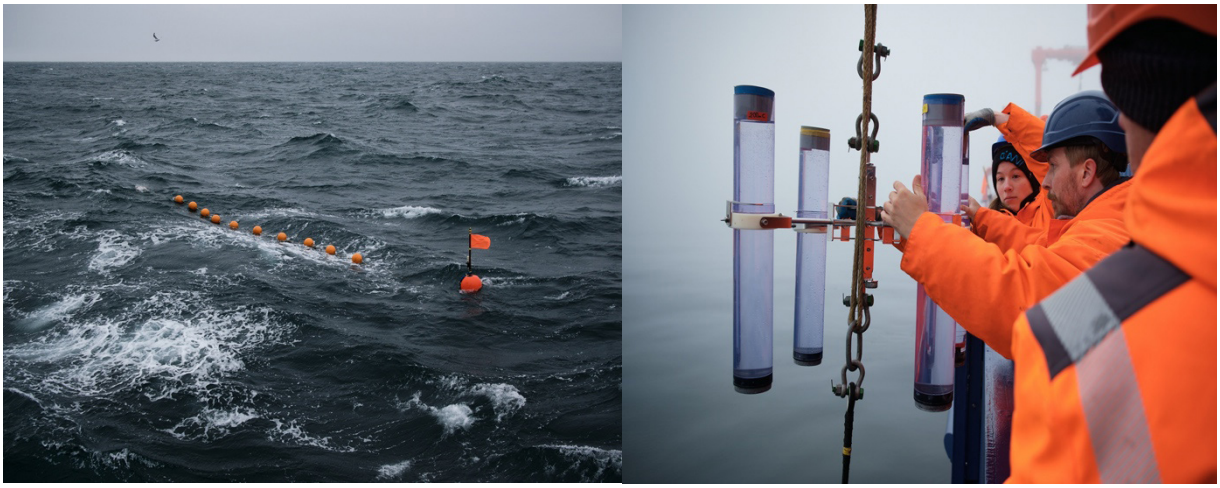

Fig. 12.2: Images of the drifting sediment trap close to the ice edge at East-Greenland (left); one of the trap stations with the four sediment trap cylinders (right); (photos: Tim Kalvelage)

Each sediment trap deployment was equipped with the *in-situ* Settling Cam (ISC) to measure size- and type-specific settling velocities of the exported particles. The traps near the glaciers consisted of the *In-situ* Settling Cam at 50 m depth and a sediment trap station 100 m depth. The traps closer to the fjord mouth consisted of three sediment trap stations deployed at 50 m, 150 m, and 200 m and the *In-situ* Settling Cam was deployed at 100 m (Fig. 12.3).

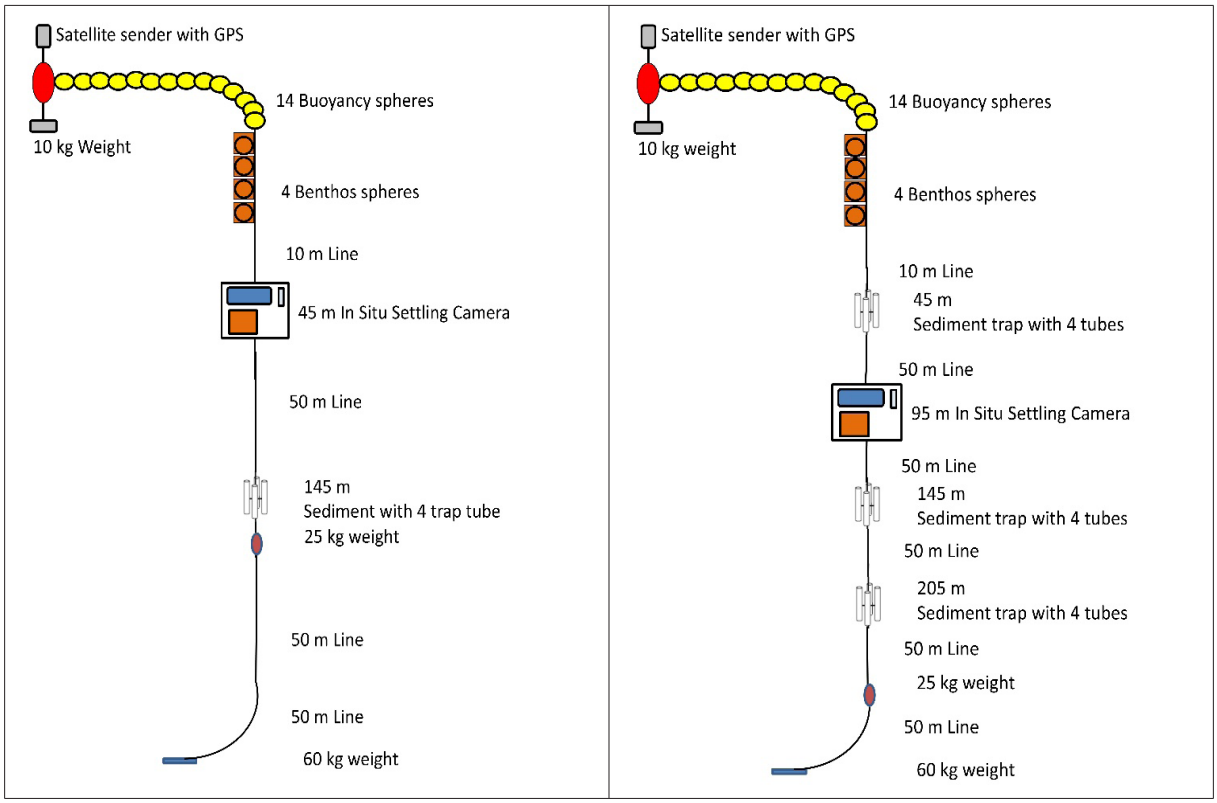

Fig. 12.3: Schematic overview of the two types of sediment trap deployments. Left is the short mooring that was deployed near the glaciers and the right image is the longer mooring that was deployed near the mouth of the fjords.

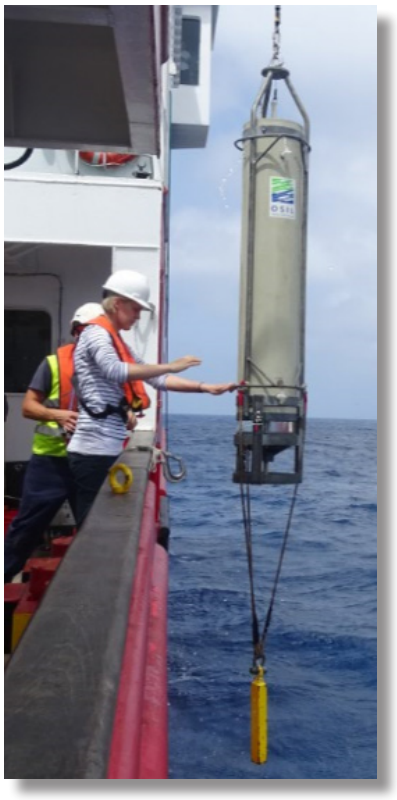

Marine Snow Catcher

A large volume sampler, the Marine Snow Catchers (MSC), was used to collected *in-situ* formed marine snow and other particles (Fig. 12.4, Table 12.3). The MSC consists of a 100L cylindrical water sampler with a particle collection tray at the bottom and will be deployed with a winch to the target depth and closed via a release mechanism. The closed MSC was placed on deck for a few hours to allow the collected particles to sink to the collection tray. After gently draining the water from the 100 L cylinder, the collection tray that contained the settling particles was removed. The collected aggregates were used to determine their size-specific sinking velocities, microscopic observations of the aggregate composition, and measurements of respiration of the aggregate attached microbes. The aggregate size, sinking velocities, and microbial respiration was measured on board in a vertical flow chamber at *in-situ* temperature.

Fig. 12.4: (Left) Deployment of the Marine Snow Catcher (MSC).

Individual aggregates were placed in the flow chamber, whereby the upward flow was increased until the aggregate remains suspended. The sinking velocity of each aggregate was calculated from the flow rate divided by the cross-sectional area of the flow chamber. Microbial respiration was estimated from the oxygen gradients through the aggregate-water interface measured using a Clark-type oxygen microelectrode mounted in a micromanipulator and calibrated at air-saturation. Similar measurements on zooplankton faecal pellets both from water column and incubations was carried out.

Table 12.3: Station number, study area, gear, deployment date, deployment time, and deployment depth for the Marine Snow Catcher (MSC).

Station Number	Study area	Gear	Date [YYYY-MM-DD]	Time [HH:MM]	Depths [m]
PS133/2_17-10	King Haakon Trough	Marine Snow Catcher x 2	2022-11-28	20:56	50
PS133/2_32-9	Cumberland Bay, Grytviken Flare	Marine Snow Catcher x 2	2022-12-02	05:12	70

Zooplankton collection

A WP2 plankton net with a mesh size of 400 µm was used to collect *in-situ* zooplankton. The collected euphausids and copepods were used for fecal pellet production for later stoichiometric and biogeochemical composition (Table 12.4).

Table 12.4: Station number, study area, gear, deployment date, deployment time, and net haul depth for the WP2 net.

Station Number	Study area	Gear	Date [YYYY-MM-DD]	Time [HH:MM]	Depths [m]
PS133/2_17-9	King Haakon Trough	WP2-Net	2022-11-28	20:34	50-0
PS133/2_23-6	Innermost King Haakon Bay	WP2-Net	2022-11-29	18:32	30-0
PS133/2_32-8	Cumberland Bay, Grytviken Flare	WP2-Net	2022-12-02	04:47	50-0
PS133/2_42-3	Confluence Zone, outer Cumberland Bay	WP2-Net	2022-12-05	03:22	50-0
PS133/2_50-4	Mid-continental shelf off Cumberland Bay	WP2-Net	2022-12-07	22:30	50-0

To investigate the bacterio- and phytoplankton interactions in the mixed layer and sediment, water and sediment were collected at nine stations where both the mulitcorer (MUC) and CTD were deployed) (Fig. 12.5) were deployed (Table 12.5, Table 12.6), and at an initial test station, where only water was sampled (St. 1). For both types of samples, some material was stored for DNA extraction, while the rest was stored and fixed in formaldehyde to allow for fluorescence *in-situ* hybridisation (FISH) at a later date.

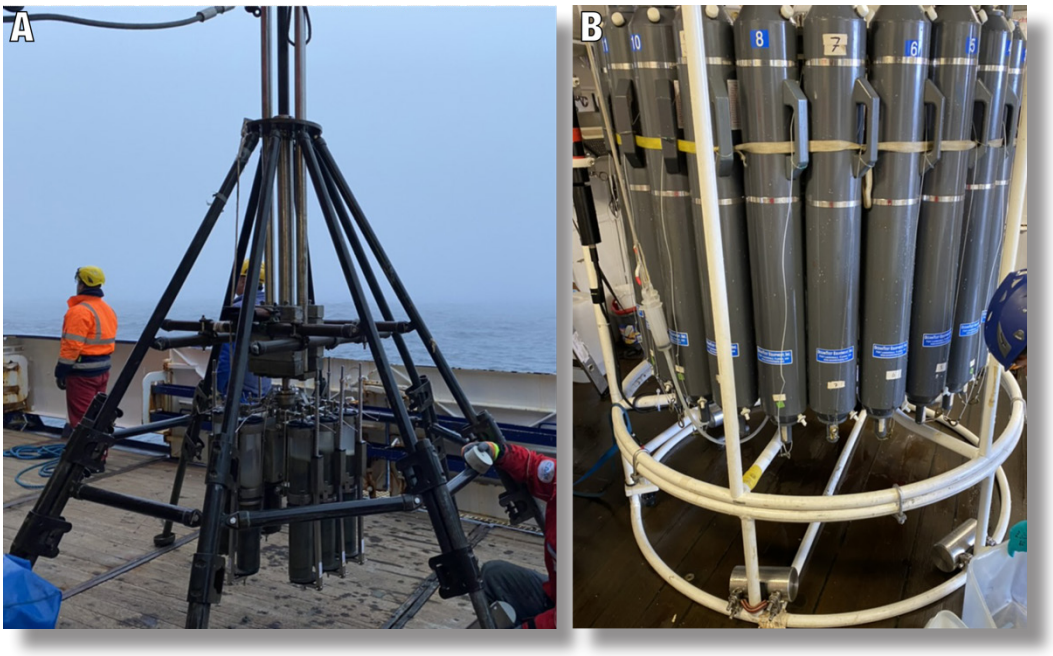

Fig. 12.5: Multicorer (A) and CTD (B) before retrieval of the samples (© Isabella Wilkie).

Table 12.5: Depths sampled at PS133/2 stations for water filtration via CTD for bacterio- and phytoplankton interactions.

Station Number	Study area	Gear	Date [YYYY-MM-DD]	Bottle no.	Depths [m]
PS133/2_1-5	Shag Rock	CTD AWI-OZE	2022-11-24	18, 24	50, 12
PS133/2_11-1	Outer Possession Bay	CTD AWI-OZE	2022-11-26	12, 24	20, 12
PS133/2_15-1	Inner Posession Bay	CTD AWI-OZE	2022-11-27	24	12
PS133/2_17-3	King Haakon Trough	CTD AWI-OZE	2022-11-28	19, 24	20, 12
PS133/2_23-1	Innermost King Haakon Bay	CTD AWI-OZE	2022-11-29	18, 21	12, 5
PS133/2_32-3	Grytviken Flare, Cumberland Bay	CTD AWI-OZE	2022-12-02	17, 20	25, 12
PS133/2_35-1	Innermost Cumberland Bay	CTD AWI-OZE	2022-12-03	8, 12	35, 5
PS133/2_37-1	Moraine Fjord, Grytviken	CTD AWI-OZE	2022-12-04	10, 16	20, 2.5
PS133/2_42-5	Confluence zone, Outer Cumberland Bay	CTD AWI-OZE	2022-12-07	17, 20	20, 5
PS133/2_50-1	Mid-continental Shelf, Cumberland Bay	CTD AWI-OZE	2022-12-07	16, 20	40, 5

Table 12.6: Cores sampled at PS133/2 stations for sediment collection via MUC.

Station Number	Study area	GEAR	Date [YYYY-MM-DD]	Core no.	Depth [m]
PS133/2_9-2	Outer Possession Bay	MUC_PS	2022-11-26	8	378.7
PS133/2_12-1	Inner Posession Bay	MUC_PS	2022-11-26	4	257.1

Station Number	Study area	GEAR	Date [YYYY-MM-DD]	Core no.	Depth [m]
PS133/2_15-5	King Haakon Trough	MUC_PS	2022-11-27	3	358.4
PS133/2_17-11	Innermost King Haakon Bay	MUC_PS	2022-11-28	5	343
PS133/2_23-10	Grytviken Flare, Cumberland Bay	MUC_PS	2022-11-30	6	153.6
PS133/2_32-17	Innermost Cumberland Bay	MUC_PS	2022-12-02	8	262.9
PS133/2_35-8	Moraine Fjord, Grytviken	MUC_PS	2022-12-03	3	161
PS133/2_42-9	Confluence zone, Outer Cumberland Bay	MUC_PS	2022-12-07	7	263.6
PS133/2_50-6	Mid-continental Shelf, Cumberland Bay	MUC_PS	2022-12-07	5	270.4

CTD work

Water samples were collected at the surface (from the Niskin bottle which was closed at the shallowest depth), as well as at the deep chlorophyll maxima (DCM) when present. 1 L of water from each depth was subsequently filtered using a Thiele filtration apparatus (Fig. 12.6), wherein the water was passed sequentially through 10 µm, 3 µm, and 0.2 µm pore-size filters. The filters were then stored at -80˚C until the DNA extraction will be conducted for metagenomic sequencing. A further sample of water from each depth was fixed using formaldehyde (final concentration of 1%) for one hour at room temperature, after which it was filtered using 0.2 µm filters. Two sets of filters were collected at each depth, those which had filtered 100 mL and those which filtered 20 mL, to account for different amounts of biomass at the different depths and sites. These filters were stored at -20˚C, and set aside for FISH and microscopy.

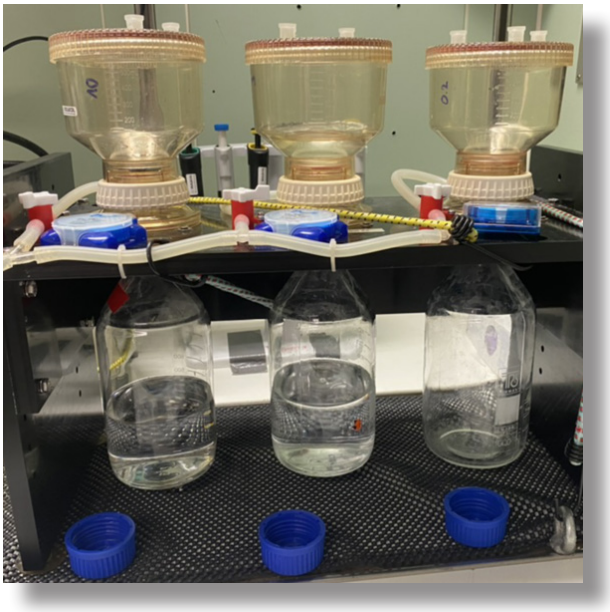

Fig. 12.6: Thiele filtration apparatus set up with 10 µm, 3 µm and 0.2 µm pore-size filters (© Isabella Wilkie).

Multicorer work

One core was taken from each site where the MUC was deployed, the overlaying bottom water was siphoned off and the surface set aside for sampling. Some bottom water was filtered using Sterivex filters, 3 filters à 100 mL for each core, for DNA extraction and metagenomic

analysis. The surface sediment itself was separated into 0-2 cm, 2-4 cm, and 4-6 cm fractions. As with the water samples, some sediment from each fraction was frozen and stored at -80˚C for future DNA extraction, while 0.5 mL of each fraction were fixed using formaldehyde (final concentration of 3%) and stored at -20˚C for FISH and microscopy.

Preliminary and expected results

The expected data set will determine vertical distribution of aggregates and zooplankton as well as biogeochemical export fluxes in waters surrounding South Georgia and will be compared to similar measurements in open waters carried out during Leg 1 (PS133-1). Our study will provide vertical profiles of aggregates and zooplankton at high spatial resolution. Rate measurements of microbial degradation from on-board measurements will help us to identify remineralization processes and by coupling these to *in-situ* flux profiles, we can quantify the role of both microbes and zooplankton for flux attenuation. This will allow us to identify important recycling and export processes through the water column. In addition, targeted experimental incubation on board will allow us to follow stoichiometric changes in different pools of organic matter and investigate the role and zooplankton and microbes for trace metals and nutrients in collaboration with the trace metal groups on board during the two legs.

The camera profiles through Cumberland Bay Fjord showed marked differences in the particle composition, size-distribution and abundance. The particles near the glacier in the innermost part of Cumberland Bay Fjord were composed of small inorganic particles, likely silt released by the melting glaciers. At the Grytviken Flare, we observed fewer particles than at the glacier and the particles were primarily organic composed of mucous and phytoplankton with some zooplankton fecal pellets. At the shelf outside Cumberland Bay Fjord, there was an increase in zooplankton fecal pellets and organic aggregates and the aggregates were generally of organic composition (Fig. 12.7).

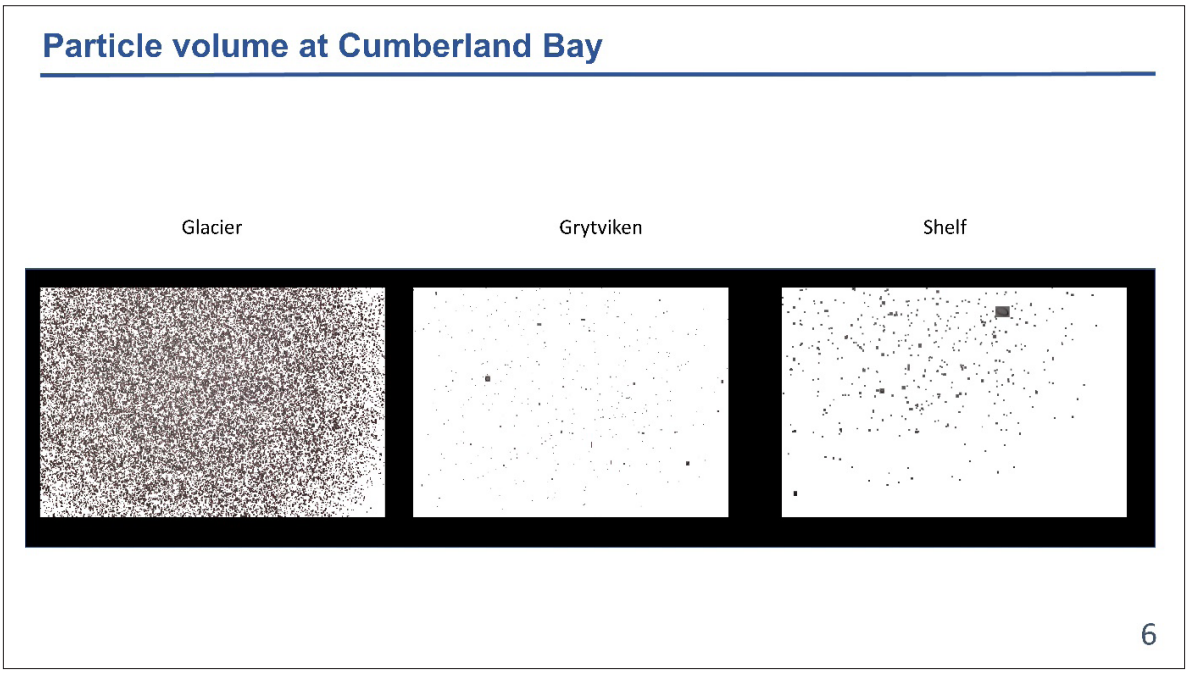

Fig. 12.7: All crops of detected particles for the upper 35 m of the water column plotted together for three locations through Cumberland Bay Fjord; left: near the glacier at the innermost part of the fjord, middle: at the Grytviken Flare, and right: at the outermost shelf of Cumberland Bay Fjord.

The total depth-specific volume of all the detected particles was highest near the glacier and lowest at the Grytviken Flare (Fig. 12.8). There seemed to be a strong input of glacial silt at 30 m near the glacier, likely the melting depth of the marine terminating glacier in Cumberland Bay Fjord. All three locations had clear indications of resuspension of sediment near the seafloor. At the shelf station there was a clear increase of organic aggregate volume at 60 m, which was near the strongly increasing salinity gradient (Fig. 12.8).

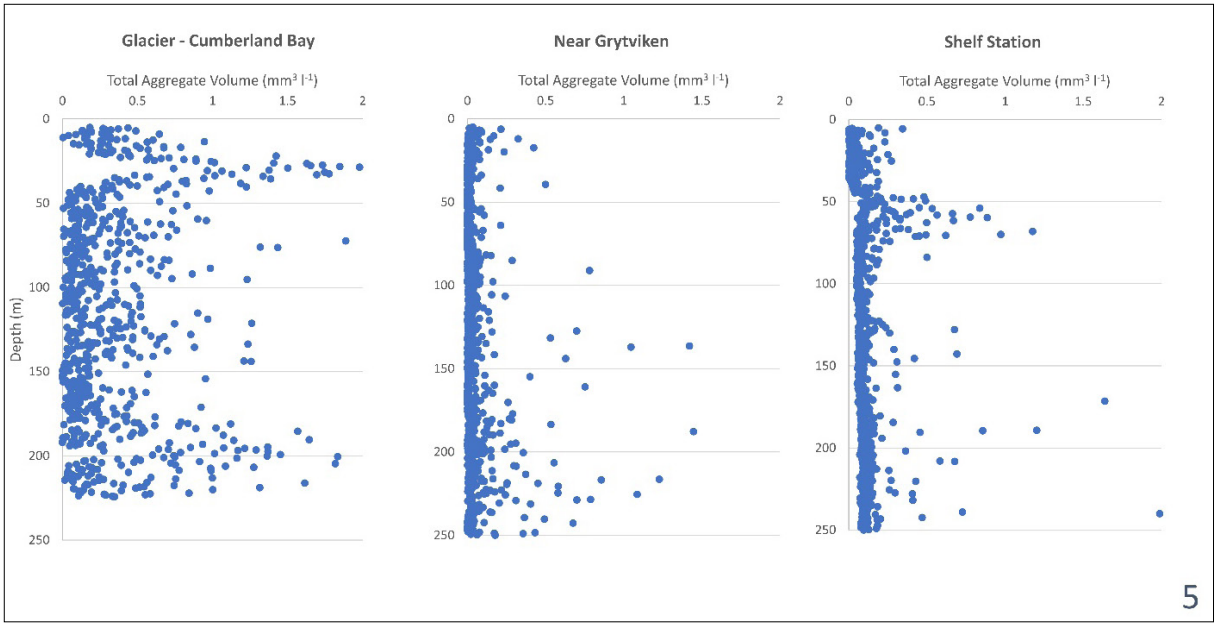

Fig. 12.8: Vertical distribution of total aggregate volume for three location through Cumberland Bay Fjord; left: near the glacier in the innermost part of the fjord, middle: near Grytviken Flare, and right: at the shelf outside Cumberland Bay Fjord.

The *in-situ* measurements of the size-specific settling velocities for the aggregates near the Grytviken Flare were measured using the *In-situ* Settling Camera (ISC). We did not find any indications of a size-to-settling relationship for the aggregates, but found that all size-ranges of particles sank with velocities between a few meters per day and up to 400 meter per day (Fig. 12.9).

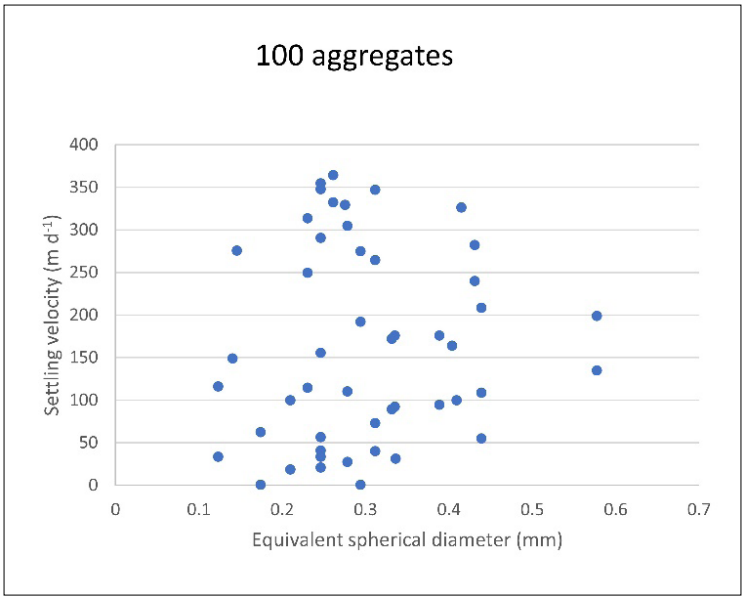

Fig. 12.9: Size-specific settling velocities of the aggregates near the Grytviken Flare.

We observed larger zooplankton through the water column with the JellyCam. Here we observed several copepods, euphausids, salps, polychaetes, and ctenophores (Fig. 12.10). We will analyse all profiles in the home laboratory and determine diel vertical distribution of zooplankton and relate this to the vertical size-distribution and abundance of settling aggregates.

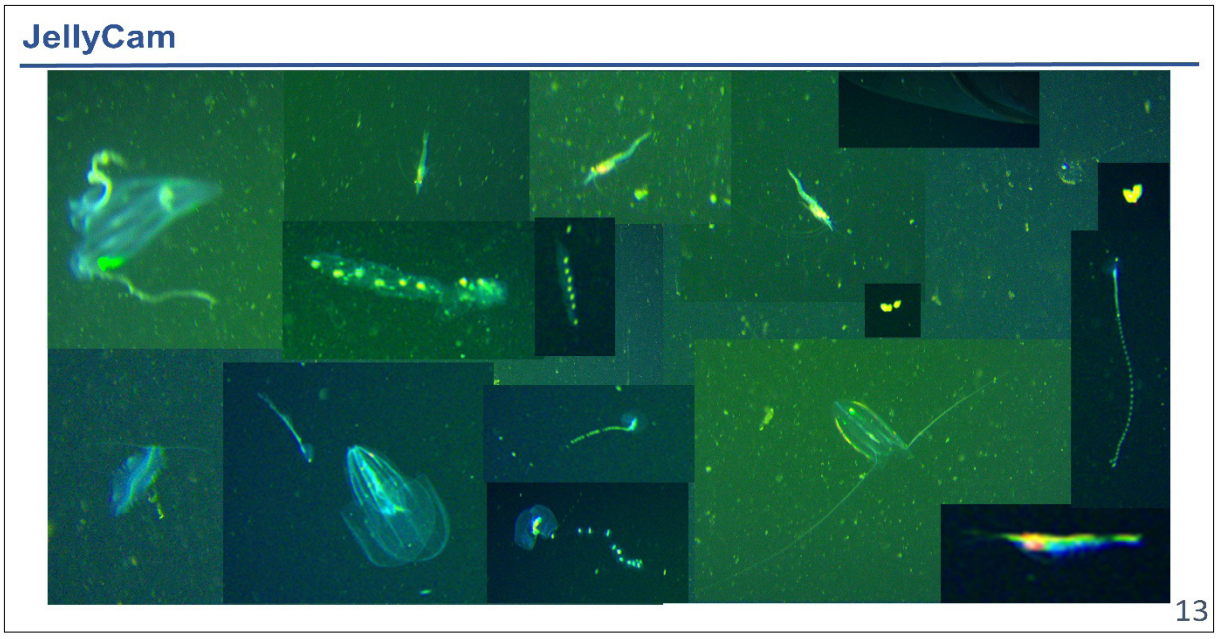

Fig. 12.10: Examples of microzooplankton observed with the JellyCam.

12.2 Nutrient Cycling in Surface Sediments

Objectives

Our main objective was to understand how turnover of nutrients in surface sediments from different depositional environments impact the water column. Originally, our main focus was planned as the sandy shelf sediments outside the troughs, however due to time constraints, we instead focussed on the nine stations where the MUC and the CTD were deployed simultaneously. Little is known about nitrogen cycling in these sediments, or how the microbially mediated processes of denitrification, dissimilatory nitrogen reduction to ammonium and anammox are linked to iron oxidation and reduction. During the voyage we aimed to:

- Quantify nitrification, denitrification/anammox and dissimilatory nitrate reduction to ammonium from different locations in the fjords using slurry incubations.
- Determine nitrification rates in the water column to better understand the coupling between the pelagic and benthic system.
- Compare the microbial communities mediating N-cycling processes in different sediment types/the water column.

Work at sea

Sediments were collected using the MUC (Table 12.7) at nine stations to set up slurry incubations. At 7 stations there was enough overlying water in the MUCs to collect 2L, which was subsequently sterile filtered using a vacuum pump and a 0.22 µm polyethersulfone filtration unit. This water was either transferred immediately to 160 mL glass serum vials (x2) or was degassed by bubbling with helium for 30 mins while stirring vigorously, before being decanted into serum vials (x8), which were overflow 0.5 times and capped with butyl stoppers, headspace free. At stations 23 (Inner King Haakon Bay) and 35 (Inner Cumberland Bay) there was not enough overlying water in the MUC so the same process was instead carried out with water collected from the deepest depth sampled by the CTD (event 23-1, bottle 1, 125 m, and event 35-4, bottle 3, 130 m, respectively). After preparation of the vials, the sediment core was sectioned into 2 cm horizons, and between 6 and 9 cm^3 was placed into the serum bottles which were capped bubble free and the bottles containing sediment from the lower two horizons were immediately degassed for 2 x 5 mins, with shaking in between. A 5 ml air headspace was added to the two bottles from the shallowest horizon and vials were left on a shaker table at 40 rpm for between 18 and 26 hours to allow them to equilibrate and to draw down the background nitrate concentration.

Sediment from each horizon was also frozen (for metagenomics), fixed with formaldehyde (for FISH) and 5 cm^3 was frozen with 6 ml of artificial seawater for later determination of intracellular nitrate concentrations.

After the pre-incubation period, ^{15}N stable isotope tracers (Table 12.8) were added to each of the bottles to track nitrogen cycling processes, shaken and subsampled at 0, 3, 6, 12 and 24 h. Subsampling was carried out by removing 6 ml of water which was filled into a 6 ml glass vial pre-filled with 100 µL of mercury chloride to stop biological activity and capped bubble free. For E3 and E4, the water was replaced passively from extra bottles which had been collected from the MUC/Niskin and also degassed. For E1, water was pipetted out of the vial and the headspace increased. From Station 23 onwards an additional 2 ml was subsampled and placed into a 6 ml vial containing a helium headspace and frozen immediately. These samples were given to Katja Laufer-Meiser (see Chapter 10) who will determine any changes in iron concentration.

Table 12.7: Details of MUC sampling.

Station Number	Study area	Date [YYYY-MM-DD]	Core no.	Depth [m]	Horizons (cm)	Volume sediment per vial (cm^3)	# of vials	Water source	Fe samples taken
PS133/2_9-2	Outer Possession Bay	2022-11-26	8	378.7	0-2 2-5 5-7	3 6 6	2 4 4	Overlying MUC	No
PS133/2_12-1	Inner Posession Bay	2022-11-26	4	257.1	0-2 2-4 4-6	6 6 6	2 4 4	Overlying MUC	No
PS133/2_15-5	King Haakon Trough	2022-11-27	3	358.4	0-2 2-4 4-6	6 6 6	2 4 4	Overlying MUC	No
PS133/2_17-11	Innermost King Haakon Bay	2022-11-28	5	343	1-3 3-5 6-8	6 6 6	2 4 4	Niskin	No
PS133/2_23-10	Grytviken Flare, Cumberland Bay	2022-11-30	6	153.6	0-2 2-4 4-6	6 6 6	2 4 4	Overlying MUC	Yes
PS133/2_32-17	Innermost Cumberland Bay	2022-12-02	8	262.9	0-2 2-4 4-6	6 6 6	2 4 4	Niskin	Yes
PS133/2_35-8	Moraine Fjord, Grytviken	2022-12-03	3	161	0-2 2-4 4-6	6 6 6	2 4 4	Overlying MUC	Yes
PS133/2_42-9	Confluence zone, Outer Cumberland Bay	2022-12-07	7	263.6	0-2 2-4 4-6	9 9 9	2 4 4	Overlying MUC	Yes
PS133/2_50-6	Mid-continental Shelf, Cumberland Bay	2022-12-07	5	270.4	0-2 2-4 4-6	9 9 9	2 4 4	Overlying MUC	Yes

Table 12.8: Details of tracer incubations.

Experiment name	Tracer added	Process targeted	Depth horizon	Number of replicates per horizon
E1	75 µM $^{15}NH_4^+$	Nitrification	1	2
E3	75 µM $^{15}NO_3^-$	Denitrification, DNRA	2 and 3	2
E4	75 µM $^{15}NH_4^+$ 75 µM $^{14}NO_2^-$	Anammox	2 and 3	2

To determine water column nitrification rates, samples were collected from the boundary layer by sampling water overlying the cores retrieved with the MUC, from above the benthic boundary layer (deepest bottle from the CTD-Rosette and from just beneath the mixed layer/ DCM (Table 12.9). 200 ml from each depth was added to 4 x 250 ml bottles and to two bottles

$^{15}NH_4^+$ and $^{14}NO_2^-$ were added to assess ammonia oxidation rates and to the other two bottles $^{15}NO_2^-$ was added to assess nitrite oxidation rates. 12 ml per bottle were subsampled and killed using mercury chloride at time intervals of 0, 3, 6, 12 and 24 hours. Mixed layer samples were taken using niskin bottles. When possible 2 L of water was also filtered onto a 0.22 µm "sterivex" filter and frozen for future DNA analysis.

Table 12.9. Stations and water depths sampled for ammonia oxidation and nitrite oxidation determination.

Station Number	Study area	Gear	Date [YYYY-MM-DD]	Bottle no.	Depths [m]
PS133/2_15-1	Inner Posession Bay	CTD AWI-OZE	2022-11-27	1, 18	340, 75 MUC
PS133/2_17-3	King Haakon Trough	CTD AWI-OZE	2022-11-28	1, 17	315, 50 MUC
PS133/2_23-1	Innermost King Haakon Bay	CTD AWI-OZE	2022-11-29	1, 14	126, 50
PS133/2_32-3	Grytviken Flare, Cumberland Bay	CTD AWI-OZE	2022-12-02	1, 16	250, 40 MUC
PS133/2_35-1	Innermost Cumberland Bay	CTD AWI-OZE	2022-12-03	3, 7	130, 50
PS133/2_42-5	Confluence zone, Outer Cumberland Bay	CTD AWI-OZE	2022-12-07	1, 15	250, 60, MUC
PS133/2_50-1	Mid-continental Shelf, Cumberland Bay	CTD AWI-OZE	2022-12-07	1, 16	254, 60, MUC

Preliminary and expected results

The expected data set will provide nitrogen cycling rates for the sediments surrounding South Georgia. By combining these with sediment and water column nutrient profiles, and other rate measurements from the sediment we will gain an almost unprecedented picture of how early diagenesis looks in these sediments and examine the impact of the glacier systems and fjord dynamics. Coastal shelf sediments play a key role in global carbon and nutrient cycling, but very little data exists from polar regions. In addition the targeted incubations on board will allow us to assess the potential interactions between nitrogen and iron cycling, transformation and release in these sediments.

The water column nitrification samples will be compared to those taken in the open waters sampled on Leg 1 (PS133/1). This will allow us to gain insights into the processes that alter nutrient stoichiometry in the water column.

Data management

Abundance data will be archived, published and disseminated according to international standards by the World Data Center PANGAEA Data Publisher for Earth & Environmental Science (https://www.pangaea.de) within two years from the end of the cruise. By default, the CC-BY license will be applied.

Any other data will be submitted to an appropriate long-term archive that provides unique and stable identifiers for the datasets and allows open online access to the data.

This expedition is supported by the Helmholtz Research Programme “Changing Earth – Sustaining our Future” Topic 2, Subtopics 1 and 4, Topic 4, Subtopic 1 and Topic 6, Subtopics 2 and 3.

In all publications based on this expedition, the **Grant No AWI_PS133/2_11** will be quoted and the following publication will be cited:

Alfred-Wegener-Institut Helmholtz-Zentrum für Polar- und Meeresforschung (2017) Polar Research and Supply Vessel POLARSTERN Operated by the Alfred-Wegener-Institute. Journal of large-scale research facilities, 3, A119. http://dx.doi.org/10.17815/jlsrf-3-163.

13. ORGANIC GEOCHEMISTRY OF THE WATER COLUMN AND SEDIMENTS

Laura Kattein[1], Hendrik Grotheer[1] [1]DE.AWI

Grant-No. AWI_PS133/2_12

Objectives

The overarching goal is to characterize and quantify the terrestrial carbon export from South Georgia and how biologically available dissolved Fe affects the biogeochemistry and biological carbon fixation in local shelf waters. Ultimately this information will aid to quantify and qualify the carbon sequestered in fjord sediments. Using radiocarbon analysis paired with molecular characterization of particulate and dissolved organic matter we aim to trace the carbon exported from its likely source on land to depositional sites in the fjords. Biological carbon fixation in shelf waters, mineralization and vertical export to the sediment will further be traced and quantified. Carbon sequestered in the sediments will therefore be a mixture of terrestrial carbon imported laterally and freshly produced marine carbon from the upper water column exported vertically that survive microbial remineralisation. Isotope ($\delta^{13}C$ and $\Delta^{14}C$) mass balance source apportionment models will be applied to quantify the relative proportions of both carbon sources to the sediment and how these changed over time.

For this, soil organic matter will be analysed and its fate along its passage from the site of erosion, through lakes and rivers, towards the fjord sediment will be characterized based on changes in its molecular and isotopic composition. Focusing on abundance and isotopic composition of terrestrial biomarkers (e.g., long chain *n*-alkanoic acids, synthesised by higher land plans), and bulk organic matter will allow to assess the terrestrial organic matter endmember for the carbon sequestration source apportionment model. Similarly, the freshly produced marine endmember will be characterized (e.g., short chain *n*-alkanoic acids, synthesized by algae) based on particulate organic matter collected from the local chlorophyl-a maximum. These two endmembers will allow to determine the extent of mixing and remineralisation in the water column and quantify the carbon sequestration in surface sediments. Information gained from the source apportionment model will be applied on short sediment cores from the fjord to investigate how sequestration rates and source proportions changed over time.

Work at sea

Dissolved Inorganic, Dissolved Organic and Particulate Organic Carbon (DIC, DOC, POC)

Radiocarbon analyses of dissolved inorganic carbon and dissolved and particulate organic carbon are useful tracers of carbon cycling mechanisms and carbon reservoir exchange pathways. DIC, DOC and POC constitute major global carbon reservoirs with paramount importance for biogeochemical cycles. Terrestrial material is exported into the oceans largely as DOC and POC, which impacts the composition of marine sediments, a connection that can be used for source appointment utilizing radiocarbon analyses. They have the potential to impact the climate on geological timescales as these reservoirs can sequester carbon for up to millennia and exchange CO_2 at the ocean/atmosphere boundary.

DIC was sampled applying a novel method developed by members of the Organic Geochemistry working group at AWI. Water obtained with the CTD-ROS was sampled immediately after recovery into pre-combusted 10 ml glass vials. After poisoning with Hg_2Cl, the vials were crimped shut with rubber membrane lids to prevent CO_2 exchange with the atmosphere. All DIC samples were taken as duplicates or triplicates and radiocarbon analyses will be conducted directly on the sealed vials at the MICADAS facility in Bremerhaven.

For DOC sample acquisition, large amounts of water (10-30 L) obtained with the CTD-ROS (for ocean/fjord stations) from different depths were filtered over pre-combusted Whatman GF/F filters (0.7 µm pore size) using a vacuum pump. The filters retain the POC fraction were stored frozen untill further analysis in Bremerhaven. An aliquot of the filtrate was sampled in acid-cleaned 0.5 L brown HDPE bottles and acidified to pH=2 using ultrahigh purity HCl or H_2SO_4. DO^{14}C analyses will be conducted at the MICADAS facility in Bremerhaven upon return. Samples taken for the dfferent analyses are listed in Table 13.1.

Tab. 13.1: Particulate organic carbon (POC) dissolved organic carbon (DOC) and dissolved inorganic carbon (DIC) samples collected with CTD-ROS Niskin-bottles. DOC fraction collected for quantification, molecular composition and radiocarbon dating (2x 500 mL acidified with HCl and 1x 500 mL with H_2SO_4 following on-board filtration over 0.75 µm GF/F filters for POC. 2-3 10 mL replicates for DIC radiocarbon analysis were sampled from the CTD-ROS and fixed with $HgCl_2$.

Station	Date	Lat. °S	Long. °W	Depth [m]	POC Volume [L]	DIC Sample [#]	DOC Sample [#]
PS133/2_15-1	27.11.2022	54° 05.052‘	037° 05.997‘	340	21.6	2	3
				12	11.9	2	3
PS133/2_17-3	28.11.2022	54° 24.077’	037° 34.073’	315	20	2	3
				175	21	2	3
				100	21.8	2	3
				12	8	2	3
PS133/2_23-1	29.11.2022	54° 09.674’	037° 21.250’	125	14	2	3
				100	14	2	3
				60	12	2	3
				12	8	2	3
PS133/2_24-1	30.11.2022	54° 12.808’	037° 32.446’	172	9	2	3
				75	14	2	3
				12	8	2	3
PS133/2_31-1	01.12.2022	54° 07.726’	036° 16.510’	263	20	2	3
				100	16	2	3
				12	8	2	3
PS133/2_32-3	02.12.2022	54° 15.892’	036° 26.200’	250	20	2	3
				200	18	2	3
				100	16.8	2	3

Station	Date	Lat. °S	Long. °W	Depth [m]	POC Volume [L]	DIC Sample [#]	DOC Sample [#]
				12	8	2	3
PS133/2_35-1	03.12.2022	54° 21.162’	036° 22.023’	100	14	2	3
				5	2.4	2	3
PS133/2_35-4	03.12.2022	54° 21.176’	036° 22.036’	130	20	2	3
PS133/2_36-1	03.12.2022	54° 17.622’	036° 27.627’	125	16.7	2	3
				100	18	2	3
				3	4.3	2	3
PS133/2_42-5	06.12.2022	54° 12.515’	036° 26.564’	250	13.2	3	3
				200	12	3	3
				150	18	3	3
				100	18	3	3
				5	6	3	3
PS133/2_48-1	07.12.2022	53° 55.442’	035° 49.668’	263	20	3	3
				200	19.4	3	3
				150	17.3	3	3
				100	18.8	3	3
				5	10	3	3
PS133/2_50-1	07.12.2022	54° 03.909’	036° 08.488’	254	22	3	3
				200	18.8	3	3
				150	20	3	3
				100	20	3	3
				5	8	3	3

Surface Water Filtration

To calculate the biomarkerbased sea surface temperature proxies TEX_{86} and UK_{37} surface water particulate organic carbon was sampled during expedition PS133/2. Comparison of calculated proxies with direct measurements of sea surface temperatures and observations of weather conditions during the cruise will increase the understanding of applicability of these proxies for paleo-environmental reconstructions. The water was obtained with a membrane pump through an inlet in the ship’s bow (~ 5 m.b.s.l.) and pumped through the internal pipeline system directly to the filtration unit, where it was passed through pre-combusted glass fibre filters (Whatman GFF, 142 mm diameter). Sampling was conducted for approximately 1h during transit times and station work, resulting in filtration volumes of ~100 l (Table 13.2). Prevailing weather conditions, water temperature and salinity were noted (Table 13.3). A total of 12 filters were obtained. The filters were stored frozen (-20°C) in pre-combusted tin foil until biomarker extraction, which will be conducted at AWI Bremerhaven in Germany.

Tab. 13.2: Sampling date, start and finish coordinates of surface water filters.

Filter #	Date	Lat. °S		Long. °W	
		Start	End	Start	End
1	23.11.2022	53° 51.306’	53° 53.643’	050° 13.189’	049° 53.537’
2	24.11.2022	54° 35.644’	54° 35.644’	043° 57.083’	043° 57.083’
3	25.11.2022	53° 16.096’	53° 11.527’	041° 40.649’	041° 10.355’
4	27.11.2022	54° 04.155’	54° 05.076’	037° 04.418’	037° 05.999’
5	27.11.2022	53° 55.268’	54° 01.620’	037° 33.909’	037° 02.982’
6	29.11.2022	54° 23.506’	54° 09.406’	037° 32.287’	037° 27.912’
7	01.- 02.12.2022	54° 15.870’	54° 15.941’	036° 25.980’	036° 26.253’
8	03.12.2022	54° 21.146’	54° 21.147’	036° 22.012’	036° 22.036’
9	04.12.2022	54° 17.571’	54° 17.611’	036° 27.603’	036° 27.590’
10	06.12.2022	53° 54.421’	53° 50.206’	036° 16.936’	036° 18.574’
11	07.12.2022	54° 03.911’	54° 04.818’	036° 08.483’	036° 07.559’
12	08.12.2022	55° 01.858’	54° 59.677’	036° 19.463’	036° 00.993’

Tab. 13.3: Physical parameters and weather conditions noted during surface filtration.

Filter #	T Water [°C]		Salinity [PSU]		Filter volume [l]	Weather
	Start	End	Start	End		
1	5.7	5.6	34.06	34.06	105	calm, covered, foggy, low waves
2	2.5	2.5	33.72	33.72	130	calm, low waves
3	3	2.8	33.81	33.77	141	sunny, calm
4	1.2	1.2	33.74	33.78	186	heavy winds, sunny to hail
5	2.1	2.3	33.76	33.81	126	night, windy and wavy
6	2.9	3	33.73	33.53	90	foggy, rainy, calm
7	3.1	2.5	33.04	33.44	126	calm, clear
8	2.3	2.3	32.1	32.39	84	sunny, calm
9	2	2.3	32.27	32.21	64	covered, calm
10	3	2.8	33.82	33.76	193	wavy, windy
11	2.7	2.7	33.69	33.69	85	wavy, cold
12	2.5	2.7	33.75	33.57	186	rough weather, high waves

Sediment sampling

Fjords are accumulation hotspots for organic matter (OM) derived from marine primary production as well as the terrestrial realm adjacent to the fjord. Radiocarbon analyses of bulk sediment samples, specific extractable compounds and pyrolytically derived OM fraction will be conducted to investigate the fate of terrestrial organic matter in fjord settings and increase the understanding of the high latitude carbon cycling. To trace organic matter transportation pathways from land into the ocean, sediment samples were collected from marine sediments in the fjords. The MUC cores were sampled in 1 cm intervals and stored frozen in pre-combusted glass petri dishes, in addition bottom water was collected for DIC radiocarbon analysis (10 mL fixed with $HgCl_2$) (Table 13.4).

Tab. 13.4: Sample list of MUC sediments and bottom water (BW DIC) collected.

Station	Date	Lat. °S	Long. °W	Depth interval samples [cm]	#Samples	#BW DIC
PS133/2_12-1	26.11.2022	54° 01.616’	037° 03.010’	0-3	3	2
PS133/2_15-5	27.11.2022	54° 05.076’	037° 05.999’	0-24	24	2
PS133/2_17-12	28.11.2022	54° 24.075’	037° 34.062’	0-10	10	2
PS133/2_23-10	29.11.2022	54° 09.551’	037° 23.188’	0-30	30	2
PS133/2_32-17	02.12.2022	54° 15.873’	036° 26.269’	0-17	17	2
PS133/2_35-6	03.12.2022	54° 20.741’	036° 22.707’	0-9	9	0
PS133/2_42-8	07.12.2022	54° 12.518’	036° 26.510’	0-15	15	3
PS133/2_42-9	07.12.2022	54° 12.522’	036° 26.523’	0-17	17	0
PS133/2_50-7	07.12.2022	54° 03.914’	036° 08.528’	0-26	26	3

Pore water sampling

In an attempt to extend the analytical capacities of the AWI MICADAS radiocarbon dating facility, pore water samples were collected from 3 additional MUC cores (Table 13.5). We aim to determine the radiocarbon age of pore water DIC and DOC which, in conjunction with other pore water data collected on parallel cores, can provide further insides on sediment geochemical processes. Pore water was collected following the sample strategie defined by the sediment geochemistry group (see above). The extracted pore water was split into 2.2 mL DIC (fixed with $HgCl_2$) subsamples and remaining pore water was transferred to 10 mL pre-combusted crimp cap vials (acidified to pH ~ 2 with HCl) for the radiocarbon analysis of DOM and samples were stored at +4 °C.

Tab. 13.5: List of MUC pore water and bottom water samples (BW DIC) collected.

Station	Date	Lat. °S	Long. °W	Depth interval samples [cm]	#Samples	#BW DIC
PS133/2_42-8	07.12.2022	54° 12.518’	036° 26.510’	0-17	17	1
PS133/2_42-9	07.12.2022	54° 12.522’	036° 26.523’	0-12	11	1
PS133/2_50-7	07.12.2022	54° 03.914’	036° 08.528’	0-25	15	1

Land based sample collection

Soil and water samples were taken during three land-based sampling campaigns that targeted the fjord-specific terrestrial surroundings. Different soil types were sampled for radiocarbon analyses and thermal stability investigations applying ramped pyrolysis/oxidation. The soil was sampled into pre-combusted 100 mL honey jars and stored frozen (-20°C) until analysis. Water was sampled for radiocarbon analysis of particulate and dissolved organic ($PO^{14}C$, $DO^{14}C$) and inorganic ($DI^{14}C$) carbon, as well as DOC molecular composition. For $DI^{14}C$, duplicates or triplicates of 10 mL were sampled into pre-combusted glass vials that were fixed with $HgCl_2$, crimped shut and stored at 4°C until analysis. For DOC investigations, different volumes were sampled in acid-cleaned brown 500 mL HDPE bottles. On board, the DOC water was filtered over pre-combusted 45 mm diameter glass-fibre filters (Whatmann, 0.7 µm), which were stored frozen (-20°C) for POC analysis. 500 mL subsamples of the filtrate were taken for $DO^{14}C$ determination and DOC molecular analyses, acidified with HCl (dublicates) and H_2SO_4 (single sample) and stored at 4°C until analysis.

Location 1: Peggotty Bluff, inner King Haakon Bay: 29.11.2022;
Landing side: 54° 08.7395' S 037° 16.7609' W (Tables 13.6 and 13.7**):**

Tab. 13.6: Information for soil samples taken during the land-based sampling campain at Peggotty Bluff, inner King Haakon Bay. Different formats of coordinates are due to the usage of different GPS devices.

Sample	Lat. °S	Long. °W
PS133/2_King Haakon Land #1	54° 08.7395'	037° 16.7609'
PS133/2_King Haakon Land #2	54° 08.7449'	037° 16.7609'
PS133/2_King Haakon Land #3	54° 08.6577'	037° 16.6623'
PS133/2_King Haakon Land #4	54° 08.6592'	037° 16.6999'
PS133/2_King Haakon Land #5	54° 08.6776'	037° 16.7096'
PS133/2_King Haakon Land #6	54° 08.6511'	037° 16.6820'
PS133/2_King Haakon Land #7	54° 08.6776'	037° 16.7096'
PS133/2_King Haakon Land #8	54° 08.6244'	037° 16.6224'
PS133/2_King Haakon Land #9	54° 08.6921'	037° 16.6876'
PS133/2_King Haakon Land #10	54° 08.6833'	037° 16.6967'
PS133/2_King Haakon Land #11 Sed. SW B	S 54° 08' 41"	W 37° 16' 36"
PS133/2_King Haakon Land #12 Sed. SW A	54° 8' 45''	037° 16' 34''

Tab. 13.7: Information for water samples taken during the land-based sampling campaign at Peggotty Bluff, inner King Haakon Bay. POC volume is the amount of water filtered on board, DIC and DOC Sample [#] show how many DIC and DOC replicates were collected. Different formats of coordinates are due to the usage of different GPS devices. SW=Schmelzwasser (melt water). In addition to terrestrial water, a marine water sample was taken from the surface water in the bay in front of the landing side.

Sample	Lat. °S	Long. °W	POC Volume [l]	# DIC [10 ml]	# DOC
PS133/2_King Haakon Land SW 1	54° 08' 42''	037° 16'34''	0.7	2x	2x HCl
PS133/2_King Haakon Land SW 2	54° 8' 43''	037° 16'33''	2	2x	2x HCl
PS133/2_King Haakon Land SW 3	54° 8' 39''	037° 16'38''	1.4 (filter 1) 1.35 (filter 2)	2x	2x HCl, 1x H_2SO_4
PS133/2_King Haakon Land Eisenhaltige Quelle	54° 08.6776'	037° 16.7096'	2.5	2x	2x HCl, 1x H_2SO_4
PS133/2_King Haakon Bay Surface Water	54° 08.847'	037° 16.878	3.2	-	2x HCl, 1x H_2SO_4

Location 2: Moraine Fjord, Cumberland Bay Fjord: 04.12.2022
Landing Side: 54° 21.9184' S 036° 29.4427' W (Tables 13.8 and 13.9; Fig. 13.1)**:**

Tab. 13.8: Information for soil samples taken during the land-based sampling campain at Moraine Fjord, Cumberland Bay Fjord Area.

Sample	Lat. °S	Long. °W
PS133/2_Moraine Fjord Land #13	54° 22.1595'	036° 29.6102'
PS133/2_Moraine Fjord Land #14	54° 22.1399'	036° 29.7256'
PS133/2_Moraine Fjord Land #15 See mix	54° 22.1589'	036° 29.5614'
PS133/2_Moraine Fjord Land #15 See oben	54° 22.1589'	036° 29.5614'
PS133/2_Moraine Fjord Land #15 See unten	54° 22.1589'	036° 29.5614'

Tab. 13.9: Information for water samples taken during the land-based sampling campaign at Moraine Fjord, in the Cumberland Bay Fjord Area. POC volume is the amount of water filtered on board, DIC and DOC Sample [#] shows how many DIC and DOC replicates were collected.

Sample	Lat. °S	Long. °W	POC Volume [l]	# DI14C [10 ml]	DOC
PS133/2_MF_FW_S1	54° 22.1399'	036° 29.7256'	0.5 (filter 1) 0.75 (filter 2) 0.75 (filter 3)	3x	1x HCl 1x H_2SO_4
PS133/2_MF_FW_S2	54° 22.1589'	036° 29.5614'	2.5	3x	1x HCl 1x H_2SO_4

Location 3: Grytviken, samples taken during hike starting from Grytviken Whaling station towards Penguin River: 05.12.2022 (Tables 13.10 and 13.11; Fig. 13.1)**:**

Tab. 13.10: Information for soil samples taken during the land-based sampling campaign in the Grytviken area.

Sample	Lat. °S	Long. °W
PS133/2 Grytviken Land # 16	54° 17.6983'	036° 30.0319'
PS133/2 Grytviken Land # 17 Mix	54° 17.6780'	036° 30.0087'
PS133/2 Grytviken Land # 18	54° 17.6780'	036° 30.0087'
PS133/2 Grytviken Land # 19	54° 17.5744'	036° 30.0782'
PS133/2 Grytviken Land # 20	54° 17.1127'	036° 30.8068'
PS133/2 Grytviken Land # 21 oben	54° 16.8677'	036° 30.6433'
PS133/2 Grytviken Land # 22 unten	54° 16.8677'	036° 30.6433'

Tab. 13.11: Information for water samples taken during the land-based sampling campaign in the Grytviken area. POC volume is the amount of water filtered on board, DIC and DOC Sample [#] show how many DIC and DOC replicates were collected.

Sample	Lat. °S	Long. °W	POC Volume [l]	# DI^{14}C [10 ml]	DOC
PS133/2_GV_FW_S1	54° 17.1785’	036° 30.4906’	0.2 (filter 1) 0.2 (filter 2) 0.2 (filter 3) 0.2 (filter 4)	3x	1x HCl 1x H_2SO_4
PS133/2_GV_FW_S2	54° 17.1823’	036° 30.6073’	3	3x	1x HCl 1x H_2SO_4
PS133/2_GV_FW_S3	54° 17.3040’	036° 30.4181’	0.3 (filter 1) 0.3 (filter 2) 0.3 (filter 3) 0.3 (filter 4)	3x	1x HCl 1x H_2SO_4
PS133/2_GV_FW_S4	54° 17.7197’	036° 29.6495’	2.5	3x	1x HCl 1x H_2SO_4
PS133/2_GV_FW_S6	54° 16.8677’	036° 30.6433’	2.5	3x	1x HCl 1x H_2SO_4

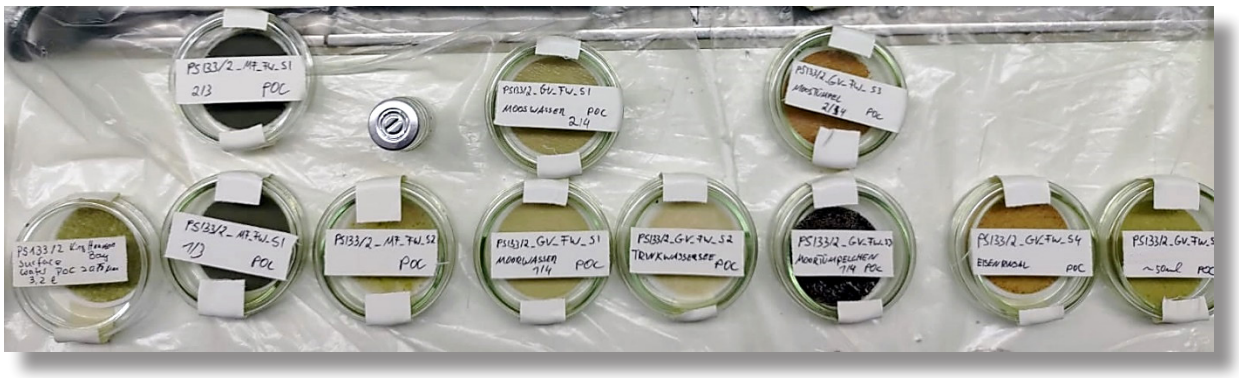

Fig. 13.1: Picture of POC filters obtained from water samples taken from the Moraine Fjord and Grytviken land sampling campaigns. Different shades and intensities of colouration indicate the presence of diverse particulate matter composition.

Preliminary and expected results

We will generate lateral and vertical profiles of the ^{14}C abundance in the marine carbon pools (POC, DOC, DIC), and pair the isotopic information with molecular characterization of POC and DOC. The expected data set will quantify and characterize terrestrial and marine organic carbon export to the fjord sediments. Further the generated data will allow to examine how organic carbon fluxes varied over the last hundreds of years in response to climatic perturbations. All analyses will be conducted upon completion of the expedition.

Data management

Data will be archived, published and disseminated according to international standards by the World Data Center PANGAEA Data Publisher for Earth & Environmental Science (https://www.pangaea.de) within two years after the end of the cruise at the latest. By default, the CC-BY license will be applied.

Any other data will be submitted to an appropriate long-term archive that provides unique and stable identifiers for the datasets and allows open online access to the data.

This expedition is supported by the Helmholtz Research Programme “Changing Earth – Sustaining our Future” Topic 2, Subtopics 1 and 4, Topic 4, Subtopic 1 and Topic 6, Subtopics 2 and 3.

In all publications based on this expedition, the **Grant No. AWI_PS133/2_12** will be quoted and the following publication will be cited:

Alfred-Wegener-Institut Helmholtz-Zentrum für Polar- und Meeresforschung (2017) Polar Research and Supply Vessel POLARSTERN Operated by the Alfred-Wegener-Institute. Journal of large-scale research facilities, 3, A119. http://dx.doi.org/10.17815/jlsrf-3-163.

14. NUTRIENTS AND DISSOLVED ORGANIC MATTER

Kai-Uwe Ludwichowski[1], Erik Stein[1] [1]DE.AWI/Nutrient Facility
not on board: Martin Graeve[1], Boris Koch[1]

Grant-No. AWI_PS133/2_13

Objectives

The determination of nutrients and biogeochemical parameters is closely connected to the physical and planktological investigations. The development of phytoplankton blooms is especially dependent on the available nutrients. Nutrients are also well suited as tracers for the identification of water masses. Our interests on this expedition was focussed to shed light on the sources and transport pathways of Fe and on nutrient distribution in the upper water layer. During the CTD-transects, all inorganic nutrients (nitrate, nitrite, ammonium, silicate and phosphate) were measured in the samples drawn from the rosette bottle system. In addition, dissolved organic matter (DOM) samples have been taken for bulk determinations (DOC/DON).

Work at sea

283 nutrient-samples were collected with the rosette water sampler at various depths (Table 14.1). Phosphate (Murphy and Riley, 1962), silicate (Strickland and Parsons, 1968), nitrite, nitrate (Grasshoff et al., 1983) and ammonia (Kerouel and Aminot, 1997) were determined immediately on board using a Seal 500 auto-analyser system according to standard methods. Additional 104 nutrient-samples from experiments carried out on board of *Polarstern* were measured (Table 14.1). For 128 DOC samples, 50 mL of each seawater sample was filtered through annealed glass fibre filters (Whatman, 450°C, 5 h, 0.7 µm nominal pore size) with a maximum pressure < 200 mbar. DOC-samples were stored at -20°C in pre-cleaned high-density polyethylene (HDPE) bottles.

Tab. 14.1: Overview of samples taken for nutrient and DOC analyses (AWI).

Station	Cast	Nutrients	DOC	Nutrient Experiments
1	5	5	0	
5	1	8	0	
9	1	11	7	
11	1	9	7	
15	1	17	7	
17	3	15	7	
18	1	12	6	
19	1	10	6	
20	1	13	7	
23	1	14	7	
24	1	10	7	
28	1	15	7	

Station	Cast	Nutrients	DOC	Nutrient Experiments
31	1	15	7	
32	3	13	7	
35	1	9	6	
37	1	9	3	
38	1	6	3	89
39	1	6	3	8
40	2	6	4	7
45	1	11	6	
42	5	14	7	
48	1	14	7	
50	1	14	7	

Preliminary Results

The oceanographic and experimental nutrient samples already measured on board and the DOC samples that will be measured later in Bremerhaven, contribute to the study of the oceanographic coupling between South Georgia and the Antarctic Circumpolar Current ACC, the particle dynamics, the sources and biogeochemical processes that control the transport and transformation of ferrous components along the flow path of the ACC. Raw nutrient data, available approximately two days after sampling, will give us an overview of water masses, biological activity, and the operation of our sampling system. Later, the nutrient data will be used for numerous studies during the cruise to reveal a variety of physical and biological processes.

Data management

We sampled a large variety of interconnected parameters. We plan that the full data set will be available at least half a year after the cruise. DOC-samples, which were not analyzed on board, will be measured immediately after their arrival at AWI. Data will be archived, published and disseminated according to international standards by the World Data Center PANGAEA Data Publisher for Earth & Environmental Science (https://www.pangaea.de) within two years after the end of the cruise at the latest. By default, the CC-BY license will be applied. Data on carbon and nitrogen isotope ratios of POC will be provided upon request to all cruise participants and later also uploaded to the PANGAEA Data archive.

This expedition was supported by the Helmholtz Research Programme “Changing Earth – Sustaining our Future” Topic 2, Subtopics 1 and 4, Topic 4, Subtopic 1 and Topic 6, Subtopics 2 and 3.

In all publications based on this expedition, the Grant No. AWI_PS133/2_13 will be quoted and the following publication will be cited:

Alfred-Wegener-Institut Helmholtz-Zentrum für Polar- und Meeresforschung (2017) Polar Research and Supply Vessel POLARSTERN Operated by the Alfred-Wegener-Institute. Journal of Large-Scale Research Facilities, 3, A119. http://dx.doi.org/10.17815/jlsrf-3-163.

References

Grasshoff K, Ehrhardt M, Kremling K (1983) Methods of Seawater Analysis. 2nd Edition, Verlag Chemie Weinhein, New York.

Kerouel R, Aminot A (1997) Fluorometric determination of ammonia in sea and estuarine waters by direct segmented flow analysis. Marine Chemistry 57:265-275.

Murphy J, Riley JP (1962) A modified single solution method for the determination of phosphate in natural waters. Analytica Chimica Acta, 27:31-36.

Strickland JDH, Parsons TR (1968) A practical handbook of seawater analysis. Research Board of Canada, Bulletin. No 167.

15. DANKSAGUNG

Sabine Kasten DE.AWI

Im Namen des gesamten Wissenschaftsteams der Expedition PS133/2 bedanke ich mich ganz herzlich bei Kapitän Moritz Langhinrichs und der Besatzung der *Polarstern* für die hervorragende Unterstützung und Hilfsbereitschaft bei der Koordination, Vorbereitung und Durchführung unserer wissenschaftlichen Arbeiten an Bord.

Mein Dank geht außerdem an die zahlreichen Kolleginnen und Kollegen der AWI Abteilung *Logistik und Forschungsplattformen* und deren Unterabteilungen sowie die vielen Mitarbeitenden der anderen Abteilungen am AWI, die uns in der Planung, Vorbereitung, Abwicklung und Öffentlichkeitsarbeit der und in Zusammenhang mit der Expedition und z.B. auch dem 40-jährigen *Polarstern*-Geburtstag in perfekter und kompetenter Weise unterstützt haben. Am Ende dieses letzten Kapitels des Fahrtberichts der Expedition PS133/2 geht mein besonderes Dankeschön an das AWI-Direktorium, an Stefan Hain und an Michael Thurmann (Reederei Laeisz), ohne die wir es sicher nicht geschafft hätten in Punta Arenas noch zeitnah einen Liegeplatz an der benötigten Pier zu erhalten. Nur aufgrund dieses bemerkenswerten Engagements war es möglich, mit nur minimaler Verspätung zu unserer Expedition PS133/2 „Island Impact“ aufzubrechen und die geplanten wissenschaftlichen Arbeiten sehr erfolgreich und in vollem Umfang durchzuführen.

APPENDIX

A.1 TEILNEHMENDE INSTITUTE / PARTICIPATING INSTITUTES

A.2 FAHRTTEILNEHMER:INNEN / CRUISE PARTICIPANTS

A.3 SCHIFFSBESATZUNG / SHIP‘S CREW

A.4 STATIONSLISTE / STATION LIST

A.5 KERN-LOGS DER SCHWERELOTKERNE DER GRUPPE MARINE GEOLOGIE / CORE LOGS OF GRAVITY CORES TAKEN FOR / BY THE MARINE GEOLOGY GROUP

A.6 VERTEILUNGSPROTOKOLLE DER MUC KERNE / MUC CORE DISTRIBUTION PROTOCOLS

A.1 TEILNEHMENDE INSTITUTE / PARTICIPATING INSTITUTES

Affiliation	Address
AR.Armada	Departamento Hidrografía SERVICIO DE HIDROGRAFÍA NAVAL MINISTERIO DE DEFENSA Av. Manuel Augusto Montes de Oca 2124 Ciudad Autónoma de Buenos Aires Celular: +5493584248016 Argentina
AR.IAA	Instituto Antártico Argentino 25 de Mayo 1143 1650 San Martin Argentina
DE.AWI	Alfred-Wegener-Institut Helmholtz-Zentrum für Polar- und Meeresforschung Postfach 120161 27515 Bremerhaven Germany
DE.DWD	Deutscher Wetterdienst Seewetteramt Bernhard Nocht Str. 76 20359 Hamburg Germany
DE.GEOMAR	GEOMAR Helmholtz-Zentrum für Ozeanforschung Kiel Wischhofstr. 1-3 24148 Kiel Germany
DE.MARUM	MARUM – Zentrum für Marine Umweltwissenschaften der Universität Bremen Leobener Str. 8 28359 Bremen Germany
DE.MPIMM	Max-Planck-Institut für Marine Mikrobiologie Celsiusstraße 1 28359 Bremen Germany

Affiliation	Address
DE.NHC	Helikopter Service Northern HeliCopter GmbH Gorch-Fock-Str. 103 26721 Emden Germany
DE.UNI-Bremen	Universität Bremen Klagenfurter Strasse 2-4 28359 Bremen Germany
DE.UNI-Heidelberg	Universität Heidelberg Grabengasse 1 69117 Heidelberg Germany
DE.UNI-Köln	Universität zu Köln Zülpicher Str. 49b 50764 Köln Germany
GOV.FLORIDA	University of South Florida 830 1st St S 33701 St. Petersburg USA
PL.PAS	Polish Academy of Sciences Twarda, 51/55 818 Warszawa Poland
UK:BAS	British Antarctic Survey High Cross Madingley Road CB3 0ET Cambridge UK
UK.GLA	University of Glasgow Scottish Universities Environmental Research Centre Rankine Avenue G75 0QF East Kilbride UK

Affiliation	**Address**
UK.NCL	Newcastle University School of Natural and Environmental Sciences Claremont Road NE1 7RU Newcastle UK
UK.SOTON	University of Southampton University Road S017 1BJ Southampton UK

A.2 FAHRTTEILNEHMER:INNEN / CRUISE PARTICIPANTS

Name/ Last name	Vorname/ First name	Institut/ Institute	Beruf/ Profession	Fachrichtung/ Discipline
Anderson	Madeline	UK.BAS	PhD Student	Biology
Anselin	Josephine	UK.BAS	PhD Student	Oceanography
Bussmann	Ingeborg	DE.AWI	Scientist	Geology
Cattana	Lucia	AR.Armada	Observer	Geology
Chang	Jun Hao	DE.UNI-Köln	PhD Student	Geochemistry
Colias Blanco	Manuel	DE.NHC	Technician	Helikopter Service
Dohrmann	Ingrid	DE.AWI	Technician	Geochemistry
Ebner	Berenice	DE.AWI	PhD Student	Geochemistry
Geibert	Walter	DE.AWI	Scientist	Geochemistry
Gentz	Torben	DE.AWI	Scientist	Geochemistry
Gischler	Michael	DE.NHC	Pilot	Helikopter Service
Glawatty	Tanja	DE.AWI	Administrative Assistence	Biology
Grotheer	Hendrik	DE.AWI	Scientist	Geochemistry
Höhn	Malte	DE.AWI	Engineer	Geochemistry
Hübner	Joshua	DE.AWI	Student	Chemistry
Iversen	Morten	DE.AWI	Scientist	Biology
Jones	Rhiannon	UK.SOTON	PhD Student	Oceanography
Kasten	Sabine	DE.AWI	Scientist	Geochemistry
Kattein	Laura	DE.AWI	PhD Student	Geochemistry
Knobelsdorf	Michael	DE.DWD	Scientist	Meteorology
Koch	Florian	DE.AWI	Scientist	Biology
Koehler	Dennis	DE.AWI	Engineer	Geochemistry
Koehler	Neele	DE.UNI-Bremen	Student	Geology
Köster	Male	DE.AWI	Scientist	Geochemistry
Krock	Bernd	DE.AWI	Scientist	Chemistry
Laufer-Meiser	Katja	DE.GEOMAR	Scientist	Biology
Lensch	Norbert	DE.AWI	Technician	Geology
Lesic	Nina-Marie	DE.MARUM	PhD Student	Geology
Leusch	Maja	DE.UNI-Bremen	Student	Geochemistry
Linse	Katrin	UK.BAS	Scientist	Biology
Ludwichowski	Kai-Uwe	DE.AWI	Engineer	Chemistry
Marchant	Hannah	DE.MARUM	Scientist	Geochemistry
Müller	Daniel	DE.AWI	PhD Student	Geochemistry
Nadolsky	Christina	DE.AWI	PhD Student	Geochemistry
Oetjens	Annika	DE.UNI-Heidelberg	Student	Physics
Otte	Frank	DE.DWD	Scientist	Meteorology
Porrmann	Simon	DE.AWI	Student	Geophysics
Rubiano	Catalina	GOV.FLORIDA	Student	Oceanography

Name/ Last name	**Vorname/ First name**	**Institut/ Institute**	**Beruf/ Profession**	**Fachrichtung/ Discipline**
Schaubensteiner	Stefan	DE.NHC	Pilot	Helikopter Service
Sekudewicz	Ilona	PL.PAS	PhD Student	Geochemistry
Spahic	Susanne	DE.AWI	Technician	Biology
Staubwasser	Michael	DE.UNI-Köln	Scientist	Geochemistry
Stein	Erik	DE.AWI	Technician	Chemistry
Stimac	Ingrid	DE.AWI	Technician	Geochemistry
Stimpfle	Jasmin	DE.AWI	PhD Student	Biology
Streuff	Katharina	DE.UNI-Bremen	Scientist	Geology
Weiss	Josefine-Friederike	DE.AWI	PhD Student	Biology
Wilkie	Isabella	DE.MPIMM	PhD Student	Biology
Willis Poratti	Graciana	AR.IAA	Scientist	Biology
Wunder	Lea	DE.UNI-Bremen	PhD Student	Biology

A.3 SCHIFFSBESATZUNG / SHIP‘S CREW

Name / Last Name	**Vorname / First Name**	**Position / Rank**
Langhinrichs	Moritz	Master
Langhinrichs	Jacob	Chiefmate
Ziemann	Olaf	Chief
Eckenfels	Hannes	2nd Mate
Peine	Lutz	2nd Mate
Strauß	Erik	2nd Mate
Hofmann	Jörg	Comm. Off.
Guba	Klaus	Ships Doc
Ehrke	Tom	2nd. Eng
Krinfeld	Oleksandr	2nd. Eng
Rusch	Torben	2nd. Eng
Pommerencke	Bernd	SET
Frank	Gerhard	ELO
Krüger	Lars	ELO
Schwedka	Thorsten	ELO
Winter	Andreas	ELO
Brück	Sebastian	Bosun
Keller	Jürgen Eugen	Carpen.
Buchholz	Joscha	MP Rat.
Decker	Jens	MP Rat.
Lutz	Johannes Paul	MP Rat.
Möller	Falko	MP Rat.
Schade	Tom	MP Rat.
Stellmanns	Thies Christian	MP Rat.
Weiß	Daniel	MP Rat.
Bäcker	Andreas	AB
Niebuhr	Tims	AB
Plehn	Marco Markus	Storekk.
Arnold-Becker	André	MP Rat.
Clasen	Nils	MP Rat.
Fink	Anna-Maria	MP Rat.

Name / Last Name	**Vorname / First Name**	**Position / Rank**
Probst	Lorenz	MP Rat.
Waterstradt	Felix	MP Rat.
Matter	Sebastian	Cook
Silinski	Frank	Cooksm.
Witusch	Petra	Chief Stew.
Ilk	Romy	Nurse
Fehrenbach	Martina	2nd Stew
Golla	Gerald	2nd Stew.
Shi	Wubo	2nd Stew.
Silinski	Carmen	2nd Stew.
Hu	Guo Yong	Laundrym.

A.4 STATIONSLISTE / STATION LIST PS133/2

Station list of expedition PS133/2 from Punta Arenas to Bremerhaven;
the list details the action log for all stations along the cruise track.

See https://www.pangaea.de/expeditions/events/PS133/2 to display the station (event) list for expedition PS133/2.
This version contains Uniform Resource Identifiers for all sensors listed under https://sensor.awi.de. See https://www.awi.de/en/about-us/service/computing-centre/data-flow-framework.html for further information about AWI's data flow framework from sensor observations to

Event label	Optional label	Date/Time	Latitude	Longitude	Depth [m]	Gear	Action	Comment
PS133/2-track		2022-11-19T00:00:00	-53,14470	-70,90910		CT	Station start	Punta Arenas - Cape Town
PS133/2-track		2022-12-19T00:00:00	-33,90680	18,43370		CT	Station end	Punta Arenas - Cape Town
PS133/2_0_Underway-28		2022-11-19T06:00:00	-53,12535	-70,85847		SWEAS	Station start	
PS133/2_0_Underway-28		2022-12-10T16:39:55	-52,26904	-25,03360		SWEAS	Station end	
PS133/2_0_Underway-6		2022-11-20T17:24:59	-53,08346	-70,70302		MYON	Station start	
PS133/2_0_Underway-6		2022-12-10T16:39:55	-52,26904	-25,03360		MYON	Station end	
PS133/2_0_Underway-14		2022-11-20T17:25:40	-53,08133	-70,69962		NEUMON	Station start	
PS133/2_0_Underway-14		2022-12-10T16:39:55	-52,26904	-25,03360		NEUMON	Station end	
PS133/2_0_Underway-24		2022-11-21T11:59:04	-52,90599	-65,58358		TSG	Station start	TSK2
PS133/2_0_Underway-24		2022-12-10T16:39:55	-52,26904	-25,03360		TSG	Station end	TSK2
PS133/2_0_Underway-23		2022-11-21T11:59:51	-52,90619	-65,57979		TSG	Station start	TSK1
PS133/2_0_Underway-23		2022-12-10T16:39:55	-52,26904	-25,03360		TSG	Station end	TSK1
PS133/2_0_Underway-22		2022-11-21T12:00:29	-52,90637	-65,57672		SNDVELPR	Station start	
PS133/2_0_Underway-22		2022-12-10T16:39:55	-52,26904	-25,03360		SNDVELPR	Station end	
PS133/2_0_Underway-18		2022-11-21T12:00:52	-52,90648	-65,57487		pCO2	Station start	
PS133/2_0_Underway-18		2022-12-10T16:39:55	-52,26904	-25,03360		pCO2	Station end	
PS133/2_0_Underway-17		2022-11-21T12:01:10	-52,90657	-65,57342		pCO2	Station start	
PS133/2_0_Underway-17		2022-12-10T16:39:55	-52,26904	-25,03360		pCO2	Station end	

** Comments are limited to 130 characters. See https://www.pangaea.de/expeditions/events/PS133/2 to show full comments in conjunction with the station (event) list for expedition PS133/2*

Event label	Optional label	Date/Time	Latitude	Longitude	Depth [m]	Gear	Action	Comment
PS133/2_0_Underway-11		2022-11-21T12:01:24	-52,90664	-65,57229		MAG	Station start	
PS133/2_0_Underway-11		2022-12-10T16:39:55	-52,26904	-25,03360		MAG	Station end	
PS133/2_0_Underway-7		2022-11-21T12:01:58	-52,90682	-65,56946		FBOX	Station start	
PS133/2_0_Underway-7		2022-12-10T16:39:55	-52,26904	-25,03360		FBOX	Station end	
PS133/2_0_Underway-1		2022-11-21T12:02:50	-52,90709	-65,56534		ADCP	Station start	
PS133/2_0_Underway-1		2022-12-10T16:39:55	-52,26904	-25,03360		ADCP	Station end	
PS133/2_1-1		2022-11-24T14:57:15	-54,59802	-43,90934		HN	Station start	
PS133/2_1-1		2022-11-24T15:00:52	-54,59963	-43,90870		HN	Station end	
PS133/2_1-2		2022-11-24T15:37:22	-54,60650	-43,90182		CTD-TM	max depth	
PS133/2_1-3		2022-11-24T16:41:41	-54,60245	-43,89645		APN	Station start	
PS133/2_1-3		2022-11-24T17:04:55	-54,60480	-43,89679		APN	Station end	
PS133/2_1-4		2022-11-24T17:38:28	-54,59985	-43,89777		TMPUMP	max depth	
PS133/2_1-5		2022-11-25T00:05:42	-54,60019	-43,89987		CTD-RO	max depth	
PS133/2_2-1		2022-11-25T03:58:16	-54,34080	-43,53732		HN	Station start	Airsampling
PS133/2_2-1		2022-11-25T04:01:53	-54,33261	-43,52588		HN	Station end	Airsampling
PS133/2_3-1		2022-11-25T14:36:00	-53,15653	-41,26143		MBES	Station start	
PS133/2_3-1		2022-11-25T17:36:40	-53,27284	-40,97922		MBES	Station end	
PS133/2_4-1		2022-11-25T15:55:14	-53,20678	-41,13842		HN	Station start	Airsampling
PS133/2_4-1		2022-11-25T15:57:37	-53,20830	-41,13471		HN	Station end	Airsampling
PS133/2_5-1		2022-11-26T01:01:37	-53,50028	-39,08016		CTD-TM	max depth	
PS133/2_5-2		2022-11-26T02:06:30	-53,50007	-39,07999		APN	Station start	
PS133/2_5-2		2022-11-26T02:21:50	-53,49962	-39,07913		APN	Station end	
PS133/2_6-1		2022-11-26T03:58:04	-53,60942	-38,69601		HN	Station start	Airsampling
PS133/2_6-1		2022-11-26T04:01:09	-53,61326	-38,68247		HN	Station end	Airsampling
PS133/2_7-1		2022-11-26T06:12:58	-53,76510	-38,14738		EK80	Station start	
PS133/2_7-1		2022-11-26T09:05:19	-53,77625	-38,13054		EK80	Station end	
PS133/2_8-1		2022-11-26T09:05:55	-53,77667	-38,12984		MBES	Station start	

Event label	Optional label	Date/Time	Latitude	Longitude	Depth [m]	Gear	Action	Comment
PS133/2_8-1		2022-11-26T10:15:13	-53,77031	-38,13856		MBES	Station end	
PS133/2_9-1		2022-11-26T10:52:39	-53,76986	-38,14041		CTD-RO	max depth	
PS133/2_9-2		2022-11-26T11:46:47	-53,77012	-38,14030		MUC	max depth	
PS133/2_9-3		2022-11-26T13:05:57	-53,77007	-38,14033		GC	max depth	
PS133/2_10-1		2022-11-26T16:01:41	-53,88520	-37,60826		HN	Station start	Airsampling
PS133/2_10-1		2022-11-26T16:04:07	-53,88729	-37,59698		HN	Station end	Airsampling
PS133/2_11-1		2022-11-26T19:12:40	-54,03565	-37,05680		CTD-RO	max depth	
PS133/2_11-2		2022-11-26T20:35:03	-54,03583	-37,05699		CTD-TM	max depth	
PS133/2_11-3		2022-11-26T21:21:30	-54,03545	-37,05671		APN	Station start	
PS133/2_11-3		2022-11-26T21:37:49	-54,03534	-37,05597		APN	Station end	
PS133/2_12-1		2022-11-26T22:14:29	-54,02694	-37,05017		MUC	max depth	
PS133/2_12-2		2022-11-26T23:08:23	-54,02727	-37,05019		MUC	max depth	
PS133/2_12-3		2022-11-27T00:15:33	-54,02700	-37,04969		GC	max depth	
PS133/2_13-1		2022-11-27T02:51:19	-54,02406	-37,06429		MBES	Station start	
PS133/2_13-1		2022-11-27T13:34:48	-54,08343	-37,09845		MBES	Station end	
PS133/2_14-1		2022-11-27T03:41:00	-53,99912	-37,00442		HN	Station start	Airsampling
PS133/2_14-1		2022-11-27T03:42:42	-54,00150	-37,00741		HN	Station end	Airsampling
PS133/2_15-1		2022-11-27T14:03:54	-54,08419	-37,09995		CTD-RO	max depth	
PS133/2_15-2		2022-11-27T14:52:30	-54,08416	-37,10093		APN	Station start	
PS133/2_15-2		2022-11-27T15:08:30	-54,08441	-37,10070		APN	Station end	
PS133/2_15-4		2022-11-27T15:40:26	-54,08407	-37,10025		HN	Station start	Airsampling
PS133/2_15-4		2022-11-27T15:45:51	-54,08404	-37,09972		HN	Station end	Airsampling
PS133/2_15-3		2022-11-27T15:43:33	-54,08404	-37,09996		MUC	max depth	
PS133/2_15-5		2022-11-27T16:39:37	-54,08410	-37,10019		MUC	max depth	
PS133/2_15-6		2022-11-27T17:52:16	-54,08435	-37,10028		GC	max depth	
PS133/2_15-7		2022-11-27T19:22:01	-54,08448	-37,10072		GC	max depth	
PS133/2_16-1		2022-11-28T04:04:43	-53,82508	-38,17668		HN	Station start	Airsampling

Event label	Optional label	Date/Time	Latitude	Longitude	Depth [m]	Gear	Action	Comment
PS133/2_16-1		2022-11-28T04:09:04	-53,83053	-38,18174		HN	Station end	Airsampling
PS133/2_17-1		2022-11-28T10:22:35	-54,39126	-37,53638		KMT	max depth	release
PS133/2_17-2		2022-11-28T12:29:23	-54,40128	-37,56738		CTD-TM	max depth	
PS133/2_17-3		2022-11-28T13:28:21	-54,40128	-37,56788		CTD-RO	max depth	
PS133/2_17-4		2022-11-28T14:11:30	-54,40095	-37,56838		APN	Station start	
PS133/2_17-4		2022-11-28T14:26:31	-54,40108	-37,56907		APN	Station end	
PS133/2_17-5		2022-11-28T14:33:32	-54,40120	-37,56878		INSIPU	Station start	
PS133/2_17-5		2022-11-28T18:25:22	-54,40100	-37,56768		INSIPU	Station end	
PS133/2_17-6		2022-11-28T16:08:43	-54,39867	-37,56879		HN	Station start	Airsampling
PS133/2_17-6		2022-11-28T16:10:15	-54,39866	-37,56885		HN	Station end	Airsampling
PS133/2_17-7		2022-11-28T18:30:32	-54,40125	-37,56750		ROSINA	Station start	
PS133/2_17-7		2022-11-28T19:40:43	-54,40109	-37,56792		ROSINA	Station end	
PS133/2_17-8		2022-11-28T20:11:04	-54,40124	-37,56737		CTD-RO	max depth	
PS133/2_17-9		2022-11-28T20:34:06	-54,40108	-37,56780		WP2	Station start	
PS133/2_17-9		2022-11-28T20:52:34	-54,40122	-37,56758		WP2	Station end	
PS133/2_17-10		2022-11-28T21:11:37	-54,40123	-37,56777		MSC	Station start	
PS133/2_17-10		2022-11-28T21:34:53	-54,40115	-37,56729		MSC	Station end	
PS133/2_17-11		2022-11-28T22:16:15	-54,40111	-37,56718		MUC	max depth	
PS133/2_17-12		2022-11-28T23:11:53	-54,40124	-37,56769		MUC	max depth	
PS133/2_18-1		2022-11-29T00:55:00	-54,28862	-37,51432		CTD-RO	max depth	
PS133/2_18-2		2022-11-29T01:27:35	-54,28886	-37,51478		ROSINA	Station start	
PS133/2_18-2		2022-11-29T02:09:43	-54,28896	-37,51525		ROSINA	Station end	
PS133/2_19-2		2022-11-29T02:50:55	-54,31253	-37,54382		HN	Station start	Airsampling
PS133/2_19-2		2022-11-29T02:52:55	-54,31277	-37,54410		HN	Station end	Airsampling
PS133/2_19-1		2022-11-29T02:55:21	-54,31289	-37,54464		CTD-RO	max depth	
PS133/2_19-3		2022-11-29T03:35:46	-54,31199	-37,55124		ROSINA	Station start	
PS133/2_19-3		2022-11-29T04:24:30	-54,31297	-37,55439		ROSINA	Station end	
PS133/2_20-1		2022-11-29T05:27:52	-54,38531	-37,51234		CTD-RO	max depth	

Event label	Optional label	Date/Time	Latitude	Longitude	Depth [m]	Gear	Action	Comment
PS133/2_20-2		2022-11-29T06:06:21	-54,38513	-37,51299		ROSINA	Station start	
PS133/2_20-2		2022-11-29T07:14:53	-54,38588	-37,51334		ROSINA	Station end	
PS133/2_21-1		2022-11-29T08:05:11	-54,39189	-37,53777		PELAGRA	Station start	recovered
PS133/2_21-1		2022-11-29T08:59:23	-54,39182	-37,53796		PELAGRA	Station end	recovered
PS133/2_22-1		2022-11-29T12:00:07	-54,16118	-37,35281		ZODIAC	Station start	
PS133/2_22-1		2022-11-29T17:17:15	-54,16239	-37,35204		ZODIAC	Station end	
PS133/2_22-2		2022-11-29T12:00:28	-54,16118	-37,35282		ZODIAC	Station start	
PS133/2_22-2		2022-11-29T17:29:40	-54,16198	-37,35255		ZODIAC	Station end	
PS133/2_23-1		2022-11-29T14:09:35	-54,16123	-37,35417		CTD-RO	max depth	
PS133/2_23-2		2022-11-29T15:47:52	-54,16070	-37,35007		APN	Station start	
PS133/2_23-2		2022-11-29T16:31:31	-54,16132	-37,35256		APN	Station end	
PS133/2_23-3		2022-11-29T16:34:34	-54,16134	-37,35304		HN	Station start	Airsampling
PS133/2_23-3		2022-11-29T16:39:37	-54,16139	-37,35375		HN	Station end	Airsampling
PS133/2_23-4		2022-11-29T16:40:48	-54,16143	-37,35380		ROSINA	Station start	
PS133/2_23-4		2022-11-29T17:07:58	-54,16229	-37,35280		ROSINA	Station end	
PS133/2_23-5		2022-11-29T17:59:54	-54,16053	-37,35513		CTD-RO	max depth	
PS133/2_23-6		2022-11-29T18:32:20	-54,16056	-37,35495		WP2	Station start	
PS133/2_23-6		2022-11-29T18:45:25	-54,16041	-37,35498		WP2	Station end	
PS133/2_23-7		2022-11-29T22:15:54	-54,16089	-37,35410		CTD-TM	max depth	
PS133/2_23-8		2022-11-29T22:57:02	-54,16136	-37,35368		PELAGRA	Station start	
PS133/2_23-8		2022-11-29T23:42:55	-54,16105	-37,35434		PELAGRA	Station end	
PS133/2_23-9		2022-11-30T00:25:05	-54,15931	-37,38682		MUC	max depth	
PS133/2_23-10		2022-11-30T01:05:06	-54,15918	-37,38647		MUC	max depth	
PS133/2_23-11		2022-11-30T02:06:28	-54,15904	-37,38625		GC	max depth	
PS133/2_23-12		2022-11-30T03:26:05	-54,15957	-37,38651		HN	Station start	Airsampling
PS133/2_23-12		2022-11-30T03:30:58	-54,15953	-37,38642		HN	Station end	Airsampling
PS133/2_23-13		2022-11-30T04:18:09	-54,15869	-37,38533		GC	max depth	
PS133/2_23-14		2022-11-30T08:00:19	-54,16121	-37,35208		PELAGRA	Station start	recovered

Event label	Optional label	Date/Time	Latitude	Longitude	Depth [m]	Gear	Action	Comment
PS133/2_23-14		2022-11-30T08:40:09	-54,16127	-37,35300		PELAGRA	Station end	recovered
PS133/2_24-1		2022-11-30T10:54:41	-54,21346	-37,54077		CTD-RO	max depth	
PS133/2_17-13		2022-11-30T13:16:45	-54,40130	-37,56719		GC	max depth	
PS133/2_17-14		2022-11-30T14:49:37	-54,40081	-37,56863		GC	max depth	
PS133/2_25-1		2022-11-30T16:18:08	-54,45470	-37,35122		DRG	Station start	
PS133/2_25-1		2022-11-30T17:08:48	-54,44866	-37,35672		DRG	Station end	
PS133/2_26-1		2022-11-30T18:51:52	-54,41352	-37,61654		GC	max depth	
PS133/2_27-1		2022-11-30T20:05:44	-54,41346	-37,58826		TMPUMP	max depth	
PS133/2_28-1		2022-12-01T01:57:15	-54,15759	-37,97596		CTD-RO	max depth	
PS133/2_29-1		2022-12-01T08:30:23	-53,77009	-38,14026		GC	max depth	
PS133/2_29-2		2022-12-01T09:24:30	-53,77004	-38,14014		GC	max depth	
PS133/2_30-1		2022-12-01T16:00:37	-53,96892	-36,89849		HN	Station start	Airsampling
PS133/2_30-1		2022-12-01T16:09:49	-53,98223	-36,86216		HN	Station end	Airsampling
PS133/2_31-1		2022-12-01T19:17:43	-54,12877	-36,27517		CTD-RO	max depth	
PS133/2_31-2		2022-12-01T20:01:30	-54,12846	-36,27589		ROSINA	Station start	
PS133/2_31-2		2022-12-01T21:27:34	-54,12912	-36,27382		ROSINA	Station end	
PS133/2_32-1		2022-12-01T22:59:49	-54,26374	-36,42199		PELAGRA	Station start	release
PS133/2_32-1		2022-12-01T23:57:39	-54,26423	-36,42287		PELAGRA	Station end	release
PS133/2_32-2		2022-12-02T00:51:40	-54,26488	-36,43796		CTD-TM	max depth	
PS133/2_32-3		2022-12-02T01:56:02	-54,26487	-36,43666		CTD-RO	max depth	
PS133/2_32-4		2022-12-02T03:00:00	-54,26595	-36,43840		APN	Station start	Net could not be deployed, technical problems
PS133/2_32-4		2022-12-02T03:10:00	-54,26573	-36,43710		APN	Station end	Net could not be deployed, technical problems
PS133/2_32-5		2022-12-02T03:14:20	-54,26576	-36,43712		ROSINA	Station start	
PS133/2_32-5		2022-12-02T03:56:23	-54,26537	-36,43726		ROSINA	Station end	
PS133/2_32-7		2022-12-02T04:11:38	-54,26492	-36,43672		HN	Station start	Airsampling
PS133/2_32-7		2022-12-02T04:17:15	-54,26499	-36,43630		HN	Station end	Airsampling

Event label	Optional label	Date/Time	Latitude	Longitude	Depth [m]	Gear	Action	Comment
PS133/2_32-6		2022-12-02T04:19:00	-54,26505	-36,43663		CTD-RO	max depth	
PS133/2_32-8		2022-12-02T04:47:32	-54,26527	-36,43766		WP2	Station start	
PS133/2_32-8		2022-12-02T04:59:16	-54,26473	-36,43812		WP2	Station end	
PS133/2_32-9		2022-12-02T05:18:25	-54,26525	-36,43746		MSC	Station start	
PS133/2_32-9		2022-12-02T05:38:53	-54,26613	-36,43742		MSC	Station end	
PS133/2_32-10		2022-12-02T06:15:47	-54,26759	-36,44149		EK80	Station start	
PS133/2_32-10		2022-12-02T07:57:55	-54,26564	-36,43747		EK80	Station end	
PS133/2_32-11		2022-12-02T10:29:23	-54,26472	-36,43805		UW-MIMS	Station start	
PS133/2_32-11		2022-12-02T15:28:25	-54,26457	-36,43763		UW-MIMS	Station end	
PS133/2_32-12		2022-12-02T16:03:01	-54,26428	-36,43723		HN	Station start	Airsampling
PS133/2_32-12		2022-12-02T16:20:48	-54,26484	-36,43618		HN	Station end	Airsampling
PS133/2_32-13		2022-12-02T16:33:20	-54,26548	-36,43672		INSIPU	Station start	
PS133/2_32-13		2022-12-02T20:28:17	-54,26461	-36,43762		INSIPU	Station end	
PS133/2_32-14		2022-12-02T20:51:13	-54,26425	-36,42252		PELAGRA	Station start	recovered
PS133/2_32-14		2022-12-02T21:33:52	-54,26498	-36,42675		PELAGRA	Station end	recovered
PS133/2_32-15		2022-12-02T21:55:37	-54,26447	-36,43727		RN	Station start	
PS133/2_32-15		2022-12-02T22:15:52	-54,26452	-36,43732		RN	Station end	
PS133/2_32-16		2022-12-02T23:01:35	-54,26512	-36,43739		GC	max depth	
PS133/2_32-17		2022-12-02T23:48:52	-54,26456	-36,43780		MUC	max depth	
PS133/2_32-18		2022-12-03T00:27:56	-54,26490	-36,43738		MUC	max depth	
PS133/2_33-1		2022-12-03T02:40:06	-54,04449	-36,27623		MBES	Station start	
PS133/2_33-1		2022-12-03T07:46:59	-54,22324	-36,40729		MBES	Station end	
PS133/2_34-1		2022-12-03T04:12:51	-54,17869	-36,21273		HN	Station start	Airsampling
PS133/2_34-1		2022-12-03T04:15:58	-54,18329	-36,21064		HN	Station end	Airsampling
PS133/2_35-1		2022-12-03T10:21:24	-54,35270	-36,36706		CTD-RO	max depth	
PS133/2_35-2		2022-12-03T10:48:30	-54,35267	-36,36742		APN	Station start	
PS133/2_35-2		2022-12-03T11:01:36	-54,35264	-36,36744		APN	Station end	

Event label	Optional label	Date/Time	Latitude	Longitude	Depth [m]	Gear	Action	Comment
PS133/2_36-1		2022-12-03T11:45:00	-54,35240	-36,36694		ZODIAC	Station start	
PS133/2_36-1		2022-12-03T17:19:21	-54,34989	-36,36933		ZODIAC	Station end	
PS133/2_36-2		2022-12-03T11:55:26	-54,35229	-36,36700		ZODIAC	Station start	
PS133/2_36-2		2022-12-03T16:58:09	-54,34888	-36,37057		ZODIAC	Station end	
PS133/2_35-3		2022-12-03T12:12:03	-54,35248	-36,36702		ROSINA	Station start	
PS133/2_35-3		2022-12-03T13:10:00	-54,35306	-36,36710		ROSINA	Station end	
PS133/2_35-4		2022-12-03T13:24:09	-54,35293	-36,36727		CTD-RO	max depth	
PS133/2_35-5		2022-12-03T15:39:06	-54,35354	-36,36593		PELAGRA	max depth	release of drifting Sediment Trap for Aggregates
PS133/2_35-6		2022-12-03T18:48:06	-54,34569	-36,37846		MUC	max depth	
PS133/2_35-7		2022-12-03T19:29:59	-54,34565	-36,37850		MUC	max depth	
PS133/2_35-8		2022-12-03T20:15:31	-54,34562	-36,37853		MUC	max depth	
PS133/2_37-1		2022-12-04T00:07:45	-54,29369	-36,46045		CTD-RO	max depth	
PS133/2_38-1		2022-12-04T01:21:12	-54,23677	-36,45493		CTD-RO	max depth	
PS133/2_38-2		2022-12-04T01:49:13	-54,23686	-36,45463		ROSINA	Station start	
PS133/2_38-2		2022-12-04T02:25:16	-54,23700	-36,45148		ROSINA	Station end	
PS133/2_39-1		2022-12-04T02:52:01	-54,23696	-36,43424		CTD-RO	max depth	
PS133/2_39-2		2022-12-04T03:21:03	-54,23736	-36,44087		ROSINA	Station start	
PS133/2_39-2		2022-12-04T04:03:37	-54,23712	-36,43691		ROSINA	Station end	
PS133/2_40-1		2022-12-04T04:17:39	-54,23793	-36,42522		ROSINA	Station start	
PS133/2_40-1		2022-12-04T04:55:29	-54,23766	-36,42680		ROSINA	Station end	
PS133/2_40-2		2022-12-04T05:12:53	-54,23754	-36,43088		CTD-RO	max depth	
PS133/2_41-1		2022-12-04T08:00:38	-54,35246	-36,36541		PELAGRA	Station start	recovered
PS133/2_41-1		2022-12-04T08:35:22	-54,35285	-36,36551		PELAGRA	Station end	recovered
PS133/2_37-2		2022-12-04T11:20:35	-54,29345	-36,46104		ZODIAC	Station start	
PS133/2_37-2		2022-12-04T12:30:00	-54,29307	-36,46092		ZODIAC	Station end	
PS133/2_37-3		2022-12-04T11:34:59	-54,29353	-36,46087		ZODIAC	Station start	
PS133/2_37-3		2022-12-04T15:56:31	-54,29244	-36,45999		ZODIAC	Station end	
PS133/2_37-4		2022-12-04T14:59:25	-54,29425	-36,46110		GC	max depth	

Event label	Optional label	Date/Time	Latitude	Longitude	Depth [m]	Gear	Action	Comment
PS133/2_37-6		2022-12-04T16:19:05	-54,29289	-36,46081		GC	max depth	
PS133/2_37-5		2022-12-04T16:53:48	-54,29339	-36,46022		ZODIAC	Station start	
PS133/2_37-5		2022-12-04T20:48:14	-54,29339	-36,45314		ZODIAC	Station end	
PS133/2_37-7		2022-12-04T17:24:47	-54,29388	-36,46033		MUC	max depth	
PS133/2_37-8		2022-12-04T17:57:52	-54,29425	-36,44666		APN	Station start	
PS133/2_37-8		2022-12-04T18:07:25	-54,29437	-36,44604		APN	Station end	
PS133/2_35-9		2022-12-04T22:30:32	-54,34565	-36,37884		GC	max depth	
PS133/2_35-10		2022-12-04T23:47:08	-54,34575	-36,37921		GC	max depth	
PS133/2_42-1		2022-12-05T02:09:54	-54,20857	-36,44323		CTD-RO	max depth	
PS133/2_42-2		2022-12-05T02:39:28	-54,20860	-36,44116		ROSINA	Station start	
PS133/2_42-2		2022-12-05T03:20:53	-54,20837	-36,44300		ROSINA	Station end	
PS133/2_42-3		2022-12-05T03:22:53	-54,20846	-36,44335		WP2	Station start	
PS133/2_42-3		2022-12-05T03:35:37	-54,20898	-36,44473		WP2	Station end	
PS133/2_42-4		2022-12-05T03:36:54	-54,20895	-36,44467		APN	Station start	
PS133/2_42-4		2022-12-05T03:53:05	-54,20829	-36,44303		APN	Station end	
PS133/2_43-1		2022-12-05T23:54:44	-54,05344	-36,07128		GC	max depth	
PS133/2_44-1		2022-12-06T01:29:26	-54,11214	-36,11697		MBES	Station start	
PS133/2_44-1		2022-12-06T23:37:04	-54,13514	-36,37929		MBES	Station end	
PS133/2_45-1		2022-12-06T06:44:08	-53,83096	-36,34600		CTD-RO	max depth	
PS133/2_45-2		2022-12-06T07:40:37	-53,83115	-36,34556		CTD-TM	max depth	
PS133/2_46-1		2022-12-06T19:20:50	-53,90700	-36,28371		GC	max depth	
PS133/2_47-1		2022-12-06T20:47:24	-53,81979	-36,31640		GC	max depth	
PS133/2_42-5		2022-12-07T00:34:25	-54,20883	-36,44230		CTD-RO	max depth	
PS133/2_42-6		2022-12-07T01:23:38	-54,20858	-36,44273		CTD-TM	max depth	
PS133/2_42-7		2022-12-07T01:56:01	-54,20878	-36,44168		INSIPU	Station start	3h pumping at 255m
PS133/2_42-7		2022-12-07T05:19:19	-54,20769	-36,44429		INSIPU	Station end	3h pumping at 255m
PS133/2_42-8		2022-12-07T06:10:32	-54,20863	-36,44184		MUC	max depth	

Event label	Optional label	Date/Time	Latitude	Longitude	Depth [m]	Gear	Action	Comment
PS133/2_42-9		2022-12-07T06:51:45	-54,20869	-36,44205		MUC	max depth	
PS133/2_42-10		2022-12-07T08:07:58	-54,20848	-36,44235		GC	max depth	
PS133/2_42-11		2022-12-07T09:17:14	-54,20837	-36,44239		GC	max depth	
PS133/2_48-1		2022-12-07T14:23:20	-53,92404	-35,82780		CTD-RO	max depth	
PS133/2_48-2		2022-12-07T15:00:05	-53,92504	-35,82886		ROSINA	Station start	
PS133/2_48-2		2022-12-07T16:01:34	-53,92462	-35,82912		ROSINA	Station end	
PS133/2_49-1		2022-12-07T17:35:12	-54,00379	-35,99565		CTD-RO	max depth	
PS133/2_49-2		2022-12-07T17:53:37	-54,00416	-35,99510		ROSINA	Station start	
PS133/2_49-2		2022-12-07T18:50:42	-54,00468	-35,99387		ROSINA	Station end	
PS133/2_50-1		2022-12-07T20:06:30	-54,06515	-36,14146		CTD-RO	max depth	
PS133/2_50-2		2022-12-07T21:15:13	-54,06520	-36,14210		CTD-TM	max depth	
PS133/2_50-3		2022-12-07T21:55:32	-54,06527	-36,14196		ROSINA	Station start	
PS133/2_50-3		2022-12-07T22:31:40	-54,06543	-36,14242		ROSINA	Station end	
PS133/2_50-4		2022-12-07T22:30:49	-54,06536	-36,14229		WP2	Station start	
PS133/2_50-4		2022-12-07T22:45:56	-54,06527	-36,14275		WP2	Station end	
PS133/2_50-5		2022-12-07T22:50:47	-54,06520	-36,14266		APN	Station start	
PS133/2_50-5		2022-12-07T23:16:05	-54,06534	-36,14248		APN	Station end	
PS133/2_50-6		2022-12-07T23:33:35	-54,06539	-36,14123		MUC	max depth	
PS133/2_50-7		2022-12-08T00:07:48	-54,06524	-36,14213		MUC	max depth	
PS133/2_51-1		2022-12-08T09:01:29	-54,95627	-36,28147		PS	Station start	
PS133/2_51-1		2022-12-08T11:49:00	-54,97138	-36,38423		PS	Station end	
PS133/2_52-1		2022-12-08T12:38:58	-55,03684	-36,31190		GC	max depth	aborted due to heavy weather conditions
PS133/2_53-1		2022-12-10T12:56:54	-52,27563	-25,03637		B_LANDER	Station start	
PS133/2_53-1		2022-12-10T16:39:55	-52,26904	-25,03360		B_LANDER	Station end	

** Comments are limited to 130 characters. See https://www.pangaea.de/expeditions/events/PS133/2 to show full comments in conjunction with the station (event) list for expedition PS133/2*

Abbreviation	Method/Device
ADCP	Acoustic Doppler Current Profiler
APN	Apstein plankton net
B_LANDER	Bottom lander
CT	Underway cruise track measurements
CTD-RO	CTD/Rosette
CTD-TM	CTD/Rosette, trace metal clean
DRG	Dredge
EK80	Echosounder, Simrad EK80
FBOX	FerryBox
GC	Gravity corer
HN	Hand net
INSIPU	In-situ pump
KMT	Sediment trap K/MT
MAG	Magnetometer
MBES	Multibeam echosounder
MSC	Marine snow catcher
MUC	MultiCorer
MYON	DESY Myon Detector
NEUMON	Neutron monitor
PELAGRA	Trap, sediment, drifting
PS	ParaSound
RN	Ring net
ROSINA	Remotely ObServing INsitu camera for Aggregates
SNDVELPR	Sound velocity probe
SWEAS	Ship Weather Station
TMPUMP	Sea water pump, trace metals
TSG	Thermosalinograph
UW-MIMS	Underwater membrane inlet mass spectrometer
WP2	WP-2 towed closing plankton net
ZODIAC	Rubber boat, Zodiac
pCO2	pCO2 sensor

A.5 Kern-Logs der Schwerelotkerne der Gruppe Marine Geologie / Core Logs of Gravity Cores taken for/by the Marine Geology Group

Cruise: PS133-2 Island Impact
Date of coring: 27.11.2022
GC-Number: GC2 AWI ID: PS133-2_12-3
Date of logging: 28.11.2022

Lat.: 54° 01.620' S Lon.: 037° 02.982' W Water depth: 257.9 m
Location: Outer Possession Bay Investigator: NL
Core length: 789 cm

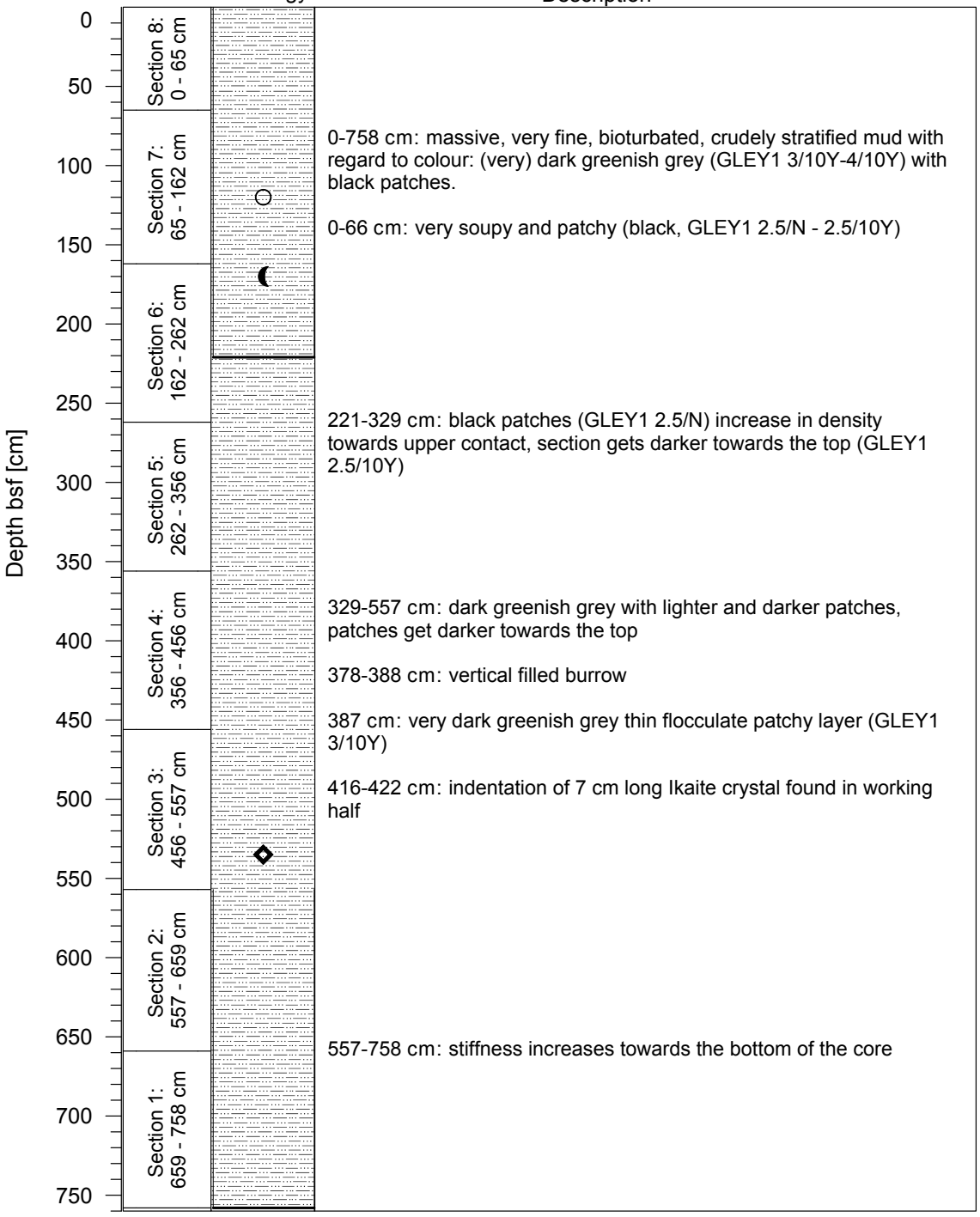

Cruise: PS133-2 Island Impact
Date of coring: 27.11.2022
GC-Number: GC4
AWI ID: PS133-2_15-7
Date of logging: 14.12.2022

Lat.: 54° 05.069' S
Lon.: 037° 06.044' W
Water depth: 357.9 m
Location: Inner Possession Bay
Investigator: KS / LC
Core length: 602 cm

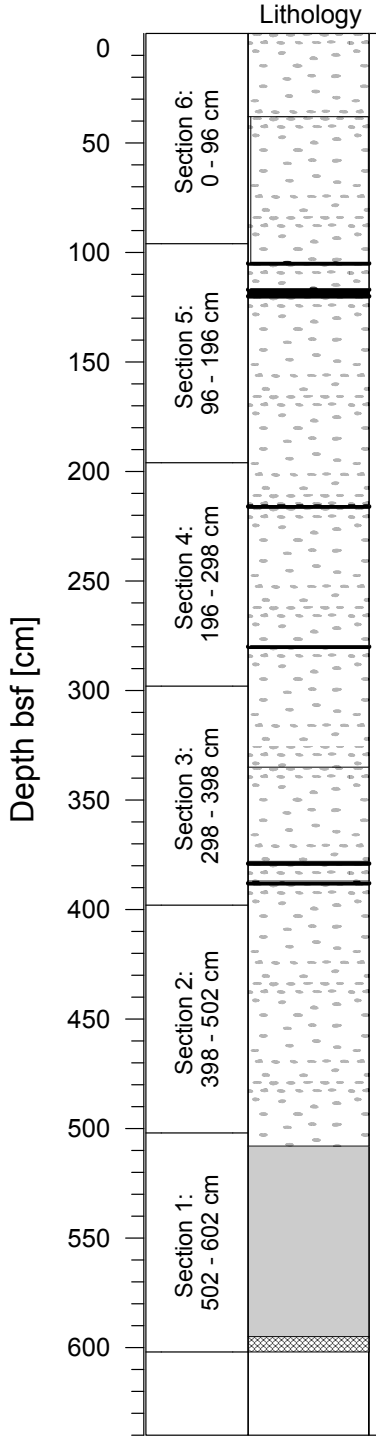

Description

0-38 cm: Dark greenish grey (GLEY1 4/10Y) homogeneous silty clay. Increasingly more mottled and seemingly very rich in organic matter. Sediment is odourless and appears to be massive to crudely stratified.

38-508 cm: Increasingly mottled, darker sediment consisting mostly of dark greenish black (GLEY1 2.5/5GY) silty clay massively intermixed with dark greenish grey clay with a very minor silt content. The sediment appears to contain no dropstones. Apart from the crude lamination, which could be an artefact from the mottled nature and the smoothening of the core surface during core splitting, no other internal structures could be observed. The sediment varies slightly in colour becoming darker or lighter but otherwise stays the same throughout the entire core.

At 105,117, 118-120, 216, ~280 cm: Intensely black, almost glowing layer containing extremely fine-grained material. Appears to be containing almost exclusively diatoms, although no smear slides could be obtained. Colour code is GLEY1 2.5N "black".

At 335 cm: Transition into darker, probably organic, matter that consists of homogeneous, relatively uniformly coloured clay. Colours vary between very dark grey (GLEY1 3/N), very dark greenish grey (GLEY1 3/5GY) and black (GLEY1 2.5/N

Between 483 and 485 cm: slightly lighter section, similar to core top, but still same material

508-602 cm: very homogeneous, completely uniformly coloured clay of a deep black (Gley1 2.5/N) colour. Mottles are no longer visible due to the dark overall colour of the sediment. No internal structures are visible and there seem to be no dropstones or shells.
From 595 cm: Liner empty but some sediment conserved at the sides, which has oxidised to a slightly lighter dark greenish grey (GLEY1 4/10Y) clay.

Cruise: PS133-2 Island Impact
Date of coring: 30.11.2022
GC-Number: GC5 AWI ID: PS133-2_17-13
Date of logging: 9.12.2022

Lat.: 54° 24.078' N Lon.: 37° 34.031' W Water depth: 344 m
Location: King Haakon Trough Investigator: NL
Core length: 895 cm

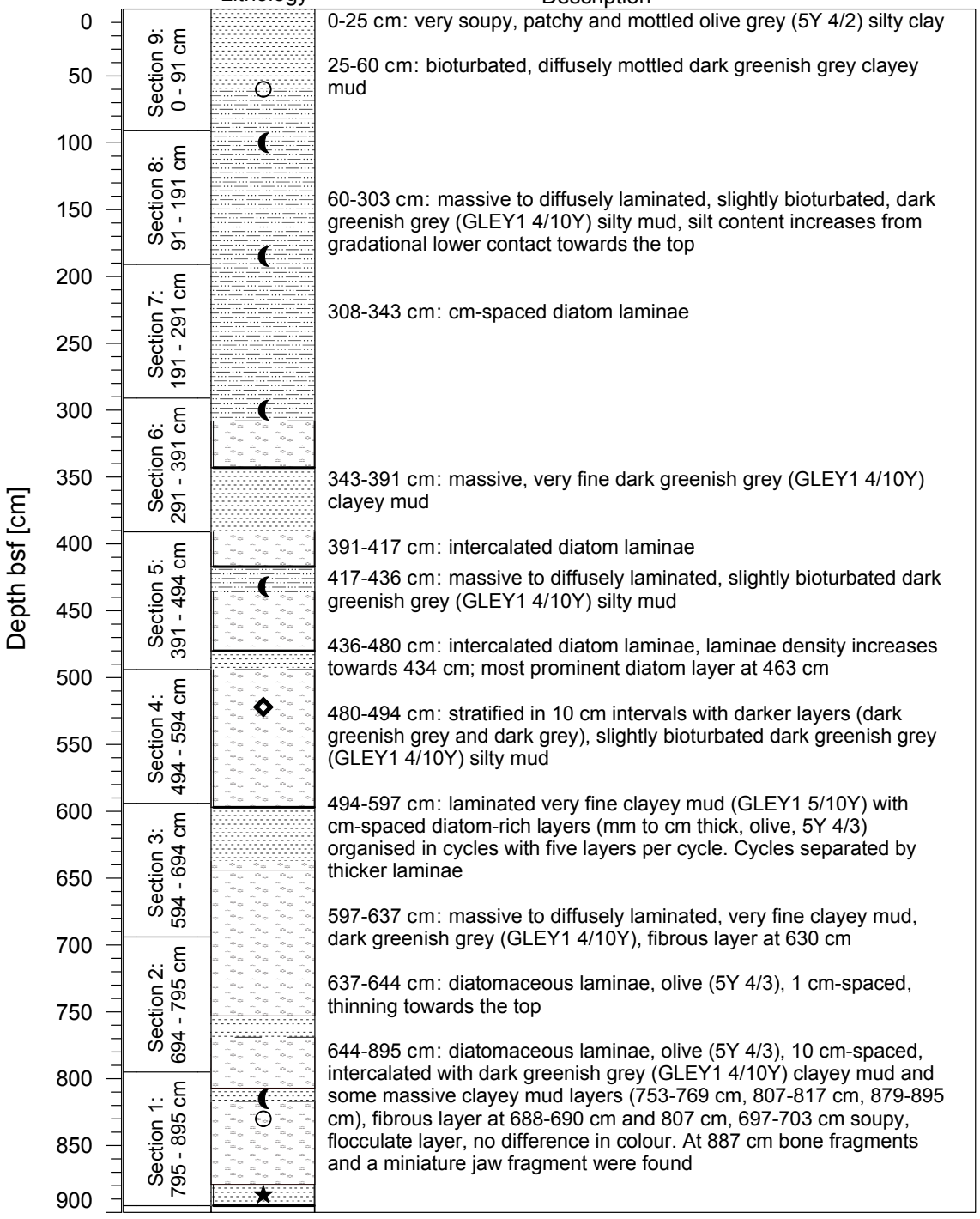

Cruise: PS133-2 Island Impact
GC-Number: GC9 AWI ID: PS133-2_26-1
Date of coring: 30.11.2022
Date of logging: 10.12.2022

Lat.: 54° 24.811' N Lon.: 037° 36.993' N Water depth: 357.4 m
Location: King Haakon Trough Investigator: NL
Core length: 985 cm

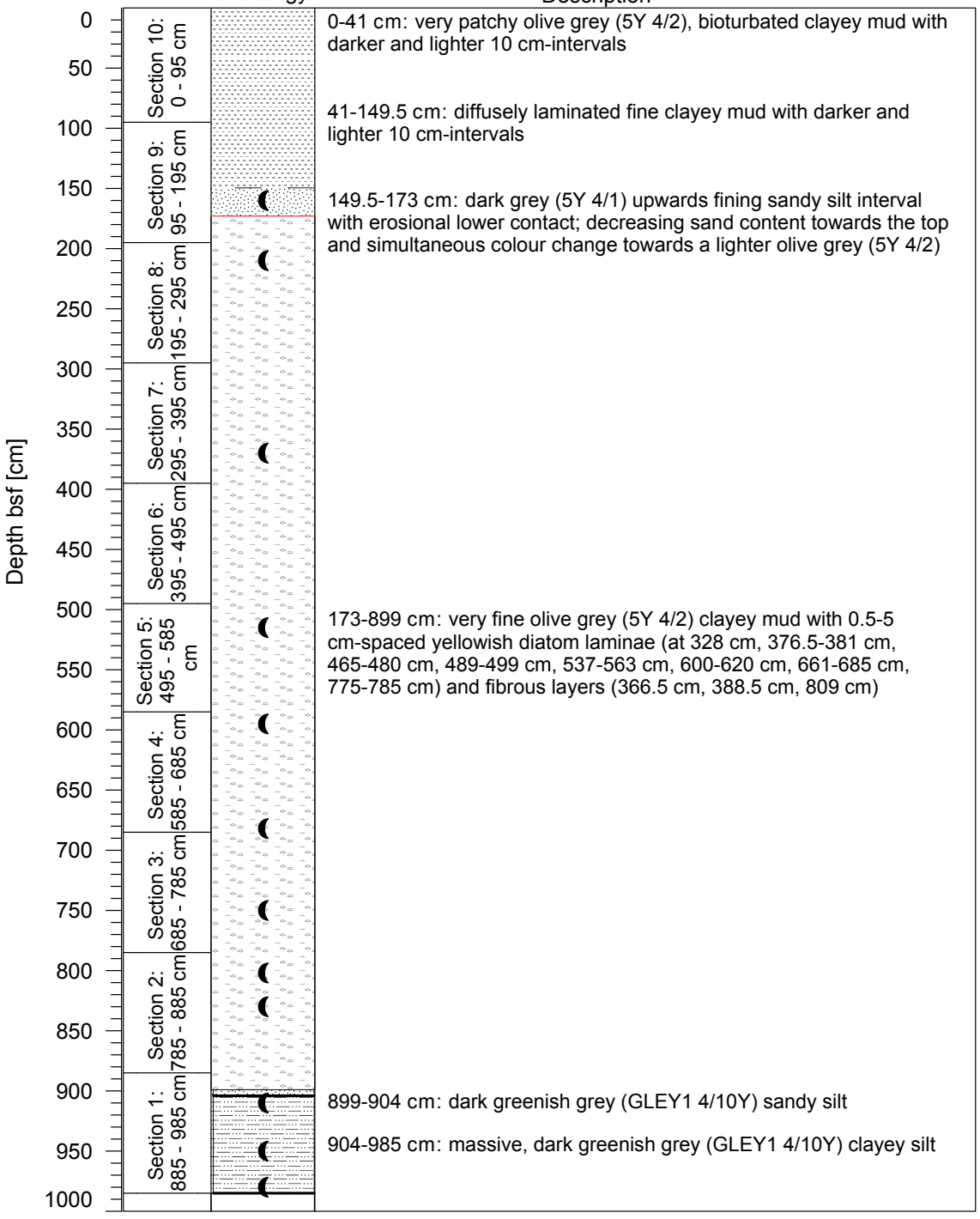

Cruise: PS133-2 Island Impact
Date of coring: 5.12.2022
GC-Number: GC19 AWI ID: PS133-2_43-1
Date of logging: 12.12.2022

Lat.: 54° 03.207' S Lon.: 036° 04.277' W Water depth: 257 m
Location: Cumberland Bay, outer continental shelf Investigator: KS / LC
Core length: 369.5 c

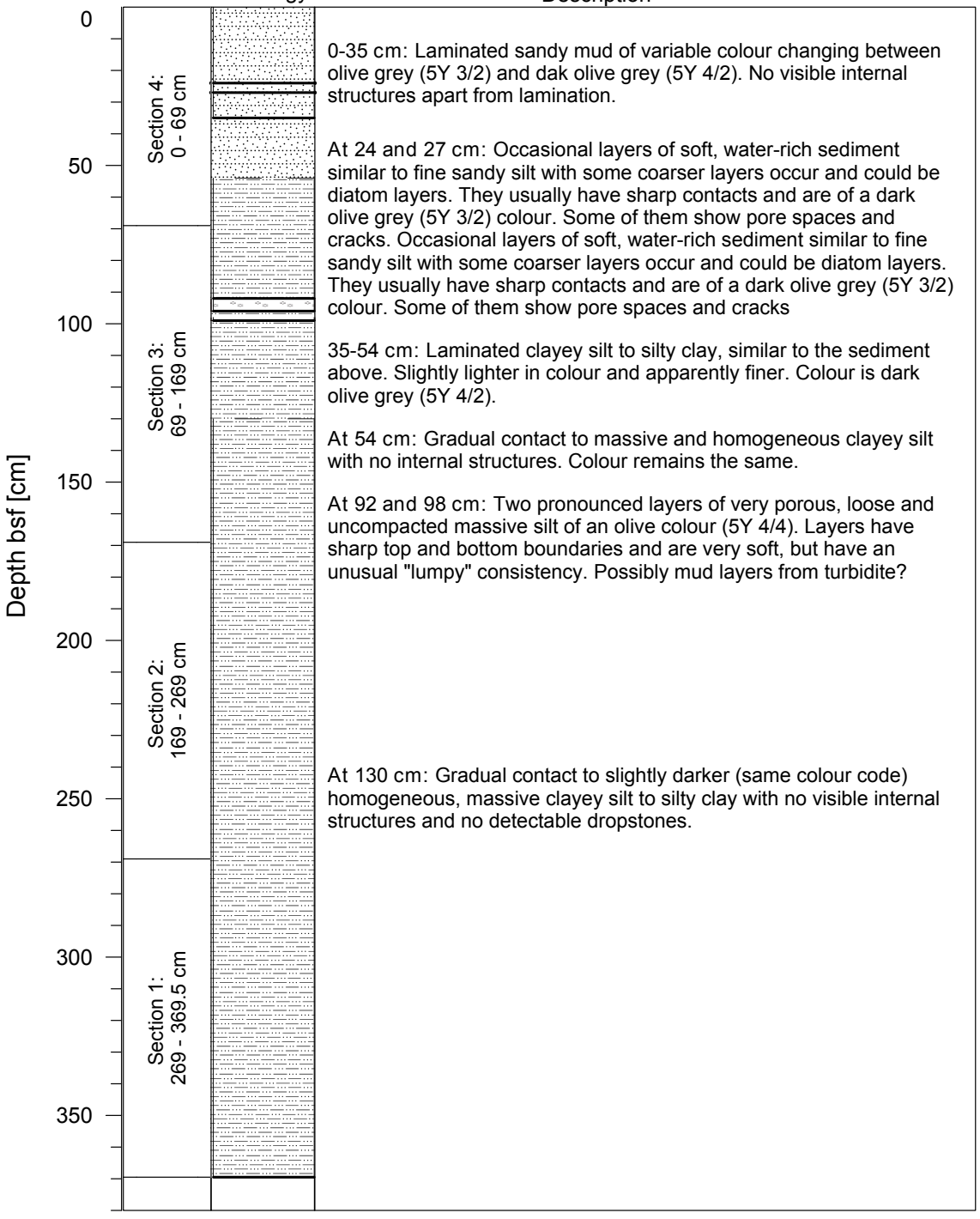

0-35 cm: Laminated sandy mud of variable colour changing between olive grey (5Y 3/2) and dak olive grey (5Y 4/2). No visible internal structures apart from lamination.

At 24 and 27 cm: Occasional layers of soft, water-rich sediment similar to fine sandy silt with some coarser layers occur and could be diatom layers. They usually have sharp contacts and are of a dark olive grey (5Y 3/2) colour. Some of them show pore spaces and cracks. Occasional layers of soft, water-rich sediment similar to fine sandy silt with some coarser layers occur and could be diatom layers. They usually have sharp contacts and are of a dark olive grey (5Y 3/2) colour. Some of them show pore spaces and cracks

35-54 cm: Laminated clayey silt to silty clay, similar to the sediment above. Slightly lighter in colour and apparently finer. Colour is dark olive grey (5Y 4/2).

At 54 cm: Gradual contact to massive and homogeneous clayey silt with no internal structures. Colour remains the same.

At 92 and 98 cm: Two pronounced layers of very porous, loose and uncompacted massive silt of an olive colour (5Y 4/4). Layers have sharp top and bottom boundaries and are very soft, but have an unusual "lumpy" consistency. Possibly mud layers from turbidite?

At 130 cm: Gradual contact to slightly darker (same colour code) homogeneous, massive clayey silt to silty clay with no visible internal structures and no detectable dropstones.

Cruise: PS133-2 Island Impact
GC-Number: GC20 AWI ID: PS133-2_46-1

Date of coring: 6.12.2022
Date of logging: 12.12.2022

Lat.: 53° 54.420' S Lon.: 036° 17.023' W Water depth: 230.1 m
Location: Cumberland Bay, outer continental shelf Investigator: KS / LC

Core length: 232 cm

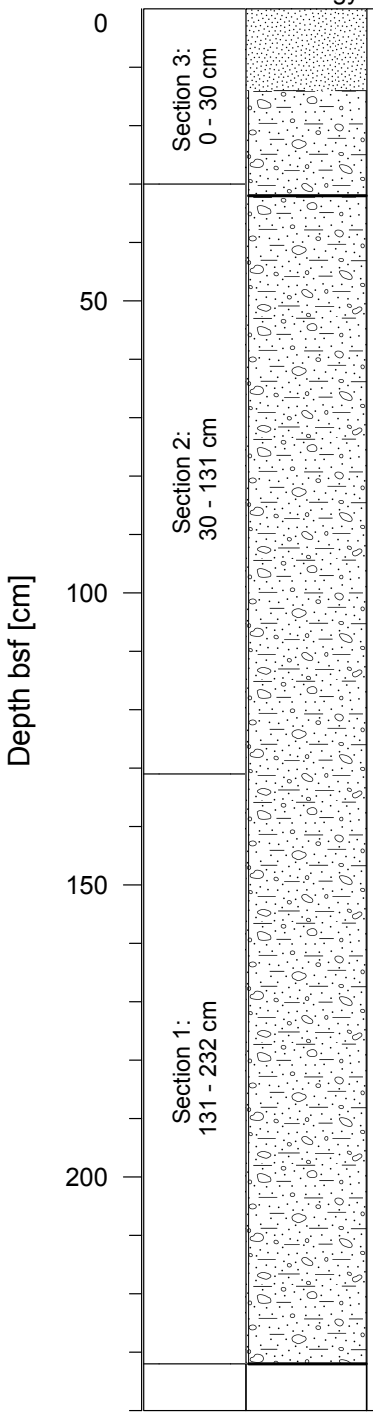

Description

0-14 cm: Massive silty/sandy mud with dropstones. Matrix is mostly mud with fine sand of an olive grey colour (5Y 4/2) and is generally well-sorted. Dropstones are generally around 1.5 cm in diameter and angular to sub-angular. Shear strength is below 3 kPa.

14-32 cm: Crudely stratified matrix-supported diamict with a sandy mud matrix containing medium to coarse sand. Colour is variable between very dark grey and dark grey (GLEY1 3/N or 2.5Y 4/1). Frequent small dropstones of a black colour occur and some sponge fibres or spicules could be observed. Dropstones appear concentrated in a cluster between 6 and 18 cm but are not spread across the entire core liner. They also occur scattered throughout. They are very angular and mostly flat. A large dropstone of 6 x 9 cm occurs between 10 and 18 cm

32-232 cm: Massive matrix-supported very dark grey (5Y 2.5/1 to 5Y 3/1) diamicton with a matrix of sandy mud containing medium to coarse sand. Frequent smaller and larger dropstones occur that can be up to 6 cm in diameter. Large dropstones were observed at 72, 90, 111 and 208 cm. Towards the bottom of the core the diamict becomes stiffer with shear strength values up to 13 kPa. Clay content seems to increase, giving a more cohesive consistency to the diamicton. At the bottom, however, the matrix seems to contain mostly fine sand with some coarser particles.

A.6 Muc Core Distribution Protocols/Verteilungsprotokolle der Muc-Kerne

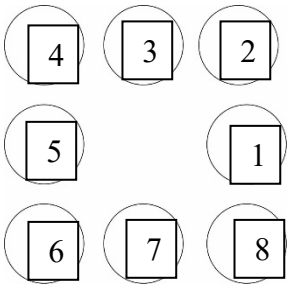

MUC core log **Site:** ……Church Trough

Station PS133-2_9_2……**MUC-**1……**Date**…26.11……..2022

Depth…379.**m**…….. Comment……8/8 core……
(SSR core next to porewater; sediment grain size longest, undisturbed core)

Core ID	Segment depth (cm)	Analysis & scientist	Comments
1	34.5	Macrobiology, MA	Disturbed, surface water for Florian & Walter
2	28	Macrobiology, MA	
3	34	Pore water, MK	
4	33	Fe kinetics, KLM	
5	32.5	Living Microbio, KLM	
6	36.5	SRR, KLM	
7	22	Macrobiology, MA	Disturbed, surface water for Florian & Walter
8	32	N-cycling	

Name	Analysis	Number of cores	Comment
Katrin Linse	Photo, length	x	
Male Koester (MK)	Pore water	1	
	O_2		
	PB, Porosity, TOC,		
	Delta 56 Fe		
	aDNA		
Katja Laufer-Meiser (KLM)	DNA, SRR &CH4	1	
	Fe Kinetics	1	
	Living community	1	
Madeline Anderson (MA)	Macrobiology	3	
Bernd Krock (BK)	Diatoms		
Hannah Marchant (HKM)	N-cycling, Metagen.	1	surface water
Henrick Grotheer (HG)	Surface isotope		
Florian Koch (FK)	Surface waters		surface water
Walter Geibert (WG)	Surface waters		surface water
		8	

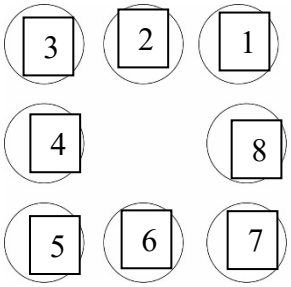

MUC core log **Site:** ……off Possession Bay……

Station PS133-2_12_1……**MUC-**2……**Date**…26.11……..2022

Depth…257.**m**…….. Comment……8/8 core……
(SSR core next to porewater; sediment grain size longest, undisturbed core)

Core ID	Segment depth (cm)	Analysis & scientist	Comments
1	31	Fe kinetics, KLM	
2	26	Diatoms, BK	Water Hannah
3	29	Surface isotope, HG	
4	31	N-cycling, HM	tilted
5	19	Macrobiology, MA	disturbed
6	28	Living Microbio, KLM	tilted
7	31	Pore water, MK	
8	30	SRR, KLM	

Name	Analysis	Number of cores	Comment
Katrin Linse	Photo, length	x	
Male Koester (MK)	Pore water	1	Next to SRR
	O_2		
	PB, Porosity, TOC, corn s		
	Delta 56 Fe		Only CB & KHB
Katja Laufer-Meiser (KLM)	DNA, SRR &CH4	1	Next to Pore water
	Fe Kinetics	1	
	Living community	1	
Madeline Anderson (MA)	Macrobiology	1	Surface water to Walter & Florian
Bernd Krock (BK)	Diatoms	1	From SSR
Hannah Marchant (HKM)	N-cycling	1	surface water
Isa Wilkie	Metagenomics		
Henrick Grotheer (HG)	Surface isotope	1	
Florian Koch (FK)	Surface waters		surface water
Walter Geibert (WG)	Surface waters		surface water
		8	

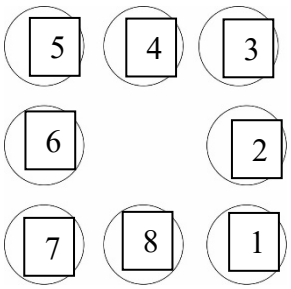

MUC core log **Site:** ……off Possession Bay……
Station PS133-2_12_2……**MUC-**3……**Date**…26.11……..2022

Depth…256.**m**…….. Comment……8/8 core……no surface waters needed (SSR core next to porewater; sediment grain size longest, undisturbed core)

Core ID	Segment depth (cm)	Analysis & scientist	Comments
1	32	Macrobiology, MA	
2	34	Macrobiology, MA	
3	32	Macrobiology, MA	
4	32	Macrobiology, MA	
5	27.5	Macrobiology, MA	
6	31	Macrobiology, MA	
7	32.5	Macrobiology, MA	
8	34	Macrobiology, MA	

Name	Analysis	Number of cores	Comment
Katrin Linse	Photo, length	x	
Male Koester (MK)	Pore water		Next to SRR
	O_2		
	PB, Porosity, TOC, corn s		
	Delta 56 Fe		Only CB & KHB
Katja Laufer-Meiser (KLM)	DNA, SRR &CH4		Next to Pore water
	Fe Kinetics		
	Living community		
Madeline Anderson (MA)	Macrobiology	8	Surface water to Walter & Florian
Bernd Krock (BK)	Diatoms		From SSR
Hannah Marchant (HKM)	N-cycling		surface water
Isa Wilkie	Metagenomics		
Henrick Grotheer (HG)	Surface isotope		
Florian Koch (FK)	Surface waters		surface water
Walter Geibert (WG)	Surface waters		surface water
		8	

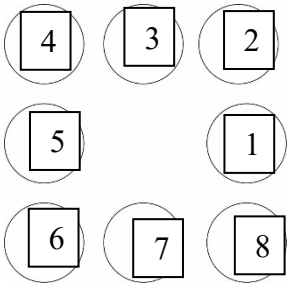

MUC core log **Site:** ……in Possession Bay……

Station PS133-2_15_3……**MUC-**4……**Date**…27.11……..2022

Depth…357.**m**…….. Comment……8/8 core……partially closed…
(SSR core next to porewater; sediment grain size longest, undisturbed core)

Core ID	Segment depth (cm)	Analysis & scientist	Comments
1	25	O2, MK	
2	17.5	Macrobiology, MA	
3	14.5	Macrobiology, MA	
4	15.5	Macrobiology, MA	tilted
5	23.5	Pb, MK	
6	27	Macrobiology, MA	Leaking, sipunculid between stopper / core
7	27	Pore water, MK	
8	23	SSR, KLM	

Name	Analysis	Number of cores	Comment
Katrin Linse	Photo, length	x	
Male Koester (MK)	Pore water	1	Next to SRR
	O_2	1	
	PB, Porosity, TOC, corn	1	
	Delta 56 Fe		Only CB & KHB
Katja Laufer-Meiser (KLM)	DNA, SRR &CH4	1	Next to Pore water
	Fe Kinetics		
	Living community		
Madeline Anderson (MA)	Macrobiology	4	Surface water to Walter & Florian
Bernd Krock (BK)	Diatoms	x	From SSR
Hannah Marchant (HKM)	N-cycling		surface water
Isa Wilkie	Metagenomics		
Henrick Grotheer (HG)	Surface isotope		
Florian Koch (FK)	Surface waters	x	surface water
Walter Geibert (WG)	Surface waters		surface water
		8	

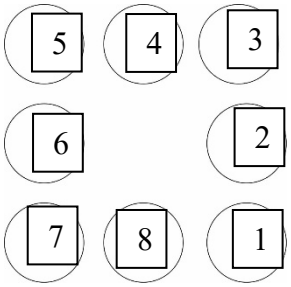

MUC core log **Site:** ……in Possession Bay……

Station PS133-2_15_5……**MUC-**5……**Date**…27.11……..2022

Depth…357.**m**…….. Comment……8/8 cores……, 10 cm oxidised layer…
(SSR core next to porewater; sediment grain size longest, undisturbed core)

Core ID	Segment depth (cm)	Analysis & scientist	Comments
1	26.5	Fe kinetics, KLM	
2	27	Microbiology living, KLM	
3	25.5	Metagenome, HM	
4	29	Surface isotope, HG	
5	28	Macrobiology, MA	tilted
6	29.5	Macrobiology, MA	
7	27	Macrobiology, MA	
8	27.5	Macrobiology, MA	

Name	Analysis	Number of cores	Comment
Katrin Linse	Photo, length	x	
Male Koester (MK)	Pore water		Next to SRR
	O_2		
	PB, Porosity, TOC, etc		
	Delta 56 Fe		Only CB & KHB
Katja Laufer-Meiser (KLM)	DNA, SRR &CH4		Next to Pore water
	Fe Kinetics	1	
	Living community	1	
Madeline Anderson (MA)	Macrobiology	4	Surface water to Walter & Florian
Bernd Krock (BK)	Diatoms		From SSR
Hannah Marchant (HKM)	N-cycling	1	surface water
Isa Wilkie	Metagenomics		
Henrick Grotheer (HG)	Surface isotope	1	
Florian Koch (FK)	Surface waters		surface water
Walter Geibert (WG)	Surface waters		surface water
		8	

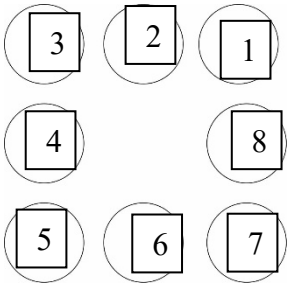

MUC core log **Site:** …P1…King Haakon Trough…near Annenkov Trough…

Station PS133-2_17_11……**MUC-**6……**Date**…28.11……..2022

Depth…343.**m**…….. Comment……8/8 core……
(SSR core next to porewater; sediment grain size longest, undisturbed core)

Core ID	Segment depth (cm)	Analysis & scientist	Comments
1	43	Pore water, MK	
2	45.5	Delta 56 FE, MK	
3	41	SRR, KLM	
4	44.5	O2, MK	22 cm oxic layer
5	40.5	Isa	Disturbed at bottom
6	36.5	FE Kinetics, KLM	Large sipunculid
7	46	Pb, MK	
8	46	Microbio living, KLM	tilted

Name	Analysis	Number of cores	Comment
Katrin Linse	Photo, length		
Male Koester (MK)	Pore water	1	Next to SRR
	O_2	1	
	PB, Porosity, TOC, etc	1	
	Delta 56 Fe	1	Only CB & KHB
Katja Laufer-Meiser (KLM)	DNA, SRR &CH4	1	Next to Pore water
	Fe Kinetics	1	
	Living community	1	
Madeline Anderson (MA)	Macrobiology		Surface water to Walter & Florian
Bernd Krock (BK)	Diatoms		From SSR
Hannah Marchant (HKM)	N-cycling	1	surface water
Isa Wilkie	Metagenomics		
Henrick Grotheer (HG)	Surface isotope		
Florian Koch (FK)	Surface waters		surface water
Walter Geibert (WG)	Surface waters		surface water
		8	

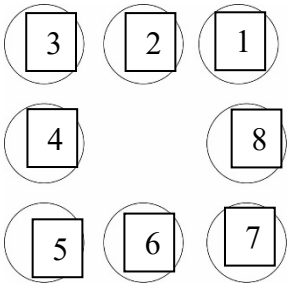

MUC core log **Site:** …P1…King Haakon Trough…near Annenkov Trough……

Station PS133-2_17_12……**MUC-**7……**Date**…28.11……..2022

Depth…343.**m**…….. Comment……7/8 core……
(SSR core next to porewater; sediment grain size longest, undisturbed core)

Core ID	Segment depth (cm)	Analysis & scientist	Comments
1	43	Macrobiology, MA	
2	45.5	Macrobiology, MA	
3	45	Macrobiology, MA	
4	42.5	Isotope, HG	
5	46	Microbio living, KLM	
6	-		Did not close
7	43	Macrobiology, MA	
8	42	Macrobiology, MA	

Name	Analysis	Number of cores	Comment
Katrin Linse	Photo, length		
Male Koester (MK)	Pore water		Next to SRR
	O_2		
	PB, Porosity, TOC, corn s		
	Delta 56 Fe		Only CB & KHB
Katja Laufer-Meiser (KLM)	DNA, SRR &CH4		Next to Pore water
	Fe Kinetics		
	Living community	1	
Madeline Anderson (MA)	Macrobiology	5	Surface water to Walter & Florian
Bernd Krock (BK)	Diatoms		From SSR
Hannah Marchant (HKM)	N-cycling, Metagenome		surface water
Henrick Grotheer (HG)	Surface isotope	1	
Florian Koch (FK)	Surface waters		surface water
Walter Geibert (WG)	Surface waters		surface water
		7	

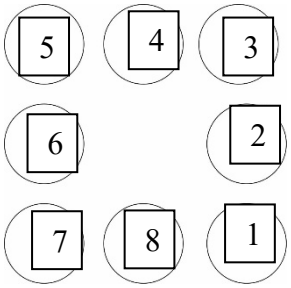

MUC core log **Site:** ……inner King Haakon Bay……

Station PS133-2_23_9……**MUC-**8……**Date**…29.11...2022 **Depth**…154.**m**

Comment 7/8 cores; FeS crystals in sediment, potential gas tunnels in upper 20 cm…
(SSR core next to porewater; sediment grain size longest, undisturbed core)

Core ID	Segment depth (cm)	Analysis & scientist	Comments
1	44.5	Pore water, MK	
2	-		
3	43.5	SRR, KLM	
4	47	Fe kinetics, KLM	
5	43	Living Microbio, KLM	
6	44	O2, MK	
7	46	Living Microbio, KLM	
8	44.5	Delta 56 Fe, MK	undisturbed

Name	Analysis	Number of cores	Comment
Katrin Linse	Photo, length		
Male Koester (MK)	Pore water	1	Next to SRR
	O_2		
	PB, Porosity, TOC, etc	1	
	Delta 56 Fe	1	Only CB & KHB
Katja Laufer-Meiser (KLM)	DNA, SRR &CH4	1	Next to Pore water
	Fe Kinetics	1	
	Living community	2	
Madeline Anderson (MA)	Macrobiology		Surface water to Walter & Florian
Bernd Krock (BK)	Diatoms		From SSR
Hannah Marchant (HKM)	N-cycling		surface water
Isa Wilkie	Metagenomics		
Henrick Grotheer (HG)	Surface isotope		
Florian Koch (FK)	Surface waters	5, 7, 3, 2	surface water
Walter Geibert (WG)	Surface waters		surface water
		7	

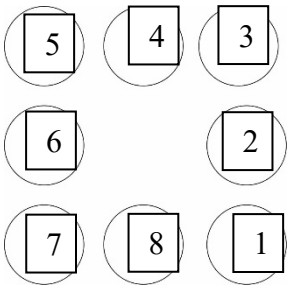

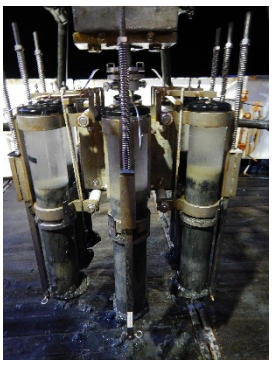

MUC core log **Site:** ……inner King Haakon Bay…

Station PS133-2_23_10……**MUC-**9……**Date**…29.11...2022 **Depth**…154.**m**

Comment 8/8 cores; Fe sulfsate cristals in sediment, potential gas tunnels in upper 20 cm… (SSR core next to porewater; sediment grain size longest, undisturbed core)

Core ID	Segment depth (cm)	Analysis & scientist	Comments
1	47.5	Macrobiology, MA	
2	49	Macrobiology, MA	
3	43.5	Macrobiology, MA	
4	46	Macrobiology, MA	
5	43.5	Macrobiology, MA	
6	43	Metagenomics HKM	
7	43	Microbiology living, KLM	
8	43	Surface isotope, HG	

Name	Analysis	Number of cores	Comment
Katrin Linse	Photo, length		
Male Koester (MK)	Pore water		Next to SRR
	O_2		
	PB, Porosity, TOC, etc		
	Delta 56 Fe		Only CB & KHB
Katja Laufer-Meiser (KLM)	DNA, SRR &CH4		Next to Pore water
	Fe Kinetics		
	Living community	1	
Madeline Anderson (MA)	Macrobiology	5	Surface water to Walter & Florian
Bernd Krock (BK)	Diatoms		From SSR
Hannah Marchant (HKM)	N-cycling, metagenome	1	surface water
Henrick Grotheer (HG)	Surface isotope	1	
Florian Koch (FK)	Surface waters		surface water
Walter Geibert (WG)	Surface waters	1,2,3,4,5,6,7	surface water
		8	

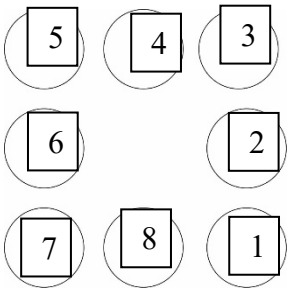

MUC core log **Site:** ……Grytviken Flare…

Station PS133-2_32_17……**MUC-**10……**Date**…2.12……..2022

Depth…256.**m**…….. Comment……8/8 core……
(SSR core next to porewater; sediment grain size longest, undisturbed core)

Core ID	Segment depth (cm)	Analysis & scientist	Comments
1	18	Macrobiology, MA	
2	19	Macrobiology, MA	Tilted and leaking
3	20	aDNA, Fine	
4	14	Macrobiology, MA	
5	18	Surface isotope, HG	tilted
6	14.5	Macrobiology, MA	
7	15	Macrobiology, MA	
8	16.5	N-cycling, Metagen, HM	

Name	Analysis	Number of cores	Comment
Katrin Linse	Photo, length		
Male Koester (MK)	Pore water		Next to SRR
	O_2		
	PB, Porosity, TOC, corn s		
	Delta 56 Fe		Only CB & KHB
Katja Laufer-Meiser (KLM)	DNA, SRR &CH4		Next to Pore water
	Fe Kinetics		
	Living community		
Madeline Anderson (MA)	Macrobiology	5	Surface water to Walter & Florian
Bernd Krock (BK)	Diatoms		From SSR
Hannah Marchant (HKM)	N-cycling	1	surface water
Isa Wilkie	Metagenomics		
Henrick Grotheer (HG)	Surface isotope	1	
Florian Koch (FK)	Surface waters		surface water
Walter Geibert (WG)	Surface waters		surface water
Josefine Weiss (JW)	aDNA	1	
		8	

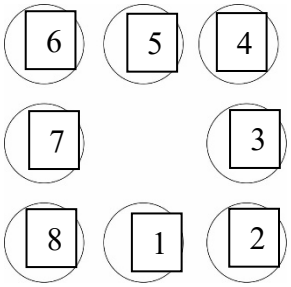

MUC core log **Site:** ……Grytviken Flare…

Station PS133-2_32_18……**MUC-**11……**Date**…2.12……..2022

Depth…256.**m**…….. Comment……8/8 core……
(SSR core next to porewater; sediment grain size longest, undisturbed core)

Core ID	Segment depth (cm)	Analysis & scientist	Comments
1	17.5	Macrobiology, MA	
2	17.5	SSR, KLM	
3	19	Pore water, MK	
4	17.5	Microbiology living, KLM	Lost some sediment on bottom
5	13.5	O2, MK	
6	17.5	Microbiology living, KLM	
7	19	Delta 56 Fe, MK	
8	18	Fe kinetics, KLM	

Name	Analysis	Number of cores	Comment
Katrin Linse	Photo, length	x	
Male Koester (MK)	Pore water	1	Next to SRR
	O_2		
	PB, Porosity, TOC, etc	1	
	Delta 56 Fe	1	Only CB & KHB
Katja Laufer-Meiser (KLM)	DNA, SRR &CH4	1	Next to Pore water
	Fe Kinetics	1	
	Living community	2	
Madeline Anderson (MA)	Macrobiology	1	Surface water to Walter & Florian
Bernd Krock (BK)	Diatoms		From SSR
Hannah Marchant (HKM)	N-cycling, metagenome		surface water
Henrick Grotheer (HG)	Surface isotope		
Florian Koch (FK)	Surface waters		surface water
Walter Geibert (WG)	Surface waters		surface water
Josefine Weiss (JW)	aDNA		
		8	

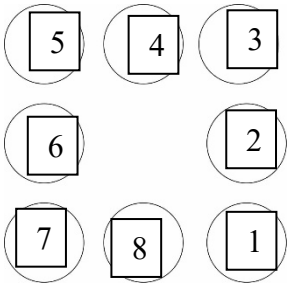

MUC core log **Site:** ……off Nordenskjold Glacier

Station PS133-2_35_6……**MUC-**12……**Date**…3.12……..2022

Depth…160.**m**…….. Comment……7/8 core……very silty mud……
(SSR core next to porewater; sediment grain size longest, undisturbed core)

Core ID	Segment depth (cm)	Analysis & scientist	Comments
1	21	Pore water, MK	
2	42	Delte 56 Fe, MK	
3	35	SRR, KL	
4	-	-	
5	15	Surface isotope, HG	Lost stuff
6	34	Microbiology living, KLM	Very fluffy sediment
7	20	Microbiology living, KLM	
8	22	FE kinetics, KLM	tilted

Name	Analysis	Number of cores	Comment
Madeline Anderson, KL	Photo, length	x	
Male Koester (MK)	Pore water	1	Next to SRR
	O_2		
	PB, Porosity, TOC, etc	1	
	Delta 56 Fe	1	Only CB & KHB
Katja Laufer-Meiser (KLM)	DNA, SRR &CH4	1	Next to Pore water
	Fe Kinetics	1	
	Living community	2	
Madeline Anderson (MA)	Macrobiology		
Bernd Krock (BK)	Diatoms		From SSR
Hannah Marchant (HKM)	N-cycling		surface water
Isa Wilkie	Metagenomics		
Henrick Grotheer (HG)	Surface isotope	1	
Florian Koch (FK)	Surface waters		surface water
Walter Geibert (WG)	Surface waters		surface water
		8	

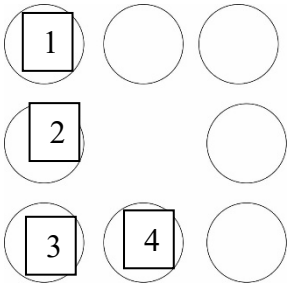

MUC core log **Site:** ……off Nordenskjold Glacier

Station PS133-2_35_7……**MUC-**13……**Date**…3.12.……..2022

Depth…160.**m**…….. Comment……4/8 core……very silty mud……
(SSR core next to porewater; sediment grain size longest, undisturbed core)

Core ID	Segment depth (cm)	Analysis & scientist	Comments
1	12	Macrobiology, MA	
2	17.5	Macrobiology, MA	
3	23	Macrobiology, MA	
4	13.5	Macrobiology, MA	
5	-	-	
6	-	-	
7	-	-	
8	-	-	

Name	Analysis	Number of cores	Comment
Madeline Anderson, KL	Photo, length	x	
Male Koester (MK)	Pore water		Next to SRR
	O_2		
	PB, Porosity, TOC, etc		
	Delta 56 Fe		Only CB & KHB
Katja Laufer-Meiser (KLM)	DNA, SRR &CH4		Next to Pore water
	Fe Kinetics		
	Living community		
Madeline Anderson (MA)	Macrobiology	4	Surface water to WG & FK
Bernd Krock (BK)	Diatoms		From SSR
Hannah Marchant (HKM)	N-cycling		surface water
Isa Wilkie	Metagenomics		
Henrick Grotheer (HG)	Surface isotope		
Florian Koch (FK)	Surface waters		surface water
Walter Geibert (WG)	Surface waters		surface water
		4	

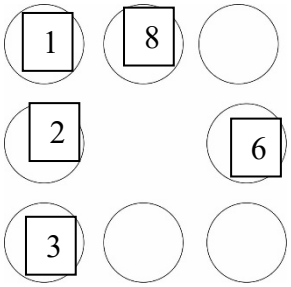

MUC core log **Site:** ……off Nordenskjold Glacier

Station PS133-2_35_8……**MUC-**14……**Date**…3.12.……..2022

Depth…160.**m**…….. Comment……5/8 core……very silty mud……
(SSR core next to porewater; sediment grain size longest, undisturbed core)

Core ID	Segment depth (cm)	Analysis & scientist	Comments
1	24	Macrobiology, MA	
2	37	Pb, Porosity etc, MK	
3	30	N-cycling, HM	
4	-	-	
5	-	-	
6	30	aDNA, MK	
7	-	-	
8	17	- Macrobiology, MA	

Name	Analysis	Number of cores	Comment
Madeline Anderson, KL	Photo, length	x	
Male Koester (MK)	Pore water		Next to SRR
	aDNA	1	
	PB, Porosity, TOC etc	1	
	Delta 56 Fe		Only CB & KHB
Katja Laufer-Meiser (KLM)	DNA, SRR &CH4		Next to Pore water
	Fe Kinetics		
	Living community		
Madeline Anderson (MA)	Macrobiology	2	Surface water to Walter & Florian
Bernd Krock (BK)	Diatoms		From SSR
Hannah Marchant (HKM)	N-cycling, metagenome	1	surface water
Henrick Grotheer (HG)	Surface isotope		
Florian Koch (FK)	Surface waters		surface water
Walter Geibert (WG)	Surface waters		surface water
		5	

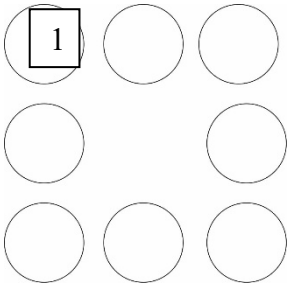

MUC core log **Site:** ……off KEP……

Station PS133-2_37_3……**MUC-**15……**Date**…4.12.……..2022

Depth…134.**m**…….. Comment……1/8 core……
(SSR core next to porewater; sediment grain size longest, undisturbed core)

Core ID	Segment depth (cm)	Analysis & scientist	Comments
1	4	Macrobiology, MA	
2			
3			
4			
5			
6			
7			
8			

Name	Analysis	Number of cores	Comment
Madeline Anderson, KL	Photo, length	x	
Male Koester (MK)	Pore water		Next to SRR
	O_2		
	PB, Porosity, TOC, etc		
	Delta 56 Fe		Only CB & KHB
Katja Laufer-Meiser (KLM)	DNA, SRR &CH4		Next to Pore water
	Fe Kinetics		
	Living community		
Madeline Anderson (MA)	Macrobiology	1	Surface water to Walter & Florian
Bernd Krock (BK)	Diatoms		From SSR
Hannah Marchant (HKM)	N-cycling		surface water
Isa Wilkie	Metagenomics		
Henrick Grotheer (HG)	Surface isotope		
Florian Koch (FK)	Surface waters		surface water
Walter Geibert (WG)	Surface waters		surface water

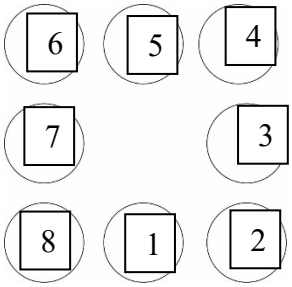

MUC core log **Site:** ……Cumberland Bay Confluence

Station PS133-2_42_8……**MUC-**16……**Date**…7.12.……..2022

Depth…264.**m**…….. Comment……8/8 cores ; no water samples taken…… (SSR core next to porewater; sediment grain size longest, undisturbed core)

Core ID	Segment depth (cm)	Analysis & scientist	Comments
1	18	SRR, KLM	
2	19	Microbiology living, KLM	No overstanding water
3	20	Surface isotope, HG	
4	18.5	?, Male	Clear water
5	18	Fe kinetics, KLM	
6	20	?, Male	
7	22	Microbiology living, KLM	No overstanding water
8	18	Surface isotope, HG	

Name	Analysis	Number of cores	Comment
Madeline Anderson, KL	Photo, length	x	
Male Koester (MK)	Pore water	1	Next to SRR
	O_2		
	PB, Porosity, TOC, etc	1	
	Delta 56 Fe		Only CB & KHB
Katja Laufer-Meiser (KLM)	DNA, SRR &CH4	1	Next to Pore water
	Fe Kinetics	1	
	Living community	2	
Madeline Anderson (MA)	Macrobiology		Surface water to Walter & Florian
Bernd Krock (BK)	Diatoms		From SSR
Hannah Marchant (HKM)	N-cycling		surface water
Isa Wilkie	Metagenomics		
Henrick Grotheer (HG)	Surface isotope	2	
Florian Koch (FK)	Surface waters		surface water
Walter Geibert (WG)	Surface waters		surface water
		8	

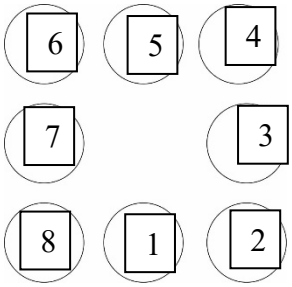

MUC core log **Site:** ……Cumberland Bay Confluence

Station PS133-2_42_9……**MUC-**17……**Date**…7.12.……..2022

Depth…264.**m**…….. Comment……8/8 cores ; no water samples taken…… (SSR core next to porewater; sediment grain size longest, undisturbed core)

Core ID	Segment depth (cm)	Analysis & scientist	Comments
1	23	aDNA, MK	
2	20	Surface isotope, HG	
3	22	?, Male	
4	22	?, KLM	
5	19	Microbiology living, KLM	
6	20	Surface isotope, HG	
7	21	N-cycling, Meta, HM	
8	21	Microbiology living, KLM	

Name	Analysis	Number of cores	Comment
Madeline Anderson, KL	Photo, length	x	
Male Koester (MK)	Pore water		Next to SRR
	O_2	1	
	PB, Porosity, TOC, etc		
	Delta 56 Fe		Only CB & KHB
	aDNA	1	
Katja Laufer-Meiser (KLM)	DNA, SRR &CH4		Next to Pore water
	Fe Kinetics		
	Living community	3	
Madeline Anderson (MA)	Macrobiology		Surface water to Walter & Florian
Bernd Krock (BK)	Diatoms		From SSR
Hannah Marchant (HKM)	N-cycling		surface water
Isa Wilkie	Metagenomics	1	
Henrick Grotheer (HG)	Surface isotope	2	
Florian Koch (FK)	Surface waters		surface water
Walter Geibert (WG)	Surface waters		surface water
		8	

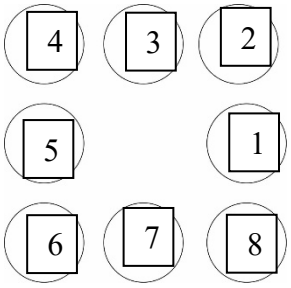

MUC core log **Site:** ……Shelf off Cumberland Bay

Station PS133-2_50_6……**MUC-**18……**Date**…7.12.……..2022

Depth…270.**m**…….. Comment……1/8 core……
(SSR core next to porewater; sediment grain size longest, undisturbed core)

Core ID	Segment depth (cm)	Analysis & scientist	Comments
1	29	aDNA, MK	leaking
2	28.5		
3	29	O2, MK	
4	27		
5	26	N-cycling, HM	
6	20		turbid
7	23.5		
8	25	Pore water, MK & KLM	tilted

Name	Analysis	Number of cores	Comment
Madeline Anderson, KL	Photo, length	x	
Male Koester (MK)	Pore water		Next to SRR
	O_2	1	
	PB, Porosity, TOC, etc		
	Delta 56 Fe		Only CB & KHB
	aDNA	1	
Katja Laufer-Meiser (KLM)	DNA, SRR &CH4		Next to Pore water
	Fe Kinetics		
	Living community	2	
Madeline Anderson (MA)	Macrobiology		Surface water to Walter & Florian
Bernd Krock (BK)	Diatoms		From SSR
Hannah Marchant (HKM)	N-cycling, metagenome	1	surface water
Henrick Grotheer (HG)	Surface isotope		
Florian Koch (FK)	Surface waters		surface water
Walter Geibert (WG)	Surface waters		surface water
		8	

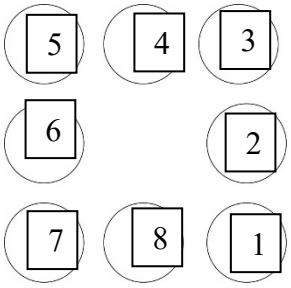

MUC core log **Site:** ……Shelf off Cumberland Bay……

Station PS133-2_50_7……**MUC-**19……**Date**…7.12.……..2022

Depth…270.**m**…….. Comment……1/8 core……
(SSR core next to porewater; sediment grain size longest, undisturbed core)

Core ID	Segment depth (cm)	Analysis & scientist	Comments
1	26.5	Microbiology living, KLM	
2	27	Surface isotopes, HG	
3	28	Fe kinetics, KLM	
4	27.5	Microbiology living, KLM	
5	27	SRR, KLM	
6	30	Pore water, MK	
7	27.5	Surface isotopes, HG	
8	29	Delta 56 Fe, MK	

Name	Analysis	Number of cores	Comment
Madeline Anderson, KL	Photo, length	x	
Male Koester (MK)	Pore water	1	Next to SRR
	O_2		
	PB, Porosity, TOC, etc		
	Delta 56 Fe	1	Only CB & KHB
	aDNA		
Katja Laufer-Meiser (KLM)	DNA, SRR &CH4	1	Next to Pore water
	Fe Kinetics	1	
	Living community	2	
Madeline Anderson (MA)	Macrobiology		
Bernd Krock (BK)	Diatoms		From SSR
Hannah Marchant (HKM)	N-cycling, Metagenome		surface water
Henrick Grotheer (HG)	Surface isotope	2	
Florian Koch (FK)	Surface waters		surface water
Walter Geibert (WG)	Surface waters		surface water
		8	

Die **Berichte zur Polar- und Meeresforschung** (ISSN 1866-3192) werden beginnend mit dem Band 569 (2008) als Open-Access-Publikation herausgegeben. Ein Verzeichnis aller Bände einschließlich der Druckausgaben (ISSN 1618-3193, Band 377-568, von 2000 bis 2008) sowie der früheren **Berichte zur Polarforschung** (ISSN 0176-5027, Band 1–376, von 1981 bis 2000) befindet sich im electronic Publication Information Center **(ePIC)** des Alfred-Wegener-Instituts, Helmholtz-Zentrum für Polar- und Meeresforschung (AWI); see https://epic.awi.de. Durch Auswahl "Reports on Polar- and Marine Research" (via "browse"/"type") wird eine Liste der Publikationen, sortiert nach Bandnummer, innerhalb der absteigenden chronologischen Reihenfolge der Jahrgänge mit Verweis auf das jeweilige pdf-Symbol zum Herunterladen angezeigt.

The **Reports on Polar and Marine Research** (ISSN 1866-3192) are available as open access publications since 2008. A table of all volumes including the printed issues (ISSN 1618-3193, Vol. 377-568, from 2000 until 2008), as well as the earlier **Reports on Polar Research** (ISSN 0176-5027, Vol. 1–376, from 1981 until 2000) is provided by the electronic Publication Information Center **(ePIC)** of the Alfred Wegener Institute, Helmholtz Centre for Polar and Marine Research (AWI); see URL https://epic.awi.de. To generate a list of all Reports, use the URL http://epic.awi.de and select "browse"/"type" to browse "Reports on Polar and Marine Research". A chronological list in declining order will be presented, and pdf-icons displayed for downloading.

Zuletzt erschienene Ausgaben:

Recently published issues:

775 (2023) The Expedition PS133/2 of the Research Vessel POLARSTERN to the Scotia Sea in 2022, edited by Sabine Kasten with contributions of the participants

774 (2023) The Expedition PS133/1 of the Research Vessel POLARSTERN to the Atlantic Ocean in 2022, edited by Christine Klaas with contributions of the participants

773 (2023) A computational approach of locomotion, energy demand and dispersal of the common comatulid crinoid *Promachocrinus kerguelensis* (Echinodermata) and its circum-Antarctic success, by Nils Owsianowski

772 (2023) Russian-German Cooperation: Expeditions to Siberia in 2021, edited by Anne Morgenstern, Birgit Heim, Luidmila A. Pestryakova, Dmitry Yu. Bolshiyanov, Mikhail N. Grigoriev, Dmitry Ayunov, Antonia Dill, and Iuliia Jünger

771 (2023) The Expedition PS132 of the Research Vessel POLARSTERN to the Atlantic Ocean in 2022, edited by Karen H. Wiltshire and Angelika Dummermuth with contributions of the participants

770 (2023) The Expedition PS131 of the Research Vessel POLARSTERN to the Fram Strait in 2022, edited by Torsten Kanzow with contributions of the participants

769 (2023) The Expedition TRITON2021 of the Hendes Dansk Majestæt Skib TRITON to the Atlantic Ocean in 2021, edited by Rebecca McPherson, Carina Engicht and Torsten Kanzow

768 (2022) Mit Erich von Drygalski in die Ostantarktis – Paul Björvigs Tagebuch von der ersten deutschen Südpolarexpedition 1901-1903. Aus dem Norwegischen übersetzt von Volkert Gazert und herausgegeben von Cornelia Lüdecke

767 (2022) Expeditions to Antarctica: ANT-Land 2021/22 Neumayer Station III, Kohnen Station, Flight Operations and Field Campaigns, edited by Christine Wesche and Julia Regnery with contributions of the participants

ALFRED-WEGENER-INSTITUT
HELMHOLTZ-ZENTRUM FÜR POLAR-
UND MEERESFORSCHUNG

BREMERHAVEN

Am Handelshafen 12
27570 Bremerhaven
Telefon 0471 4831-0
Telefax 0471 4831-1149
www.awi.de

HELMHOLTZ